Instituto Teófilo Hernando de I+D del Medicamento
Departamento de Farmacología y Terapéutica
Facultad de Medicina
Universidad Autónoma de Madrid

Contribución de los receptores nicotínicos a la neuroprotección y a la neuroinflamación

Esther Parada Pérez

Licenciada en Farmacia

Directores de Tesis: Dra. Manuela G. López y Dr. Francisco Javier Egea

Instituto Teófilo Hernando

Universidad Autónoma de Madrid

Departamento de Farmacología y Terapéutica
Facultad de Medicina
Universidad Autónoma de Madrid

Dra. Manuela García Lopez, Profesora Titular del Departamento de Farmacología y Terapéutica de la Facultad de Medicina,

Dr. Francisco Javier Egea Maíquez, Investigador Post-Doctoral adjunto al Departamento de Farmacología y Terapéutica de la Facultad de Medicina

CERTIFICAN que Doña Esther Parada Pérez ha realizado bajo su dirección el presente trabajo: “Contribución de los receptores nicotínicos a la neuroprotección y a la neuroinflamación”, como Tesis para alcanzar el grado de Doctor por la Universidad Autónoma de Madrid

Para que conste a efectos oportunos, expiden y firman la presente en Madrid a 10 de Febrero de 2014

Dra. Manuela García López
Profesora Titular de Farmacología

Dr. Francisco Javier Egea Maíquez
Investigador post-doctoral senior

Esta tesis doctoral se encuadra dentro de una de las principales líneas de trabajo del Instituto Teófilo Hernando (ITH): el estudio de la muerte neuronal y la búsqueda de fármacos neuroprotectores para el tratamiento de enfermedades neurodegenerativas. En nuestro trabajo, nos hemos centrado en los accidentes cerebrosvasculares. Para ello, hemos desarrollado modelos de isquemia cerebral tanto *in vitro* como *in vivo* y también hemos testado el perfil farmacológico de agonistas nicotínicos y otras moléculas prometedoras.

La enfermedad cerebrovascular es una alteración fisiológica del flujo cerebral cuyas consecuencias producen elevados índices de muerte e incapacidad. Los esfuerzos de la comunidad científica están encaminados a conseguir fármacos neuropotectores que sean capaces de frenar la muerte cerebral producida por la isquemia. Para conseguir esto, ampliar la ventana terapéutica de actuación, conocer los mecanismos de muerte celular y las dianas farmacológicas de tratamiento, son algunas de las premisas que deberíamos seguir para realizar un estudio encaminado al conocimiento de esta patología.

En los modelos de isquemia que aquí se plantean, hemos querido evaluar la capacidad neuroprotectora y antiinflamatoria de compuestos relacionados con los receptores nicotínicos (agonistas selectivos del subtipo α7 nAChRs e inhibidores acetilcolinesterásicos). También hemos querido estudiar los mecanismos de acción que tenían lugar al activar estos receptores, así como las proteínas que estaban implicadas, en concreto el papel que desempeñaba la expresión de la enzima antioxidante HO-1.

Hemos querido además, evaluar la capacidad glioprotectora y antioxidante de inductores directos de HO-1, como son la melatonina y la curcumina, así como la participación de los receptores nicotínicos en los mecanismos de acción que estábamos observando.

1. La isquemia cerebral

1.1. Fisiopatología del ictus

El ictus es la segunda causa de muerte en el mundo y la principal causa de discapacidad (Thrift *et al.* 2001). Datos de la "American Heart Association" (Lloyd-Jones 2010) indican que en EEUU, cada 40 segundos una persona sufre un accidente cerebrovascular. Mejorar las tasas de mortalidad y las complicaciones derivadas de esta enfermedad, es un objetivo socio-sanitario prioritario.

Los accidentes cerebrovasculares pueden ser de tipo isquémico (representando entre el 80 y el 85 % de todos los ictus) o de tipo hemorrágico (representando el 15-20% restante). En los de tipo isquémico, se produce una interrupción brusca del flujo sanguíneo cerebral que altera de forma transitoria o permanente, la función de una determinada región que, en la mayoría de los casos, es la arteria cerebral media o sus ramificaciones (Thrift *et al*. 2001, Durukan & Tatlisumak 2007).

Cuando se produce la oclusión de un vaso, el flujo sanguíneo cerebral desciende rápidamente (por debajo de 10-15 mL/100g/min), se produce entonces la muerte celular rápida y característica del núcleo del infarto. En este núcleo, las neuronas mueren por necrosis, fruto de un fracaso energético agudo con pérdida de la morfología celular, que finalmente lleva a la lisis. El área adyacente que circunscribe al foco isquémico, denominada área de penumbra, presenta sin embargo, unas características fisiológicas distintas, preservando aún la morfología celular y el metabolismo energético. Dado que el flujo sanguíneo desciende hasta 20 mL/100 g/min, la integridad de las células, así como su función, aunque alterada, es potencialmente recuperable (Fig 1).

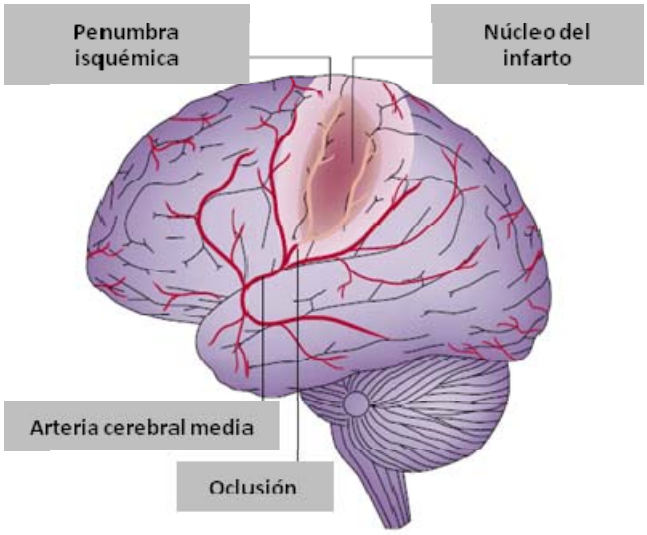

Fig1: Representación de un infarto cerebral por oclusión de la arteria cerebral media, en el cual está definido, tanto el núcleo del infarto (parte más profunda con daño estructural irreparable), como la penumbra isquémica (porción periférica que podría recuperar la función perdida)

Tras la obstrucción de un vaso sanguíneo en un evento de tipo isquémico, lo primero que se observa es la caída brusca del flujo sanguíneo, la primera consecuencia lleva a la acumulación de lactato y la disminución del pH (acidosis láctica) a través de la glucolisis anaerobia. La acidosis láctica puede aumentar la producción de especies reactivas de oxígeno (ROS, del inglés reactive oxygen species), interferir con la síntesis proteica y empeorar el daño isquémico (Mergenthaler *et al.* 2004). El resultado es una disminución en los niveles de ATP, ya que el metabolismo oxidativo está comprometido. En el núcleo del infarto los niveles de ATP disminuyen entre un 80-85% (Folbergrova *et al.* 1995). Debido a esta reducción en los niveles de ATP, en la neurona presináptica se produce un fallo en el control de las bombas de Na^+ /K^+ ATPasa, que conlleva la apertura de los canales de Na^+, K^+ y Ca^{2+}, con la consecuente entrada desmedida de iones Ca^{2+} y Na^+ y salida de K^+ (conocida como la despolarización anóxica). La consecuencia de esta despolarización celular es la liberación de glutamato (principal neurotransmisor excitador) a la hendidura sináptica, que activa los receptores NMDA, AMPA, Kainato (KA) y los receptores metabotrópicos de glutamato (mGLURs), que tiene como consecuencia una sobrecarga de Ca^{2+} en los terminales postsinápticos. Este aumento de Ca^{2+} intracelular origina numerosas alteraciones celulares que contribuyen a aumentar la lesión y la muerte de las neuronas por necrosis, entre ellas destacan la activación de lipasas, proteasas y peroxidasas, liberación de radicales, alteración de macromoléculas y ruptura de la membrana celular. Todos estos

eventos, que ocurren tras la oclusión de un vaso sanguíneo cerebral, se conocen como "cascada isquémica" (Fig2).

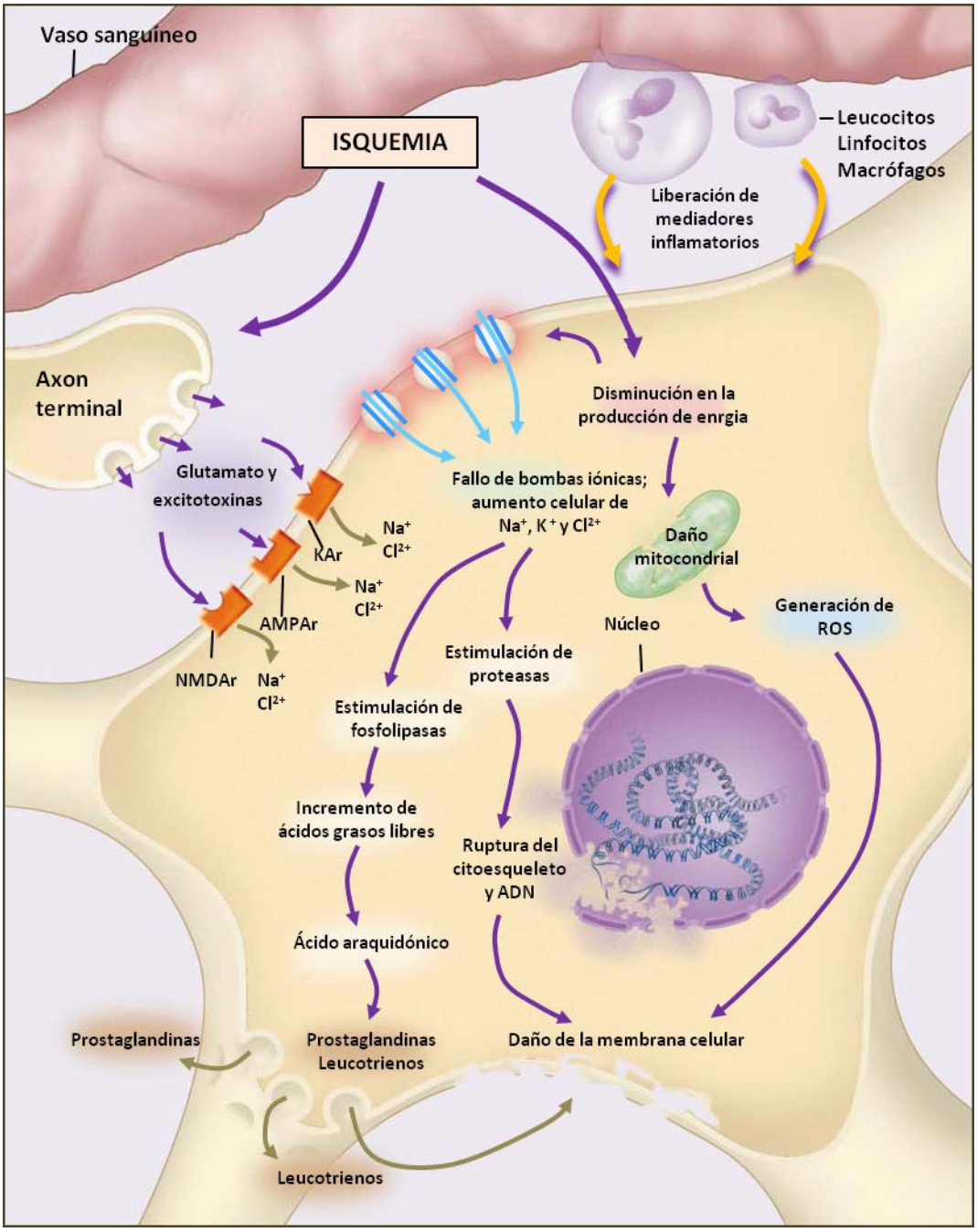

Fig2: Imagen representativa de la cascada isquémica

Durante la isquemia, se produce la hidrolisis del ATP en AMP, lo que conlleva a una acumulación de hipoxantina. La sobrecarga de Ca^{2+} que se produce en este periodo, agudiza la conversión de xantina deshidrogenasa en xantina oxidasa, debido a la activación de Ca^{2+}-calmodulina (CaM). Cuando se produce la reperfusión, la presencia de oxígeno activa la reacción que produce la xantina oxidasa, convirtiendo la

hipoxantina acumulada durante la isquemia en xantina, a través de la vía del ácido úrico. Ésto genera grandes cantidades de anión superóxido (O_2^-), cuya producción masiva, además de inactivar distintas enzimas, es precursora de del H_2O_2, que es un potente oxidante relativamente estable. La acumulación de H_2O_2, en presencia de hierro u otros metales como manganeso o cobre, desencadena la reacción de Haber-Weiss, catalizada por hierro y descrita por Fenton:

$$O_2^- + H_2O \text{ ----} Fe^3 \text{ ------>} O_2 + OH^- + OH^-$$

En ésta reacción, el producto es el radical hidroxilo (OH^-), que es muy inestable y altamente reactivo (Fig 3). El hierro (Fe^3) es el elemento conductor de dicha reacción, existe de forma abundante en el cuerpo humano, formando parte de diversas proteínas tales como los citocromos, la transferrina, la hemoglobina u otros, sin embargo, las condiciones anaerobias favorecen su separación (White *et al.* 1985, Babbs 1985, Komara *et al.* 1986).

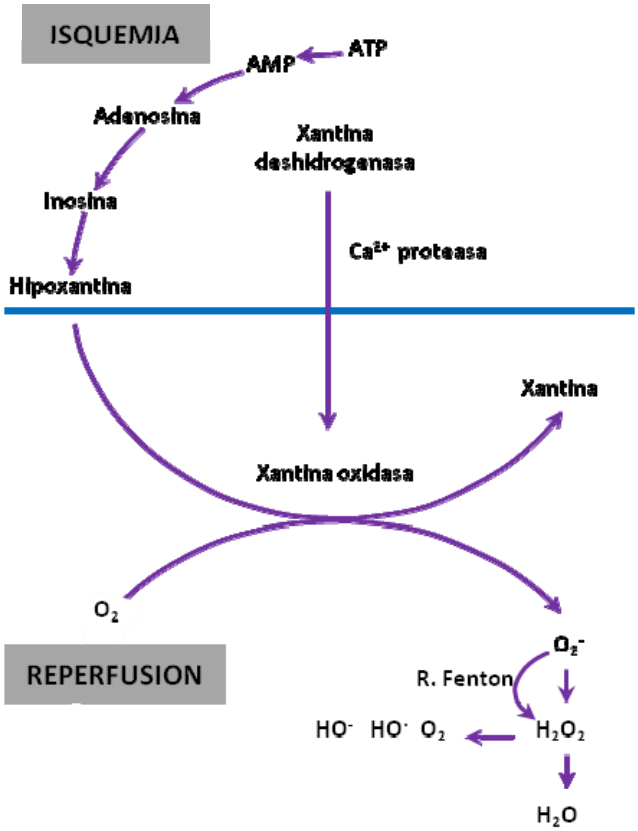

Fig 3: Esquema representativo de las principales alteraciones bioquímicas que se producen durante la isquemia-reperfusión.

Otro de los inconvenientes que se producen en la reperfusión es el originado a raíz de la restauración de los niveles de ATP, ya que puede producir una absorción activa del calcio por parte de la mitocondria, lo que contribuye al aumento masivo de calcio en el interior celular (Safar 1986)

El objetivo principal de la neuroprotección es el de interferir con las alteraciones bioquímicas que se producen en el «área de penumbra», con el fin de bloquear la citada *cascada* y, así, evitar o retrasar la evolución hacia la muerte celular. Durante los últimos 20 años, los buenos resultados obtenidos con distintos compuestos neuroprotectores en modelos experimentales de infarto cerebral, han motivado su evaluación en fases clínicas. Lamentablemente, cuando estos compuestos han llegado a la fase clínica, muchos de ellos hasta la fase III, han fallado estrepitosamente (Green 2002, Xu & Pan 2013). Para minimizar esta gran discordancia entre los resultados pre-clínicos y clínicos, un grupo de expertos (Stroke Therapy Academic Industry Roundtable–STAIR-) ha establecido una serie de recomendaciones para guiar el diseño preclínico de los nuevos estudios (véase http://www.thestair.org/). Entre ellos destacan la realización de estudios ciegos, el control de las variables fisiológicas durante los experimentos y la evaluación del potencial protector de las moléculas, tanto en fase aguda, como a largo plazo. En cuanto a los modelos de isquemia propiamente dichos y la especie a elegir, los criterios STAIR defienden que los estudios de eficacia se realicen en animales adultos (principalmente envejecidos), sin distinción de sexo y con enfermedades concomitantes, como por ejemplo diabetes o hipertensión (STAIR & Development. 1999, Liu *et al.* 2009, Kahle & Bix 2012, Fisher *et al.* 2009).

1.2.Muerte celular en la isquemia cerebral

En la isquemia cerebral, se producen tres tipos principales de muerte celular: necrosis, apoptosis y autofagia. La necrosis, se acompaña de hinchazón de las organelas celulares y edema celular, con la consiguiente ruptura de membranas y lisis de la célula, cuya consecuencia es el vertido de los componentes intracelulares al espacio extracelular, causando edema en el tejido e induciendo una respuesta inflamatoria. La necrosis, comparada coloquialmente con un "suicidio celular", se ha considerado tradicionalmente como una forma de muerte pasiva, sin embargo, recientes investigaciones han descubierto que podría tratarse de otra forma más de muerte celular

dirigida o programada. Cuando se identificaron las caspasas por primera vez, como los principales mediadores de la apoptosis, se planteó la hipótesis de que muchos de sus sustratos eran proteínas esenciales cuya destrucción aseguraba la muerte celular. Sin embargo, existe una muerte celular independiente de caspasas. Cuando la apoptosis se ha iniciado, en muchas ocasiones, el uso de agentes antiapoptoticos o inhibidores de caspasas es ineficaz. En estas condiciones, las células que normalmente morirían por apoptosis, presentan todas las características de la necrosis. Estos resultados conducen a la idea de que la necrosis se puede "programar", de modo que existan eventos de señalización celular que inician la destrucción por necrosis en un proceso denominado necroptosis (Xu & Zhang 2011, Galluzzi & Kroemer 2008, Degterev *et al.* 2005).

La apoptosis es un proceso complejo, finamente regulado por diferentes vías de señalización celular. Tras iniciarse la apoptosis, se suceden una serie de cambios bioquímicos que incluyen: encogimiento celular, condensación de la cromatina, formación de vesículas citoplasmáticas y fragmentación del ADN nuclear. La apoptosis se caracteriza por la exposición de residuos de fosfatidil serina en la membrana plasmática, así como por la activación de caspasas. Estos últimos, son los principales ejecutores de la muerte celular por apoptosis (Broughton *et al.* 2009, Mehta *et al.* 2007).

La autofagia, otro tipo de muerte celular programada, se caracteriza por la formación de vesículas llamadas autofagosomas en el interior celular, cuyo contenido alberga macromoléculas y organelas propias de la célula. En este proceso de "autodestrucción celular", las mitocondrias intactas proporcionan energía a la célula, para que se produzca la degradación del aparato de golgi, polirribosomas, retículo endoplásmico y, finalmente, la desintegración del núcleo (Xu & Zhang 2011). La autofagia, es un proceso catabólico natural, que se da en la célula en situaciones de remodelación celular o para facilitar la eliminación de células dañadas. Sin embargo, la autofagia se ha visto alterada en numerosas enfermedades neurodegenerativas, como la enfermedad de Alzhemier, de Parkinson o la isquemia cerebral (Nixon 2013).

Como hemos visto anteriormente, el área de penumbra isquémica representa la región celular recuperable en un ictus. En éste área, las células mueren eminentemente por apoptosis y autofagia, mientras que en el núcleo del infarto, donde existe una depleción casi total de los niveles de ATP, la muerte celular se produce principalmente por necrosis (Fig 4).

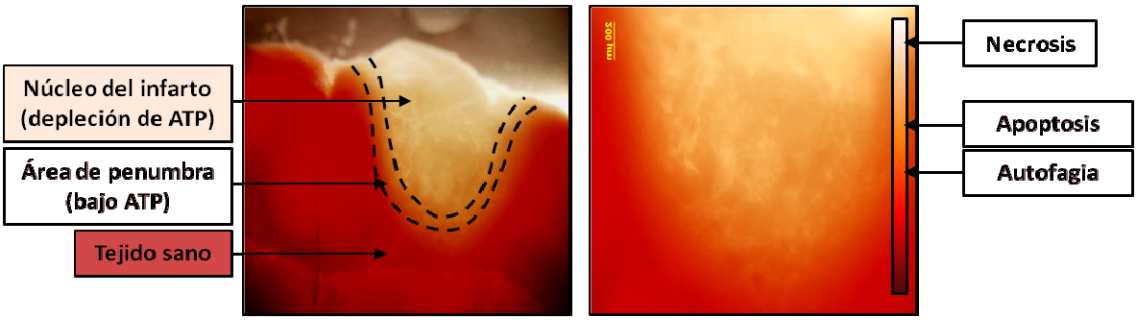

Fig 4: Corte coronal de cerebro de ratón infartado teñido con TTC. En la región infartada, podemos ver una zona resistente a la tinción, en color blanco (núcleo del infarto) y una zona sana, teñida de color rojo. También se aprecia a simple vista, una región punteada, que corresponde al peri-infarto o denominada área de penumbra isquémica (izda), donde la muerte principal de las células se produce por autofagia y necrosis, mientras que en el núcleo del infarto, predomina la muerte por necrosis (dcha)

2. Procesos inflamatorios en el ictus

Los procesos inflamatorios suceden, tanto en condiciones agudas, como en condiciones crónicas de neurodegeneración. La inflamación tiene un papel vital en el desarrollo de la enfermedad de tipo isquémica. De hecho, pacientes que han sufrido un ictus con inflamación sistémica concomitante, poseen peor pronóstico (Emsley & Hopkins 2008, McColl *et al.* 2009). La respuesta inflamatoria del sistema nervioso central es distinta a la que ocurre en otros tejidos. La isquemia focal induce un reclutamiento y activación de células inflamatorias, incluyendo neutrófilos, células T, monocitos y macrófagos. La activación de estas células, unida a las de las células gliales residentes del sistema nervioso central (astrocitos y microglía), produce la expresión y liberación de mediadores de la inflamación como proteínas de fase aguda, eicosanoides y distintas citoquinas (Barone & Feuerstein 1999). Esta respuesta aguda puede inhibir la respuesta inflamatoria, disminuyendo el volumen de infarto y mejorando los déficits neurológicos que acontecen en la isquemia (Wang 2005, Yilmaz & Granger 2008).

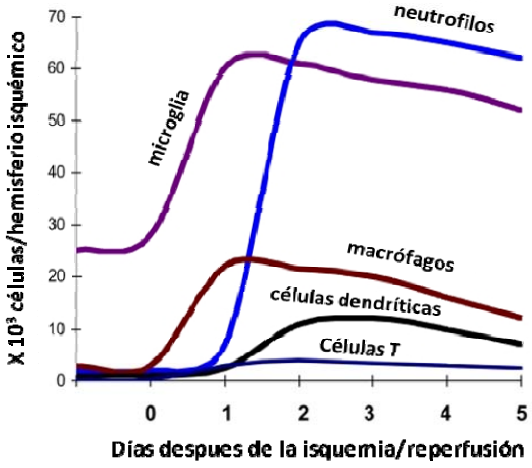

Fig 5: Imagen representativa, tiempo/dependiente, que muestra el reclutamiento de células inflamatorias en el parénquima cerebral, después de una isquemia focal en ratón (Jin *et al.* 2010).

2.1.Importancia de la microglía

Los primeros estudios que intuyen la presencia en el cerebro de la microglía, son los realizados por Santiago Ramón y Cajal, quien descubrió un tipo celular diferente al que denomino glía adendrítica o "tercer elemento de los centros nerviosos". Sin embargo, no fue hasta 1919, cuando Rio Hortega describió este tipo celular tal y como lo conocemos ahora: una célula de origen mesodérmico que se encuentra mayoritariamente en la materia gris, altamente ramificada, con capacidad migratoria y fagocítica (Del Rio-Hortega 1921, del Rio-Hortega 1993, Rezaie & Male 2002, del Rio-Hortega 1933)).

En el cerebro adulto, la microglía se encuentra, generalmente, en un estado quiescente, caracterizado morfológicamente por poseer somas de tamaño medio y múltiples ramificaciones; sin embargo, frente a un daño cerebral o estímulo inflamatorio, la microglía sufre un rápido cambio morfológico, clásicamente conocido como activación microglíal. En este nuevo estado, las ramificaciones de la microglía se retraen, los somas se engrosan (Fig. 6), además, expresa una serie de receptores de membrana distintos a los que están presentas en un estado quiescente (CD14, complejo mayor de histocompatibilidad II (CMH II), receptores de quimioquinas y otros marcadores) (Block *et al.* 2007, Rock *et al.* 2004).

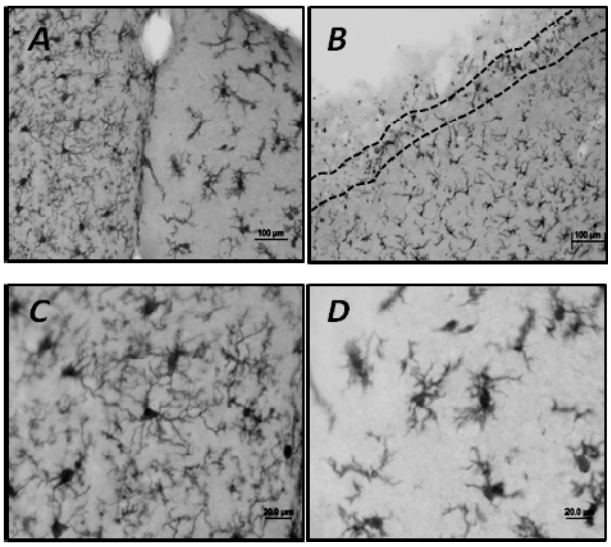

Fig 6: Tinción inmunohistoquímica con el marcador especifico de microglía/macrófagos Iba1. En la imagen (A) se observan las diferencias morfologícas entre la microglía correspondiente al hemisferio infartado (ipsilateral-dcha) y la del hemisferio sano (contralateral-izda). La imagen (B) muestra la acumulación de microglía en el borde del infarto. Magnificaciones de la morfología característica de microglía quiescente (C) y microglía activada (D).

La microglía activada puede tener un papel beneficioso para las neuronas que han sufrido un daño, eliminando restos celulares de neuronas muertas, liberando factores tróficos y antiinflamatorios, o facilitando la reparación tisular y promoviendo la migración de células madre a sitios concretos de inflamación o daño (Muller *et al.* 2006, Hanisch & Kettenmann 2007, Morgan *et al.* 2004). Sin embargo, la microglía activada también puede tener un papel tóxico, agravando el daño tisular y produciendo factores neurotóxicos como NO, mieloperoxidasa, prostaglandinas y anion superóxido y liberando citoquinas proinflamatorias como TNF e IL1β (Taylor & Sansing 2013).

Por ello, la microglía es probablemente una de las células más complejas del SNC, la inexactitud del término "microglía activada" ha promovido la necesidad de crear nuevas y distintas clasificaciones que definan correctamente los cambiantes estados de esta célula. Uno de los esquemas que pretenden explicar la diversidad de fenotipos de la microglía es el propuesto por Perry y colaboradores, (Perry *et al.* 2010). En este esquema la microglía se divide en: 1) clásicamente activada, 2) cicatrizante y 3) reguladora. Todo ello considerando que la microglía no se instaura dentro de un fenotipo concreto, sino que cambia de un estado a otro según la fisiopatología del SNC lo requiera (Fig. 7). Uno de los ejemplos más ilustrativos de esta naturaleza es el

descrito por Davalos y colaboradores (Davalos *et al.* 2005). Estos experimentos *in vivo*, demuestran claramente, que la microglía no se encuentra en un estado quiescente como tal, sino que explora continuamente el cerebro y actúa casi instantáneamente frente a una lesión aguda (Fig. 8).

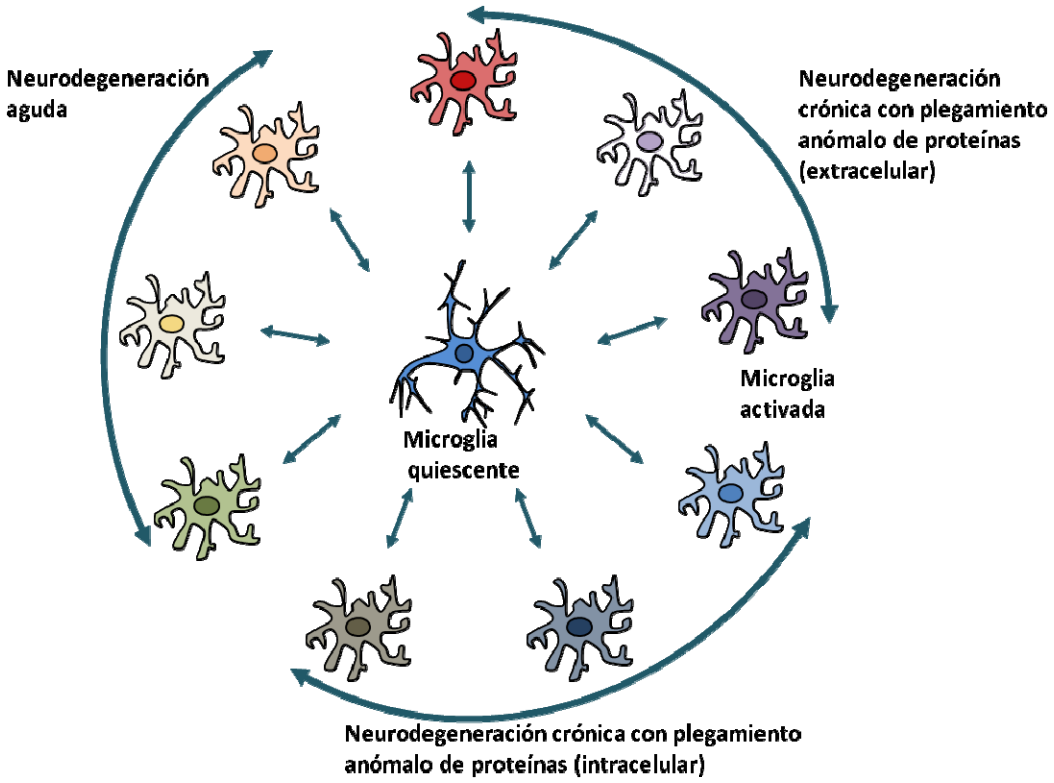

Fig 7: Esta imagen, pretende ilustrar los fenotipos cambiantes de la microglía (Perry *et al*. 2010). La microglía puede adoptar distintos fenotipos según el tipo de enfermedad, el estado, duración y muchas otras variables. Por ejemplo, la microglía que se activa en una neurodegeneración aguda, tendrá distintos fenotipos dependiendo del tamaño de la lesión, tiempo de examinación después de ésta o edad del paciente; estos diversos fenotipos están representados como microglía activada, con distintos colores. Del mismo modo, se representa la reversibilidad de estos estados. Tanto la morfología característica como la expresión de marcadores de membrana, son buenos indicadores para poder identificar estos estados.

Después de una lesión isquémica, los receptores de membrana de microglía /macrófagos responden, de manera rápida, a sustancias diversas que se encuentran en altas concentraciones, en el lugar donde se ha producido el infarto. Estas proteínas se llaman DAMPs, (del inglés, **D**amage-**A**ssociated **M**olecular **P**attern **M**olecules). Entre ellas destacan HSP (**H**eat **S**hock **P**rotein), HMGB1 (**H**igh **M**ovility **G**roup **B**ox 1), histonas, lípidos oxidados, ADN y ATP (Bianchi 2007, Kono & Rock 2008). Dentro de los receptores que son capaces de detectar estas señales DAMPs, se encuentran los receptores SRs (**S**cavenger **R**eceptors), TLRs (**T**oll **L**ike **R**eceptors) y RAGEs

(**R**eceptors for **A**dvanced **G**lycation **E**nd **P**roducts). Las células de la microglía responden rápidamente a estas señales, migrando a las zonas donde se produce la degeneración del tejido, y se acumulan entorno al borde del infarto, delimitando así la zona de penumbra. La función de la microglía en este proceso, sigue siendo actualmente motivo de debate en la comunidad científica.

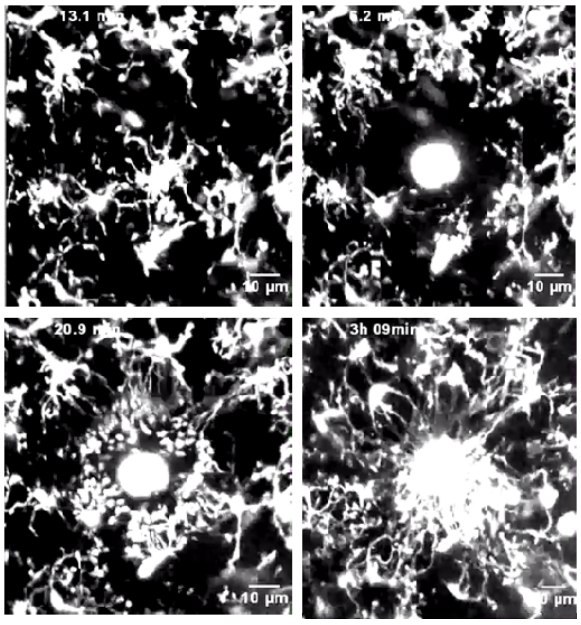

Fig 8: Estas imágenes, extraídas del estudio de Davalos y colaboradores (Davalos *et al.* 2005), nos ilustran, *in vivo,* y a tiempo real, el rápido movimiento de la microglía hacia los sitios de lesión. En la esquina superior izquierda, vemos la microglía de un ratón normal antes de producirle una lesión por ablación laser (esquina superior derecha). Podemos ver cómo, en apenas 20 minutos, la microglía responde a esta agresiva devastación de tejido, migrando hacia el lugar donde se ha producido el daño, alcanzando su máximo de confluencia a las 3 horas (imágenes inferiores izda -dcha).

Tradicionalmente, la microglía ha desempeñado un papel neurotóxico en la isquemia cerebral, liberando citoquinas proinflamatorias como IL1β o TNF (Gregersen *et al.* 2000, Mabuchi *et al.* 2000) que favorecen el reclutamiento de neutrófilos y monocitos de los vasos sanguíneos (Danton & Dietrich 2003, Allan & Rothwell 2003), contribuyendo así al aumento de la lesión isquémica. Sin embargo, cada vez se defiende más el papel neuroprotector de la microglía en la isquemia cerebral, entre sus acciones beneficiosas se encuentran la de liberar factores trófico, que contribuyen a la regeneración del tejido como TGFβ , IGF, BDNF, bFGF, VEGF y GDNF (Merson *et al.* 2010, Kiefer *et al.* 1995, Battista *et al.* 2006, Madinier *et al.* 2009); reducir la producción de NO o liberar citoquinas antiinflamatorias como TGFβ o IL10 (Hu *et al.* 2012). Otra prueba que apoya el efecto protector de la microglía en la isquemia se

encuentra en que los ratones deficitarios en microglía, poseen mayor vulnerabilidad a la isquemia (Lalancette-Hebert *et al.* 2007). Por otro lado, el transplante de microglía exógena ha mostrado efectos beneficioso, tanto *in vivo* como *in vitro*, en modelos de isquemia focal y privación de oxígeno y glucosa, respectivamente (Neumann *et al.* 2008, Narantuya *et al.* 2010).

Ante esta gran controversia, un trabajo de investigación reciente demuestra que la microglía tiene un efecto dual dentro de la misma patología y depende, fundamentalmente, del transcurso del tiempo. Es decir, ante un estímulo de isquemia focal, la población microglíal predominante varía, desde un fenotipo antiinflamatorio (primeros días después de la lesión), hasta un fenotipo proinflamatorio (varios días después de la lesión) (Hu *et al.*).

2.2. Terapia antiinflamatoria e implicación de los receptores nicotínicos

Como hemos visto anteriormente, debido al importante papel que juega la inflamación en la patología isquémica, instaurar una terapia antiinflamatoria coadyuvante que ayude a limitar la respuesta inmune y a reparar el tejido dañado, se postula como una de las dianas farmacológicas más prometedoras en el tratamiento de esta enfermedad (Jordan *et al.* 2008).

El efecto antiinflamatorio que se produce tras la activación del receptor nicotínico alfa siete, se puso de manifiesto en los trabajos de grupo del Dr. Kevin Tracey entre los años 2000 y 2003 (Borovikova *et al.* 2000, Tracey 2002, Wang *et al.* 2003). En estos trabajos, se estudió el efecto antiinflamatorio que tiene la estimulación del nervio vago (ENV) y la importancia de la activación de este receptor a nivel periférico, para el control de la inflamación en modelos de sepsis.

Desde estos primeros estudios, son muchos los grupos que han querido averiguar el efecto de esta estimulación en modelos de isquemia cerebral, y aunque los datos que tenemos hasta ahora parecen prometedores, aún habría que profundizar más en este campo para que se puedan instaurar en la práctica clínica post-ictus (Cheyuo *et al.* 2011). Entre los estudios en los cuales se pone de manifiesto el efecto neuroprotector de la estimulación del nervio vago, se encuentran el de Ay y colaboradores y el de Miyamoto y colaboradores. En el primero, la ENV produce una reducción del volumen de infarto, así como una mejora del déficit cognitivo en un modelo de isquemia

transitoria en rata (Ay *et al.* 2009). En el segundo trabajo, la ENV produjo un 50% de reducción en las células apoptóticas, una reducción en la liberación de glutamato y un aumento del flujo sanguíneo cerebral durante la reperfusión, en un modelo de isquemia global en jerbo (Miyamoto *et al.* 2003).

En la línea del empleo de técnicas no invasivas para el tratamiento de este tipo de enfermedades, una reciente publicación sugiere que, la ruta protectora y antiinflamatoria que se produce en la EN, también se puede conseguir mediante electroacupuntura. Así, se ha demostrado el efecto beneficioso de esta práctica en un modelo de isquemia focal en rata y su implicación directa con la activación del receptor α7 nAChR (Wang *et al.* 2012). La ENV podría por tanto convertirse, con el tiempo, en una práctica clínica factible para los pacientes que han sufrido un ictus; de hecho, en la actualidad se emplea en el tratamiento de otras enfermedades como la epilepsia (Vijgen *et al.* 2013, Bergey 2013).

Desde el punto de vista farmacológico, existe también un extenso número de publicaciones, en las que se estudia el efecto de distintos compuestos que interaccionan con los receptores nicotínicos, para reparar el daño producido en la isquemia. El subtipo de receptor, en el cual se han focalizado la mayor parte de estos trabajos, es el receptor nicotínico α7. En este sentido, el modulador alostérico positivo PNU-120596, ha mostrado reducir los volúmenes de infarto y mejorado el déficit cognitivo en ratas sometidas a la oclusión de la arteria cerebral media en rata (Kalappa *et al.* 2013, Sun *et al.* 2013). Por otro lado, los agonistas nicotínicos α7, como el PNU 282987 o el PHA-543613 han mostrado buenos perfiles neuroprotectores y antiinflamatorios, en varios modelos de isquemia hemorrágica (Duris *et al.* 2011, Krafft *et al.* 2011, Krafft *et al.* 2013).

Estas evidencias científicas, ponen de manifiesto la importancia de este subtipo de receptor como diana para conseguir un efecto antiinflmamatorio y neuroprotector en situaciones de compromiso de flujo cerebral De hecho, los ratones nulos para la expresión de receptores α7 nAChR, presentan mayores volúmenes de infarto y un mayor déficit cognitivo respecto a los ratones salvajes cuando se les somete a una isquemia cerebral (Liu *et al.* 2012).

3. Receptores nicotínicos de acetilcolina

3.1. Estructura, composición y función de los nAChR

Los receptores nicotínicos de acetilcolina (nAChR) pertenecen a la superfamilia de canales iónicos regulados por ligando y se localizan, tanto en el sistema nervioso central, como en el sistema periférico. Los nAChR, son glucoproteínas transmembrana de 270-290 KDa que se componen de 5 subunidades insertadas en la membrana lipídica; cada una de estas subunidades, consta de 4 hélices α transmembrana denominadas M1, M2, M3 y M4 (Corbin *et al.* 1998). Hasta la fecha, se conoce la existencia de 9 subunidades α en neuronas (α2-α10) y 3 subunidades β (β2-β4). Estas subunidades pueden encontrarse en su forma homomérica (todas las subunidades iguales) o heteromérica (subunidades distintas). Las neuronas expresan gran diversidad de nAChR que, junto a los receptores de tipo muscarínico, son capaces de elevar la concentración de calcio citosólico ($[Ca^{2+}]_c$) tras su activación con un agonista endógeno, la acetilcolina (ACh). En cuanto a la localización de estas subunidades en las distintas regiones del sistema nervioso central, la siguiente tabla nos muestra un ejemplo de la amplia diversidad de subtipos distintos que podemos encontrar, aunque en el cerebro de los humanos, los subtipos más abundantes son los formados por las subunidades α7, α4β2 y α3β4 (Lindstrom 2003).

	α3	α4	α5	α6	α7	β2	β3	β4
Corteza cerebral								
Frontal		●	●		●	●		
Parietal		●				●		
Occipital								
Temporal	●	●	●	●	●	●	●	●
Insular								
Entorrinal	●	●			●	●		●
Subiculum	●	●			●	●		●
Hipocampo	●	●			●	●		●
Tálamo								
Ganglio Basal								
Caudado	●	●			●	●		
Putamen	●	●	●	●	●	●	●	
Globo pálido								
Tronco del encéfalo								
Cerebro medio		●				●		
Pons								
Medulla oblongata								
Cerebelo	●	●		●	●	●		●

FigXX: Distribución de los distintos subtipos nAChR en el sistema Nerviosos Central (Imagen adaptada (Gotti & Clementi 2004))

En el individuo adulto se ha descrito la implicación de los nAChR en numerosas funciones del sistema nervioso: el aprendizaje y la memoria, la atención, el control de la actividad motora, la percepción sensorial y del dolor o la regulación corporal de la temperatura. Generalmente, estos efectos son debidos a la existencia de receptores nicotínicos que contienen la subunidad α7 en la terminación presináptica, que actúan modulando la secreción de neurotransmisores (Wonnacott 1997). Sin embargo, el papel de estos receptores, a nivel postsináptico, también es muy importante, sobre todo en el control de la transmisión en ganglios periféricos, hipocampo y corteza sensorial (Jones *et al.* 1999).

3.2. Los receptores nicotínicos: dianas terapéuticas para el desarrollo de nuevos fármacos

En los últimos años, se ha postulado la implicación de estos receptores en diversas patologías neurodegenerativas. En cerebros de pacientes con enfermedad de Alzheimer, se ha visto una disminución de la expresión de estos receptores, así como de la cantidad de ACh liberada y, en general, un actividad colinérgica mermada (Bartus *et al.* 1982, Francis *et al.* 1999). Agonistas nicotínicos que remeden la disminución de ACh que se produce en esta enfermedad, han mostrado ser efectivos en estudios preclínicos tanto *in vitro* como *in vivo* (Arias *et al.* 2004, Bitner *et al.* 2010). Estos prometedores resultados han alentado el comienzo de diversos ensayos clínicos (Frolich *et al.* 2011).

Igual que ocurre en la enfermedad de Alzhéimer, la expresión y función de estos receptores también está alterada en otras patologías como la enfermedad de Parkinson o esquizofrenia. La síntesis de fármacos que tengan como diana la activación o modulación de estos receptores, es por tanto objetivo de distintas compañías farmacéuticas, que han visto este mecanismo de acción como una futura estrategia para el tratamiento de enfermedades neurodegenerativas (Posadas *et al.* 2013, Kawamata & Shimohama 2011).

3.3. Rutas intracelulares de señalización activadas por los receptores nicotínicos

Aunque sabemos que la activación de los receptores nicotínicos está implicada en varios modelos de neuroprotección, los mecanismos que suceden a esta activación aún no son totalmente conocidos. La neuroprotección por activación de nAChRs es, en general, dependiente de la entrada de Ca^{2+} (Donnelly-Roberts *et al.* 1996, Dajas-Bailador *et al.* 2000, Ferchmin *et al.* 2003). Sin embargo, cuando se activa selectivamente el subtipo α7 nAChR, la protección obtenida parece ser independiente de la entrada de Ca^{2+} al interior celular (Del Barrio *et al.* 2011b, del Barrio *et al.* 2011a). Esta entrada de calcio, a través de receptores no- α7, es la que desencadena el inicio de la activación de distintas quinasas, con el objetivo de proteger a la célula. Entre estas quinasas, cabe destacar el papel de la proteína quinasa C (PKC), proteína quinasa A (PKA), Ca^{2+}/calmodulina quinasa-II (CAMK-II y fosfoinositol-3-quinasa (PI3K). Otra de las quinasas que se puede activar por receptores nicotínicos, pero de forma independiente a la entrada de calcio, es la proteína jannus quinasa 2 (JAK2). Se ha descubierto, recientemente, que esta proteína se encuentra unida físicamente a la subunidad α7 nAChR (Marrero & Bencherif 2009). Debido a esto, la fosforilación de JAK2, tras la activación de receptores α7 nAChR, se ha postulado como vital en el efecto protector y antiinflamatorio observado con el uso de agonistas α7 nAChR, como: colina, nicotina o PNU282987 (Del Barrio et al. 2011b, Shaw *et al.* 2002, Smedlund *et al.* 2011). Aunque la activación de esta ruta parecía exclusiva del receptor receptores α7 nAChR, algunos autores afirman que también puede darse por activacion de otros subtipos de receptores nicotínicos, como los subtipos α4β2 (Hosur & Loring 2011).

La activación de todas estas proteínas, está relacionada con la supervivencia celular en distintos modelos de toxicidad (Jin *et al.* 2004, Marrero & Bencherif 2009, Egea *et al.* 2007).

4. El factor de transcripción NRf2: el regulador maestro de la respuesta antioxidante

El factor de transcripción Nrf2 (en inglés, nuclear factor-erythroid 2-related factor 2) es uno de los factores de transcripción esenciales, implicados en la regulación del equilibrio redox de la célula (Itoh *et al.* 1997). Este factor de transcripción, se une en el citoplasma,a la proteína Kelch ECH associating protein 1 (Keap1), en condiciones normales. Nrf2 es conducida por Keap1 hacia una degradación por el protosoma (Fig 9). Sin embargo, el estrés oxidativo, electrófilos u otros agentes pueden producir la escisión del complejo Nrf2/Keap1, promoviendo la translocación al núcleo de Nrf2 y facilitando su unión a una secuencia específica del ADN, conocida como ARE (de sus siglas en inglés: "**A**ntioxidant **R**esponse **E**lement"). La respuesta Nrf2-ARE, controla la expresión de enzimas de fase 2 implicadas en citoprotección frente al estrés oxidativo, como hemoxigenasa 1 (HO-1), glutamato cisteína ligasa (GCL) o flavoproteína NADPH:quinona oxidorreductasa 1 (NQO1)

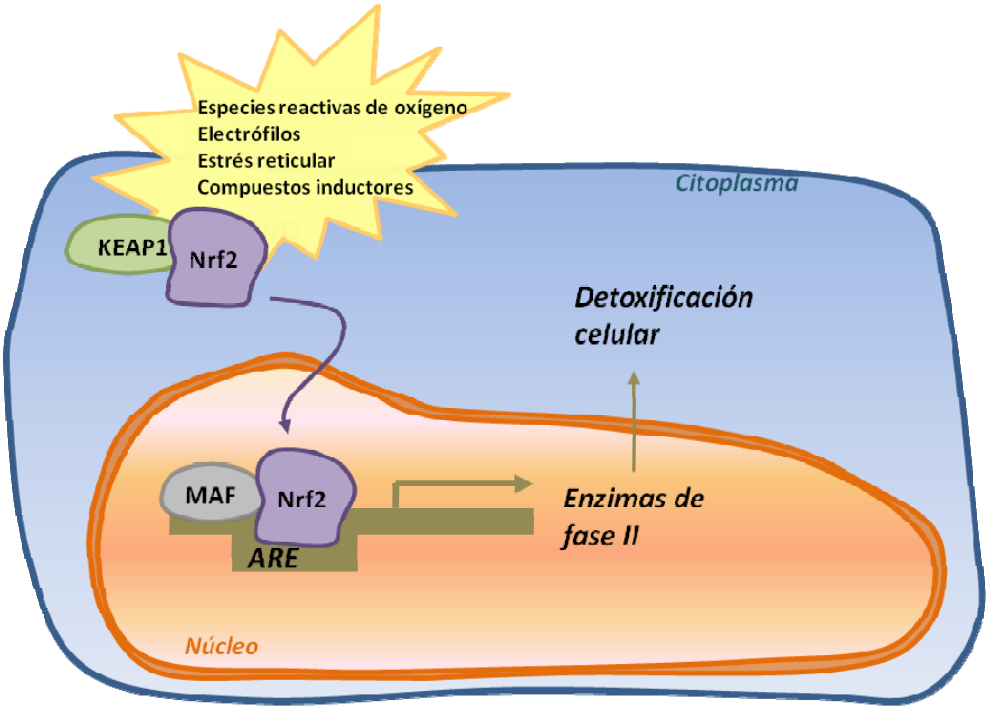

Fig 9: Esquema adaptado (Davinelli *et al.* 2012) que ilustra la activación de la ruta Nrf2-ARE para generar la sobreexpresión de enzimas antioxidantes.

4.1. La hemoxigenasa-1 (HO-1): una proteína con propiedades antioxidantes y antiinflamatorias

Tal como se ha citado anteriormente, la hemoxigenasa 1 (HO-1) es la enzima encargada del catabolismo oxidativo del grupo hemo (Fig 9), generando tres subproductos: biliverdina (convertida a bilirrubina por la NADPH biliverdina reductasa), monóxido de carbono (CO) y hierro (Fe^{2+}). El grupo hemo cumple una función fisiológica esencial, como es la de formar parte de diversas proteínas, como son la hemoglobina, mioglobina y citocromo (Wijayanti *et al.* 2004), sin embargo , es el causante de efectos proinflamatorios y de incrementar el estrés oxidativo, cuando no se encuentra unido a proteínas (Paine *et al.* 2010).

Existen dos isoformas genéticamente diferentes de la HO: la HO-1, que es inducible, y la HO-2, que es constitutiva (Ryter *et al.* 2006). Los niveles de HO-1 son muy bajos en condiciones basales, sin embargo, su expresión se ha visto aumentada rápidamente para proteger a las células frente a distintos agentes tóxicos, como estrés oxidativo (Poss & Tonegawa 1997), isquemia focal (Nimura *et al.* 1996) o glutamato (Parfenova *et al.* 2006).

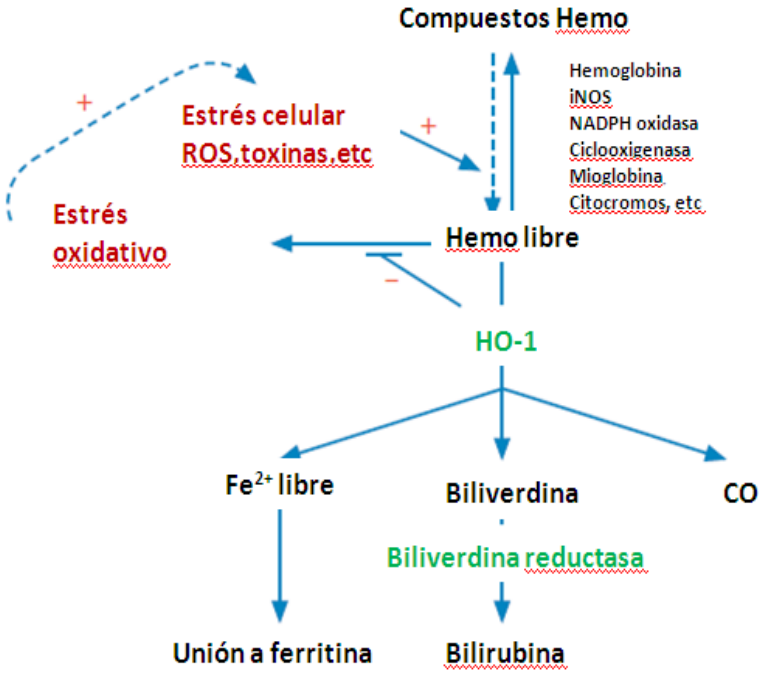

Fig 9: Esquema adaptado (Ferenbach *et al.* 2010) en el que se muestran los productos que surgen de la catabolisis oxidativa del grupo Hemo: Fe^{3+}.

La HO-1 juega un papel importante en el sistema de defensa antioxidante del organismo. Se ha demostrado, que los ratones deficitarios de esta enzima son más susceptibles al estrés oxidativo y a la muerte celular (Yet *et al.* 2003).Tanto la bilirrubina, como la biliverdina, poseen propiedades antioxidantes, y ambas previenen la oxidación de ácidos grasos poliinsaturados, inhiben la degradación de la vitamina E y actúan como secuestradores de varios radicales, como son el peroxilo y anión superóxido (Stocker *et al.* 1987, Ryter & Tyrrell 2000).

El monóxido de carbono (CO), otro subproducto generado tras el catabolismo del grupo hemo, posee propiedades vasodilatadoras, mediante la activación de la vía de guanilato-ciclasa-GMPc (Dong *et al.* 2007, Wilkinson & Kemp 2011). Esta molécula gaseosa tiene la capacidad de difundirse libremente de una célula a otra, e influir así en los mecanismos de transducción de señales intracelulares. Es considerado un mensajero químico muy importante, cuyo mecanismo de actuación recuerda al de un neurotransmisor. Al igual que la proteína HSP (heats shock protein), la capacidad protectora de HO-1 y de sus subproductos, hace que forme parte de los *vitagenes*, genes implicados en la preservación de la homeostasis celular, durante condiciones de estrés (Calabrese *et al.* 2004).

El papel inmunomodulador y antiinflamatorio de HO-1, se puso de manifiesto cuando se describió que la inhibición de esta enzima producía un claro aumento de la inflamación en ratas inyectadas con carragenina (Willis *et al.* 1996). Otro ejemplo de este efecto lo vemos en los estudios realizados en ratones nulos para HO-1 o Nrf2, ya que estos animales desarrollan una inflamación crónica y poseen mayor susceptibilidad a la sepsis inducida por endotoxinas (Poss & Tonegawa 1997, Thimmulappa *et al.* 2006b, Thimmulappa *et al.* 2006a). Aunque el efecto antiinflamatorio de HO-1 está documentado, el mecanismo por el cual ejercen dicha acción aún no está del todo esclarecida. En este sentido, algunos estudios señalan al monóxido de carbono (CO) como el responsable de dicho efecto (Loboda *et al.* 2008, Immenschuh *et al.* 2010, Paine *et a*l. 2010).

Respecto a la implicación especifica del eje NRf2/ARE en el SNC, se ha observado que los ratones nulos para este factor de transcripción expresan mayores niveles cerebrales de marcadores proinflamatorios (TNF, IL6, F480 e iNOS) cuando son expuestos a la endotoxina LPS, en comparación con los animales salvajes (Innamorato *et al.* 2008).

Como hemos visto anteriormente, la microglía es la célula inmunomoduladora por excelencia del SNC. Cada vez son más los estudios que relacionan los efectos antiinflamatorios de diversos compuestos con un aumento en la expresión de HO-1 en microglía. Un ejemplo de esto, lo vemos en los estudios realizados por Lin y colaboradores, donde el licopeno (uno de los carotenoides mas abundante presente en los tomates) recude la expresión de COX2 via HO-1 en la línea microglíal BV2 (Lin *et al.* 2014). El poder antiinflamatorio de compuestos como etilpiruvato, xanthohumol, ácido docosahexaenoico o dimetil fumarato y su implicación directa con un aumento de HO-1 en microglía, son sólo más ejemplos de la importancia de este efecto (Lu *et al.* 2010, Kim *et al.* 2013, Lee *et al.* 2011, Foresti *et al.* 2013).

4.2. Inductores Nrf2/HO-1 como estrategia incipiente para el tratamiento y prevención de enfermedades neurodegenerativas

Algunos de los compuestos más estudiados para regular la expression de Nrf2/HO-1, han sido: sulforafano, curcumina, 3H-1,2-Ditiol-3-Tiona (D3T), terc Butil Hidroquinona (tBHQ) o melatonina. La administración de estos compuestos, ha resultado ser neuroprotectora en modelos de isquemia cerebral, Alzhemier, Parkinson, o traumatismo craneal (Hong *et al.* 2010, Yang *et al.* 2009, Zhao *et al.* 2006, Burton *et al.* 2006, Nouhi *et al.* 2011, Hsu *et al.* 2012).

Estos antecedentes han motivado el comienzo de ensayos clínicos diversos que pretenden poner a prueba el efecto antiinflamatorio y antioxidante de estas moléculas, como posible tratamiento frente a distintas enfermedades neurodegenerativas. La curcumina por ejemplo, tiene un amplio rango de actividades farmacológicas, incluyendo las antinflamatorias, antimicrobianas, antioxidantes y antitumorales. Los ensayos clínicos en estudio engloban enfermedades como cáncer de colon, cáncer pancreático, psoriasis, Alzheimer o epilepsia (Hatcher *et al.* 2008, Maheshwari *et al.* 2006).

Otro compuesto inductor de la ruta activada por Nrf2 es el dimetil fumarato. Ha mostrado tener propiedades antiapoptoticas, cardioprotectoras y antiinflamatorias, por todo ello ha suscitado el interés de la comunidad científica para el tratamiento de la enfermedad de esclerosis multiple (Phillips & Fox 2013, Stangel & Linker 2013). Cada vez más se realizan estudios con éxito en los cuales esta molécula se ensaya frente a otras patologías como la infección por el virus de la inmunodeficiencia humana (VIH) o la cardiopatía isquémica (Gill & Kolson 2013, Ashrafian *et al.* 2012).

En base a las evidencias anteriormente citadas, la modulación de Nrf2 y HO-1 se postula como una buena estrategia farmacológica potencialmente interesante para el tratamiento y prevención de enfermedades neurodegenerativas y envejecimiento celular (Zhang *et al.* 2013).

Free Radical Biology & Medicine 49 (2010) 1815–1821

Contents lists available at ScienceDirect

Free Radical Biology & Medicine

journal homepage: www.elsevier.com/locate/freeradbiomed

Original Contribution

Poststress treatment with PNU282987 can rescue SH-SY5Y cells undergoing apoptosis via α7 nicotinic receptors linked to a Jak2/Akt/HO-1 signaling pathway

Esther Parada [a,b,1], Javier Egea [a,b,d,1], Alejandro Romero [a,b,d], Laura del Barrio [a,b], Antonio G. García [a,b,c], Manuela G. López [a,b,d,*]

[a] Instituto Teófilo Hernando, Facultad de Medicina, Universidad Autónoma de Madrid, 4-28029 Madrid, Spain
[b] Departamento de Farmacología y Terapéutica, Facultad de Medicina, Universidad Autónoma de Madrid, 4-28029 Madrid, Spain
[c] Servicio de Farmacología Clínica, Hospital Universitario de la Princesa, Madrid, Spain
[d] Instituto de Investigación Sanitaria del Hospital Universitario La Paz (IdiPAZ), Madrid, Spain

RESUMEN

La mayoría de los estudios de neuroprotección mediada por agonistas nicotínicos, han demostrado ser eficaces cuando se administran antes del estímulo tóxico. En este trabajo hemos investigado si el agonista del receptor nicotínico α7 (nAChR) PNU282987 puede prevenir la muerte celular una vez que las células ya han sido sometidas a un estímulo oxidativo. La combinación de rotenona (30 µM) más oligomicina A (10 µM) (Rot / oligo) se ha usado como un modelo *in vitro* de producción de ROS mitocondrial . Las células de neuroblastoma humano SH-SY5Y fueron incubadas con rot / oligo durante 8 horas y se dejaron durante otras 16 h en MEM/F-12. Bajo estas condiciones experimentales, se produjo una muerte celular por apoptosis del 30%. El PNU282987, administrado después del estímulo anteriormente citado (PST / PNU) redujo esta muerte celular de una manera concentración-dependiente. La co-incubación del PNU282987 con 100 nM metillicaconitina (un antagonista selectivo de α7 nAChR) , 10 M mecamilamina (un antagonista no selectivo de receptores nAChR) , 3 µM LY294002 (un inhibidor de PI3K) , o 10 µM AG490 (un inhibidor de JAK2) revistó la protección conferida por PST / PNU . Por otra parte, el aumento de ROS, caspasa - 3 activa, y la apoptosis causada por la rot/oligo, también se vio reducida por PST / PNU. Además, PNU282987 aumentó la expresión de hemo oxigenasa - 1 (HO - 1) , una enzima de defensa celular contra el estrés oxidativo ; este aumento fue revertido por AG490 o LY294002 . El inhibidor de la actividad de HO-1 (Sn (IV) protoporfirina –IX) también revirtio la protección celular de PST / PNU . Estos resultados sugieren que la activación del receptor α7 nAChR está vinculada a la cascada de señalización Jak2/PI3K/Akt para inducir la enzima antioxidante HO - 1 y conferir neuroprotección .

Contents lists available at ScienceDirect

Free Radical Biology & Medicine

journal homepage: www.elsevier.com/locate/freeradbiomed

Original Contribution

Poststress treatment with PNU282987 can rescue SH-SY5Y cells undergoing apoptosis via α7 nicotinic receptors linked to a Jak2/Akt/HO-1 signaling pathway

Esther Parada [a,b,1], Javier Egea [a,b,d,1], Alejandro Romero [a,b,d], Laura del Barrio [a,b], Antonio G. García [a,b,c], Manuela G. López [a,b,d,*]

[a] Instituto Teófilo Hernando, Facultad de Medicina, Universidad Autónoma de Madrid, 4-28029 Madrid, Spain
[b] Departamento de Farmacología y Terapéutica, Facultad de Medicina, Universidad Autónoma de Madrid, 4-28029 Madrid, Spain
[c] Servicio de Farmacología Clínica, Hospital Universitario de la Princesa, Madrid, Spain
[d] Instituto de Investigación Sanitaria del Hospital Universitario La Paz (IdiPAZ), Madrid, Spain

a r t i c l e i n f o

Article history:
Received 29 June 2010
Revised 1 September 2010
Accepted 20 September 2010
Available online 27 September 2010

Keywords:
Neuroprotection
PNU282987
Heme oxygenase-1
Nicotinic receptors
Free radicals

a b s t r a c t

Most neuroprotection studies with nicotinic agonists have shown efficacy when given before the stressor. Here we have investigated whether the α7 nicotinic acetylcholine receptor (nAChR) agonist PNU282987 can prevent cell death once the cells have already undergone an oxidative stress. The combination of rotenone (30 μM) plus oligomycin A (10 μM) (rot/oligo) has been used as an in vitro model of mitochondrial ROS production. SH-SY5Y cells incubated with rot/oligo for 8 h and left for another 16 h in MEM/F-12 experienced 30% apoptotic cell death. Under these experimental conditions, PNU282987 administered after rot/oligo (PST/PNU) prevented cell death in a concentration-dependent manner. Co-incubation of PNU282987 with 100 nM methyllycaconitine (a selective α7 nAChR antagonist), 10 μM mecamylamine (a nonselective nAChR antagonist), 3 μM LY294002 (a PI3K inhibitor), or 10 μM AG490 (a Jak2 inhibitor) prevented the protection afforded by PST/PNU. Moreover, the increase in ROS, active caspase-3, and apoptosis caused by rot/oligo was also prevented by PST/PNU. Furthermore, PNU282987 increased the expression of heme oxygenase-1 (HO-1), a critical cell defense enzyme against oxidative stress; this increase was prevented by AG490 or LY294002. The HO-1 inhibitor Sn(IV) protoporphyrin-IX also inhibited the PST/PNU protecting effects. These results suggest that activation of α7 nAChR linked to the Jak2/PI3K/Akt cascade induces the antioxidant enzyme HO-1 to provide neuroprotection.

Excessive production of reactive oxygen species (ROS) produces an imbalance in the redox system of cells. They can potentially damage various types of macromolecules, including proteins, lipids, and nucleic acids [1], a phenomenon collectively referred to as oxidative stress. Oxidative stress leads to apoptotic or necrotic cell death in distinct cytotoxic models such as glutamate- [2] or hydrogen peroxide-induced cytotoxicity [3]; it has also been implicated in neurodegenerative diseases [4] and in acute and chronic inflammation [5]. The major sources of mitochondrial ROS are complexes I and III of the electron transport chain. Blockade of these complexes produces an increment of ROS that causes cell death [6,7].

Heme oxygenase-1 (HO-1) provides an inducible defense mechanism that confers protection in cells and tissues in response to noxious stimuli, such as oxidative stress [8], hydrogen peroxide [3], focal ischemia [9], and glutamate [2]. HO-1 serves a vital metabolic function as the rate-limiting step in the oxidative catabolism of the heme group to generate carbon monoxide (CO), biliverdin (BV), and ferrous iron; the BV generated is subsequently converted to bilirubin by NADPH biliverdin reductase. These three by-products have been related to cell protection in distinct cellular models [3,10]. The fact that HO-1 has an essential role in stress adaptation is corroborated in humans, in that a child diagnosed with HO-1 deficiency exhibited anemia, endothelial cell damage, tissue iron deposition, and increased inflammatory indices [11]. HO-1 induction can be mediated by the phosphoinositide (PI)-3K/Akt pathway [12]; however, little is known about the possible involvement of α7 nicotinic acetylcholine receptors (nAChRs) in HO-1 overexpression.

Neuronal nAChRs are a family of ligand-gated ion channels and are members of the Cys-loop receptor superfamily [13]. In the mammalian brain, the α4β2 and α7 subtypes are the most abundant nAChRs [14]. Both nAChRs participate in cognitive processes, such as learning and memory; in the modulation of neurotransmitter release; and in neuroprotection. Particularly interesting is the observation that α7 nAChR activation protects against a wide variety of cytotoxic stimuli,

Abbreviations: PST/PNU, poststress (rotenone + oligomycin A) treatment with PNU282987; rot/oligo, rotenone + oligomycin A; ROS, reactive oxygen species; nAChR, nicotinic acetylcholine receptor; HO-1, NADPH oxidase; HO-1, heme oxygenase-1.

* Corresponding author. Instituto Teófilo Hernando, Facultad de Medicina, Universidad Autónoma de Madrid, 4-28029 Madrid, Spain. Fax: +34 914975380.
E-mail address: manuela.garcia@uam.es (M.G. López).

[1] These authors contributed equally to this work.

0891-5849/$ - see front matter © 2010 Elsevier Inc. All rights reserved.
doi:10.1016/j.freeradbiomed.2010.09.017

such as glutamate [15], amyloid-β [16,17], oxygen and glucose deprivation [18], and kainic acid [19]. In these studies, the experimental protocols included a period of preexposure of the cells to the nAChR agonist followed by a second incubation period in which cells were exposed to the same nAChR agonist together with the stressor. This is far from the clinical situation in which treatment of a patient suffering a cerebrovascular disease commences several hours after such accident; at this stage, neuronal damage caused by excessive free radical production after an ischemic–reperfusion insult has already initialized.

In this study we explored two questions: (i) whether there was a time window for α7 nAChR-mediated neuroprotection after cell exposure to an oxidative stress and (ii) if neuroprotection exerted by α7 nAChR stimulation was linked to HO-1. We used the selective α7 nAChR agonist PNU282987 [20] to test whether its addition to SH-SY5Y cells that were previously challenged with an oxidative stress could afford neuroprotection by modifying the expression of HO-1. We selected as cytotoxic stimulus a model of ROS production [21], the combination of rotenone plus oligomycin A (rot/oligo), which inhibits mitochondrial respiration complexes I and V, respectively [21,22]. We have found that poststress treatment with PNU282987 afforded protection through activation of the α7 nAChR/Jak2/Akt axis, which results in overexpression of the potent antioxidant enzyme HO-1; this enzyme induction leads to a reduction of oxidative stress and apoptotic cell death. To our knowledge, this is the first study involving HO-1 in the neuroprotectant actions of α7 nAChR agonists; this study has the added value of showing that this protection occurred when cells were already exposed to oxidative stress, suggesting the existence of a "therapeutic window of opportunity" that could potentially have clinical interest in the context of offering pharmacological neuroprotection after a brain ischemic episode.

Materials and methods

Materials

F-12 nutrient mixture, Eagle's minimum essential medium (MEM), rotenone, oligomycin A, mecamylamine, methyllycaconitine, and MTT (3-(4,5-dimethylthiazol-2-yl)-2,5-diphenyltetrazolium bromide) were obtained from Sigma (Madrid, Spain). Chelerythrine, 2-(2-amino-3-methoxyphenyl)-4H-1-benzopyran-4-one (PD98059), and LY294002 were purchased from Tocris (Biogen Científica, Madrid, Spain). Sn(IV) protoporphyrin-IX dichloride (SnPP) and Co(III) protoporphyrin-IX dichloride (CoPP) were obtained from Frontier Scientific Europe (Lancashire, UK). 2′,7′-Dichlorofluorescein diacetate (H_2DCFDA) was purchased from Molecular Probes (Invitrogen, Madrid, Spain). Penicillin, pyruvate, and 5% heat-inactivated fetal bovine serum (FBS) were purchase from Invitrogen.

Culture of SH-SY5Y cells

SH-SY5Y cells were maintained in a 1:1 mixture of F-12 nutrient mixture (Ham 12) and Eagle's MEM supplemented with 15 nonessential amino acids, 1 mM sodium pyruvate, 10% heat-inactivated FBS, 100 units/ml penicillin, and 100 μg/ml streptomycin. Cultures were seeded into flasks containing supplemented medium and kept at 37 °C in a humidified atmosphere of 5% CO_2 and 95% air. For assays, SH-SY5Y cells were subcultured in 48-well plates at a seeding density of 1×10^5 cells per well. Cells were treated with the drugs before confluence in MEM/F-12 with 1% FBS. Cells were used at a passages below 13.

Quantification of viability by MTT in SH-SY5Y cells

Cell viability, virtually the mitochondrial activity of living cells, was measured by quantitative colorimetric assay with MTT, as described previously [23]. Briefly, 50 μl of the MTT labeling reagent, at a final concentration of 0.5 mg/ml, was added to the MEM/F-12 of each well at the end of the rot/oligo period and the plate was placed in a humidified incubator at 37 °C with 5% CO_2 and 95% air (v/v) for an additional 2 h. Then the insoluble formazan was dissolved with dimethyl sulfoxide; colorimetric determination of MTT reduction was measured at 540 nm. Control cells treated with vehicle (MEM/F-12) were taken as 100% viable.

Measurement of apoptosis and necrosis with annexin V–phycoerythrin (PE)/7-amino-actinomycin-D (7-AAD) double staining

Apoptosis was determined by flow cytometry using an annexin V-PE and 7-AAD double staining kit (BD Bioscience, Madrid, Spain) according to the manufacturer's instructions. Briefly, cells were collected by centrifugation and resuspended in 100 μl of 1× binding buffer with 5 μl annexin V-PE and 5 μl 7-AAD. After incubation at room temperature for 15 min in the dark, 400 μl of 1× binding buffer was added. Cells were then subjected to FACS analysis (Beckman Coulter, Madrid, Spain). At least 20,000 events per assay well were included and represented as dot plots. Annexin$^+$/7-AAD$^-$ cells were considered early apoptotic cells, annexin$^+$/7-AAD$^+$ late apoptotic cells, and annexin$^-$/7-AAD$^-$ viable cells.

ROS measurement

To measure cellular ROS, we used the molecular probe H_2DCFDA [24]. SH-SY5Y cells were loaded with 10 μM H_2DCFDA, which diffuses through the cell membrane and is hydrolyzed by intracellular esterases to the nonfluorescent form dichlorofluorescein (DCFH). DCFH reacts with intracellular H_2O_2 to form dichlorofluorescin, a green-fluorescent dye. Fluorescence was measured in a fluorescence microplate reader (FLUOstar Galaxy; BMG Labtech, Offenburg, Germany). Wavelengths of excitation and emission were 485 and 520 nm, respectively.

Immunoblotting and image analysis

After the various treatments, SH-SY5Y cells (5×10^6) were washed once with cold phosphate-buffered saline and lysed in 100 μl ice-cold lysis buffer (1% Nonidet P-40, 10% glycerol, 137 mM NaCl, 20 mM Tris-HCl, pH 7.5, 1 μg/ml leupeptin, 1 mM phenylmethylsulfonyl fluoride, 20 mM NaF, 1 mM sodium pyrophosphate, and 1 mM Na_3VO_4). Protein (30 μg) from this cell lysate was resolved by SDS-PAGE and transferred to Immobilon-P membranes (Millipore Corp., Billerica, MA, USA). Membranes were incubated with anti-Akt (1:1000), anti-phospho-Akt (1:1000; Santa Cruz Biotechnology, Santa Cruz, CA, USA), anti-HO-1 (1:1000; Chemicon, Temecula, CA, USA), anti-cleaved caspase-3 (1:1000; Cell Signaling Technology, Danvers, MA, USA), or anti-β-actin (1:100,000; Sigma). Appropriate peroxidase-conjugated secondary antibodies (1:10,000) were used to detect proteins by enhanced chemiluminescence. Different band intensities corresponding to immunoblot detection of protein samples were quantified using the Scion Image program. Immunoblots correspond to a representative experiment that was repeated three or four times with similar results.

Statistics

Data are given as means ± SEM. Differences between groups were determined by applying a one-way ANOVA followed by a Newman-Keuls test or Student t test when appropriate. Differences were considered statistically significant when $p < 0.05$.

Results

Apoptotic cell death induced by rot/oligo

We first established the experimental conditions that were most appropriate to induce apoptotic cell death with the combination of 30 μM rotenone plus 10 μM oligomycin A (rot/oligo). For this purpose, cells were incubated for various time periods (1, 2, 4, 8, and 24 h) with rot/oligo; at the end of each period, we replaced rot/oligo with basal medium and the cells remained in this medium for the remaining time to complete 24 h, i.e., 23, 22, 20, 16, and 0 h, respectively (Fig. 1A). Finally, we analyzed cell death by flow cytometry. Fig. 1B shows that apoptotic cell death increased with the time of incubation with rot/oligo. Moreover, necrotic cell death was augmented significantly only after 24 h incubation with rot/oligo. Basal apoptotic cell death amounted to 8.4 ± 1.7%; 8 h treatment with rot/oligo followed by 16 h with basal medium significantly augmented apoptosis to 25.5 ± 2.1%. We selected this time of incubation of rot/oligo because it produced the maximum increase in apoptosis without augmenting necrosis.

Antiapoptotic effect of PNU282987 added after rot/oligo to SH-SY5Y cells

Nicotinic agonists are widely used to afford neuroprotection against various cytotoxic stimuli (see the introduction). Most of these studies involved preincubation with the agonists. Hence, we tried to afford protection by adding the α7 nAChR agonist once the 8-h period of rot/oligo ended (Fig. 2A).

As Fig. 2B shows, 8 h incubation with rot/oligo followed by 16 h with medium reduced cell viability by 40%, measured as reduction of MTT. However, PNU282987 (1, 3, and 10 μM) incubated for 16 h after the 8-h rot/oligo period produced a concentration-dependent protective effect; the maximum protective effect was achieved with 10 μM PNU282987 (50% neuroprotection; Fig. 2B). This poststress treatment with PNU282987 will be referred to from here on as PST/PNU. Interestingly, PNU282987 co-incubated with or administered after the toxic stimulus afforded the same protection (Fig. 2C). Considering this result, we decided to continue the work using the PST/PNU protocol with 10 μM PNU282987.

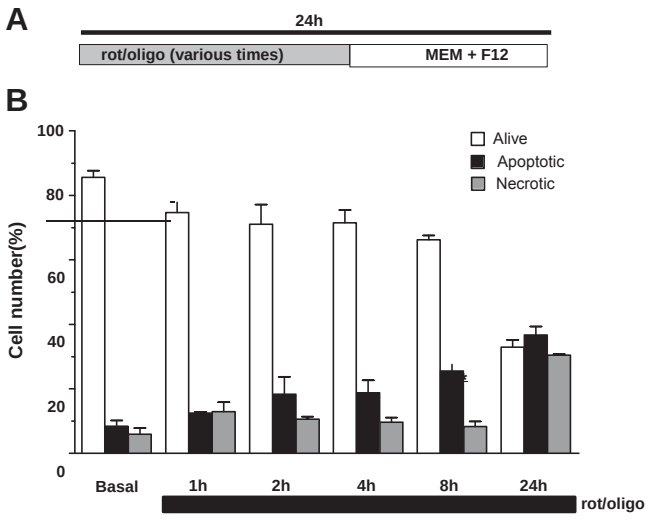

Fig. 1. Time course of rot/oligo-induced apoptosis. (A) Protocol used to elicit cell death with 30 μM rotenone plus 10 μM oligomycin for various times (1, 2, 4, 8, and 24 h) followed by cell incubation with MEM/F-12 to complete a 24-h period (23, 22, 20, 16, and 0 h). (B) The percentage of alive, apoptotic, and necrotic cells exposed for various times to rot/oligo was measured by flow cytometry (see Materials and methods). Data are means ± SEM of four different cell batches; ***p < 0.001, significantly different from basal apoptotic cell death.

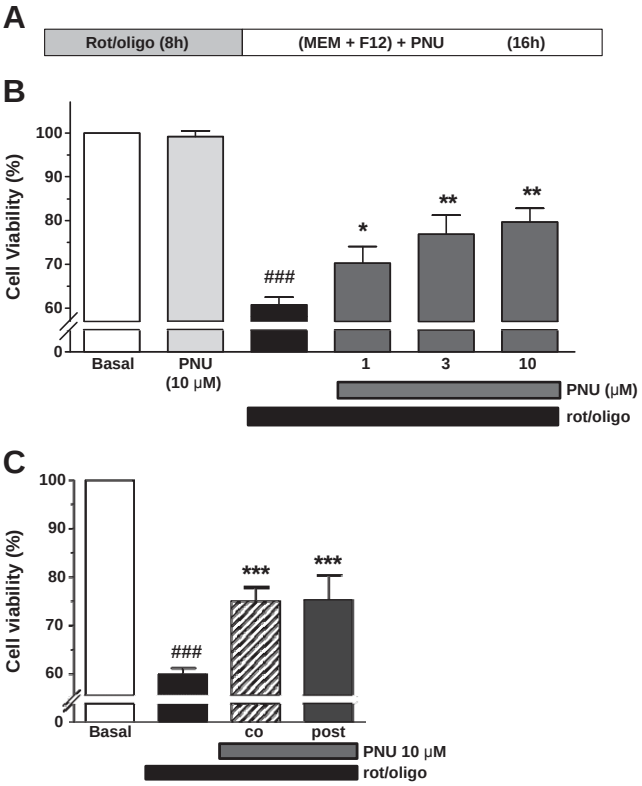

Fig. 2. Added after the period of rot/oligo exposure, PNU282987 afforded protection in a concentration-dependent manner. (A) Protocol used to elicit toxicity (8 h incubation with rot/oligo) and protection (16 h of PNU282987 treatment). (B) Concentration–response curve of PNU282987 incubated for 16 h, after the 8-h rot/oligo period. (C) The cytoprotective effect afforded by PNU282987 co-incubated with rot/oligo or administered post-rot/oligo. Values are expressed as means ± SEM of seven different cell batches; ###p < 0.001 compared to basal; ***p < 0.001, **p < 0.01, and *p < 0.05 with respect to rot/oligo-treated cells.

Next we sought to corroborate these data by measuring apoptosis by flow cytometry. Basal apoptosis (measured as annexin V-positive cells) amounted to 8.2 ± 0.9% (Figs. 3A and D), and cell treatment for 8 h with rot/oligo followed by 16 h basal medium increased apoptosis to 30.3 ± 2.7% (Figs. 3B and D). However, PST/PNU treatment produced a significant reduction in annexin V-positive cells (24.7 ± 1.5%; p b 0.05) (Figs. 3C and D). Next we decided to corroborate the antiapoptotic effect afforded by PST/PNU by measuring active caspase-3 by Western blot. Fig. 3E shows that rot/oligo produced a threefold increase in caspase-3 activation, compared to control cells. Again, PST/PNU significantly reduced the amount of active caspase-3 produced by rot/oligo alone ($p < 0.05$). These results suggest that poststress cell treatment with PNU282987 was capable of rescuing SH-SY5Y cells from apoptotic death by decreasing active caspase-3.

The antiapoptotic effect of PST/PNU is mediated by α7 nAChRs

Although it is accepted that PNU282987 behaves as a selective α7 nAChR agonist, we wanted to prove that to afford protection, PNU282987 was definitely acting on such receptor. Thus, the PST/PNU protocol was performed in the absence or the presence of 10 μM mecamylamine, a nonselective nAChR antagonist, or 100 nM methyllycaconitine (MLA), a selective α7 nAChR antagonist (Fig. 4). Treatment for 8 h with rot/oligo followed by 16 h in MEM/F-12 reduced cell viability to 61.4 ± 2.6%; once again, PST/PNU treatment afforded 50% neuroprotection. However, the protective effect afforded by PST/PNU was significantly reduced by MLA and by mecamylamine, suggesting that the protective signal was indeed being initiated by α7 nAChR activation.

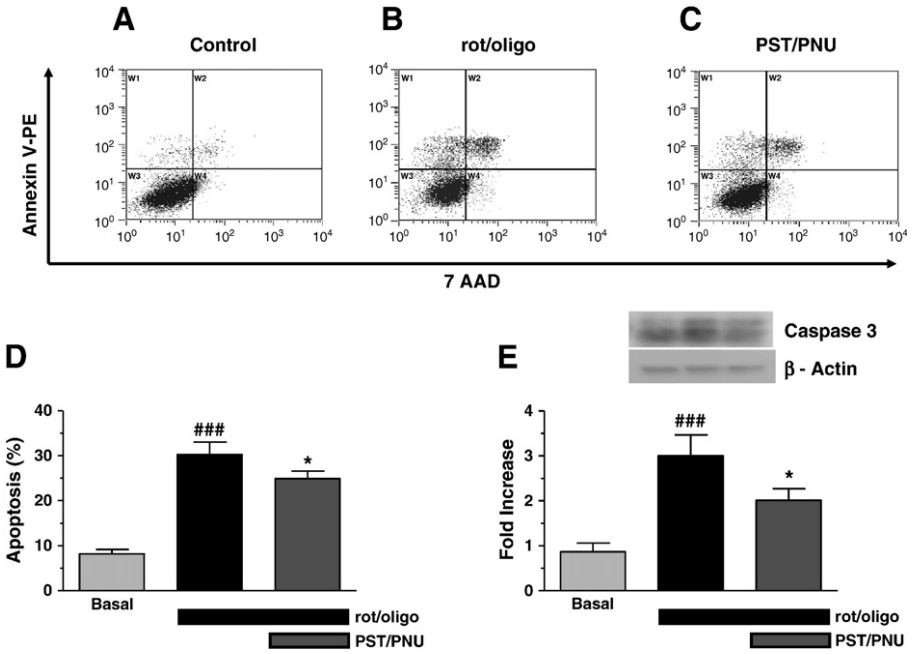

Fig. 3. PST/PNU reduced apoptosis and caspase-3 activation. Representative scatter diagrams of (A) control cells, (B) cells exposed to rot/oligo for 8 h, and (C) cells treated with 10 μM PNU282987 for 16 h post-rot/oligo. Cells were collected by centrifugation and stained with annexin V-PE/7-AAD and analyzed by FACS. (D) Averaged data of the apoptotic population (annexin$^+$/7-AAD$^-$ and annexin$^+$/7-AAD$^+$) for each variable; data correspond to the means and SEM of five experiments from different cell cultures. (E) The top shows a representative immunoblot of cleaved caspase-3 from untreated cells (track 1), cells incubated for 8 h with rot/oligo (track 2), and cells incubated for 16 h with 10 μM PNU282987 poststressor (track 3). Densitometric quantitation of cleaved caspase-3 protein levels using β-actin for normalization is shown in the bar graph. Data are means ± SEM of at least five different cell batches. $^{###}p < 0.001$, significantly different from untreated cells; $^{*}p < 0.05$ with respect to rot/oligo.

PST/PNU reduced the production of ROS generated by rot/oligo

Oxidative stress is a mechanism that can drive cells to enter into apoptosis through excessive production of ROS. Therefore, ROS production was measured with the fluorescent probe H_2DCFDA using the protocol previously shown in Fig. 2A. Treatment with rot/oligo for 8 h followed by 16 h in MEM/F-12 (Fig. 5B) doubled the amount of ROS produced in SH-SY5Y compared to basal cells (Fig. 5A). PST/PNU reduced ROS production to control levels (Figs. 5C and D).

Effects of PST/PNU on the activation of the Jak2/Akt pathway

α7 nAChRs can activate various signaling pathways related to neuroprotection, such as Jak2, Akt, or Erk1/2 [17,21]. To explore the intracellular pathways involved in the protective effect of PST/PNU, we used AG490 (10 μM, a Jak2 blocker) [3], chelerythrine (1 μM, a protein kinase C blocker) [25], LY294002 (3 μM, a PI3K blocker) [26], and PD98059 (5 μM, a MEK1/2 blocker) [27]. Hence, as Fig. 6A shows, neither chelerythrine nor PD98059 significantly affected the protective effect afforded by the PST/PNU. In contrast, AG490 and LY294002 prevented the protective effect afforded by PST/PNU, suggesting that Jak2 and Akt were participating in the protective effect of α7 nAChR activation.

It was therefore relevant to corroborate by Western blot that PNU282987 was indeed activating Jak2 and Akt. Fig. 6B shows a

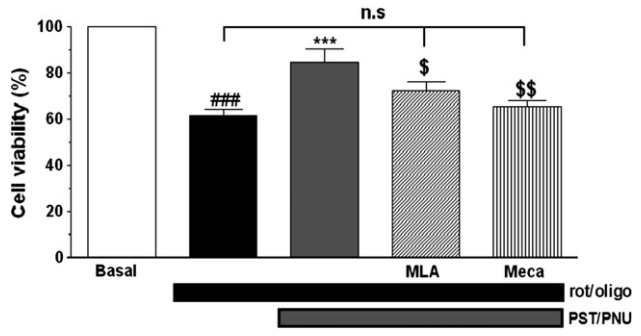

Fig. 4. Neuroprotection afforded by PST/PNU is mediated by α7 nAChR. Cells were incubated for 8 h with rot/oligo followed by 10 μM PNU282987 for 16 h (PST/PNU) with or without 10 μM mecamylamine (meca) or 0.1 μM methyllycaconitine (MLA). Cell viability was measured using the MTT assay. Data are means ± SEM of nine different cell batches. $^{###}p < 0.001$, significantly different from untreated cells, $^{***}p < 0.001$ with respect to rot/oligo; $^{\$\$}p < 0.01$, $^{\$}p < 0.05$, significantly different from PST/PNU-treated cells.

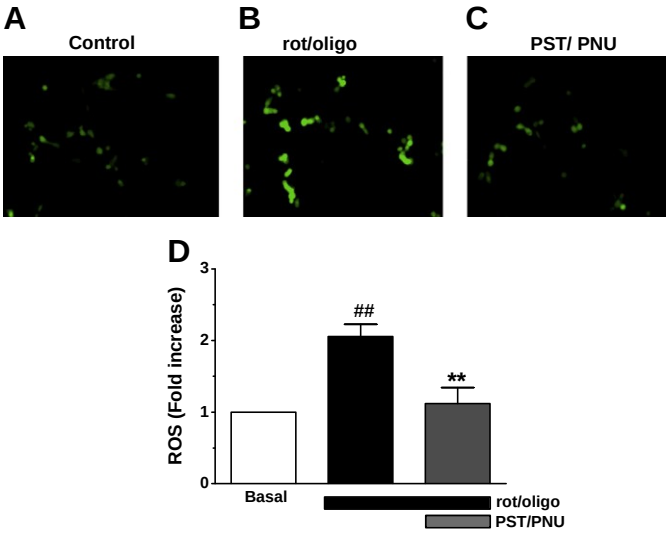

Fig. 5. Effect of PST/PNU on rot/oligo-induced cellular ROS production. Photomicrographs (original magnification 20×) of cells loaded with the fluorescent probe H_2DCFDA are shown. (A) Untreated cells; (B) cells exposed to rot/oligo for 8 h followed by 16 h with MEM/F-12, and (C) cells treated for 16 h with PNU282987 after the rot/oligo period (PST/PNU). (D) Statistics of the effect of PST/PNU on ROS production elicited by rot/oligo treatment. Values are expressed as means ± SEM of five different cell batches; $^{##}p < 0.01$ compared to basal; $^{**}p < 0.01$ with respect to rot/oligo.

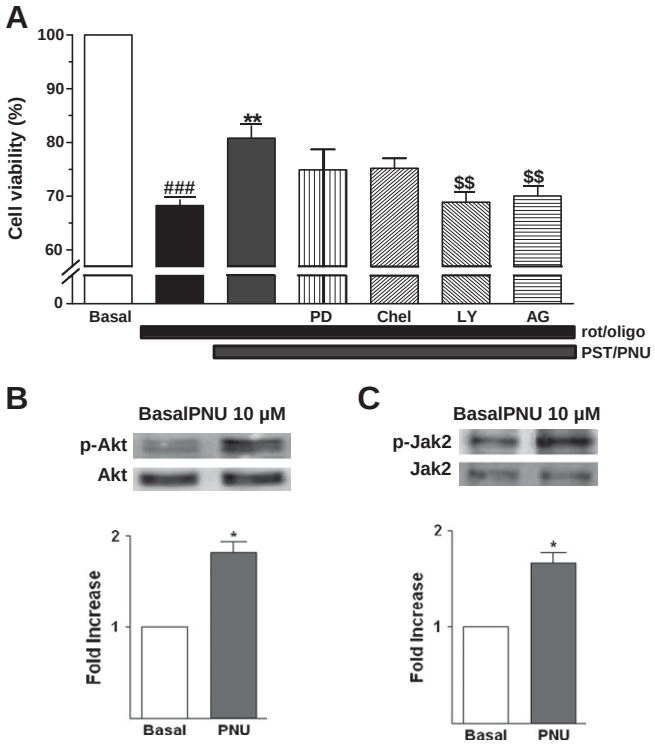

Fig. 6. PST/PNU neuroprotection was mediated by Jak2 and AKT activation. Cells were incubated for 8 h with rot/oligo followed by 16 h treatment with 10 µM PNU282987 (PST/PNU) in the absence or the presence of 5 µM PD98059, 1 µM chelerythrine, 3 µM LY294002, or 10 µM AG490. (A) Averaged data of eight experiments from different cell cultures in which cell viability was measured with the MTT assay. Data are means ± SEM. $^{\#\#\#}p < 0.001$, significantly different from untreated cells; $^{**}p < 0.01$ with respect to rot/oligo; $^{\$\$}p < 0.01$, significantly different from PNU282987-treated cells. Representative immunoblots of (B) Akt and (C) Jak2 phosphorylation. Cells were incubated for 15 min with MEM/F-12 (basal) or 10 µM PNU282987. Histograms represent mean increases (±SEM) in Akt (B, bottom) and Jak2 (C, bottom). $^{*}p < 0.05$ with respect to basal.

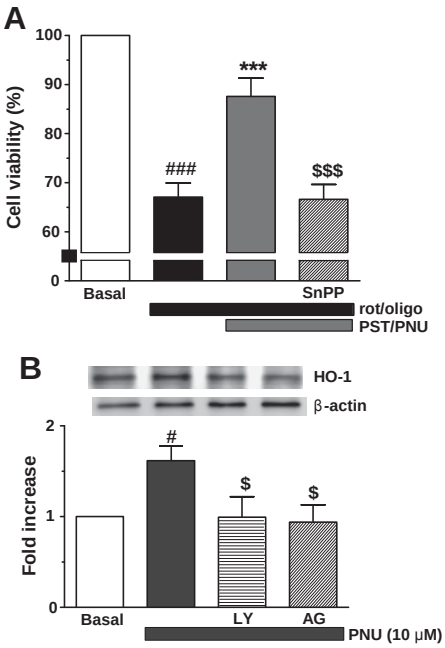

Fig. 7. Neuroprotection elicited by PST/PNU is associated with HO-1 induction by PNU282987. (A) The protective effect of PST/PNU and its reversal by SnPP. Cells were exposed to rot/oligo for 8 h followed by 16 h with 10 µM PNU282987 (PST/PNU) in the absence or the presence of 3 µM SnPP. (B) A representative immunoblot of HO-1 induction by PNU282987 in the absence or presence of 3 µM LY294002 or 10 µM AG490. The histogram presents the densitometric quantification of HO-1 induction using β-actin for normalization. Values are means ± SEM of six experiments. $^{\#\#\#}p < 0.001$, $^{\#}p < 0.05$, significantly different from untreated cells; $^{***}p < 0.001$ in comparison with rot/oligo; $^{\$\$}p < 0.001$, $^{\$}p < 0.05$ with respect to PNU282987-treated cells.

Western blot of phospho-Akt and total Akt. In control cells, Akt phosphorylation was quite low; however, incubation with 10 µM PNU282987 for 15 min induced a significant increase in Akt phosphorylation (1.8-fold above basal). Fig. 6C shows a representative Western blot of phospho-Jak2 and total Jak2. As in the case of Akt, basal phosphorylation of Jak2 was low. Incubation with 10 µM PNU282987 for 15 min induced a significant phosphorylation of Jak2 (1.6-fold above basal). Taken together, these data support the involvement of Jak2 and Akt in the protective effect of α7 nAChR activation.

The protective effect of PST/PNU is mediated by HO-1 induction

According to the protocol shown in Fig. 2A, SH-SY5Y cells were incubated with rot/oligo for 8 h followed by PST/PNU, in the absence or presence of SnPP (3 µM, an inhibitor of HO-1 activity). Interestingly, SnPP prevented the neuroprotective effect afforded by PST/PNU, by reducing cell viability to almost the level of control cells (Fig. 7A). The possibility that PST/PNU was affording protection by inducing HO-1 was tested in the following experiment. Cells were incubated for 16 h with vehicle or 10 µM PNU282987 and cell lysates were resolved by SDS-PAGE and analyzed by immunoblot with anti-HO-1 antibody (Fig. 7B). PNU282987 significantly increased by 1.6-fold the amount of HO-1 expression compared with control cells. To further analyze the roles of Jak2 and Akt in the up-regulation of HO-1, we inhibited the PI3K/Akt pathway with the PI3K inhibitor LY294002 and Jak2 with AG490. As shown in Fig. 7B, both LY294002 and AG490 inhibited the induction of HO-1 produced by PNU282987. These data support the involvement of HO-1 in the protective effect afforded by α7 nAChR.

CoPP protects SH-SY5Y cells by inducing HO-1 against rot/oligo

Another means of inducing HO-1 is incubating the cells with CoPP. We therefore used this compound to corroborate that HO-1 induction leads to protection against rot/oligo. Poststress treatment with CoPP (0.1, 0.3, 1, and 3 µM) for 16 h after the 8-h rot/oligo treatment protected against cell death in a concentration-dependent manner (Fig. 8A); cell viability was augmented to 70% at the concentration of 1 µM. To see if this maximal protective concentration was inducing HO-1, cells were incubated for 16 h with vehicle or 1 µM CoPP. CoPP produced a significant induction of HO-1 expression compared to control cells (Fig. 8B). To corroborate the participation of HO-1 in the protective effect of CoPP, SH-SY5Y cells were incubated for 8 h with rot/oligo followed by 1 µM CoPP with or without 3 µM SnPP, a HO-1 inhibitor. As shown in Fig. 8C, SnPP inhibited the neuroprotective effect of 1 µM CoPP, which indicates that HO-1 was necessary for the protection exerted by CoPP.

Discussion

Central to this study is the finding that the selective α7 nAChR agonist PNU282987 can protect SH-SY5Y cells against apoptotic cell death, even if added after an 8-h stress period based on the production of excessive ROS by rot/oligo. The features of such protection are as follows: (i) it takes place regardless of whether PNU282987 was co-incubated with rot/oligo or added immediately after the 8-h period of cell incubation with rot/oligo and left for an additional 16-h period in the absence of the stressor (so-called poststress treatment) (Fig. 2C); (ii) it is linked to the α7 subtype of nAChR because MLA, a selective high-affinity antagonist of such receptors [28], mitigated the

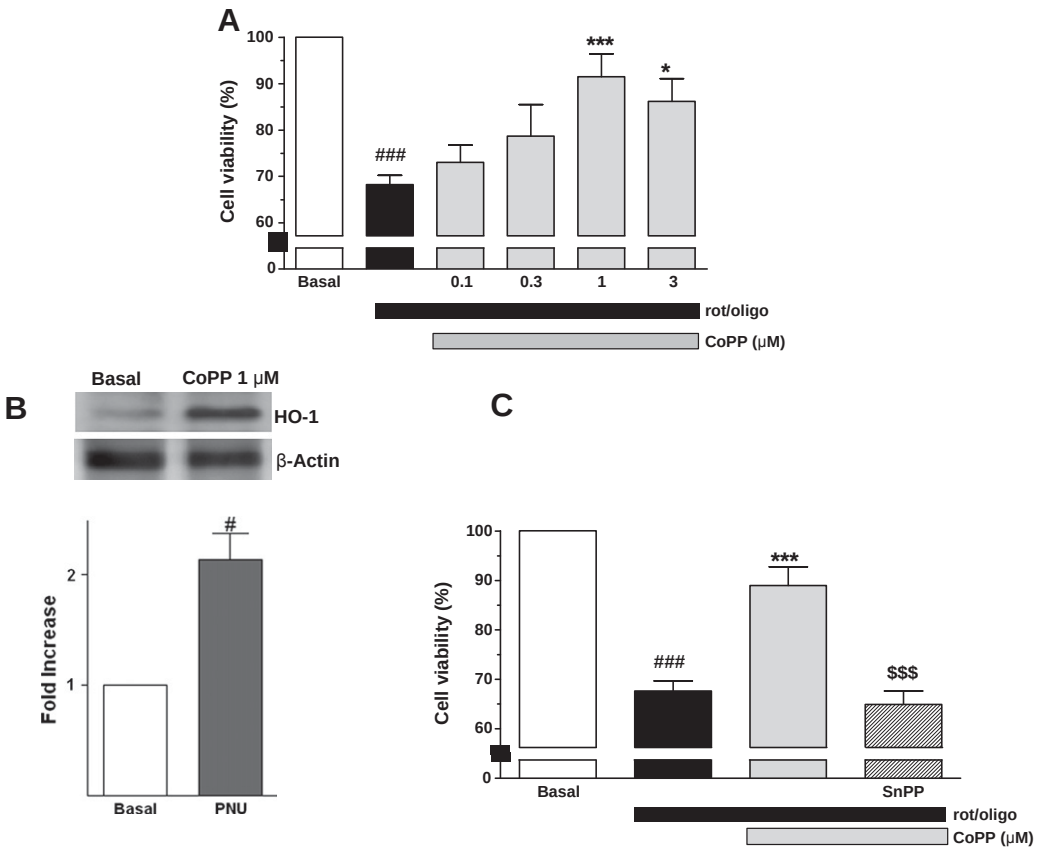

Fig. 8. HO-1 induction by CoPP protects against rot/oligo-induced cell death in a concentration-dependent manner. Experiments were run in parallel following the protocol shown in Fig. 2A. (A) A concentration−response curve for CoPP incubated for 16 h after the rot/oligo insult. (B) A representative immunoblot of HO-1 induction and mean increases ± SEM (bottom) of four different cell batches; $^{\#}p < 0.05$ compared to basal. Cells were incubated for 16 h with MEM/F-12 (basal) or 1 μM CoPP. (C) The protective effect of 1 μM CoPP and its reversal by 3 μM SnPP. Cells were incubated for 16 h with 1 μM CoPP after the rot/oligo period, in the absence or the presence of 3 μM SnPP. Cell viability was measured with the MTT assay. Data are means ± SEM of at least five different cell batches. $^{\#\#\#}p < 0.001$ compared to untreated cells; $^{***}p < 0.001$ and $^{*}p < 0.05$ in comparison with the rot/oligo-lesioned cells; $^{\$}$ $^{\$\$}p < 0.001$ compared to CoPP posttreated cells.

protective action of PST/PNU; it occurred under conditions which cells exposed to 8-h rot/oligo were still in a reversible apoptotic phase. This is shown by the fact that PST/PNU reduced annexin V-positive cells (Figs. 3A−D) and could reduce augmentation of cleaved caspase-3 (Fig. 3E), whose activation drives cells into the irreversible apoptotic cascade.

The protective effects of PST/PNU seem to be linked to a drastic decrease in excessive ROS production of mitochondrial origin (Fig. 5). In searching for a mechanism to explain this effect, we found that PNU282987 augmented the expression of HO-1 (Fig. 7B), a stress defense enzyme; it is known that overexpression of phase II enzymes such as HO-1 improves the imbalance between the overproduction of ROS (in our case, due to rot/oligo cell incubation) and the ROS-scavenging activity of antioxidant enzymes such as HO-1 [29]. Thus, by enhancing HO-1 expression, PNU282987 could restore the balance between ROS production and scavenging in cells stressed with rot/oligo. That the PNU282987 protective effects were linked to HO-1 was supported by two additional findings: (1) the HO-1 inhibitor SnPP antagonized the protective actions of PST/PNU (Fig. 7A) and (2) the HO-1 inducer CoPP caused cytoprotection against rot/oligo and such an effect was blocked by SnPP (Figs. 8A, B, and C).

The question remains as to how PST/PNU augmented HO-1 expression to enhance ROS scavenging and produce neuroprotection. These effects seemed to be mediated by the Jak2/PI3K/Akt signaling pathway, as the following pharmacological experiments suggest: (i) the Jak2 blocker AG490 antagonized the protective effects of PST/PNU and (ii) the PI3K blocker LY294002 also inhibited such an effect (Fig. 6A). Moreover PNU282987 induced Akt and Jak2 phosphorylation (Figs. 6B and C). The scheme of Fig. 9 summarizes the proposed

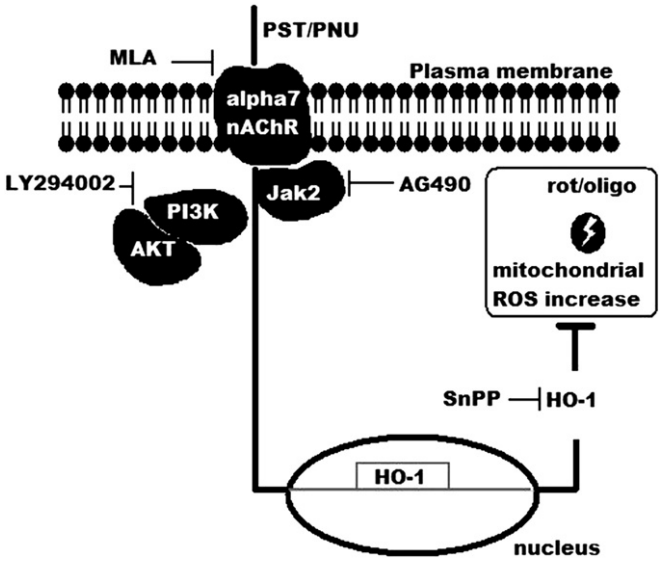

Fig. 9. Schematic diagram of the signaling pathway related to HO-1 induction via α7 nicotinic receptors. PNU282987 given poststress (rot/oligo), by acting on α7 nAChR, activates Jak-2, PI3K, and Akt, which finally causes HO-1 induction, which mitigates ROS production caused by blockade of mitochondrial complexes I and V with rotenone and oligomycin A, respectively. Different antagonists have been used to explore the participation of the various proteins in the protective signaling pathway activated by the α7 nAChR agonist PNU282987: MLA for the α7 nAChR, AG490 for Jak2, LY294002 for PI3K/Akt, and SnPP for HO-1.

mechanism of action explaining the neuroprotective effects of PST/PNU.

Most in vitro experiments performed in cell lines or primary neuronal cultures use a protocol based on the belief that a given compound will afford neuroprotection more efficaciously if added before the stressor used to cause cell damage and apoptotic or necrotic death. Although this argument seems relevant, it is also true that a neuroprotective compound with potential therapeutic interest will be used clinically after neurons already have become vulnerable; such is the case of the penumbra ischemic area after an acute ischemic stroke [30] or neurodegenerative diseases that are diagnosed after neuronal damage is already established [31]. Therefore, efforts have to be made to establish the appropriate experimental conditions that, though far from clinical reality, simulate more closely a therapeutic window of opportunity. In our model we subjected SH-SY5Y cells to a ROS stressor targeted to the mitochondria; we selected an exposure time that allowed the cells to enter into a reversible apoptotic phase, and we were successful in rescuing such cells by incubating them with a PST/PNU strategy. This model should inspire the search for novel neuroprotective compounds under conditions closer to the clinic and may be useful for screening large chemical libraries because of its simplicity.

In conclusion, we show here that activation of the α7 nAChR can exert neuroprotection against the stressor rot/oligo by enhancing the expression of HO-1 and augmenting the capability of cells for ROS scavenging. Coupling of plasmalemmal α7 nAChRs and HO-1 over-expression is exerted through the Jak2/PI3K/Akt signaling pathway. These effects are exerted under the unusual experimental conditions of stimulating the α7 nAChRs after the cells were already subjected to an 8-h treatment with the stressor. Therefore, activation of this receptor could potentially prevent apoptotic cell death, once initiated by mitochondrial blockade, by increasing the cell antioxidant defense.

Acknowledgments

This work was supported in part by grants from the Spanish Ministry of Science and Innovation, Ref. SAF2009-12150, to M.G.L.; the Spanish Ministry of Health (Instituto de Salud Carlos III) RETICS-RD06/0026 and Comunidad Autónoma de Madrid, Ref. SAL2006/0275, to A.G.G. and M.G.L.; and Fundación CIEN, IS Carlos III, MICINN, No. PI016/09 and Agencia Lain Entralgo, CN No. NDE07/09, Comunidad de Madrid, Spain, to A.G.G. We also thank the Fundación Teófilo Hernando for its continued support and Mr. Tolsá Torrenova for language editing.

References

[1] Circu, M. L.; Aw, T. Y. Reactive oxygen species, cellular redox systems, and apoptosis. Free Radic. Biol. Med. 48:749–762; 2010.

[2] Parfenova, H.; Basuroy, S.; Bhattacharya, S.; Tcheranova, D.; Qu, Y.; Regan, R. F.; Leffler, C. W. Glutamate induces oxidative stress and apoptosis in cerebral vascular endothelial cells: contributions of HO-1 and HO-2 to cytoprotection. Am. J. Physiol. Cell Physiol. 290:C1399–C1410; 2006.

[3] Kim, Y. S.; Zhuang, H.; Koehler, R. C.; Dore, S. Distinct protective mechanisms of HO-1 and HO-2 against hydroperoxide-induced cytotoxicity. Free Radic. Biol. Med. 38:85–92; 2005.

[4] Mariani, E.; Polidori, M. C.; Cherubini, A.; Mecocci, P. Oxidative stress in brain aging, neurodegenerative and vascular diseases: an overview. J. Chromatogr. B Anal. Technol. Biomed. Life Sci. 827:65–75; 2005.

[5] Rosales-Corral, S.; Reiter, R. J.; Tan, D. X.; Ortiz, G. G.; Lopez-Armas, G. Functional aspects of redox control during neuroinflammation. Antioxid. Redox Signaling 13: 193–247; 2010.

[6] Turrens, J. F. Mitochondrial formation of reactive oxygen species. J. Physiol. 552: 335–344; 2003.

[7] Trojanowski, J. Q. Rotenone neurotoxicity: a new window on environmental causes of Parkinson's disease and related brain amyloidoses. Exp. Neurol. 179:6–8; 2003.

[8] Poss, K. D.; Tonegawa, S. Reduced stress defense in heme oxygenase 1-deficient cells. Proc. Natl Acad. Sci. USA 94:10925–10930; 1997.

[9] Nimura, T.; Weinstein, P. R.; Massa, S. M.; Panter, S.; Sharp, F. R. Heme oxygenase-1 (HO-1) protein induction in rat brain following focal ischemia. Brain Res. Mol. Brain Res. 37:201–208; 1996.

[10] Vitali, S. H.; Mitsialis, S. A.; Christou, H.; Fernandez-Gonzalez, A.; Liu, X.; Kourembanas, S. Mechanisms of heme oxygenase-1-mediated cardiac and pulmonary vascular protection in chronic hypoxia: roles of carbon monoxide and bilirubin. Chest 128:578S–579S; 2005.

[11] Yachie, A.; Niida, Y.; Wada, T.; Igarashi, N.; Kaneda, H.; Toma, T.; Ohta, K.; Kasahara, Y.; Koizumi, S. Oxidative stress causes enhanced endothelial cell injury in human heme oxygenase-1 deficiency. J. Clin. Invest. 103:129–135; 1999.

[12] Hwang, Y. P.; Jeong, H. G. Ginsenoside Rb1 protects against 6-hydroxydopamine-induced oxidative stress by increasing heme oxygenase-1 expression through an estrogen receptor-related PI3K/Akt/Nrf2-dependent pathway in human dopaminergic cells. Toxicol. Appl. Pharmacol. 242:18–28; 2010.

[13] Lester, H. A.; Dibas, M. I.; Dahan, D. S.; Leite, J. F.; Dougherty, D. A. Cys-loop receptors: new twists and turns. Trends Neurosci. 27:329–336; 2004.

[14] Gotti, C.; Fornasari, D.; Clementi, F. Human neuronal nicotinic receptors. Prog. Neurobiol. 53:199–237; 1997.

[15] Stevens, T. R.; Krueger, S. R.; Fitzsimonds, R. M.; Picciotto, M. R. Neuroprotection by nicotine in mouse primary cortical cultures involves activation of calcineurin and L-type calcium channel inactivation. J. Neurosci. 23:10093–10099; 2003.

[16] Arias, E.; Gallego-Sandin, S.; Villarroya, M.; Garcia, A. G.; Lopez, M. G. Unequal neuroprotection afforded by the acetylcholinesterase inhibitors galantamine, donepezil, and rivastigmine in SH-SY5Y neuroblastoma cells: role of nicotinic receptors. J. Pharmacol. Exp. Ther. 315:1346–1353; 2005.

[17] Shaw, S.; Bencherif, M.; Marrero, M. B. Janus kinase 2, an early target of alpha 7 nicotinic acetylcholine receptor-mediated neuroprotection against Abeta-(1–42) amyloid. J. Biol. Chem. 277:44920–44924; 2002.

[18] Egea, J.; Rosa, A. O.; Sobrado, M.; Gandia, L.; Lopez, M. G.; Garcia, A. G. Neuroprotection afforded by nicotine against oxygen and glucose deprivation in hippocampal slices is lost in alpha7 nicotinic receptor knockout mice. Neuroscience 145:866–872; 2007.

[19] Shin, E. J.; Chae, J. S.; Jung, M. E.; Bing, G.; Ko, K. H.; Kim, W. K.; Wie, M. B.; Cheon, M. A.; Nah, S. Y.; Kim, H. C. Repeated intracerebroventricular infusion of nicotine prevents kainate-induced neurotoxicity by activating the alpha7 nicotinic acetylcholine receptor. Epilepsy Res. 73:292–298; 2007.

[20] Hajos, M.; Hurst, R. S.; Hoffmann, W. E.; Krause, M.; Wall, T. M.; Higdon, N. R.; Groppi, V. E. The selective alpha7 nicotinic acetylcholine receptor agonist PNU-282987 [N-[(3R)-1-azabicyclo[2.2.2]oct-3-yl]-4-chlorobenzamide hydrochloride] enhances GABAergic synaptic activity in brain slices and restores auditory gating deficits in anesthetized rats. J. Pharmacol. Exp. Ther. 312:1213–1222; 2005.

[21] Egea, J.; Rosa, A. O.; Cuadrado, A.; Garcia, A. G.; Lopez, M. G. Nicotinic receptor activation by epibatidine induces heme oxygenase-1 and protects chromaffin cells against oxidative stress. J. Neurochem. 102:1842–1852; 2007.

[22] Hoglinger, G. U.; Lannuzel, A.; Khondiker, M. E.; Michel, P. P.; Duyckaerts, C.; Feger, J.; Champy, P.; Prigent, A.; Medja, F.; Lombes, A.; Oertel, W. H.; Ruberg, M.; Hirsch, E. C. The mitochondrial complex I inhibitor rotenone triggers a cerebral tauopathy. J. Neurochem. 95:930–939; 2005.

[23] Denizot, F.; Lang, R. Rapid colorimetric assay for cell growth and survival: modifications to the tetrazolium dye procedure giving improved sensitivity and reliability. J. Immunol. Meth. 89:271–277; 1986.

[24] Ha, H. C.; Woster, P. M.; Yager, J. D.; Casero Jr., R. A. The role of polyamine catabolism in polyamine analogue-induced programmed cell death. Proc. Natl Acad. Sci. USA 94:11557–11562; 1997.

[25] Herbert, J. M.; Augereau, J. M.; Gleye, J.; Maffrand, J. P. Chelerythrine is a potent and specific inhibitor of protein kinase C. Biochem. Biophys. Res. Commun. 172: 993–999; 1990.

[26] Vlahos, C. J.; Matter, W. F.; Hui, K. Y.; Brown, R. F. A specific inhibitor of phosphatidylinositol 3-kinase, 2-(4-morpholinyl)-8-phenyl-4H-1-benzopyran-4-one (LY294002). J. Biol. Chem. 269:5241–5248; 1994.

[27] Alessi, D. R.; Cuenda, A.; Cohen, P.; Dudley, D. T.; Saltiel, A. R. PD 098059 is a specific inhibitor of the activation of mitogen-activated protein kinase kinase in vitro and in vivo. J. Biol. Chem. 270:27489–27494; 1995.

[28] Ward, J. M.; Cockcroft, V. B.; Lunt, G. G.; Smillie, F. S.; Wonnacott, S. Methyllycaconitine: a selective probe for neuronal alpha-bungarotoxin binding sites. FEBS Lett. 270:45–48; 1990.

[29] Salinas, M.; Diaz, R.; Abraham, N. G.; Ruiz de Galarreta, C. M.; Cuadrado, A. Nerve growth factor protects against 6-hydroxydopamine-induced oxidative stress by increasing expression of heme oxygenase-1 in a phosphatidylinositol 3-kinase-dependent manner. J. Biol. Chem. 278:13898–13904; 2003.

[30] Weinberger, J. M. Evolving therapeutic approaches to treating acute ischemic stroke. J. Neurol. Sci. 249:101–109; 2006.

[31] Xu, K.; Xu, Y. H.; Chen, J. F.; Schwarzschild, M. A. Neuroprotection by caffeine: time course and role of its metabolites in the MPTP model of Parkinson's disease. Neuroscience 167:475–481; 2010.

Neuropharmacology 62 (2012) 1082-1090

Contents lists available at SciVerse ScienceDirect

Neuropharmacology

journal homepage: www.elsevier.com/locate/neuropharm

Galantamine elicits neuroprotection by inhibiting iNOS, NADPH oxidase and ROS in hippocampal slices stressed with anoxia/reoxygenation

J. Egea [a,b,d,*], M.D. Martín-de-Saavedra [a,b], E. Parada [a,b], A. Romero [a,b,d,1], L. del Barrio [a,b], A.O. Rosa [a,b,2], A.G. García [a,b,c], M.G. López [a,b,d]

[a] Instituto Teófilo Hernando, Universidad Autónoma de Madrid, Spain
[b] Departamento de Farmacología y Terapéutica, Facultad de Medicina, Universidad Autónoma de Madrid, Spain
[c] Servicio de Farmacología Clínica, Instituto de Investigación Sanitaria, Hospital Universitario de la Princesa, Madrid, Spain
[d] Instituto Universitario la Paz-IdiPaz, Universidad Autónoma de Madrid, Spain

RESUMEN

La galantamina es una de las terapias actuales en el tratamiento de la enfermedad de Alzheimer, esta enfermedad, puede llevar asociado un daño isquémico que contribuye a agravar la patología neurodegenerativa y el déficit cognitivo. Estudios anteriores del grupo, muestran que la galantamina posee efecto neuroprotector en modelos de isquemia cerebral tanto in vivo como in vitro. En este trabajo, nos planteamos evaluar los mecanismos de señalización intracelular implicados en la protección mediada pos galantamina en un modelo in vitro de isquemia/reperfusion. Para ello, usamos rodajas de hipocampo de rata, sometidas a un periodo de privación de oxigeno y glucosa (OGD) seguido de reoxigenación. En estas condiciones experimentales, la galantamina ofreció protección significativa de manera concentración-dependiente, obteniéndose la máxima protección a la concentración de 15 µM. El efecto neuroprotector de galantamina fue revertido por mecamilamina y por AG490 , sin embargo no se observaron diferencias significativas con atropina, indicando asi que los receptores nicotínicos y la proteína jak2 participaban en el efecto protector. La galantamina redujo la translocacion al nucleo de p65, la expresión de iNOS y la producción de NO, de forma dependiente de la activación de jak2. El tratamiento con galantamina, redujo también la producción de ROS mediada por la activación de NADPH oxidase (NOX).

En conclusión, el efecto neuroprotector de galantamina frente a isquemia/reperfusión, esta mediado por la activación de una ruta protectora que involucra a los de receptores nicotínicos y de la proteína jak2

Contents lists available at SciVerse ScienceDirect

Neuropharmacology

journal homepage: www.elsevier.com/locate/neuropharm

Galantamine elicits neuroprotection by inhibiting iNOS, NADPH oxidase and ROS in hippocampal slices stressed with anoxia/reoxygenation

J. Egea [a,b,d,*], M.D. Martín-de-Saavedra [a,b], E. Parada [a,b], A. Romero [a,b,d,1], L. del Barrio [a,b], A.O. Rosa [a,b,2], A.G. García [a,b,c], M.G. López [a,b,d]

[a] Instituto Teófilo Hernando, Universidad Autónoma de Madrid, Spain
[b] Departamento de Farmacología y Terapéutica, Facultad de Medicina, Universidad Autónoma de Madrid, Spain
[c] Servicio de Farmacología Clínica, Instituto de Investigación Sanitaria, Hospital Universitario de la Princesa, Madrid, Spain
[d] Instituto Universitario la Paz-IdiPaz, Universidad Autónoma de Madrid, Spain

ARTICLE INFO

Article history:
Received 16 June 2011
Received in revised form
25 October 2011
Accepted 31 October 2011

Keywords:
Galantamine
Ischemia
Neuroprotection
ROS

ABSTRACT

Galantamine is a drug currently used to treat Alzheimer's disease (AD); in this group of patients it has been observed that concomitant ischemic brain injury can accelerate their cognitive deficit. We have previously shown that galantamine can afford neuroprotection on in vitro and in vivo models related to brain ischemia. In this context, this study was planned to investigate the intracellular signaling pathways implicated in the protective effect of galantamine on an in vitro brain ischemia-reperfusion model, namely rat hippocampal slices subjected to oxygen and glucose deprivation (OGD) followed by reoxygenation. Galantamine protected hippocampal slices subjected to OGD in a concentration-dependent manner; at 15 mM, cell death was reduced to almost control levels. The neuroprotective effects of galantamine were reverted by mecamylamine and AG490, but not by atropine, indicating that nicotinic receptors and Jak2 participated in this action. Galantamine also prevented p65 translocation into the nucleus induced by OGD; this effect was also linked to nicotinic receptors and Jak2. Furthermore, galantamine reduced iNOS induction and production of NO caused by OGD via Jak2. ROS production by NADPH oxidase (NOX) activation was also inhibited by galantamine. In conclusion, galantamine afforded neuroprotection under OGD-reoxygenation conditions by activating a signaling pathway that involves nicotinic receptors, Jak2 and the consequent inhibition of NOX and NFkB/iNOS.

This article is part of a Special Issue entitled 'Post-Traumatic Stress Disorder'.

1. Introduction

Based on its ability to improve cognition in clinical trials (Tariot et al., 2000; Wilcock et al., 2000), galantamine was introduced in the clinic as a therapy to treat Alzheimer's disease (AD). At that time it was known that galantamine was a mild inhibitor of acetylcholinesterase (AChE) (Thomsen and Kewitz, 1990) and an allosteric modulator of neuronal nicotinic receptors for acetylcholine (nAChRs) (Schrattenholz et al., 1996). Thus, cognition enhancement was attributed to the ability of galantamine to augment cholinergic neurotransmission (Santos et al., 2002). Later on, galantamine was shown to exert neuroprotection on AD in vitro models based on neuronal cultures subjected to oxidative stress or amyloid beta (Aβ) stress (Arias et al., 2004, 2005; Kihara et al., 2004). It was subsequently demonstrated that galantamine also afforded neuroprotection in rat hippocampal slices subjected to oxygen and glucose deprivation followed by a reoxygenation period (OGD) (Sobrado et al., 2004). It is also interesting that galantamine also behaved as a neuroprotective agent on an in vivo model of global cerebral ischemia, even when given after the ischemic insult (Ji et al., 2007; Lorrio et al., 2007). This effect was also mediated by nAChRs (Lorrio et al., 2007).

There is a great deal of literature reporting that various nAChR agonists produce neuroprotection (Egea et al., 2007a, 2007b; Gahring et al., 2003; Hejmadi et al., 2003; Stevens et al., 2003). However, the intracellular signaling pathway(s) involved in such

* Corresponding author. Instituto Teófilo Hernando, Departamento de Farmacología y Terapéutica, Facultad de Medicina, Universidad Autónoma de Madrid, Calle Arzobispo Morcillo, 4, 28029 Madrid, Spain. Tel.: þ34 91 4975387; fax: þ34 91 4975380.
E-mail address: javier.egea@uam.es (J. Egea).
[1] Present address: Department of Toxicology and Pharmacology, Faculty of Veterinary Medicine, Universidad Complutense de Madrid, 28040 Madrid, Spain.
[2] Present address: Department of Physiology and Biophysics, University of São Paulo, São Paulo, Brazil.

0028-3908/$ – see front matter © 2011 Elsevier Ltd. All rights reserved.
doi:10.1016/j.neuropharm.2011.10.022

action is unclear. One possibility is that a brain cholinergic anti-inflammatory pathway may be involved in nAChR-mediated neuroprotection. Cytoplasmic Janus protein tyrosine kynases (Jaks) are crucial components of diverse signal transduction pathways that govern cellular survival, proliferation, differentiation and apoptosis (Rane and Reddy, 2000) as well as inflammation (de Jonge et al., 2005). Concerning inflammation, it should be noted that Jak activation inhibits the translocation of NFkB to the nucleus, thus preventing the expression of genes coding for pro-inflammatory cytokines like IL-1 and TNF-α, as well as enzymes like inducible nitric oxide synthase (iNOS) and cyclooxygenase 2 (COX-2) (Madrigal et al., 2006; Sethi et al., 2008).

Another relevant protagonist in the cascade of events leading to neuronal death during a brain ischemic–reperfusion episode is the overproduction of reactive oxygen species (ROS). NADPH oxidase (NOX) is one of the main contributors to such excessive ROS, as shown on in vitro (Abramov et al., 2007) and in vivo models of ischemia (Chen et al., 2009). Another contributor to ROS generation is nitric oxide (NO), generated by inducible NO synthase (iNOS); this enzyme is expressed in in vitro (Cardenas et al., 2000) and in vivo models of brain ischemia (Iadecola et al., 1995). A link between excessive ROS production and neuroinflammation may be found in the fact that iNOS expression and its activity are regulated by inflammatory cytokines (Galea et al., 1992).

This study focuses on the effects of galantamine on the two pathways involved in neuronal death occurring during an ischemic insult, namely the neuroinflammatory pathway (nAChR–Jak–NFkB) and the ROS pathway (iNOS/NOX). We have used an in vitro model of brain injury, i.e. rat hippocampal slices subjected to the OGD protocol under different drug treatments. We demonstrate here that galantamine produces neuroprotection by activating the nAChR–Jak axis that inhibits NFkB translocation and the subsequent neuroinflammation, as well as through the mitigation of ROS production by inhibiting NOX and iNOS expression. These data are relevant in the clinical context of galantamine efficacy in improving cognition, behavior and daily life activities in patients with mix AD-cerebrovascular disease (Erkinjuntti et al., 2003).

2. Materials and methods

2.1. Materials

The fluorescent dyes propidium iodide, Hoechst 33342, hydroethidine and DAF-AM were from Invitrogen (Madrid, Spain). Anti-iNOS was purchased from BD Europe Transduction Lab (Madrid, Spain), anti-phospho-Jak2 and anti-Jak2 were from Cell Signalling (Izasa S.A., Barcelona, Spain), anti-b-actin, mecamylamine and MTT (3-(4,5-dimethylthiazol-2-yl)-diphenyltetrazolium bromide) from Sigma (Madrid, Spain) and LY294002 and galantamine from Tocris (Biogen Científica, Madrid, Spain).

2.2. Animal usage and hippocampal slice preparation

Experiments were performed in hippocampal slices from adult male Sprague–Dawley rats (275–325 g) from a colony of our animal quarters. The experiments were performed after approval of the protocol by the institutional Ethics Committee of Universidad Autónoma de Madrid, Spain according to the European Guidelines for the use and care of animals for research. All efforts were made to minimize animal suffering and to reduce the number of animals used in the experiments.

We used the protocol described by Egea and co-workers (Egea et al., 2007b) with slight modifications. Rats were quickly decapitated under sodium pentobarbital anesthesia (60 mg/kg, i.p.), forebrains were rapidly removed from the skull and placed into ice-cold Krebs bicarbonate dissection buffer (pH 7.4), containing: NaCl 120 mM, KCl 2 mM, $CaCl_2$ 0.5 mM, $NaHCO_3$ 26 mM, $MgSO_4$ 10 mM, KH_2PO4 1.18 mM, glucose 11 mM and sucrose 200 mM. The chamber solutions were pre-bubbled with either 95% O_2/5% CO_2 or 95% N_2/5% CO_2 gas mixtures, for at least 45 min before slice immersion, to ensure O_2 saturation or removal. The hippocampi were quickly dissected, glued down leaning vertically against agar blocks in a small chamber, submerged in cold, oxygenated dissection buffer and sectioned in transverse slices of 200 μm thick using a vibratome (Leica; Heidelberg, Germany). After an initial stabilization period of 30 min, the slices corresponding to the control group were incubated 15 min in a Krebs solution with the following composition: NaCl 120 mM, KCl 2 mM, $CaCl_2$ 2 mM, $NaHCO_3$ 26 mM, $MgSO_4$ 1.19 mM, KH_2PO_4 1.18 mM and glucose 11 mM; this solution was equilibrated with 95% O_2/5% CO_2. Oxygen and glucose deprivation was induced by incubating the slices in a glucose-free Krebs solution, equilibrated with a 95% N_2/5% CO_2 gas mixture; glucose was replaced by 2-deoxyglucose. After this OGD period, the slices were returned back to an oxygenated normal Krebs solution containing glucose (reoxygenation period). Experiments were performed at 37 °C. A control and OGD group was included in all experiments. The OGD-reoxygenation protocol employed was 15 min OGD followed by 60 min reoxygenation.

2.3. Monitoring of superoxide anion production

Superoxide anion production was evaluated in real-time by the oxidized hydroethidine (Het) method (Bindokas et al., 1996). Het (3.2 μM) was dissolved in oxygenated Krebs solution. Ethidium fluorescence was excited at 485 nm, and emitted fluorescence was measured at >580 nm. The average fluorescence intensity of the Et was monitored using a 10X objective in the pyramidal cell layer of the CA1 region every 30 s during 10 min of the reoxygenation period. Fluorescence analysis was performed using the Metamorph programme version 7.0. Each value was divided by the initial fluorescence value for the purpose of normalization. The slope of the fluorescence change from 0 to 10 min after the stress was calculated as an indication of the rate of superoxide anion production.

2.4. Cell culture and ROS imaging

Mixed cultures of hippocampal and glial cells were prepared as described previously (Abramov et al., 2004) from Sprague–Dawley rat pups 2–4 postpartum. Hippocampi were removed into ice-cold HBSS (Lonza, Madrid, Spain). The tissue was minced and trypsinized (0.1%, 15 min 37 °C), triturated, and plated on poli-D-lysine-coated coverslips and cultured in Neurobasal medium supplemented with B-27 and 2 mM L-glutamine. Cultures were maintained at 37 °C in a humidified atmosphere of 5% CO_2 and 95% air, fed twice a week, and maintained for 7 d before experimental use.

For measurement of hydroethidine (HEt) fluorescence, dihydroethidium (2 μM) was present in all solutions during these experiments, and no preincubation was used, to limit the intracellular accumulation of oxidized product. Fluorescence measurements were obtained on a fluorescence inverted microscope equipped with a 40X objective. HEt were monitored in single cells using excitation light provided by a Xenon lamp. Ethidium fluorescence was excited at 485 nm, and emitted fluorescence was measured at >580 nm.

2.5. Quantification of cell death in propidium iodide and Hoechst 33342 stained hippocampal slices

At the end of the experiment, the hippocampal slices were loaded with 1 μg/ml propidium iodide (PI) and Hoechst 33342 (Hoechst) during the last 5 min of incubation. Mean PI and Hoechst fluorescence in CA1 and CA3 regions in each slice, after a given treatment, were analyzed. Fluorescence was measured in a fluorescence inverted NIKON eclipse T2000-U microscope. Wavelengths of excitation and emission for PI and Hoechst were 530 or 350, and 580 or 460 nm, respectively. Images were taken at CA1 and CA3 at magnifications of 100X. Fluorescence analysis was performed using the Metamorph programme version 7.0. To calculate cell death, we divided the mean PI fluorescence by the mean Hoechst fluorescence. Data were normalized with respect to control values that were considered as 1.

2.6. Quantification of viability by MTT in hippocampal slices

Hippocampal cell viability was also determined through the ability of the cells to reduce MTT (Mosmann, 1983). Hippocampal slices were collected immediately after the reoxygenation period and were incubated with MTT (0.5 mg/ml) in Krebs bicarbonate solution for 30 min at 37 °C. The tetrazolium ring of MTT can be cleaved by active dehydrogenases in order to produce a precipitated formazan. The formazan produced in the hippocampal slices was solubilized by adding 200 μl dimethyl sulfoxide (DMSO), resulting in a colored compound whose optical density was measured in an ELISA microplate reader at 540 nm. Absorbance values obtained in control slices was taken as 100% viability.

2.7. Measurement of NO production in hippocampal slices

NO release was estimated from the amounts of nitrites (NO_2^-) in the incubation solution. NO_2^- was determined by a colorimetric assay based on the Griess reaction (1% sulphanilamide, 0.1% naphthylethylenediamine dihydrochloride and 2–5 % H_3PO_4) and modified by Marzinzig et al. (Marzinzig et al., 1997). Samples of the solution bathing the hippocampal slices were taken at times 0, 1 and 2 h of the reoxygenation period and measured spectrophotometrically at 540 nm, using a microplate reader (Labsystems iEMS reader MF). The values found for NO_2^- were compared with a standard curve of $NaNO_2$. Data were normalized with respect to NO_2^- released in the OGD group at time 0 min of reoxygenation period, in each experiment.

2.8. Preparation of nuclear and cytosolic extracts

Cytosolic and nuclear fractions were prepared as previously described (Rojo et al., 2006) with slight modifications. Briefly, hippocampal slices were mechanically disaggregated in three volumes of cold buffer A (20 mmol/L HEPES, pH 7.0; 0.15 mmol/L EDTA, 0.015 mmol/L EGTA, 10 mmol/L KCl, 1% Nonidet P-40, 1 μg/ml leupeptin and 1 mM phenylmethylsulfonyl fluoride). The homogenates were placed in ice during 10 min. Then, the homogenates were centrifuged at 2300 rpm for 5 min. The supernatant, corresponding to the cytosolic fraction, was resolved in SDS-PAGE and blotted. The nuclear pellet was resuspended in five pellet volumes of cold buffer B (10 mmol/L HEPES, pH 8.0; 0.1 mmol/L EDTA, 25% glycerol, 0.1 mol/L NaCl, 1 μg/ml leupeptin and 1 mM phenylmethylsulfonyl fluoride). After centrifugation in the same conditions indicated above, the nuclei were resuspended in two pellet volumes of hypotonic cold buffer A. Nuclear debris was removed by centrifugation at 2300 rpm for 5 min at 4 °C. The supernatant corresponding to the nuclear fraction was resolved in SDS-PAGE and blotted.

2.9. Western blot analysis

Slices of each group were lysed in 100 μl ice-cold lysis buffer (1% Nonidet P-40, 10% glycerol, 137 mM NaCl, 20 mM Tris-HCl, pH 7.5, 1 μg/ml leupeptin, 1 mM phenylmethylsulfonyl fluoride, 20 mM NaF, 1 mM sodium pyrophosphate, and 1 mM Na_3VO_4). Proteins (30 μg) from these lysates were resolved by SDS-PAGE and transferred to Immobilon-P membranes (Millipore Corp.). Membranes were incubated with anti-iNOS (1:1000), anti-β-actin (1:1000), anti-phospho-Jak2 (1:1000); anti-Jak2 (1:1000) and anti-TATA binding protein (TBP, 1:1000). Appropriate peroxidase-conjugated secondary antibodies (1:10000) were used to detect proteins by enhanced chemiluminescence. Protein bands were scanned and density was analyzed with the MCID Image Analysis software (InterFocus Imaging Ltd, Cambridge, UK).

2.10. Data analysis

Data are represented as means ± standard error of the mean. Comparisons between experimental and control groups were performed by One-way ANOVA followed by Newman-Keuls post-hoc test when appropriate. Differences were considered to be statistically significant when $p < 0.05$. All statistical procedures were carried out using Statistica software version 6.0 for an IBM compatible computer.

3. Results

3.1. Galantamine reduced cell death caused by OGD-reoxygenation in CA1 and CA3 hippocampal regions

To evaluate cell death, propidium iodide fluorescence in a given area of CA1 or CA3 was divided by Hoechst 33342 fluorescence in the same area (Top part of Fig. 1 illustrates an example of CA1); this value was normalized to 1 in control slices. Under these experimental conditions, 15 min OGD followed by 60 min reoxygenation doubled the amount of cell death in CA1 and CA3. We did not find differences between cell death caused by OGD in CA1 and CA3 regions (Fig. 1B and C).

Using this experimental protocol we performed a concentration-response curve with galantamine (1-15 μM); galantamine was present during the OGD period and throughout the whole experiment. Galantamine afforded concentration-dependent protection in CA1 (Fig. 1B) and CA3 (Fig. 1C) regions; the concentration of 15 μM afforded maximum protection (see also images on top part of Fig. 1), reaching almost control levels.

We corroborated these results by measuring cell viability by MTT. Fifteen min OGD followed by 1 h reoxygenation produced 35% decrease of cell viability with respect to control slices; galantamine was able to increase cell viability in a concentration-dependent manner. At 15 μM, galantamine increased cell viability almost to control levels (Fig. 1D). Therefore, this was the concentration selected for the following experiments.

3.2. Implication of acetylcholine receptors in the protective effects of galantamine

To determine the participation of acetylcholine receptors in the neuroprotective effects of galantamine, we used the nicotinic antagonist mecamylamine and the muscarinic antagonist atropine. As illustrated in Fig. 2, at 30 μM mecamylamine antagonized the galantamine effect (Fig. 2A and B). On the other hand, at 100 or 1000 nM atropine was not able of antagonizing the neuroprotection afforded by galantamine (Fig. 2C and D). By themselves, neither mecamylamine nor atropine afforded any significant effect on OGD-induced cell death. These data indicate that nAChRs are implicated in the neuroprotective effect of galantamine.

The neuroprotective effect of galantamine has been related to its action on nicotinic receptors since it can act as an acetylcholinesterase (AChE) inhibitor (Thomsen and Kewitz, 1990) as well as a positive allosteric modulator of the nAChRs (Schrattenholz et al., 1996). To determine if the inhibition of AChE was participating in the neuroprotective effect of galantamine, we used tacrine as a control, a potent inhibitor of AChE. Thus, we performed a concentration-response curve of tacrine (0.3-3 μM) and observed that at these concentrations that blocks 100% AChE activity, tacrine did not protect against OGD-reoxygenation (Fig. 3A). Therefore, we discarded that the neuroprotective effect of galantamine against OGD was mediated by AChE inhibition.

The neuroprotective effects of certain AChE inhibitors such as donepezil or galantamine, have been related to their actions on the α7 nAChRs (Arias et al., 2005; Shen et al., 2010). To corroborate that α7 nAChRs activation could be participating in the neuroprotective effect observed with galantamine in this model, we used the selective α7 nAChR agonist PNU 282987 (Gronlien et al., 2007). Hence, we performed a concentration-response curve of PNU 282987 (3-30 μM) and at the end of the experiment, we measured cell viability using MTT. Fifteen min OGD followed by 1 h reoxygenation produced 35% decrease of cell viability with respect to control slices and PNU 282987 was able to increase cell viability in a concentration-dependent manner. At 30 μM, PNU 282987 afforded the maximum effect (65% protection) (Fig. 3B). Therefore, these results point to α7 nAChR activation as the responsible for the neuroprotective effect of galantamine.

3.3. Implication of Jak2 in the neuroprotective effect of galantamine

It has been described that stimulation of α7 nAChR transduces signals to PI3K and Akt via Jak2 (Shaw et al., 2002). To evaluate if Jak2 was participating in the neuroprotective effect afforded by galantamine, we used the Jak2 inhibitor AG490 at 30 μM. As represented in Fig. 4A and B, AG490 blocked the protective effect afforded by galantamine in hippocampal slices subjected to OGD-reoxygenation, both in CA1 and CA3 regions.

To further corroborate that galantamine was activating Jak2, protein was extracted from hippocampal slices incubated for 30 min with 15 μM galantamine and immunoblots for pJak2 were performed; pJak2 was increased over two-fold by galantamine treatment and AG490 significantly reduced to almost basal levels its phosphorylation (Fig. 4C). The Jak2 inhibitor per se did not modify phosphorylation of Jak2.

Taken together, these results suggest that Jak2 is involved in the neuroprotective signal cascade induced by galantamine.

3.4. Galantamine inhibits the inflammatory NFkB pathway and iNOS induction: implication of nicotinic receptors and Jak2

Translocation of p65 to the nucleus produces an increment of pro-inflammatory cytokines and the induction of distinct proteins such as COX-2 and iNOS (Du et al., 2009), which augment the ROS production such as NO. Furthermore, ROS are involved in neurotoxicity and neuronal death following an ischemic insult (Coyle and Puttfarcken, 1993). Thus, in this study we examined the effect of galantamine on p65 translocation, induction of iNOS and NO

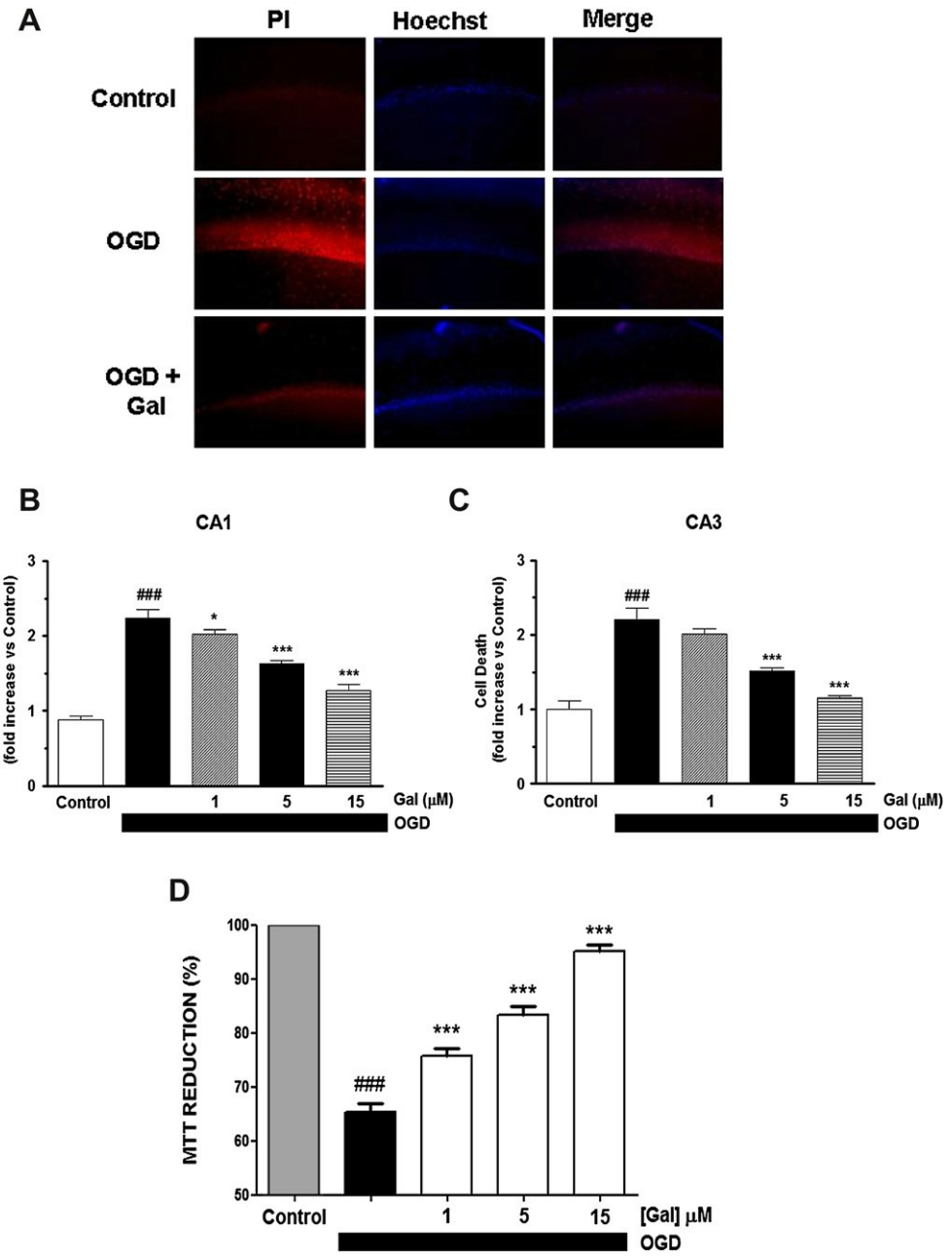

Fig. 1. Galantamine reduces cell death of hippocampal slices subjected to OGD and reoxygenation. Slices were subjected to 15 min OGD followed by 1 h reoxygenation in the absence (OGD) or presence of 1-15 μM galantamine (Gal); another group of slices were kept during the same period of time with oxygen and glucose (Control). (A) Illustrates fluorescence images of propidium iodide, Hoechst and Merge of CA1. (B) and (C) represent cell death measured as the ratio PI/Hoechst and normalized respect to control obtained after the different treatments in CA1 and CA3, respectively. (D) Shows hippocampal viability measured by MTT. Data are means ± s.e.m. of 5 animals (n ¼ 5). $^{###}p < 0.001$ comparing control respect to OGD, $^{*}p < 0.05$ and $^{***}p < 0.001$ comparing OGD respect to OGD plus galantamine.

production in rat hippocampal slices subjected to OGD followed by reoxygenation.

We first measured by immunoblot the presence of p65 in cytosolic and nuclear extracts obtained from hippocampal slices subjected to the different experimental conditions. Under OGD conditions, p65 was increased in the nuclear fraction as an indication of its translocation to the nucleus. Galantamine treatment reduced to control levels p65 translocation; both mecamylamine and AG490 inhibited galantamine's action on p65 translocation (Fig. 5).

We next measured by western blot analysis iNOS production in ischemic slices treated or untreated with galantamine. In Fig. 6A, 15 min OGD followed by 1 h reoxygenation, increased by 2-fold iNOS with respect to control slices; this increase was reduced to almost basal levels in galantamine-treated slices. Moreover, the reduction of iNOS was reverted by AG490 indicating that galantamine reduces iNOS induction by activating Jak2. To corroborate this data, we measured the release of nitrites (NO_2^-) as an indirect measurement of NO production using the Griess method. As illustrated in Fig. 6B, 15 min OGD increased by 3 and 3.6 fold NO production measured at 1 and 2 h of reoxygenation with respect to control slices. In galantamine treated slices NO_2^- release was significantly reduced by 53, 54% at 1 and 2 h of reoxygenation, respectively ($p < 0.05$).

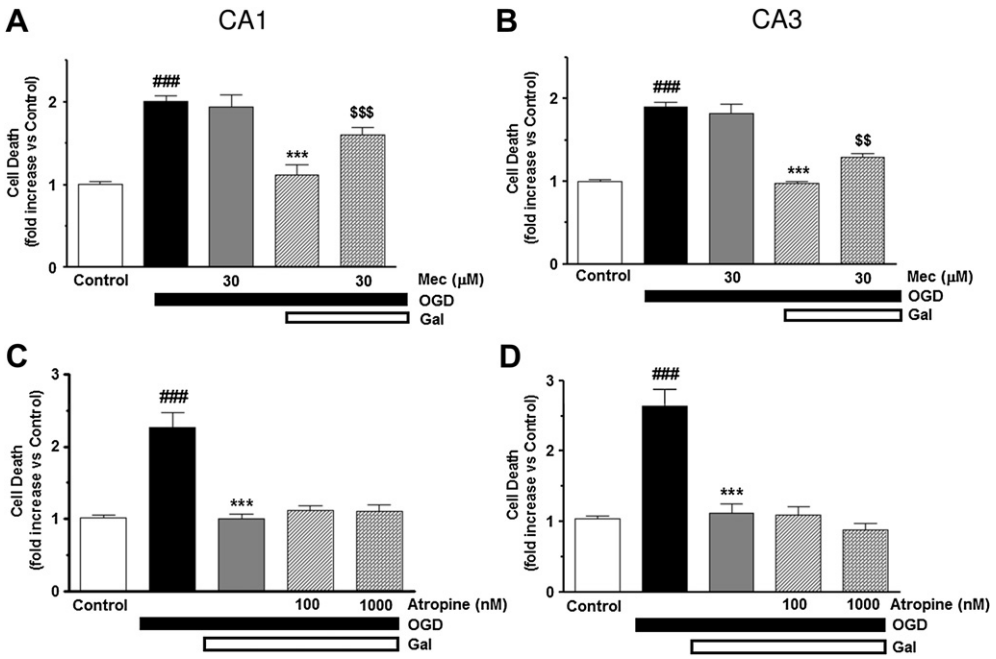

Fig. 2. Implication of nicotinic but not muscarinic receptors in the protective effect of galantamine. Slices were subjected to 15 min OGD followed by 1 h reoxygenation. Under these experimental conditions, slices were treated with 15 μM galantamine, alone or in the presence of 30 μM mecamylamine (A and B) or 100 or 1000 nM atropine (C and D). Antagonists were added to the bath solution 30 min before the OGD period. Cell death was evaluated by quantification of the ratio PI/Hoechst (see Material and Methods) in CA1 and CA3. Data correspond to the mean ± s.e.m. of 5 animals (n ¼ 5); all variables were run in parallel. $^{###}p < 0.001$ respect to control, $^{***}p < 0.001$ OGD-reoxygenation and $^{\$\$}p < 0.01$, $^{\$\$\$}p < 0.001$ with respect to galantamine.

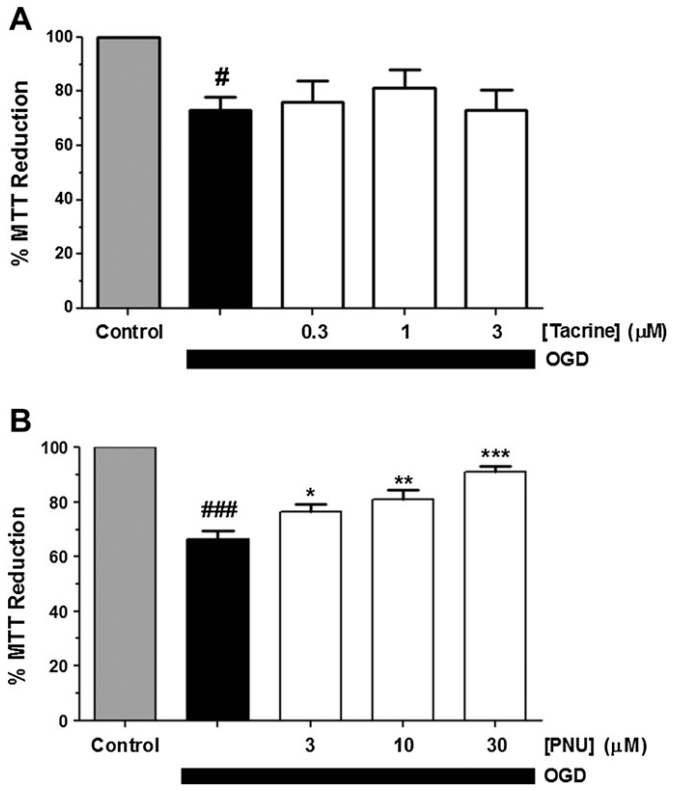

Fig. 3. α7 agonism but not tacrine protect hippocampal slices against OGD and reoxygenation. Slices were subjected to 15 min OGD followed by 1 h reoxygenation in the absence (OGD) or presence of 0.3-3 μM tacrine (A) or 3-30 μM PNU282987 (PNU) (B); another group of slices were kept during the same period of time with oxygen and glucose (Control). At the end of the experiment, cell viability was measured using MTT. Data are means ± s.e.m. of 5 animals (n ¼ 5); all variables were run in parallel. $^{#}p < 0.05$ and $^{###}p < 0.001$ respect to control, $^{*}p < 0.05$, $^{**}p < 0.01$ and $^{***}p < 0.001$ respect to OGD-reoxygenation.

3.5. Galantamine inhibits NADPH oxidase activation

Another source of ROS generation during reoxygenation is the activation of the NADPH oxidase (NOX) complex (Abramov et al., 2007). The fact that galantamine given post-ischemia in vivo, is able to afford neuroprotection (Lorrio et al., 2007) and that NOX inhibitors protect against cell death also given post-ischemia, prompted us to measure if galantamine could inhibit NOX activation. To activate NOX we used the phorbol ester phorbol myristate acetate (PMA). We found that application of PMA (10 nM) produced a rapid and significant increase (1.65-fold increase) in free radical generation (Fig. 7A). PMA-activated ROS production was suppressed by 76% when cells were co-incubated with 15 μM galantamine (Fig. 7A) or with the NOX inhibitor diphenylene iodonium (DPI 0.5 μM) (data not shown). This data indicates that galantamine could be inhibiting NOX activation in primary co-cultures.

To corroborate the in vitro data mentioned above, we next measured superoxide anion production during the first 10 min of the reoxygenation period, following the OGD period, in hippocampal slices. After exposing the hippocampal slices to 15 min OGD, the slope of the fluorescence during reoxygenation became much steeper than the slope of fluorescence of control slices (Fig. 7B). The rate of superoxide production of the slices subjected to OGD increased by 2.8-fold with respect to control slices (Fig. 7C). Superoxide anion production induced by OGD was suppressed by 55% when slices were incubated with 15 μM galantamine (Fig. 7B, C). Taken together, these results indicate that galantamine could inhibit NOX activation and the subsequent ROS production.

4. Discussion

In this study we have shown that galantamine provides protection of hippocampal slices subjected to OGD-reoxygenation through a multifunctional mechanism, rather than a single one. By acting on nicotinic receptors, galantamine-induced phosphorylation of Jak2

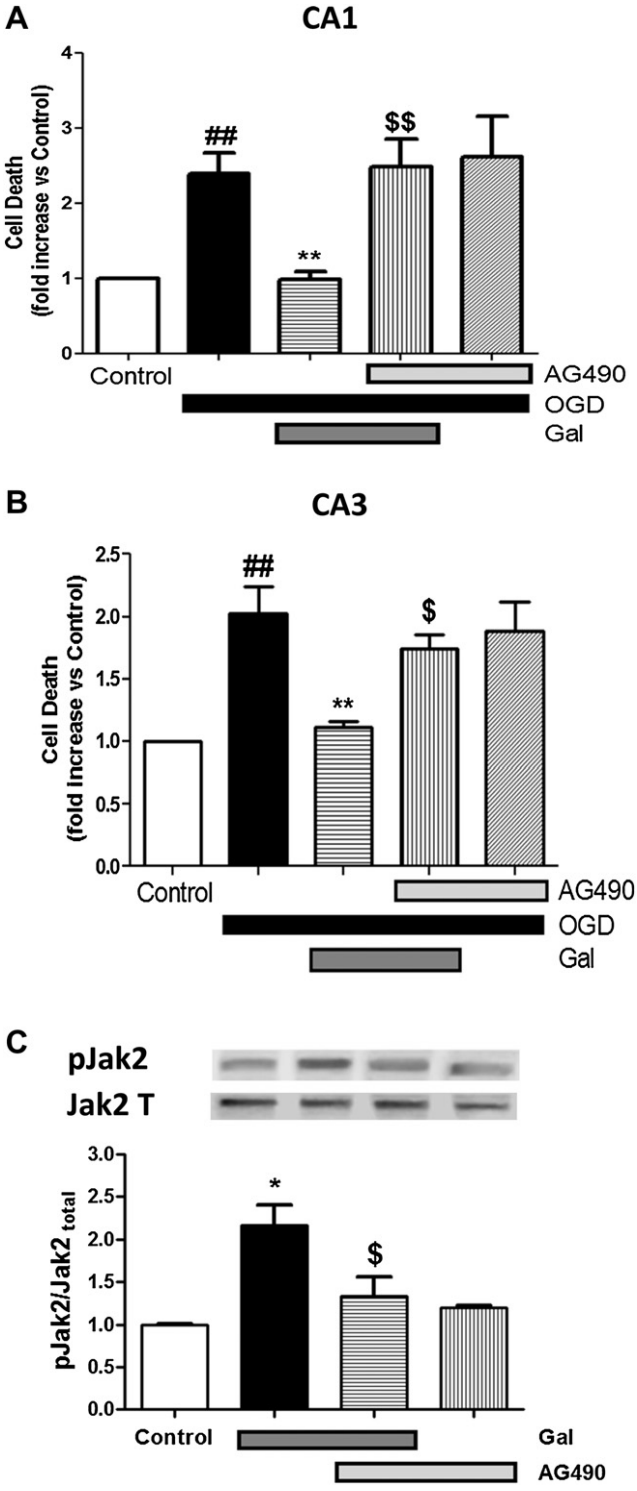

Fig. 4. Implication of Jak2 in the neuroprotective action of galantamine. The Jak2 antagonist AG490 (30 μM) inhibited the neuroprotective action of galantamine in CA1 (A) and CA3 regions (B). Data correspond to the mean ± s.e.m. of 5 animals. $^{\#\#}p < 0.01$ comparing control and OGD; $^{**}p < 0.01$ comparing OGD in the absence or presence of galantamine; $^{\$}p < 0.05$, $^{\$\$}p < 0.01$ comparing galantamine in the absence or presence of AG490. (C) Incubation of hippocampal slices for 30 min with galantamine increased pJak2 and AG490 significantly reduced its activation. AG490, per se, had no effect on pJak2. Data correspond to the mean ± s.e.m. of 4 animals. $^{*}p < 0.05$, $^{**}p < 0.01$ comparing OGD with respect to galantamine; $^{\$}p < 0.05$, comparing galantamine in the absence or presence of AG490.

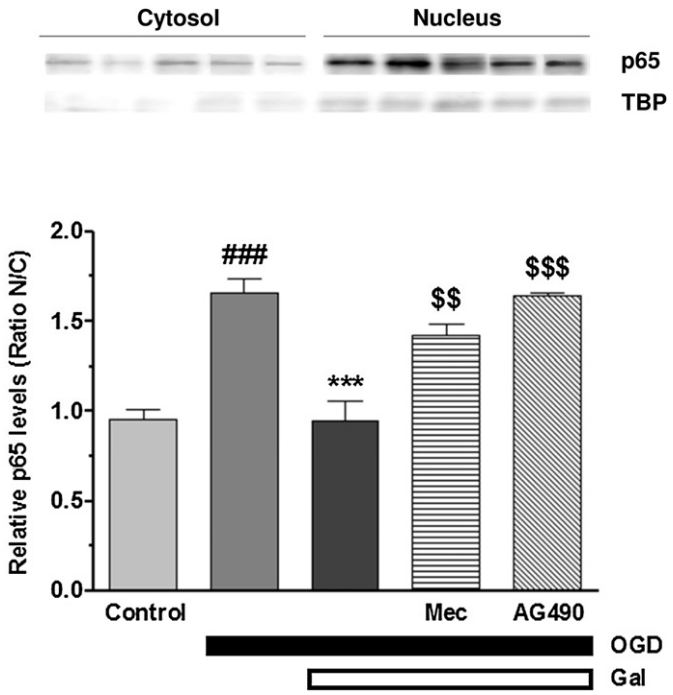

Fig. 5. Galantamine prevents activation of NFkB upon OGD: implication of Jak2. (A) The top part of the figure illustrates representative bands showing the expression of p65 in cytosolic and nuclear extracts obtained from hippocampal slices subjected to the experimental conditions shown in the bar graph. Translocation of p65 to the nucleus is represented as the ratio of the band densities obtained in the nuclear fraction/cytosolic fraction. TATA binding protein (TBP) is a control of the nuclear fraction. OGD caused an increment in p65 translocation while galantamine prevented it; the effects of galantamine were reverted by mecamylamine (30 μM) and AG490 (30 μM). Data correspond to the mean ± s.e.m. of 5 animals. $^{\#\#\#}p < 0.001$ in comparison to control; $^{***}p < 0.001$ in comparison to OGD in the absence of drug; $^{\$\$}p < 0.01$ and $^{\$\$\$}p < 0.001$ in comparison to galantamine.

that inhibited the NFkB inflammatory pathway. Moreover, galantamine reduced ROS production by inhibiting iNOS induction and NOX activation.

Signaling through nAChRs is being increasingly recognized to play an important role in different processes such as neurite outgrowth, synaptic transmission, control and synthesis of neurotrophic factors, neuroprotection (Belluardo et al., 2000) and inflammation (Borovikova et al., 2000). The implication of nAChRs in the protective effects afforded by galantamine have been previously described in vitro (Arias et al., 2005; Parada et al., 2010; Takada-Takatori et al., 2006) and in vivo (Lorrio et al., 2007); these results have been corroborated in this study as shown in the mecamylamine experiments and the use of the selective a7 nAChR agonist PNU 282987. Furthermore, galantamine could also potentiate GABA and NMDA currents (Moriguchi et al., 2004; Pereira et al., 2002). In fact, GABA agonists have shown to afford protection against cerebral ischemic injury (Gilby et al., 2005; Xu et al., 2008). Hence, our data does not exclude the possibility that the protective effect afforded by galantamine could be due to changes in GABA release resulting from galantamine application during OGD. Muscarinic receptors have also been implicated in neuroprotection against glutamate-induced toxicity (Zhou et al., 2008). However, the participation of these receptors in the protective effect of galantamine in our model has been discarded as revealed by the atropine experiments.

Jak2 has been related with neuroprotective effects of nAChRs agonists like nicotine or GTS-21 (Kox et al., 2009; Shaw et al., 2002). The neuroprotective effect mediated by nicotine implicated the

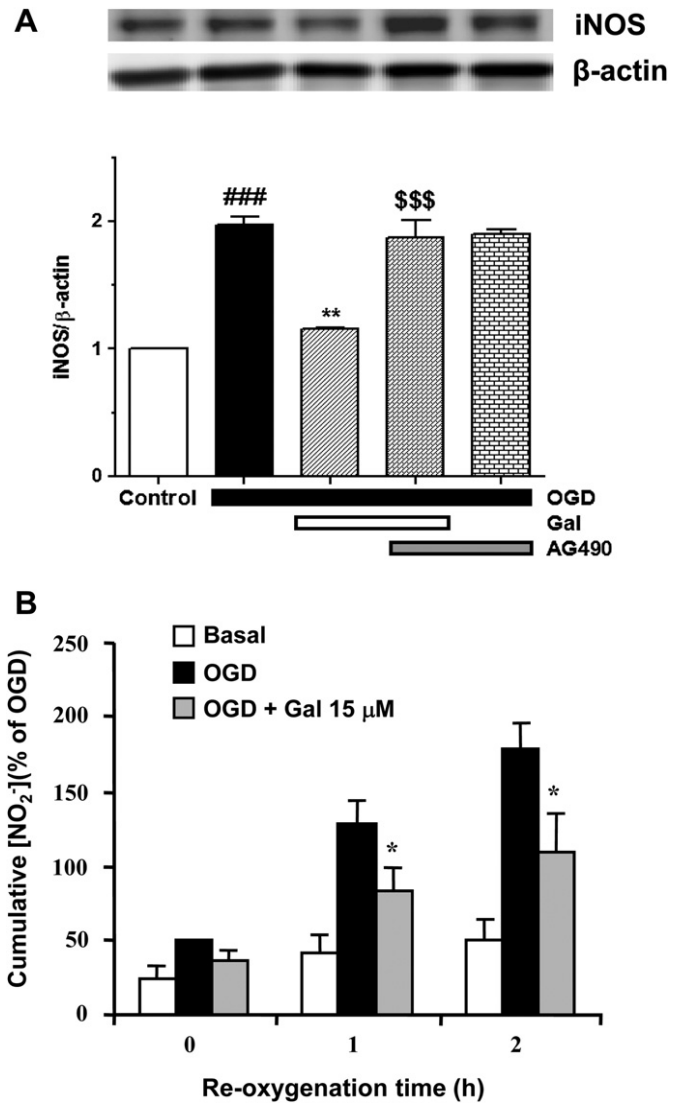

Fig. 6. Galantamine reduces iNOS induction and NO production induced by OGD-reoxygenation: implication of Jak2. Rat hippocampal slices were subjected to 15 min OGD followed by 1 h reoxygenation in the absence (OGD) or presence of galantamine 15 μM (Gal) or AG490 30 μM; another group of slices were kept during the same period of time with oxygen and glucose (Control). (A) Illustrates representative western blot that correspond to the experimental variables plotted in the bar graph below and correspond to the expression of iNOS. OGD increased iNOS and galantamine markedly reduced its induction; AG490 blocked galantamine's action. AG490 has no effect on iNOS per se. Data correspond to the mean and s.e.m. of 6 animals (n ¼ 6). $^{###}p < 0.001$ in comparison to control; $^{**}p < 0.01$ in comparison to OGD in the absence of drug; $^{\$\$\$}p < 0.001$ in comparison to galantamine. (B) Effects of galantamine 15 μM on NO_2^- release from hippocampal slices subjected to OGD and reoxygenation. Slices were run in parallel to measure NO_2^- released in basal or OGD conditions, in the absence or the presence of galantamine. The drug was present during the OGD and the reoxygenation period. Cumulative release of NO_2^- throughout the experiment is represented as % of NO_2^- released after OGD. Data correspond to the mean and s.e.m. of 6 animals. $^{*}p < 0.05$ comparing OGD respect to OGD plus galantamine.

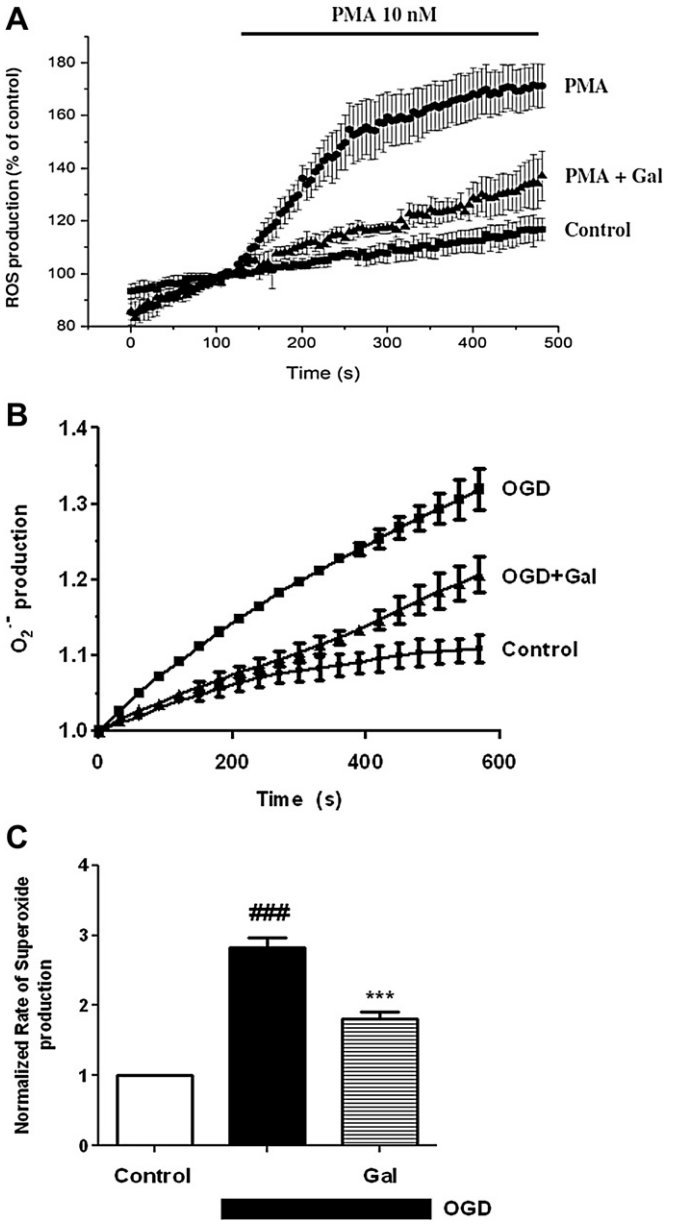

Fig. 7. Galantamine inhibits superoxide anion production in astrocytes and hippocampal slices subjected to OGD. (A) The rate of appearance of the Et fluorescent product was clearly increased in rat astrocytes exposed to PMA (10 nM; 42 cells, n ¼ 5) which caused a 1.65-fold increase in the HEt signal. In astrocytes pre-incubated for 5 min with galantamine 15 μM, galantamine inhibits ROS production by 76% (39 cells, n ¼ 5). (B) The slope of the fluorescence change was increased in hippocampal slices subjected to OGD with respect to control slices. Galantamine 15 μM inhibits ROS production by 55%. (C) Represents the relative slope of the fluorescence changes during 10 min of reoxygenation. Data were normalized with respect to control slope that was considered as 1 and represents the mean ± s.e.m. of 4 animals. $^{###}p < 0.001$ comparing control respect to OGD, $^{***}p < 0.001$ comparing OGD respect to OGD plus galantamine.

tyrosine phosphorylation of PI3K (Kihara et al., 2001) and Akt (Arias et al., 2005), two enzymes linked to cell survival. Furthermore, Jak2 mediates the induction of Bcl-2 and inhibits cell death in hematopoietic cells (Sakai and Kraft, 1997), and treatment with the inhibitor AG490 reduces the phosphorylation of PI3K resulting in an increase in caspase-3 activity and Bax protein in acute myocardial infarction (Negoro et al., 2000). Moreover, activation of neuronal erythropoietin receptors prevents apoptosis by triggering cross-talk between the signaling pathways of Jak2 and the NFkB (Digicaylioglu and Lipton, 2001). Our results are in line with those described above. In our study, 30 min incubation of hippocampal slices with galantamine activated Jak2 and the Jak2 inhibitor AG490 reverted Jak2 phosphorylation resulting in a reversion of the neuroprotective effect afforded by galantamine. Since the nicotinic antagonist mecamylamine prevented galantamine-induced activation of Jak2, it seems that this drug could be acting by

a mechanism similar to that described previously for nicotine against amyloid beta-induced toxicity (Shaw et al., 2002).

Another interesting finding in this study is related to the anti-neuroinflammatory actions of galantamine. Ischemic brain damage elicits inflammation in the injured areas (Feuerstein et al., 1998) and plays a critical role not only in the initiation and propagation of ischemia/hypoxia-evoked neuroinflammation but also in the resolution of brain damage (Rothwell and Luheshi, 2000). In the past years, a novel link between vagus nerve and inflammatory responses has been established. In fact, it has been demonstrated that the efferent vagus nerve can modulate the inflammatory response in a reflex-like fashion termed "the cholinergic anti-inflammatory pathway" (Borovikova et al., 2000; Sugano et al., 1998). In different cell types including monocytes, macrophages and endothelial cells, studies have indicated that the anti-inflammatory potential of nAChRs is mediated by inhibition of the transcription factor NFkB (de Jonge et al., 2005). Activation of NFkB requires ubiquitination of the IkB. This process will allow the nuclear translocation of the p65 and/or p50 subunits in order to modulate the transcription of NFkB responsive genes such as IL-6 and iNOS (Madrigal et al., 2006; Sugano et al., 1998). Furthermore, accumulating evidence indicates that the therapeutic effects of AChE inhibitors in AD are mediated through ACh enhancement of neuronal transmission and anti-inflammatory activity (Tabet, 2006). Here we found that OGD-reoxygenation augmented p65 translocation and that galantamine impaired such translocation; this effect was prevented by mecamylamine and AG490. These results indicate that by acting on nicotinic receptors, galantamine activates Jak2 that in turn prevents p65 translocation to the nucleus. Thus, it seems that galantamine is endowed with immunomodulatory actions.

Under ischemic conditions, NO is produced in excessive amount and turns its physiological neuromodulatory actions into neurotoxic effects. NO released by the novo expression of iNOS contributes to the damage found in ischemia. In fact, iNOS knockout mice present smaller infarcts (–30%) and better neurological outcomes after middle cerebral artery occlusion in comparison to their littermates (Iadecola et al., 1995). Moreover, iNOS inhibitors and NO scavengers are neuroprotective against OGD-reoxigenation models (Cardenas et al., 1998). In this study, OGD-reoxygenation increased iNOS and the formation of NO and, galantamine was able to block the induction of iNOS and NO production. iNOS is among the different genes that are responsive to NFkB (Madrigal et al., 2006); therefore a possible explanation for iNOS reduction in galantamine treated slices could be the inhibition of NFkB due to Jak2 activation. On the other hand, we have seen that: i) treatment of hippocampal primary cultures with galantamine is able to reduce NOX activation induced by PMA, and ii) treatment of hippocampal slices subjected to OGD with galantamine is able to reduce superoxide produced by NOX activation in the first 10 min of reoxygenation. A major source of ROS production during reoxygenation, after an ischemic insult, is the activation of NOX enzyme (Abramov et al., 2007). It has been demonstrated that post-ischemic inhibition of NOX is a good strategy to afford neuroprotection since apocynin, a NADPH oxidase inhibitor, reduced brain infarction and alleviated post-ischemic inflammation progress (Chen et al., 2009). Moreover, genetic ablation of the gp91phox subunit of NOX reduced brain infarction by 50% at 22 h of reperfusion after 2 h of focal ischemia (Walder et al., 1997). Hence, by inhibiting iNOS induction and NOX activation, galantamine reduces free radical production induced by OGD and thereby affords protection.

In conclusion, we have shown that galantamine activates a survival pathway in rat hippocampal slices subjected to OGD-reoxygenation. Such pathway involves nAChRs and Jak2 activation, inhibition of NFkB translocation to the nucleus, inhibition

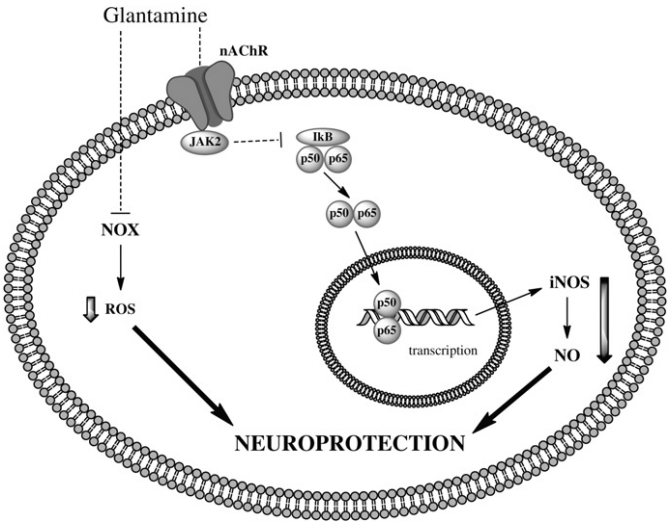

Fig. 8. Schematic diagram illustrating the putative points of regulation by galantamine during hippocampal OGD-reoxygenation to cause neuroprotection. Activation of the nicotinic receptor for acetylcholine (nAChR), activates Jak2, giving rise on the one hand to inhibition of NADPH oxidase (NOX) and on the other, to inhibition of p65 translocation to the nucleus, thereby inhibiting the induction of iNOS and the subsequent NO production and cell death.

of iNOS induction and NO production and inhibition of NOX activation, that ultimately afford neuroprotection (see Fig. 8 for a summary of this pathway). Therefore, Jak2 seems to be the initial kinase activated by galantamine through nAChRs to induce neuroprotective and anti-inflammatory actions under brain ischemia-reoxygenation conditions.

Acknowledgments

This work was supported in part by grants from Spanish Ministry of Science and Innovation Ref. SAF2009-12150 to MGL, the Spanish Ministry of Health (Instituto de Salud Carlos III) RETICS-RD06/0026 and Comunidad Autónoma de Madrid Ref. SAL2006/0275 to AGG and MGL, Agencia Lain Entralgo Ref. NDG07/9 and Fundación C.I.E.N., Instituto Carlos III Ref. 85016/09. MDMS has a pre-doctoral fellowship from the Spanish Ministry of Science and Innovation. We would also like to thank "Fundación Teófilo Hernando" for its continued support.

References

Abramov, A.Y., Canevari, L., Duchen, M.R., 2004. Beta-amyloid peptides induce mitochondrial dysfunction and oxidative stress in astrocytes and death of neurons through activation of NADPH oxidase. J. Neurosci. 24, 565e575.

Abramov, A.Y., Scorziello, A., Duchen, M.R., 2007. Three distinct mechanisms generate oxygen free radicals in neurons and contribute to cell death during anoxia and reoxygenation. J. Neurosci. 27, 1129e1138.

Arias, E., Ales, E., Gabilan, N.H., Cano-Abad, M.F., Villarroya, M., Garcia, A.G., Lopez, M.G., 2004. Galantamine prevents apoptosis induced by beta-amyloid and thapsigargin: involvement of nicotinic acetylcholine receptors. Neuropharmacology 46, 103e114.

Arias, E., Gallego-Sandin, S., Villarroya, M., Garcia, A.G., Lopez, M.G., 2005. Unequal neuroprotection afforded by the acetylcholinesterase inhibitors galantamine, donepezil, and rivastigmine in SH-SY5Y neuroblastoma cells: role of nicotinic receptors. J. Pharmacol. Exp. Ther. 315, 1346e1353.

Belluardo, N., Mudo, G., Blum, M., Amato, G., Fuxe, K., 2000. Neurotrophic effects of central nicotinic receptor activation. J. Neural. Transm. Suppl., 227e245.

Bindokas, V.P., Jordan, J., Lee, C.C., Miller, R.J., 1996. Superoxide production in rat hippocampal neurons: selective imaging with hydroethidine. J. Neurosci. 16, 1324e1336.

Borovikova, L.V., Ivanova, S., Zhang, M., Yang, H., Botchkina, G.I., Watkins, L.R., Wang, H., Abumrad, N., Eaton, J.W., Tracey, K.J., 2000. Vagus nerve stimulation attenuates the systemic inflammatory response to endotoxin. Nature 405, 458e462.

Cardenas, A., De Alba, J., Moro, M.A., Leza, J.C., Lorenzo, P., Lizasoain, I., 1998. Protective effect of N-(3-(aminomethyl)benzyl) acetamidine, an inducible nitric oxide synthase inhibitor, in brain slices exposed to oxygen-glucose deprivation. Eur. J. Pharmacol. 354, 161–165.

Cardenas, A., Moro, M.A., Hurtado, O., Leza, J.C., Lorenzo, P., Castrillo, A., Bodelon, O.G., Bosca, L., Lizasoain, I., 2000. Implication of glutamate in the expression of inducible nitric oxide synthase after oxygen and glucose deprivation in rat forebrain slices. J. Neurochem. 74, 2041–2048.

Coyle, J.T., Puttfarcken, P., 1993. Oxidative stress, glutamate, and neurodegenerative disorders. Science 262, 689–695.

Chen, H., Song, Y.S., Chan, P.H., 2009. Inhibition of NADPH oxidase is neuroprotective after ischemia-reperfusion. J. Cereb. Blood Flow Metab. 29, 1262–1272.

de Jonge, W.J., van der Zanden, E.P., The, F.O., Bijlsma, M.F., van Westerloo, D.J., Bennink, R.J., Berthoud, H.R., Uematsu, S., Akira, S., van den Wijngaard, R.M., Boeckxstaens, G.E., 2005. Stimulation of the vagus nerve attenuates macrophage activation by activating the Jak2-STAT3 signaling pathway. Nat. Immunol. 6, 844–851.

Digicaylioglu, M., Lipton, S.A., 2001. Erythropoietin-mediated neuroprotection involves cross-talk between Jak2 and NF-kappaB signalling cascades. Nature 412, 641–647.

Du, J., Wei, N., Guan, T., Xu, H., An, J., Pritchard, K.A., Shi, Y., 2009. Inhibition of CDKs by roscovitine suppressed LPS-induced *NO production through inhibiting NF {kappa}B activation and BH4 biosynthesis in macrophages. Am. J. Physiol. Cell Physiol.

Egea, J., Rosa, A.O., Cuadrado, A., Garcia, A.G., Lopez, M.G., 2007a. Nicotinic receptor activation by epibatidine induces heme oxygenase-1 and protects chromaffin cells against oxidative stress. J. Neurochem. 102, 1842–1852.

Egea, J., Rosa, A.O., Sobrado, M., Gandia, L., Lopez, M.G., Garcia, A.G., 2007b. Neuroprotection afforded by nicotine against oxygen and glucose deprivation in hippocampal slices is lost in alpha7 nicotinic receptor knockout mice. Neuroscience 145, 866–872.

Erkinjuntti, T., Kurz, A., Small, G.W., Bullock, R., Lilienfeld, S., Damaraju, C.V., 2003. An open-label extension trial of galantamine in patients with probable vascular dementia and mixed dementia. Clin. Ther. 25, 1765–1782.

Feuerstein, G., Wang, X., Barone, F.C., 1998. Cytokines in brain ischemia–the role of TNF alpha. Cell Mol. Neurobiol. 18, 695–701.

Gahring, L.C., Meyer, E.L., Rogers, S.W., 2003. Nicotine-induced neuroprotection against N-methyl-D-aspartic acid or beta-amyloid peptide occur through independent mechanisms distinguished by pro-inflammatory cytokines. J. Neurochem. 87, 1125–1136.

Galea, E., Feinstein, D.L., Reis, D.J., 1992. Induction of calcium-independent nitric oxide synthase activity in primary rat glial cultures. Proc. Natl. Acad. Sci. U S A 89, 10945–10949.

Gilby, K.L., Sydserff, S.G., Robertson, H.A., 2005. Differential neuroprotective effects for three GABA-potentiating compounds in a model of hypoxia-ischemia. Brain Res. 1035, 196–205.

Gronlien, J.H., Hakerud, M., Ween, H., Thorin-Hagene, K., Briggs, C.A., Gopalakrishnan, M., Malysz, J., 2007. Distinct profiles of alpha7 nAChR positive allosteric modulation revealed by structurally diverse chemotypes. Mol. Pharmacol. 72, 715–724.

Hejmadi, M.V., Dajas-Bailador, F., Barns, S.M., Jones, B., Wonnacott, S., 2003. Neuroprotection by nicotine against hypoxia-induced apoptosis in cortical cultures involves activation of multiple nicotinic acetylcholine receptor subtypes. Mol. Cell Neurosci. 24, 779–786.

Iadecola, C., Zhang, F., Xu, S., Casey, R., Ross, M.E., 1995. Inducible nitric oxide synthase gene expression in brain following cerebral ischemia. J. Cereb. Blood Flow Metab. 15, 378–384.

Ji, X., Li, C., Lu, Y., Chen, Y., Guo, L., 2007. Post-ischemic continuous administration of galantamine attenuates cognitive deficits and hippocampal neurons loss after transient global ischemia in gerbils. Neurosci. Lett. 416, 92–95.

Kihara, T., Sawada, H., Nakamizo, T., Kanki, R., Yamashita, H., Maelicke, A., Shimohama, S., 2004. Galantamine modulates nicotinic receptor and blocks Abeta-enhanced glutamate toxicity. Biochem. Biophys. Res. Commun. 325, 976–982.

Kihara, T., Shimohama, S., Sawada, H., Honda, K., Nakamizo, T., Shibasaki, H., Kume, T., Akaike, A., 2001. alpha 7 nicotinic receptor transduces signals to phosphatidylinositol 3-kinase to block A beta-amyloid-induced neurotoxicity. J. Biol. Chem. 276, 13541–13546.

Kox, M., van Velzen, J.F., Pompe, J.C., Hoedemaekers, C.W., van der Hoeven, J.G., Pickkers, P., 2009. GTS-21 inhibits pro-inflammatory cytokine release independent of the Toll-like receptor stimulated via a transcriptional mechanism involving JAK2 activation. Biochem. Pharmacol. 78, 863–872.

Lorrio, S., Sobrado, M., Arias, E., Roda, J.M., Garcia, A.G., Lopez, M.G., 2007. Galantamine postischemia provides neuroprotection and memory recovery against transient global cerebral ischemia in gerbils. J. Pharmacol. Exp. Ther. 322, 591–599.

Madrigal, J.L., Garcia-Bueno, B., Caso, J.R., Perez-Nievas, B.G., Leza, J.C., 2006. Stress-induced oxidative changes in brain. CNS Neurol. Disord. Drug Targets 5, 561–568.

Marzinzig, M., Nussler, A.K., Stadler, J., Marzinzig, E., Barthlen, W., Nussler, N.C., Beger, H.G., Morris Jr., S.M., Bruckner, U.B., 1997. Improved methods to measure end products of nitric oxide in biological fluids: nitrite, nitrate, and S-nitrosothiols. Nitric Oxide 1, 177–189.

Moriguchi, S., Marszalec, W., Zhao, X., Yeh, J.Z., Narahashi, T., 2004. Mechanism of action of galantamine on N-methyl-D-aspartate receptors in rat cortical neurons. J. Pharmacol. Exp. Ther. 310, 933–942.

Mosmann, T., 1983. Rapid colorimetric assay for cellular growth and survival: application to proliferation and cytotoxicity assays. J. Immunol. Methods 65, 55–63.

Negoro, S., Kunisada, K., Tone, E., Funamoto, M., Oh, H., Kishimoto, T., Yamauchi-Takihara, K., 2000. Activation of JAK/STAT pathway transduces cytoprotective signal in rat acute myocardial infarction. Cardiovasc. Res. 47, 797–805.

Parada, E., Egea, J., Romero, A., Del Barrio, L., Garcia, A.G., Lopez, M.G., 2010. Post-stress treatment with PNU 282987 can rescue SH-SY5Y cells undergoing apoptosis via alpha7 nicotinic receptors linked to a Jak2/Akt/HO-1 signaling pathway. Free Radic. Biol. Med. 49, 1815–1821.

Pereira, E.F., Hilmas, C., Santos, M.D., Alkondon, M., Maelicke, A., Albuquerque, E.X., 2002. Unconventional ligands and modulators of nicotinic receptors. J. Neurobiol. 53, 479–500.

Rane, S.G., Reddy, E.P., 2000. Janus kinases: components of multiple signaling pathways. Oncogene 19, 5662–5679.

Rojo, A.I., Salina, M., Salazar, M., Takahashi, S., Suske, G., Calvo, V., de Sagarra, M.R., Cuadrado, A., 2006. Regulation of heme oxygenase-1 gene expression through the phosphatidylinositol 3-kinase/PKC-zeta pathway and Sp1. Free Radic. Biol. Med. 41, 247–261.

Rothwell, N.J., Luheshi, G.N., 2000. Interleukin 1 in the brain: biology, pathology and therapeutic target. Trends Neurosci. 23, 618–625.

Sakai, I., Kraft, A.S., 1997. The kinase domain of Jak2 mediates induction of bcl-2 and delays cell death in hematopoietic cells. J. Biol. Chem. 272, 12350–12358.

Santos, M.D., Alkondon, M., Pereira, E.F., Aracava, Y., Eisenberg, H.M., Maelicke, A., Albuquerque, E.X., 2002. The nicotinic allosteric potentiating ligand galantamine facilitates synaptic transmission in the mammalian central nervous system. Mol. Pharmacol. 61, 1222–1234.

Schrattenholz, A., Pereira, E.F., Roth, U., Weber, K.H., Albuquerque, E.X., Maelicke, A., 1996. Agonist responses of neuronal nicotinic acetylcholine receptors are potentiated by a novel class of allosterically acting ligands. Mol. Pharmacol. 49, 1–6.

Sethi, G., Sung, B., Aggarwal, B.B., 2008. Nuclear factor-kappaB activation: from bench to bedside. Exp. Biol. Med. (Maywood) 233, 21–31.

Shaw, S., Bencherif, M., Marrero, M.B., 2002. Janus kinase 2, an early target of alpha 7 nicotinic acetylcholine receptor-mediated neuroprotection against Abeta-(1-42) amyloid. J. Biol. Chem. 277, 44920–44924.

Shen, H., Kihara, T., Hongo, H., Wu, X., Kem, W.R., Shimohama, S., Akaike, A., Niidome, T., Sugimoto, H., 2010. Neuroprotection by donepezil against glutamate excitotoxicity involves stimulation of alpha7 nicotinic receptors and internalization of NMDA receptors. Br. J. Pharmacol. 161, 127–139.

Sobrado, M., Roda, J.M., Lopez, M.G., Egea, J., Garcia, A.G., 2004. Galantamine and memantine produce different degrees of neuroprotection in rat hippocampal slices subjected to oxygen-glucose deprivation. Neurosci. Lett. 365, 132–136.

Stevens, T.R., Krueger, S.R., Fitzsimonds, R.M., Picciotto, M.R., 2003. Neuroprotection by nicotine in mouse primary cortical cultures involves activation of calcineurin and L-type calcium channel inactivation. J. Neurosci. 23, 10093–10099.

Sugano, N., Shimada, K., Ito, K., Murai, S., 1998. Nicotine inhibits the production of inflammatory mediators in U937 cells through modulation of nuclear factor-kappaB activation. Biochem. Biophys. Res. Commun. 252, 25–28.

Tabet, N., 2006. Acetylcholinesterase inhibitors for Alzheimer's disease: anti-inflammatories in acetylcholine clothing! Age Ageing 35, 336–338.

Takada-Takatori, Y., Kume, T., Sugimoto, M., Katsuki, H., Niidome, T., Sugimoto, H., Fujii, T., Okabe, S., Akaike, A., 2006. Neuroprotective effects of galanthamine and tacrine against glutamate neurotoxicity. Eur. J. Pharmacol. 549, 19–26.

Tariot, P.N., Solomon, P.R., Morris, J.C., Kershaw, P., Lilienfeld, S., Ding, C., 2000. A 5-month, randomized, placebo-controlled trial of galantamine in AD. The Galantamine USA-10 Study Group. Neurology 54, 2269–2276.

Thomsen, T., Kewitz, H., 1990. Selective inhibition of human acetylcholinesterase by galanthamine in vitro and in vivo. Life Sci. 46, 1553–1558.

Walder, C.E., Green, S.P., Darbonne, W.C., Mathias, J., Rae, J., Dinauer, M.C., Curnutte, J.T., Thomas, G.R., 1997. Ischemic stroke injury is reduced in mice lacking a functional NADPH oxidase. Stroke 28, 2252–2258.

Wilcock, G.K., Lilienfeld, S., Gaens, E., 2000. Efficacy and safety of galantamine in patients with mild to moderate Alzheimer's disease: multicentre randomised controlled trial. Galantamine International-1 Study Group. Br. Med. J. 321, 1445–1449.

Xu, J., Li, C., Yin, X.H., Zhang, G.Y., 2008. Additive neuroprotection of GABA A and GABA B receptor agonists in cerebral ischemic injury via PI-3K/Akt pathway inhibiting the ASK1-JNK cascade. Neuropharmacology 54, 1029–1040.

Zhou, W., Zhu, X., Zhu, L., Cui, Y.Y., Wang, H., Qi, H., Ren, Q.S., Chen, H.Z., 2008. Neuroprotection of muscarinic receptor agonist pilocarpine against glutamate-induced apoptosis in retinal neurons. Cell Mol. Neurobiol. 28, 263–275.

J. Pineal Res. 2014
Doi:10.1111/jpi.12113

Journal of Pineal Research
Molecular, Biological, Physiological and Clinical Aspects of

Neuroprotective effect of melatonin against ischemia is partially mediated by alpha-7 nicotinic receptor modulation and HO-1 Overexpression

Esther Parada[1], Izaskun Buendia[1], Rafael León[1,2], Pilar Negredo[3], Alejandro Romero[1,*], Antonio Cuadrado[1,4], Manuela G. López[1,2] and Javier Egea[1,2]

[1]Departamento de Farmacología y Terapéutica, Facultad de Medicina, Instituto Teófilo Hernando, Universidad Autónoma de Madrid, Madrid, Spain; [2]Instituto de Investigación Sanitaria, Hospital Universitario de la Princesa, Madrid, Spain; [3]Departamento de Anatomía, Histología y Neurociencia, Facultad de Medicina, Universidad Autónoma de Madrid, Madrid, Spain; [4]Department of Biochemistry, Faculty of Medicine, Centro de Investigación Biomédica en Red Sobre Enfermedades Neurodegenerativas (CIBERNED), Instituto de Investigación Sanitaria La Paz (IdiPaz), Instituto de Investigaciones Biomédicas 'Alberto Sols' UAM-CSIC, Autonomous University of Madrid, Madrid, Spain; *Present address: Department of Toxicology and Pharmacology, Faculty of Veterinary Medicine, Complutense University of Madrid 28040, Madrid, Spain

Key words: HO-1, ischemia, melatonin, neuroprotection, nicotinic receptors

Address reprint requests to Javier Egea, Departamento de Farmacología y Terapéutica, Facultad de Medicina, Instituto Teófilo Hernando, Universidad Autónoma de Madrid, Calle Arzobispo Morcillo, 4. 28029 Madrid, Spain.
E-mail: javier.egea@uam.es

Received September 9, 2013;
Accepted December 13, 2013.

RESUMEN

El efecto neuroprotector de melatonina ha sido ampliamente estudiado frente al estrés oxidativo. Sin embargo, todavía no se conoce el mecanismo por el cual ofrece efectos neuroprotectores frente a isquemia. En este estudio, hemos evaluado el efecto neuroprotector/antioxidante de melatonina en cultivo organotípico de rodajas de hipocampo y en el modelo de fototrombosis en ratón. Melatonina (0.1, 1 y 10 μM) incubada post-POG protegió de manera concentración dependiente, con una protección máxima del 90% a la concentración de 10 μM. A continuación, incubamos melatonina 10 μM a diferentes tiempos post-OGD, sin embargo, a 6 h se perdía el efecto neuroprotector. El efecto neuroprotector de melatonina y la reducción de ROS inducida por la POG se revirtieron con luzindol (antagonista de melatonina) y con α-bungarotoxina (antagonista de receptores nicotínicos α7). En ratones KO para el factor de transcripción Nrf-2, el efecto protector de la melatonina se redujo un 40%, lo que indica que Nrf-2 participa en el efecto protector de melatonina. Melatonina, incubada a 0, 1 y 2 h post-POG, aumentó la expresión de hemo oxigenasa-1 y esta expresión se redujo cuando se coincubó con luzindol y α-bungarotoxina. Por último, la administración de 15 mg/kg de melatonina después de la fototrombosis in vivo, redujo el volumen de infarto (50%) y mejoró la función motora. Este efecto se revirtió parcialmente (60%) en ratones inyectados con MLA 0.1 mg/kg. Estos resultados demuestran que la post-incubación de melatonina produce un efecto neuroprotector que depende, al menos en parte, de la activación de receptores nicotínicos y de la inducción de HO-1.

J. Pineal Res. 2014
Doi:10.1111/jpi.12113

Journal of Pineal Research
Molecular, Biological, Physiological and Clinical Aspects of

Neuroprotective effect of melatonin against ischemia is partially mediated by alpha-7 nicotinic receptor modulation and HO-1 overexpression

Abstract: Melatonin has been widely studied as a protective agent against oxidative stress. However, the molecular mechanisms underlying neuroprotection in neurodegeneration and ischemic stroke are not yet well understood. In this study, we evaluated the neuroprotective/antioxidant mechanism of action of melatonin in organotypic hippocampal cultures (OHCs) as well as in photothrombotic stroke model in vivo. Melatonin (0.1, 1, and 10 μM) incubated postoxygen and glucose deprivation (OGD) showed a concentration-dependent protection; maximum protection was achieved at 10 μM (90% protection). Next, OHCs were exposed to 10 μM melatonin at different post-OGD times; the protective effect of melatonin was maintained at 0, 1, and 2 hr post-OGD treatment, but it was lost at 6 hr post-OGD. The protective effect of melatonin and the reduction in OGD-induced ROS were prevented by luzindole (melatonin antagonist) and a-bungarotoxin (a-Bgt, a selective a7 nAChR antagonist). In Nrf2 knockout mice, the protective effect of melatonin was reduced by 40% compared with controls. Melatonin, incubated 0, 1, and 2 hr post-OGD, increased the expression of heme oxygenase-1 (HO-1), and this overexpression was prevented by luzindole and a-bungarotoxin. Finally, administration of 15 mg/kg melatonin following the induction of photothrombotic stroke in vivo, reduced infarct size (50%), and improved motor skills; this effect was partially lost in 0.1 mg/kg methyllycaconitine (MLA, selective a7 nAChR antagonist)-treated mice. Taken together, these results demonstrate that postincubation of melatonin provides a protective effect that, at least in part, depends on nicotinic receptor activation and overexpression of HO-1.

Esther Parada[1], Izaskun Buendia[1], Rafael León[1,2], Pilar Negredo[3], Alejandro Romero[1,*], Antonio Cuadrado[1,4], Manuela G. López[1,2] and Javier Egea[1,2]

[1]Departamento de Farmacología y Terapéutica, Facultad de Medicina, Instituto Teófilo Hernando, Universidad Autónoma de Madrid, Madrid, Spain; [2]Instituto de Investigación Sanitaria, Hospital Universitario de la Princesa, Madrid, Spain; [3]Departamento de Anatomía, Histología y Neurociencia, Facultad de Medicina, Universidad Autónoma de Madrid, Madrid, Spain; [4]Department of Biochemistry, Faculty of Medicine, Centro de Investigación Biomédica en Red Sobre Enfermedades Neurodegenerativas (CIBERNED), Instituto de Investigación Sanitaria La Paz (IdiPaz), Instituto de Investigaciones Biomédicas 'Alberto Sols' UAM-CSIC, Autonomous University of Madrid, Madrid, Spain; *Present address: Department of Toxicology and Pharmacology, Faculty of Veterinary Medicine, Complutense University of Madrid 28040, Madrid, Spain

Key words: HO-1, ischemia, melatonin, neuroprotection, nicotinic receptors

Address reprint requests to Javier Egea, Departamento de Farmacología y Terapéutica, Facultad de Medicina, Instituto Teófilo Hernando, Universidad Autónoma de Madrid, Calle Arzobispo Morcillo, 4. 28029 Madrid, Spain.
E-mail: javier.egea@uam.es

Received September 9, 2013;
Accepted December 13, 2013.

Introduction

Melatonin, a molecule produced in multiple tissues [1], plays important roles in many biological activities and participates in the regulation of diverse body functions including cancer inhibition [2], pain suppression [3], dendrite growth stimulation [4], inhibition of inflammation [5], and many others. Melatonin and its metabolites possess a potent antioxidant activity, and part of its therapeutic applications or preventive uses are based on this property [6, 7]. This indolamine was first shown to detoxify the highly toxic hydroxyl radical [8, 9], being more effective than its analogues [10]. Furthermore, the scavenging activity of melatonin includes most of the oxygen and nitrogen reactive species (ROS and RNS, respectively) such as hydrogen peroxide [11], peroxynitrite anion [12], and superoxide anion radical [13]. It also has been demonstrated that melatonin enhances the activities of a variety of antioxidative enzymes which include glutathione peroxidase and superoxide dismutase [14, 15]. Moreover, it has been demonstrated that melatonin has synergistic interactions with other antioxidants [16] and enhances the eficacy of a variety of drugs [17, 18].

Stroke is the second most common cause of death and the leading cause of adult disability [19]. Although treatments for ischemic stroke have been rigorously investigated for two decades, to date, there is only one approved, the intravenous thrombolytic treatment using recombinant tissue plasminogen activator (rt-PA) [20]. However, its use is limited by a brief therapeutic window (3–4.5 hr) and the potential side effects (intracranial hemorrhage). There is accumulating evidence implicating reactive oxygen species (ROS) and inflammation as mediators of acute responses of brain tissue to cerebral ischemia and its chronic progression [20, 21].

Melatonin has been widely tested in various different models of brain ischemia (i.e., middle cerebral artery occlusion (MCAO) and focal photothrombotic model) due to its potent antioxidant ability described above [6–12]. The ability of melatonin to protect the brain against ischemia/reperfusion was first described by Manev et al. [22], where these authors showed that pinealectomized rats had larger infarct volumes than control animals.

The redox-sensitive nuclear factor erythroid 2-related factor 2 (Nrf2) transcription factor is a master regulator of endogenous antioxidant defenses [23, 24] and is ubiquitously expressed. Given that the brain has a relatively inefficient enzymatic antioxidative defense system, Nrf2 may act as one of the most important defense systems against oxidative stress and inflammation [25, 26]. Nrf2 regulates the expression of phase II enzymes, such as heme oxygenase-1 (HO-1), which is cytoprotective against oxidative and inflammatory stress. HO-1 has a crucial metabolic function and serves as the rate-limiting step in the oxidative catabolism of the heme group. HO-1 induction has been related to cell protection in distinct cellular models including cerebral ischemia [27, 28].

The light/dark cycle modulates the function of many tissues including central and peripheral cholinergic synapses. Peripherally, it has been shown that the number and the response of nicotinic acetylcholine receptors (nAChRs) located on sympathetic nerve terminals of rat vas deferens [29] present a circadian rhythm [30, 31], which depends on nocturnal plasma levels of melatonin. In the central nervous system, a daily variation in nicotinic function and number of binding sites was also observed. In cerebellum, Markus et al. [32] demonstrated that [^{3}H]glutamate released from synaptosomes by stimulation of a7 nAChRs is different during the light and dark phases of the day and that the number of a-[^{125}I]bungarotoxin binding sites is also under lighting control.

Recently, we showed that pre-incubation of cells with the combination of subeffective concentrations of melato- nin and galantamine induces HO-1, which protects against oxidative stress [17]. Here, we described the neuroprotective effect of melatonin against OGD–reoxygenation, which, at least in part, depends on nicotinic receptor activation and overexpression of HO-1. Furthermore, we have defined the 'therapeutic window' incubating melatonin after OGD in the reoxygenation period.

Material and methods

Materials

The fluorescent dyes, propidium iodide (PI) and Hoechst 33,342 were from Life Technologies (Madrid, Spain). Anti-HO-1 was purchased from Millipore Corp. (Madrid, Spain) and anti-b-actin and melatonin from Sigma-Aldrich (Madrid, Spain).

Organotypic slice cultures (OHCs) preparation

Organotypic slice cultures (OHCs) were conducted on 8- to 10-day-old Sprague-Dawley rats or wild-type C57BL/6 mice and Nrf2 knockout of the same littermates. All animal assays were carried out following the Guide for the Care and Use of Laboratory Animals and were previously approved by the Institutional Ethics Committee of the Autonomous University of Madrid, Spain, according to the European guidelines for the use and care of animals for research in accordance with the European Union Directive of 22 September 2010 (2010/63/UE) and with the Spanish Royal Decree of 1 February 2013 (53/2013). All efforts were made to minimize the number of animals used and their suffering.

Cultures were prepared according to the methods described by Stoppini et al. [33] with some modifications [34]. Briefly, 300-μm-thick hippocampal slices were prepared from rats or mice pups using a Mcllwain tissue chopper and separated in ice-cold Hank's balanced salt solution (HBSS) composed of (in mM) the following: glucose 15, $CaCl_2$ 1.3, KCl 5.36, NaCl 137.93, KH_2PO_4 0.44, Na_2HPO_4 0.34, $MgCl_2$ 0.49, $MgSO_4$ 0.44, $NaHCO_3$ 4.1, HEPES 25; 100 U/mL penicillin, and 0.100 mg/mL genta- micin. Hippocampal slices were placed on Millicell 0.4-μm culture inserts (Millipore Corp.) within each well of a six- well culture tray with media, where they remained for 7 days. The culture media that consist of 50% minimal essential medium (MEM), 25% Hank's balanced salt solution, and 25% heat-inactivated horse serum were purchased from Life Technologies and 100U/mL penicillin. OHCs were cultivated in a humidified atmosphere at 37°C and 5% CO_2, and the medium was changed twice a week.

Induction of oxygen and glucose deprivation in OHCs

Oxygen deprivation and glucose deprivation were used as an in vitro model of cerebral ischemia. The inserts with slice cultures were placed into 1 mL of OGD solution composed of (in mM) the following: NaCl 137.93, KCl 5.36, $CaCl_2$ 2, $MgSO_4$ 1.19, $NaHCO_3$ 26, KH_2PO_4 1.18, and 2-deoxyglucose 11 (Sigma-Aldrich, Madrid, Spain). The cultures were then placed into an airtight chamber (Billups and Rothenberg, Del Mar, CA, USA) and were exposed for 5 min to 95% N_2/5% CO_2 gas flow to ensure oxygen deprivation. After that, the chamber was sealed for 15 min at 37°C. Control cultures were maintained for the same time under normoxic atmosphere, and 2-deoxyglucose was replaced by glucose 15 mM. After OGD period, slice cultures were returned to their original culture conditions for 24 hr. Melatonin was dissolved in dimethyl sulfoxide (DMSO), and stock solutions were prepared to ensure final concentration of 0.1% of DMSO. The same concentration of DMSO was added to basal and OGD conditions.

Propidium iodide and Hoechst imaging in OHCs

At the end of the experiment, OHCs were loaded with 1 μg/mL PI and Hoechst 33,342 (Hoechst) during the last 30 min of incubation. Mean PI and Hoechst fluorescence in CA1 region in each slice were analyzed. Fluorescence was measured in a fluorescence-inverted NIKON eclipse T2000-U microscope. Wavelengths of excitation and emission for PI and Hoechst were 530 or 350, and 580 or 460 nm, respectively. Images were taken at magnifications

of 10X. Fluorescence analysis was performed using the Metamorph program version 7.0. To calculate cell death, we divided the mean PI fluorescence by the mean Hoechst fluorescence. Data were normalized with respect to control values that were considered as 1.

ROS imaging in OHCs

To measure cellular ROS, we used the molecular probe H_2DCFDA as previously described [34]. Organotypic hippocampal slices were loaded with 5 μM H_2DCFDA. Fluorescence was measured in a fluorescence-inverted NIKON eclipse T2000-U microscope. Wavelengths of excitation and emission were 485 and 520 nm, respectively. Images were taken at magnifications of 10X. Fluorescence analysis was performed using the Metamorph program version 7.0. To calculate cell death, we divided the mean PI fluorescence by the mean Hoechst fluorescence. Data were normalized with respect to control values that were considered as 1.

Western blot analysis

Slices of each group were lysed in 100 μL ice-cold lysis buffer (1% Nonidet P-40, 10% glycerol, 137 mM NaCl, 20 mM Tris– HCl, pH 7.5, 1 μg/mL leupeptin, 1 mM phenylmethylsulfonyl fluoride, 20 mM NaF, 1 mM sodium pyrophosphate, and 1 mM Na_3VO_4). Proteins (30 μg) from these lysates were resolved by SDS–PAGE and transferred to Immobilon-P membranes (Mil- lipore Corp.). Membranes were incubated with anti-HO-1 (1:1000) and anti-b-actin (1:50,000). Appropriate peroxidase- conjugated secondary antibodies (1:10,000) were used to detect proteins by enhanced chemiluminescence. Protein bands were scanned and density was analyzed using the Scion Image program.

Culture of SH-SY5Y cells

SH-SY5Y cells were maintained in a 1:1 mixture of F-12 nutrient mixture (Ham12) (Sigma-Aldrich, Madrid, Spain) and Eagle's minimum essential medium (EMEM) supplemented with 15 nonessential amino acids, 1 mM sodium pyruvate, 10% heat-inactivated fetal bovine serum (FBS), 100 units/mL penicillin, and 100 μg/mL streptomycin (reagents from Life Technologies). Cultures were seeded into flasks containing supplemented medium and maintained at 37°C in a humidified atmosphere of 5% CO_2 and 95% air. For assays, SH-SY5Y cells were subcultured in 48-well plates at a seeding density of 1×10^5 cells per well. All the cells were used at a low passage number (<13).

Luciferase assays

Transient transfections of SH-SY5Y cells were performed with the expression vectors for Renilla (Promega, Madison, CA, USA) and 3xARE-Luc (Promega). Cells were seeded on 24-well plates (100,000 cells per well), cultured for 16 hr, and transfected using lipofectamine 2000 (Life Technologies). After overnight recovery from transfection, cells were treated for 24 hr with different concentrations of melatonin or tert-butylhydroquinone (tBHQ) as a positive control of Nrf2 induction. At the end of the treatment, cells were lysed and assayed for luciferase activity with a dual-luciferase assay system (Promega) according to the manufacturer's instructions. Relative light units were measured in a GloMax 96 microplate luminometer with dual injectors (Promega).

Photothrombotic stroke model in mice

All animal assays were carried out following the European Community Council Directive issued for these purposes and were approved by the Ethics Committee of the School of Medicine, Universidad Autónoma de Madrid. Every effort was made to minimize the number of animals used and their suffering. Mice were housed individually under controlled temperature and lighting conditions with food and water provided ad libitum. To induce ischemia, C57Bl6 mice were anesthetized with 1.5% isoflurane in oxygen under spontaneous respiration. Mice were then placed in a stereotaxic frame (David Kopf Instruments, Tujunga, CA, USA), and body temperature was maintained at 37 ± 0.5°C using a servo-controlled rectal probe heating pad (Cibertec, Madrid, Spain). A midline scalp incision was made, the skull was exposed with removal of the periosteum, and both bregma and lambda points were identified. A cold-light (Zeiss KL 1500 LCD, Jena, Germany) was centered using a micromanipulator at 0.2 mm posterior and 1.5 mm lateral to bregma on the right side using a fiber optic bundle of 2 mm in diameter. According to the Paxinos mouse brain atlas, the primary motor cortex, secondary motor cortex, and primary somatosensory cortex (hindlimb and forelimb) are lying beneath this stereotaxic position. One milligram (0.1 mL) of the photosensitive dye Rose Bengal (Sigma-Aldrich, St. Louis, MO, USA) dissolved in sterile saline was injected i.p., and 5 min later, the brains were illuminated through the intact skull for 20 min. After completion of the surgical procedures, the incision was sutured and the mice were allowed to recover. Mice were randomly divided into 3 groups: Group 1: subjected to ischemia and treated with 0.9% NaCl sterile saline solution containing 5% DMSO (saline); Group 2: treated with 15 mg/kg melatonin dissolved in saline containing 5% DMSO (melatonin) [35]; Group 3: treated with the combination of melatonin and methyllycaconitine 0.1 mg/kg (melatonin + MLA). Melatonin and MLA treatments were given i.p after ischemia.

Measurement of infarct volume

Animals were sacrificed by decapitation 24 hr after the ischemic insult. The brains were quickly removed and coronally sectioned into 1-mm-thick slices. For delineation of infarct area, the brain slices were incubated in a 2% solution of triphenyltetrazolium chloride and then fixed in a buffered formalin solution, and the unstained area was defined as infarcted tissue. Morphometric determination of cortical infarct volume was obtained using an unbiased stereological estimator of volume based on Cavalieri's principle [36].

Beam walk test (BWT)

Motor coordination of mice was assessed 24 hr after the photothrombotic stroke by measuring the number of contralateral hindpaw slips in the beam walk apparatus [37]. This test takes place over 3 consecutive days: 2 days of training and 1 day of testing. In the BWT, mice have to go through a 520-mm beam with a flat surface of 10 mm width resting 50 cm above the table top on two poles. A black goal box (150 mm × 150 mm × 150 mm) is placed at the end of the beam as the finish point. The amounts of hindpaw slips that occur in the process were counted.

Data analysis

Data are represented as means ± S.E.M. Comparisons between experimental and control groups were performed by one-way ANOVA followed by Newman–Keuls post hoc test or two-way ANOVA followed by Bonferroni post hoc test when appropriate. Differences were considered to be statistically significant when $P \leq 0.05$. All statistical procedures were carried out using GraphPad Prism software version 5.0 (La Jolla, CA, USA).

Results

To evaluate the protective properties of melatonin under OGD–reoxygenation conditions, OHCs were treated with melatonin at different concentrations (0.1, 1, and 10 μM) during the 24-hr reoxygenation period, beginning just after OGD. Fifteen-minutes OGD followed by 24-hr reoxygenation increased PI fluorescence in CA1 (1.54 ± 0.08) compared with basal condition (Fig. 1), and post-OGD treatment with increasing concentrations of melatonin reduced PI uptake. Melatonin significantly reduced cell death, measured as PI uptake, at the concentrations of 0.1 μM (1.28 ± 0.06), 1 μM (1.09 ± 0.12), and 10 μM (1.14 ± 0.04) in comparison with OHCs exposed only to OGD (1.54 ± 0.08). Maximum protection was achieved at the concentration of 10 μM (90%, $P < 0.001$).

Next, OHCs were exposed to 10 μM melatonin at different post-OGD times (0, 1, 2, and 6 hr post-OGD) to define the 'therapeutic window' of the neuroprotective effect of melatonin. As shown in Fig. 2, 15-min OGD followed by 24-hr reoxygenation increased cell death by 1.6-fold. Neuroprotection provided by 10 μM melatonin was significantly preserved at 0, 1, and 2 hr post-OGD ($P < 0.05$, $P < 0.01$, and $P < 0.05$, respectively). However, this protective effect was lost when melatonin was added 6 hr post-OGD. These results suggest that melatonin has a 'therapeutic window' of at least 2 hr post-OGD to observe neuroprotection in OHCs.

In the central nervous system, a daily variation in nicotinic function and number of binding sites was observed and this efect was related to melatonin's action [32]. Hence, we wanted to prove whether part of the neuroprotective efect of melatonin against OGD–reoxygenation could be mediated by this receptor. We followed the protocol illustrated in Fig. 1 in the absence or presence of a-bungarotoxin (a-Bgt, 100 nM), a selective a7 nAChR

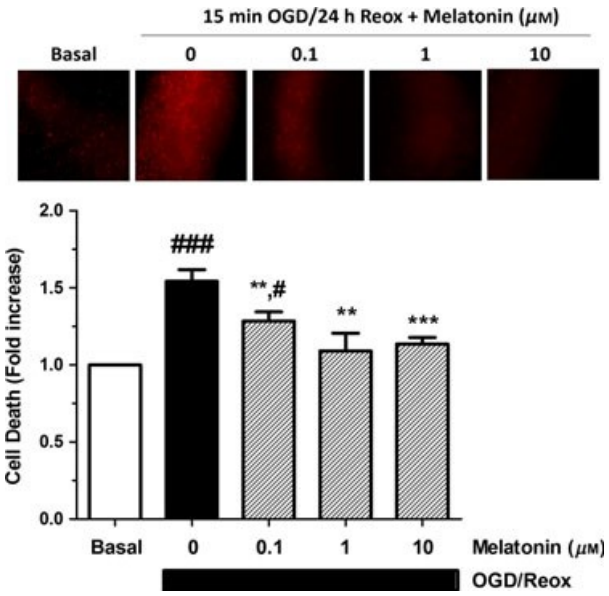

Fig. 1. Postoxygen and glucose deprivation (OGD) treatment with melatonin afforded protection in organotypic slices subjected to OGD–reoxygenation. Organotypic slices were subjected to 15 min OGD followed by 24-hr reoxygenation in the absence OGD or presence of 0.1, 1, or 10 μM melatonin; a parallel group of slices were kept during the same period of time with oxygen and glucose (Basal). Photomicrographs (original magnification 10×) of the CA1 subfield loaded with PI are shown on the top. Concentration– response curve of melatonin (0.1, 1, and 10 μM) incubated for 24 hr after the OGD period, measured by PI/Hoechst in the CA1 subfield. Values are expressed as means ± S.E.M. of five different experi- ments, $^{***}P < 0.001$, $^{**}P < 0.01$ compared with the OGD-treated slices, $^{###}P < 0.001$, $^{#}P < 0.05$, with respect to the basal.

antagonist, or luzindole 1 μM, a melatonin receptor antagonist (Fig. 3A). Inhibition of cell death associated with OGD–reoxygenation by melatonin 10 μM was abrogated by a-Bgt and luzindole, suggesting that this protective effect is indeed mediated via melatonin receptors and a7 nAChR activation. As illustrated in Fig. 3B, melatonin markedly reduced ROS production measured in OHCs subjected to OGD–reoxygenation stained with the fluorescent dye DFCDA. OGD followed by reoxygenation increased by 2.1-fold the ROS production in hippocampal slice cultures. In melatonin-treated slices, ROS production was significantly reduced almost to basal levels. As in the case of the neuroprotective effect, the reduction in ROS was prevented by the melatonin antagonist luzindole and the nicotinic antagonist a-bungarotoxin, indicating the participation of melatonin and nicotinic receptors in the reduction in ROS production by melatonin.

As stated in the introduction, melatonin possesses a potent antioxidant activity based principally on its scavenging capacity. Besides its scavenging capacity, we wanted to test the possibility that melatonin could activate the transcription factor Nrf2, a master regulator of the antioxidant defense system. Therefore, SH-SY5Y cells were transfected with 3xARE-Luc and Renilla vectors, and after overnight recovery, cells were stimulated for 24 hr with increasing concentrations of melatonin (0.01, 0.1, 1, 10, and 30 μM) and with tBHQ at 10 μM as a

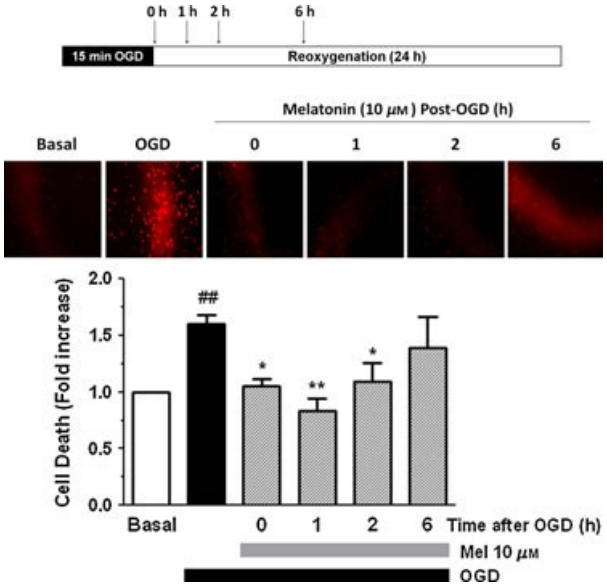

Fig. 2. Time dependence of the protective effect of melatonin administered postoxygen and glucose deprivation (OGD). Proto- col used to elicit toxicity: organotypic hippocampal cultures (OHCs) were exposed for 15 min to OGD followed by 24 hr in control solution (reoxygenation). Melatonin was added at differ- ent times post-OGD (0, 1, 2, and 6 hr) and remained until com- pletion of the 24-hr reoxygenation period. Photomicrographs (original magnification 10X) of the CA1 subfield loaded with PI are shown on the top. The bottom of the figure shows averaged data of five different experiments indicating cell death measured as the ratio PI/Hoechst fluorescence in the CA1 subfield. Values are expressed as means ± S.E.M., $^{**}P < 0.01$, $^{*}P < 0.05$ compared with the OGD-treated slices, $^{\#\#}P < 0.01$, with respect to the basal.

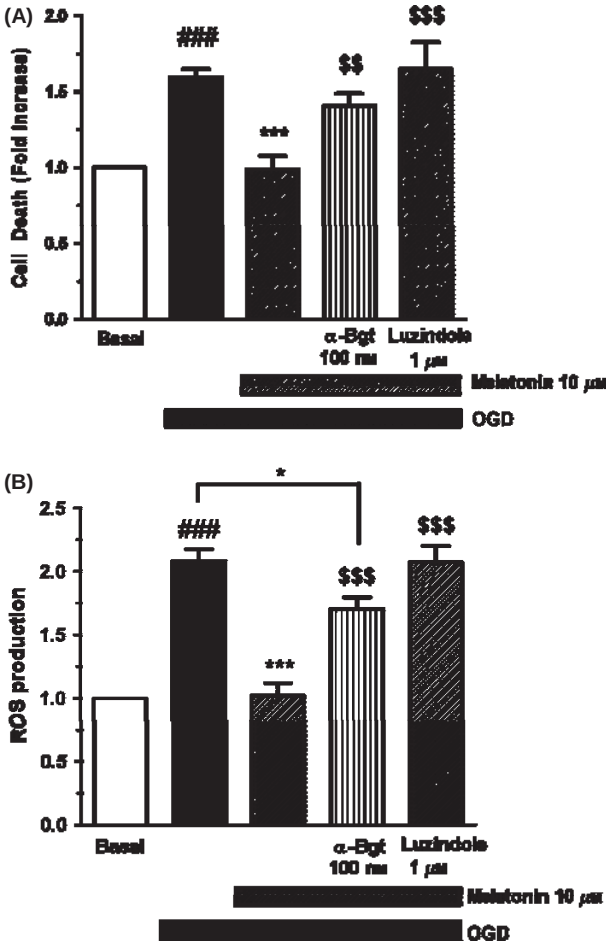

Fig. 3. Protection elicited by postoxygen and glucose deprivation (OGD) treatment with melatonin is mediated by reduction in ROS through melatonin receptors and a7 nAChRs. Organotypic hippocampal cultures (OHCs) were exposed to 15 min of OGD and then incubated with 10 μM melatonin for 24 hr in the pres- ence or absence of 100 nM a-bungarotoxin (a-Bgt) and 1 μM luzin- dole. (A) shows averaged data of five different experiments indicating cell death measured as the ratio PI/Hoechst fluorescence in the CA1 subfield. (B) shows averaged data of four different exper- iments indicating ROS production measured using DFCDA in the CA1 subfield. Values are mean ± S.E.M., $^{\#\#\#}P < 0.001$ compared with the untreated slices, $^{*}P < 0.05$ and $^{***}P < 0.001$ with respect to the OGD-treated slices, $^{\$\$\$}P < 0.001$, $^{\$\$}P < 0.01$ compared with melatonin-treated slices.

positive control. As shown in Fig. 4A, melatonin increased reporter gene activity in a concentration-dependent man- ner with a maximum of twofold at the concentration of 10 μM, similar to that obtained by the positive control tBHQ at 10 μM.

Once demonstrated that melatonin could activate the transcription factor Nrf2, we tested the participation of Nrf2 in the protective effect of melatonin in OHCs sub- jected to OGD–reoxygenation. For this purpose, we used OHCs obtained from Nrf2 knockout (−/−) and wild-type mice (+/+) of the same littermate. The protective effect afforded by 10 μM melatonin, administered post-OGD, and increased cell viability in OHCs from +/+ mice, as expected. However, this protection was reduced by 40% in OHCs from Nrf2 −/− mice (Fig. 4B). Therefore, Nrf2 seemed to be partially required in the neuroprotective effect afforded by melatonin under OGD–reoxygenation conditions.

To corroborate the overexpression of antioxidant and anti- inflammatory phase II enzymes under our experimen- tal conditions, we followed the protocol shown in Fig. 2. At the end of the experiment, OHCs were collected and cell lysates were resolved in SDS–PAGE and analyzed by immunoblot with anti-HO-1 antibody. Melatonin, at 10 μM, significantly increased by 1.7-, 1.8-, and 1.9-fold the expression of HO-1 at times 0, 1, and 2 hr post-OGD, respectively (Fig. 5A). However, when melatonin was incubated 6 hr post-OGD, there was no significant increase in HO-1 expression, agreeing with the loss of protection (Fig. 5A). Next, we wanted to prove whether HO-1 overexpression was linked to melatonin receptor and a7 nAChR activation. As shown in Fig. 5B, mela- tonin at 10 μM increased the expression of HO-1 by 1.6-fold. This effect was reversed by a-Bgt and luzindole, suggesting the participation of melatonin receptors and a7 nAChRs in the overexpression of HO-1. To sum up, melatonin augmented the expression of phase II enzymes at post-OGD times where the protective effect was observed, and this effect is related to melatonin and nicotinic receptors.

Finally, we used the photothrombotic model of stroke in mice to evaluate whether the protective effects of melatonin

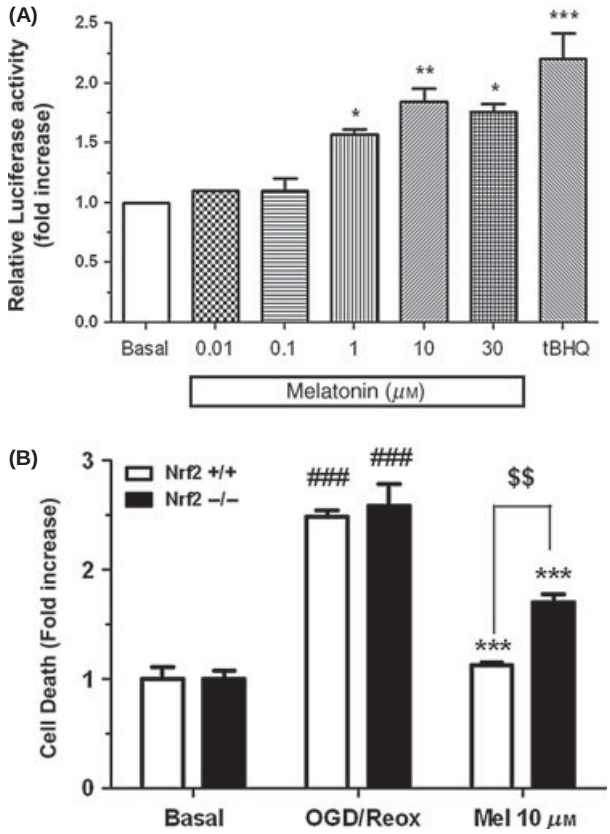

Fig. 4. The neuroprotective effect of postoxygen and glucose deprivation (OGD) treatment with melatonin is mediated by Nrf2 activation. (A) SH-SY5Y cells were transfected with the 3xARE-Luc and Renilla control vectors, and after transfection, cells were treated with melatonin (0.01, 0.1, 1, 10, and 30 μM) or with tBHQ at 10 μM for 24 hr before luciferase activity was measured. Data are means ± S.E.M. of five different experiments, *P < 0.05, ** P < 0.01, ***P < 0.001 compared with the basal. (B) Organotypic slices from Nrf2 wild-type (Nrf2 + /+) and null mice (Nrf2−/−) were subjected to 15 min OGD followed by 24-hr reoxygenation in the absence (OGD) or presence of 10 μM melatonin; another group of slices were kept during the same period of time with oxygen and glucose (Basal). Data are means ± S.E.M. of five different experiments, ***P < 0.001, compared with the OGD- treated slices, ###P < 0.001, with respect to the basal, $$P < 0.01 Nrf2 + /+ vs Nrf2−/− treated with melatonin.

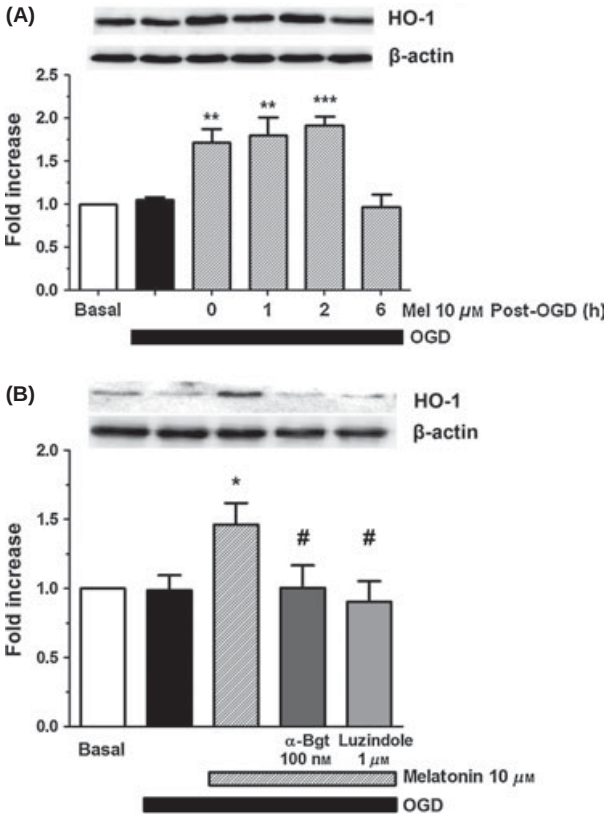

Fig. 5. The protective effect of postoxygen and glucose deprivation (OGD) administration of melatonin is linked to overexpression of HO-1 and modulation of a7 nAChRs. (A) The top part of the figure illustrates representative immunoblots showing the expression of HO-1 obtained from hippocampal slices subjected to the experimental conditions following the protocol shown in Fig. 2. Expression of HO-1 is represented as densitometric quantification using b-actin for normalization (bottom). Melatonin 10 μM caused an increment in the expression of HO-1 at times 0, 1, and 2 hr post-OGD. Data correspond to the mean ± S.E.M. of 5 experiments. **P < 0.01, ***P < 0.001 compared with control slices. (B) Representative immunoblot of HO-1 induction by melatonin in the absence or presence of 100 nM a-Bgt and 1 μM luzindole. The histogram represents the densitometric quantification of HO-1 using b-actin for normalization. Data correspond to the mean ± S.E.M. of 5 experiments. *P < 0.05 with respect to the basal, #P < 0.05 compared with the melatonin-treated slices.

act under brain ischemic conditions in vivo [38]. Following the protocol shown in Fig. 6A, ischemia induced by photothrombosis caused a mean cortical infarct volume of 15.6 ± 0.9%. Administration of melatonin (15 mg/kg, i.p.) postphotothrombosis reduced infarct volume by 45% (8.5 ± 0.7%). Co-administration of melatonin with MLA, 0.1 mg/kg, a selective a7 nAChRs antagonist, prevented the neuroprotective effect of melatonin by 59% (12.7 ± 0.8%) (Fig. 6B and C). Reduction in the infarct volume correlated with improved motor coordination measured as hindpaw slips in the beam walking test (Fig. 6D).

Discussion

In the present study, we provide novel data on the neuroprotective role of melatonin against ischemia–reoxygenation in OHCs and in an in vivo model of photothrombotic stroke. Furthermore, we have defined the 'therapeutic window' of melatonin administered post-ischemia (Fig. 2). Melatonin induces neuroprotection through a mechanism that includes the following: (i) activation of melatonin receptor, (ii) modulation of a7 nAChRs (Fig. 3), (iii) reduction in ROS production (Fig. 3), and (iv) overexpression of phase II enzymes including the anti-inflammatory and antioxidant enzyme HO-1 (Figs 4 and 5). Therefore, this work documents that the neuroprotective effect of melatonin against brain ischemia occurs both in vitro and in vivo (Fig. 6) through the same mechanism, which involves the activation of the transcription factor Nrf2. This idea is supported by the fact that (i) melatonin activated the transcription factor Nrf2, (ii) in Nrf2 knockout mice, the neuroprotective effect of melatonin

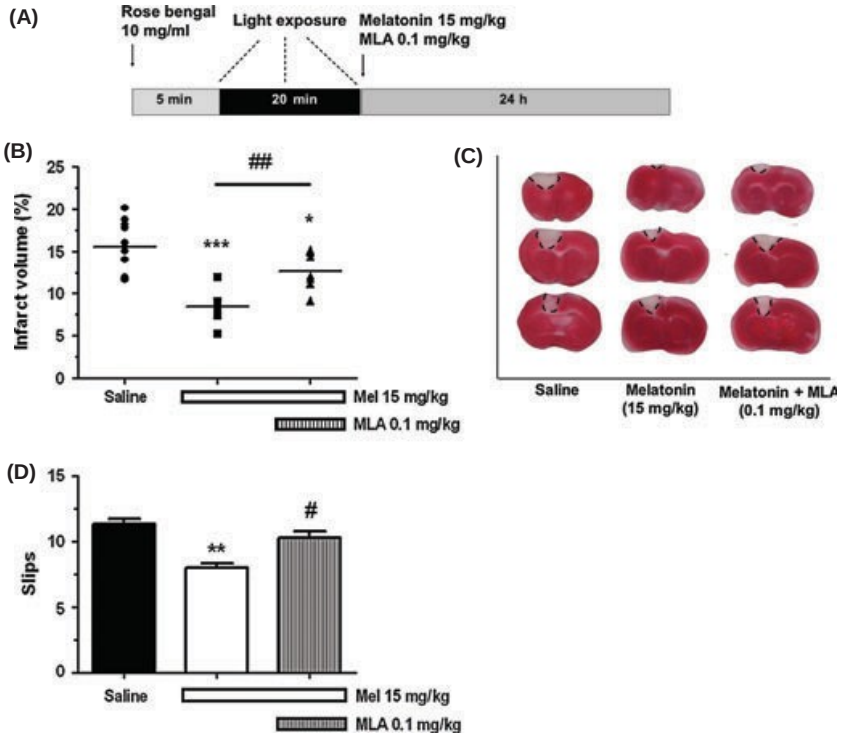

Fig. 6. Melatonin reduces infarct volume and promotes functional recovery in mice subjected to photothrombotic stroke depending on modulation of a7 nAChRs. (A) illustrates the protocol used, in which melatonin (i.p at 15 mg/Kg) and/or methyllycaconitine (MLA) (i.p. at 0.1 mg/Kg) were administered just after the photothrombotic stroke. (B) Data are expressed as percentage (%) of cortical infarct volume in mice. (C) Note that reduction in infarct in mice receiving melatonin was partially prevented by the a7 nAChR antagonist MLA. (D) Motor skills analyzed with the beam walk test 24 hr after ischemia by quantification of hindpaw slips (see Material and methods). Data are expressed as mean ± S.E.M. of 8 animals per group. *P < 0.05, ** P < 0.01, and ***P < 0.001 compared with ischemia plus saline group, $^{\#}$P < 0.05 and $^{\#\#}$ P < 0.01 in comparison with melatonin- treated group.

was reduced by 40% (Fig 4), and (iii) melatonin augmented the expression of the phase II enzyme HO-1 at post-OGD times where the protective effect was observed (Fig. 5).

Taking into account the ability of melatonin to reduce oxidative damage caused by ischemia in other organs, such as heart [39], liver [40], and kidney [41], our aim was to study the neuroprotective effect of melatonin incubated post-OGD, against cell death caused by brain ischemia. In our hands, melatonin maintains its neuroprotective effect when added 2 hr after ischemia onset. However, melatonin did not afford neuroprotection when added 6 hr after ischemia (Fig. 2). The protective effect of melatonin administrated before ischemia or reperfusion onset has been widely studied [42], and in the recent years, additional investigations have been designed to study the protective effect of melatonin postischemia, which is closer to a clinical situation, where the drug is usually applied after a stroke patient is identified. Recently, it has been reported that the neuroprotective effect of melatonin administrated 1 hr after MCAO in rats is mediated by a decrease in iNOS activity and nitrite levels [43]. Our results are in line with those described by Nair et al., and we have shown that melatonin is able to protect given postischemia in the OHC in vitro model and is able to reduce OGD-induced ROS production to basal levels (Fig. 3). Furthermore, melatonin administrated 2 hr after MCAO in mice promotes neurogenesis and reduces infarction [44]. In our hands, melatonin 15 mg/kg reduces infarct volume and improves motor skills given postischemia (Fig. 6). Given the fact that melatonin is an endogenous molecule with minimal side effects even at high pharmacological doses [45], and protects administered post-ischemia, lead us to consider melatonin as a potential neuroprotectant drug against brain ischemia.

Melatonin modulates both central and peripheral nAChRs [31, 32]. It has been shown that vas deferens contraction induced by acetylcholine in rats has a remarkable daily rhythm in nAChR activity that is driven by nocturnal plasma melatonin. In another model, using the analysis of glutamate release in cerebellar synaptosomes or cerebellar slices induced by nicotine, variability in the response was shown to be dependent on the presence or absence of melatonin. Moreover, exogenous melatonin has also been shown to improve the neuropathological, behavioral, and biochemical changes in a transgenic mouse model, by ameliorating the spatial memory impairment induced by cholinergic dysfunction [46]. Recently, it has been shown that melatonin significantly decreases duodenal mucosal paracellular permeability by a nAChR-dependent mechanism [47]. Here, we have demonstrated the importance of a7 nAChRs modulation in the neuroprotective effect of melatonin against ischemia. The protective effect observed in OHCs treated with melatonin depends, partially, on the modulation of a7 nAChRs because co-incubation with a-Bgt prevents the neuroprotective effect observed with melatonin (Fig. 3). We corroborated this result using the in vivo model of photothrombotic stroke. Co-administration of MLA with melatonin impedes both the protective effect and the improvement in motor coordination (Fig. 6). Hence, taking into account the cellular protective effects of melatonin and the dependence on this molecule for some physiological cholinergic responses, the decline in the pineal production of melatonin with age could represent a condition that favors the manifestation of age-related diseases, such as ischemia or Alzheimer's disease.

Nrf2 is a master regulator of cellular redox homeostasis and regulates the expression of different proteins with antioxidant and anti-inflammatory properties (phase II

enzymes) including HO-1. Induction of HO-1 has generally been considered to be an adaptive cellular response against the toxicity of oxidative stress [48, 49]. It has been demonstrated in a HO-1 knockout mice model that these animals develop a chronic inflammatory disease [50]. The protective effect observed in OHCs treated with melatonin depends, partially, on the activation of this transcription factor, because in $Nrf2^{-/-}$ mice, the neuroprotective effect of melatonin was reduced by 40% (Fig. 4). Moreover, the protective effect of postincubated melatonin seems to be linked to modulation of a7 nAChRs and overexpression of HO-1 (Fig. 5), which has potent antioxidant and anti-inflammatory effects. Recently, we have demonstrated the critical role of microglial α7 nAChRs activation and HO-1 overexpression in the protective effect against brain ischemia [34]. Furthermore, we have shown that the protective effect of the combination of subeffective concentrations of melatonin and galantamine depends on HO-1 overexpression [17]. Taking into account these data, we hypothesized that HO-1 overexpression due to melatonin administration depends on modulation of α7 nAChRs.

In conclusion, melatonin administered postischemia provides a neuroprotective effect that, at least in part, is related to (i) modulation of α7 nAChRs, (ii) reduction in ROS production, and (iii) activation of the transcription factor Nrf2 followed by overexpression of phase II enzymes such as HO-1, which has a potent antioxidant and anti-inflammatory effect.

Acknowledgements

This work was supported in part by grants from Spanish Ministry of Science and Innovation Ref. SAF2012-32223 to MGL and European Commission, Marie Curie Actions FP7 (FP7-People-2012-CIG-322156) to RL, and IS Carlos III, Programa Miguel Servet (CP11/00165) to RL. We would also like to thank 'Fundación Teófilo Hernando' for its continued support.

Author contributions

Esther Parada and Izaskun Buendia have contributed to acquisition of data and data analysis/interpretation. Rafael León and Pilar Negredo have contributed to acquisition of data, data analysis/interpretation, and critical revision of the manuscript. Alejandro Romero and Antonio Cuadrado have contributed to critical revision of the manuscript. Manuela G. López has contributed to concept/design, drafting of the manuscript, critical revision of the manuscript, and approval of the article. Javier Egea has contributed to concept/design, acquisition of data, data analysis/interpretation, drafting of the manuscript, critical revision of the manuscript, and approval of the article.

References

1. Reiter RJ, Tan DX, Rosales-Corral S et al. The universal nature, unequal distribution and antioxidant functions of melatonin and its derivatives. Mini Rev Med Chem 2013; 13:373–384.
2. Zha L, Fan L, Sun G et al. Melatonin sensitizes human hepatoma cells to endoplasmic reticulum stress-induced apoptosis. J Pineal Res 2012; 52:322–331.
3. Gitto E, Aversa S, Salpietro CD et al. Pain in neonatal intensive care: role of melatonin as an analgesic antioxidant. J Pineal Res 2012; 52:291–295.
4. Dominguez-Alonso A, Ramirez-Rodriguez G, Benitez-King G. Melatonin increases dendritogenesis in the hilus of hippocampal organotypic cultures. J Pineal Res 2012; 52:427–436.
5. Mauriz JL, Collado PS, Veneroso C et al. A review of the molecular aspects of melatonin's anti-inflammatory actions: recent insights and new perspectives. J Pineal Res 2012. doi: 10.1111/j.1600-079X.2012.01014.x.
6. Galano A, Tan DX, Reiter RJ. Melatonin as a natural ally against oxidative stress: a physicochemical examination. J Pineal Res 2011; 51:1–16.
7. Galano A, Tan DX, Reiter RJ. On the free radical scavenging activities of melatonin's metabolites. AFMK and AMK. J Pineal Res 2013; 54:245–257.
8. Tan DX, Chen LD, Poeggeler B et al. Melatonin: a potent, endogenous hydroxyl radical scavenger. Endocr J 1993; 1:57–60.
9. Poeggeler B, Reiter RJ, Tan DX et al. Melatonin, hydroxyl radical-mediated oxidative damage, and aging: a hypothesis. J Pineal Res 1993; 14:151–168.
10. Poeggeler B, Thuermann S, Dose A et al. Melatonin's unique radical scavenging properties – roles of its functional substituents as revealed by a comparison with its structural analogs. J Pineal Res 2002; 33:20–30.
11. Tan DX, Manchester LC, Reiter RJ et al. Melatonin directly scavenges hydrogen peroxide: a potentially new metabolic pathway of melatonin biotransformation. Free Radic Biol Med 2000; 29:1177–1185.
12. Reiter RJ, Tan DX, Manchester LC et al. Biochemical reactivity of melatonin with reactive oxygen and nitrogen species: a review of the evidence. Cell Biochem Biophys 2001; 34:237–256.
13. Ximenes VF, Silva SO, Rodrigues MR et al. Superoxide-dependent oxidation of melatonin by myeloperoxidase. J Biol Chem 2005; 280:38160–38169.
14. Rodriguez C, Mayo JC, Sainz RM et al. Regulation of antioxidant enzymes: a significant role for melatonin. J Pineal Res 2004; 36:1–9.
15. Tomas-Zapico C, Coto-Montes A. A proposed mechanism to explain the stimulatory effect of melatonin on antioxidative enzymes. J Pineal Res 2005; 39:99–104.
16. Lopez-Burillo S, Tan DX, Mayo JC et al. Melatonin, xanthurenic acid, resveratrol, EGCG, vitamin C and alpha-lipoic acid differentially reduce oxidative DNA damage induced by Fenton reagents: a study of their individual and synergistic actions. J Pineal Res 2003; 34:269–277.
17. Romero A, Egea J, Garcia AG et al. Synergistic neuroprotective effect of combined low concentrations of galantamine and melatonin against oxidative stress in SH-SY5Y neuroblastoma cells. J Pineal Res 2010; 49:141–148.
18. Reiter RJ, Tan DX, Sainz RM et al. Melatonin: reducing the toxicity and increasing the e□cacy of drugs. J Pharm Pharmacol 2002; 54:1299–1321.
19. Balami JS, Chen RL, Grunwald IQ et al. Neurological complications of acute ischaemic stroke. Lancet Neurol 2011; 10:357–371.
20. Lakhan SE, Kirchgessner A, Hofer M. Inflammatory mechanisms in ischemic stroke: therapeutic approaches. J Transl Med 2009; 7:97.

21. Jung JE, Kim GS, Chen H et al. Reperfusion and neurovascular dysfunction in stroke: from basic mechanisms to potential strategies for neuroprotection. Mol Neurobiol 2010; 41:172–179.
22. Manev H, Uz T, Kharlamov A et al. Increased brain damage after stroke or excitotoxic seizures in melatonin-deficient rats. FASEB J 1996; 10:1546–1551.
23. Kensler TW, Wakabayashi N, Biswal S. Cell survival responses to environmental stresses via the Keap1-Nrf2-ARE pathway. Annu Rev Pharmacol Toxicol 2007; 47:89–116.
24. Kaspar JW, Niture SK, Jaiswal AK. Nrf 2:INrf2 (Keap1) signaling in oxidative stress. Free Radic Biol Med 2009; 47:1304–1309.
25. Shah ZA, Li RC, Thimmulappa RK et al. Role of reactive oxygen species in modulation of Nrf2 following ischemic reperfusion injury. Neuroscience 2007; 147:53–59.
26. Innamorato NG, Rojo AI, Garcia-Yague AJ et al. The transcription factor Nrf2 is a therapeutic target against brain inflammation. J Immunol 2008; 181:680–689.
27. Kim YS, Zhuang H, Koehler RC et al. Distinct protective mechanisms of HO-1 and HO-2 against hydroperoxide-induced cytotoxicity. Free Radic Biol Med 2005; 38:85–92.
28. Yang C, Zhang X, Fan H et al. Curcumin upregulates transcription factor Nrf2, HO-1 expression and protects rat brains against focal ischemia. Brain Res 2009; 1282:133–141.
29. Carneiro RC, Markus RP. Presynaptic nicotinic receptors involved in release of noradrenaline and ATP from the prostatic portion of the rat vas deferens. J Pharmacol Exp Ther 1990; 255:95–100.
30. Carneiro RC, Cipolla-Neto J, Markus RP. Diurnal variation of the rat vas deferens contraction induced by stimulation of presynaptic nicotinic receptors and pineal function. J Pharmacol Exp Ther 1991; 259:614–619.
31. Markus RP, Zago WM, Carneiro RC. Melatonin modulation of presynaptic nicotinic acetylcholine receptors in the rat vas deferens. J Pharmacol Exp Ther 1996; 279:18–22.
32. Markus RP, Santos JM, Zago W et al. Melatonin nocturnal surge modulates nicotinic receptors and nicotine-induced [3H] glutamate release in rat cerebellum slices. J Pharmacol Exp Ther 2003; 305:525–530.
33. Stoppini L, Buchs PA, Muller D. A simple method for organotypic cultures of nervous tissue. J Neurosci Methods 1991; 37:173–182.
34. Parada E, Egea J, Buendia I et al. The microglial alpha7-acetylcholine nicotinic receptor is a key element in promoting neuroprotection by inducing heme oxygenase-1 via nuclear factor erythroid-2-related factor 2. Antioxid Redox Signal 2013; 19:1135–1148.
35. Zou LY, Cheung RT, Liu S et al. Melatonin reduces infarction volume in a photothrombotic stroke model in the wild-type but not cyclooxygenase-1-gene knockout mice. J Pineal Res 2006; 41:150–156.
36. Avendano C, Roda JM, Carceller F et al. Morphometric study of focal cerebral ischemia in rats: a stereological evaluation. Brain Res 1995; 673:83–92.
37. Quinn LP, Perren MJ, Brackenborough KT et al. A beam-walking apparatus to assess behavioural impairments in MPTP-treated mice: pharmacological validation with R-(-)-deprenyl. J Neurosci Methods 2007; 164:43–49.
38. de Ryck M, van Reempts J, Borgers M et al. Photochemical stroke model: flunarizine prevents sensorimotor deficits after neocortical infarcts in rats. Stroke 1989; 20:1383–1390.
39. Reiter RJ, Tan DX. Melatonin: a novel protective agent against oxidative injury of the ischemic/reperfused heart. Cardiovasc Res 2003; 58:10–19.
40. Okatani Y, Wakatsuki A, Reiter RJ et al. Protective effect of melatonin against mitochondrial injury induced by ischemia and reperfusion of rat liver. Eur J Pharmacol 2003; 469:145–152.
41. Sener G, Sehirli AO, Keyer-Uysal M et al. The protective effect of melatonin on renal ischemia-reperfusion injury in the rat. J Pineal Res 2002; 32:120–126.
42. Reiter RJ, Tan DX, Leon J et al. When melatonin gets on your nerves: its beneficial actions in experimental models of stroke. Exp Biol Med (Maywood) 2005; 230:104–117.
43. Nair SM, Rahman RM, Clarkson AN et al. Melatonin treatment following stroke induction modulates L-arginine metabolism. J Pineal Res 2011; 51:313–323.
44. Chern CM, Liao JF, Wang YH et al. Melatonin ameliorates neural function by promoting endogenous neurogenesis through the MT2 melatonin receptor in ischemic-stroke mice. Free Radic Biol Med 2012; 52:1634–1647.
45. Sezabra ML, Bignotto M, Pinto LR Jr et al. Randomized, double-blind clinical trial, controlled with placebo, of the toxicology of chronic melatonin treatment. J Pineal Res 2000; 29:193–200.
46. Feng Z, Chang Y, Cheng Y et al. Melatonin alleviates behavioral deficits associated with apoptosis and cholinergic system dysfunction in the APP 695 transgenic mouse model of Alzheimer's disease. J Pineal Res 2004; 37:129–136.
47. Sommansson A, Nylander O, Sjoblom M. Melatonin decreases duodenal epithelial paracellular permeability via a nicotinic receptor-dependent pathway in rats in vivo. J Pineal Res 2013; 54:282–291.
48. Vile GF, Basu-Modak S, Waltner C et al. Heme oxygenase 1 mediates an adaptive response to oxidative stress in human skin fibroblasts. Proc Natl Acad Sci U S A 1994; 91:2607–2610.
49. Gozzelino R, Jeney V, Soares MP. Mechanisms of cell protection by heme oxygenase-1. Annu Rev Pharmacol Toxicol 2010; 50:323–354.
50. Poss KD, Tonegawa S. Reduced stress defense in heme oxygenase 1-deficient cells. Proc Natl Acad Sci U S A 1997; 94:10925–10930.

ANTIOXIDANTS & REDOX SIGNALING
Volume 19, Number 11, 2013
Mary Ann Liebert, Inc.
DOI: 10.1089/ars.2012.4671

Therapeutics

ORIGINAL RESEARCH COMMUNICATION

The Microglial α7-Acetylcholine Nicotinic Receptor Is a Key Element in Promoting Neuroprotection by Inducing Heme Oxygenase-1 via Nuclear Factor Erythroid-2-Related Factor 2

Esther Parada,[1,*] Javier Egea,[1,2,*] Izaskun Buendia,[1] Pilar Negredo,[1,3,4] Ana C. Cunha,[5] Silvia Cardoso,[5] Miguel P. Soares,[5] and Manuela G. López[1,3]

[1]Instituto Teófilo Hernando and Department of Pharmacology, School of Medicine, Universidad Autónoma de Madrid, Madrid, Spain.
[2]Instituto de Investigación Sanitaria Hospital Universitario La Princesa-IP, Universidad Autónoma de Madrid, Madrid, Spain.
[3]Instituto Universitario la Paz-IdiPaz, Universidad Autónoma de Madrid, Madrid, Spain.
[4]Department of Anatomy, Histology and Neuroscience, School of Medicine, Universidad Autónoma de Madrid, Madrid, Spain.
[5]Instituto Gulbenkian de Ciência, 2780-156 Oeiras, Portugal.
*These authors contributed equally to this work.

RESUMEN

Objetivos: Nos preguntamos si la estimulación colinérgica microglial, producida después de un evento isquémic, puede actúa a través de un mecanismo que implica la activación del factor nuclear factor relacionado eritroide - 2 - 2 (Nrf2) y / o la expresión de su gen citoprotector, hemooxigenasa 1 (HO - 1). Para ello, se analizó el efecto protector del receptor nicotínico α7 (α7 nAChR), usando para ello el agonista selectivo PNU282987. Como modelos experimentales se usaron los cultivos organotípicos de hipocampo de rata (OHC)sometidos a privación de oxígeno y glucosa (OGD) como *modelo in vitro*, así como modelo *in vivo* de isquemia focal por fototrombosis en ratón.

Resultados: Los OHCs expuestos a OGD/ reoxigenación, provocaron la muerte celular, medida por yoduro de propidio y por el método de reducción de MTT. El agonista de receptores nicotínicos α7 nAChR PNU282987, redujo la muerte celular, así como la producción de especies reactivas de oxígeno y la liberación de la citoquina proinflamatoria TNF . Esto se asoció con la sobreexpresión de la enzima antioxidante HO - 1, este efecto fue revertido por un antagonista de receptores nicotínicos α7 (bungarotoxina) y por la protoporfirina de estaño - IX. El efecto protector obtenido por el PNU282987 se perdió en OHCs depletados de microglia, así como en las OHCs provenientes de ratones deficientes en el factor de transcripción Nrf2. La administración de PNU282987 1 h después de la inducción de un infarto focal por fototrombosis en ratón, redujo el tamaño del infarto y mejoró las habilidades motoras en ratones Hmox1lox/lox que expresan niveles normales de HO - 1, pero no en ratones LysMCreHmox1D / D en los cuales la expresión de HO - 1 está inhibida en las células de la línea mieloide, incluyendo la microglia.

Innovación: Este estudio sugiere la participación de los receptores α7 nAChR microgliales, apoyando así la teoría colinérgica antiinflamatorios.

Conclusión : La activación del eje nAChR/Nrf2/HO-1/α7 en microglia, regula la neuroinflamación y el estrés oxidativo , proporcionando neuroprotección frente a isquémicas cerebral

ANTIOXIDANTS & REDOX SIGNALING
Volume 19, Number 11, 2013
Mary Ann Liebert, Inc.
DOI: 10.1089/ars.2012.4671

Therapeutics

ORIGINAL RESEARCH COMMUNICATION

The Microglial α7-Acetylcholine Nicotinic Receptor Is a Key Element in Promoting Neuroprotection by Inducing Heme Oxygenase-1 via Nuclear Factor Erythroid-2-Related Factor 2

Esther Parada,[1,*] Javier Egea,[1,2,*] Izaskun Buendia,[1] Pilar Negredo,[1,3,4] Ana C. Cunha,[5] Silvia Cardoso,[5] Miguel P. Soares,[5] and Manuela G. López[1,3]

Abstract

Aims: We asked whether the neuroprotective effect of cholinergic microglial stimulation during an ischemic event acts via a mechanism involving the activation of nuclear factor erythroid-2-related factor 2 (Nrf2) and/or the expression of its target cytoprotective gene, heme oxygenase-1 (HO-1). Specifically, the protective effect of the pharmacologic alpha-7 nicotinic acetylcholine receptor (α7 nAChR) agonist PNU282987 was analyzed in organotypic hippocampal cultures (OHCs) subjected to oxygen and glucose deprivation (OGD) *in vitro* as well as in photothrombotic stroke *in vivo*. Results: OHCs exposed to OGD followed by reoxygenation elicited cell death, measured by propidium iodide and 3-(4,5-Dimethylthiazol-2-yl)-2,5-diphenyltetrazolium bromide staining. Activation of a7 nAChR by PNU282987, after OGD, reduced cell death, reactive oxygen species production, and tumor necrosis factor release. This was associated with induction of HO-1 expression, an effect reversed by a-bungarotoxin and by tin–protoporphyrin IX. The protective effect of PNU282987 was lost in microglial-depleted OHCs as well as in OHCs from Nrf2-deficient-versus-wild-type mice, an effect associated with suppression of HO-1 expression in microglia. Administration of PNU282987 1 h after induction of photothrombotic stroke *in vivo* reduced the infarct size and improved motor skills in $Hmox1^{lox/lox}$ mice that express normal levels of HO-1, but not in $LysM^{Cre}Hmox1^{D/D}$ in which HO-1 expression is inhibited in myeloid cells, including the microglia. Innovation: This study suggests the participation of the microglial a7 nAChR in the brain cholinergic anti-inflammatory pathway. Conclusion: Activation of the a7 nAChR/Nrf2/HO-1 axis in microglia regulates neuroinflammation and oxidative stress, affording neuroprotection under brain ischemic conditions. *Antioxid. Redox Signal.* 19, 1135–1148.

Introduction

Ischemic damage results from a cascade of cellular and molecular events triggered by a sudden lack of blood flow and subsequent reperfusion of the ischemic territory. Post-ischemic inflammation is characterized by an orderly sequence of events involving a rapid activation of microglial cells, followed by infiltration of various circulating leukocytes, including granulocytes (neutrophils), T-cells, and monocytes/macrophages that irrupt in the ischemic parenchyma because of the blood–brain barrier (BBB) breakdown

Innovation

We demonstrate the role of microglial alpha-7 nicotinic acetylcholine receptor (a7 nAChR) in providing neuroprotective and anti-inflammatory actions under brain ischemia conditions by a mechanism that implicates the induction of heme oxygenase-1 expression via nuclear factor erythroid-2-related factor 2 activation. Our data support the notion that microglial a7 nAChR might be targeted therapeutically to modulate the brain cholinergic anti-inflammatory pathway.

[1]Instituto Teófilo Hernando and Department of Pharmacology, School of Medicine, Universidad Autónoma de Madrid, Madrid, Spain.
[2]Instituto de Investigación Sanitaria Hospital Universitario La Princesa-IP, Universidad Autónoma de Madrid, Madrid, Spain.
[3]Instituto Universitario la Paz-IdiPaz, Universidad Autónoma de Madrid, Madrid, Spain.
[4]Department of Anatomy, Histology and Neuroscience, School of Medicine, Universidad Autónoma de Madrid, Madrid, Spain.
[5]Instituto Gulbenkian de Ciência, 2780-156 Oeiras, Portugal.
*These authors contributed equally to this work.

(23, 30). The specific role of microglia in this pathological scenario remains controversial. Microglial activation has been linked to the upregulation of the proinflammatory cytokines such interleukin (IL)-1b and tumor necrosis factor (TNF), chemokines, and reactive oxygen species (ROS), which contribute to tissue damage progression (18, 37). There is also an increasing body of evidence demonstrating the protective role of microglia in stroke. Postischemic production of TGF-b and IL-10 by microglia may facilitate tissue repair by exerting direct cytoprotective effects on surviving cells in the ischemic penumbra and promoting the resolution of inflammation (9, 34). This notion is strongly supported by a recent study showing the beneficial effects of human microglia transplanted into rats subjected to the experimental focal brain ischemia (40).

Nicotinic acetylcholine receptors (nAChRs) are a family of ligand-gated ion channels and are members of the Cys-loop receptor superfamily (35). Activation of the a7 nAChR is protective against a wide variety of cytotoxic stimuli, such as glutamate (53), oxygen and glucose deprivation (OGD) (15), and kainic acid (50). In recent years, nAChRs were shown to regulate inflammation, in particular via the a7 nAChR activation in macrophages (61), which regulates the cholinergic anti-inflammatory pathway (26, 28, 48, 61). The transcripts for the nAChR subunits a7, a3, a5, as well as b4 have been detected in multiple inflammatory cell types, including macrophages and microglia, the resident macrophages of the brain (16, 47).

The transcription factor Nrf2 (nuclear factor erythroid-2-related factor 2) is a master regulator of redox homeostasis (22). Nrf2 controls the expression of phase II enzymes that act in a cytoprotective manner against oxidative stress, including heme oxygenase-1 (HO-1) (2) and the catalytic subunit of glutamate cysteine ligase (GCL-c). HO-1 serves a vital metabolic function as the rate-limiting step in the oxidative catabolism of heme to generate carbon monoxide (CO), biliverdin, and ferrous iron (56); biliverdin is subsequently converted to bilirubin by biliverdin reductase. These three byproducts, and in particular CO, have been related to cytoprotection (5) during ischemic injury, (1) including cerebral ischemia (27, 60, 65). Moreover, CO regulates monocyte/macrophage activation (42), an effect associated with protection against different experimental models of disease (43, 51). Induction of HO-1 expression by different nicotinic receptor agonists and its importance in the maintenance of anti-inflammatory effects have been recently reported (57). On the other hand, induction of GCL-c, the rate-limiting enzyme of the novo synthesis of glutathione (GSH), by melatonin increases the levels of GSH and protects against oxidative stress (58).

Although the participation of a7 nAChR in the cholinergic anti-inflammatory pathway is well documented in the periphery (61), there is little evidence related to its participation in the central nervous system. In this context, we used a highly selective microglial-target toxin and the selective a7 nAChR agonist PNU282987 to evaluate the neuroprotective and anti-neuroinflammatory effects of the microglial a7 nAChRs. Further, we used Nrf2-deficient ($Nrf2^{-/-}$) mice and $LysM^{Cre}Hmox1^{D/D}$ mice to assess the participation of this transcription factor in the regulation of HO-1 in the microglial cells and in the neuroprotective effect mediated by a7 nAChR activation. We found that microglial-a7 nAChR activation is crucial in the neuroprotective effect afforded by PNU282987, an effect mediated via a mechanism involving Nrf2 activation and HO-1 expression.

Results

Cell death induced by OGD in OHCs

We first established the experimental conditions required to test the protective role of the a7 nAChR agonist PNU282987. To determine the optimum period of OGD and reoxygenation (Reox), organotypic hippocampal cultures (OHCs) were subjected to 15 or 30 min of OGD followed by a 24- or 48-h Reox period. Cell death was measured in the CA1 subfield, which is considered to be the most vulnerable to hypoxia/anoxia (63). OGD for 15 or 30 min increased cell death by 177%–161% and 234%–243%, as compared to normoxia, respectively. No significant differences were found between 24- and 48-h Reox, independently of the OGD periods applied (Fig. 1). We therefore selected 15-min OGD followed by 24-h Reox as the standard protocol to perform the following studies.

Effect of post-OGD administration of the a7 nAChR agonist PNU282987 on OHC viability

To evaluate the protective properties of a7 nAChR, OHCs were treated with the a7 nAChR agonist PNU282987 at different concentrations (1, 3, and 10 μM) during the 24-h Reox period (see protocol in Fig. 2A). OGD (15 min) followed by Reox (24 h) increased cell death as assessed by propidium iodide (PI) fluorescence in CA1 (compare the basal condition in Fig. 2B with Fig. 2C). Post-OGD treatment with increasing concentrations of PNU282987 reduced PI staining (Fig. 2D–F). PNU282987 significantly reduced cell death measured as PI uptake at the concentrations of 10 μM (110% – 10%) and 30 μM (142% – 12%) in comparison to OHCs subjected to OGD alone (180% – 2%) (Fig. 2G).

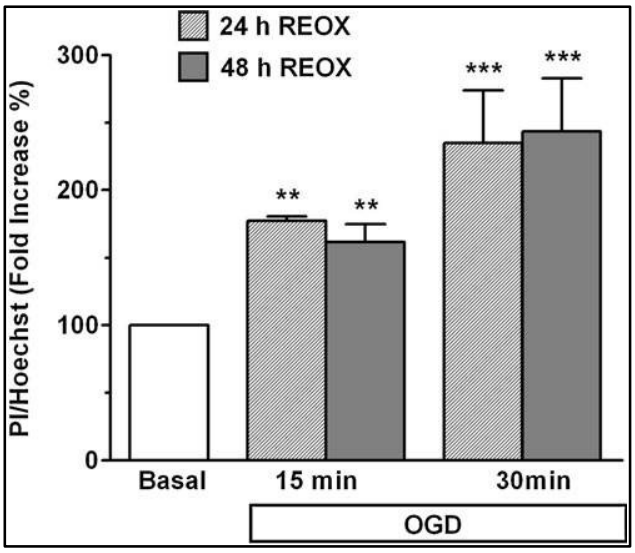

FIG. 1. Oxygen and glucose deprivation (OGD) increases cell death in organotypic hippocampal slices. Cell death was labeled with propidium iodide (PI) fluorescence corrected for the number of nuclei (Hoechst) in the CA1 subfield of rat organotypic slices after 15 or 30 min of OGD followed by 24 or 48 h of reoxygenation (Reox). Data are mean – SEM of seven independent experiments, ***$p < 0.001$, **$p < 0.01$ with respect to the basal.

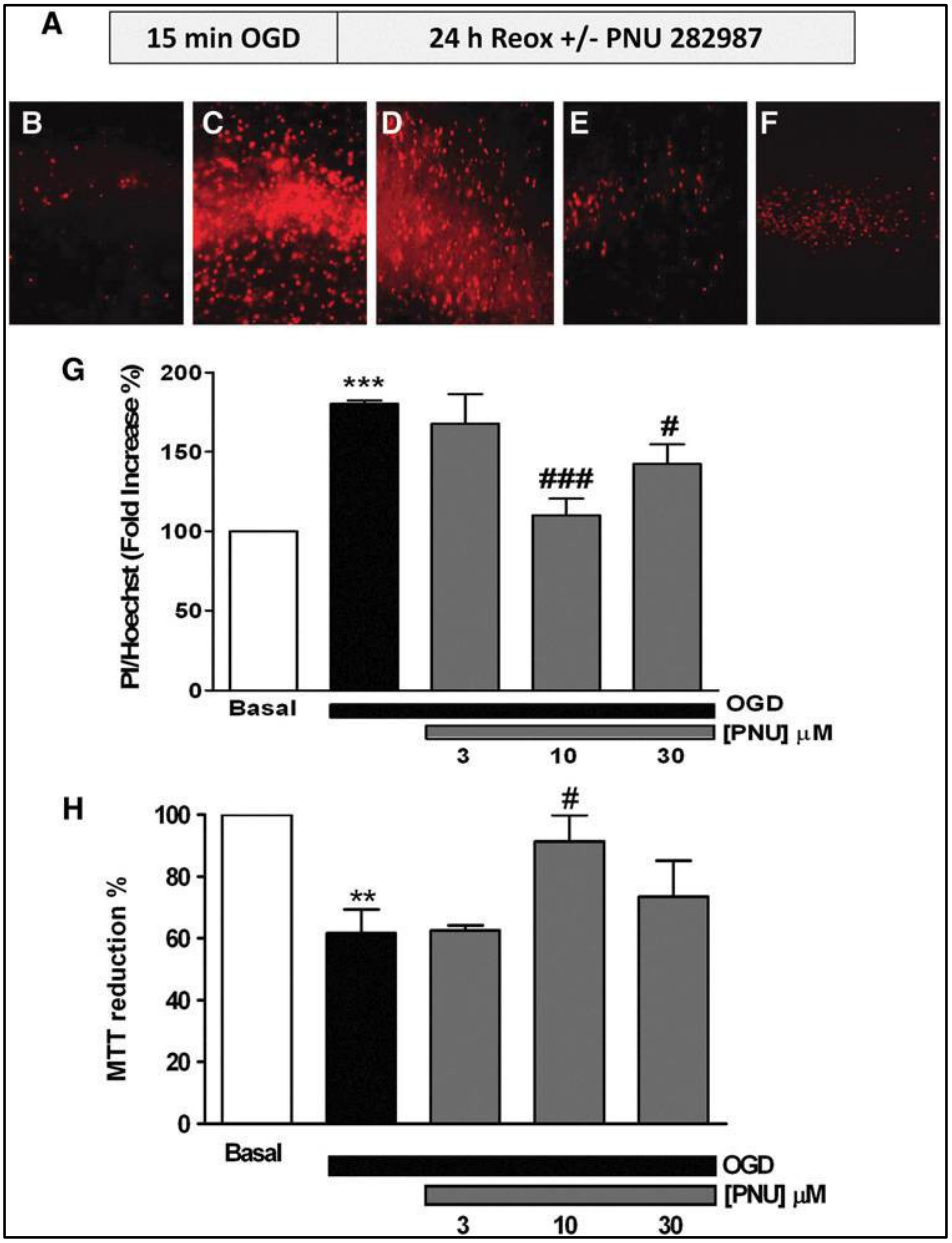

FIG. 2. Post-OGD treatment with the a7-nicotinic acetylcholine receptor (nAChR) agonist PNU282987 protects organotypic hippocampal cultures (OHCs). (A) Protocol used to elicit toxicity: OHCs were exposed for 15 min to OGD followed by 24 h in the control solution (Reox). PNU282987, when used, was present during the 24-h Reox period. (B–F) Microphotographs (original magnification 10 ·) of the CA1 subfield loaded with PI are shown. (B) Untreated slice; (C) slice exposed to OGD for 15 min followed by 24 h with a fresh medium, and slices were treated for 24 h with PNU282987 after the OGD period at 3 μM (D), 10 μM (E), or 30 μM (F). (G) The concentration–response curve of PNU282987 incubated for 24 h after the OGD period, measured as the relationship of PI/Hoechst fluorescence in the CA1 subfield. (H) Cell viability was measured by the 3-(4, 5-Dimethylthiazol-2-yl)-2,5-diphenyltetrazolium bromide (MTT) reduction activity of the organotypic slices under the same experimental conditions as in (G). Values are expressed as mean – SEM of at least five independent experiments; $^{***}p < 0.001$, $^{**}p < 0.01$ compared to the basal. $^{###}p < 0.001$, $^{#}p < 0.05$ with respect to OGD-treated slices in the absence of PNU282987. To see this illustration in color, the reader is referred to the web version of this article at www.liebertpub.com/ars

The cell viability was also assessed by the colorimetric determination of 3-(4,5-Dimethylthiazol-2-yl)-2,5-diphenyltetrazolium bromide (MTT) reduction. Considering the cell viability in basal OHCs as 100%, OGD reduced the cell viability by 40%; under these experimental conditions, maximum protection offered by PNU282987 was also achieved at 10 μM (60%; Fig. 2H). We therefore selected the concentration of 10 μM to evaluate the protective mechanism of action of a7 nAChR stimulation against OGD-induced toxicity in OHCs.

Participation of the a7 nAChR/Nrf-2/HO-1 axis in the neuroprotective effect of PNU282987

Although it is accepted that PNU282987 is a selective a7 nAChR agonist (19), we wanted to prove that the neuroprotective effect of PNU 282987 is mediated by this receptor. We used the protocol illustrated in Figure 2A in the absence or presence of a-bungarotoxin (BGT; 100 nM), a selective a7 nAChR antagonist. Inhibition of cell death associated with OGD/Reox by PNU282987 was abrogated by BGT (Fig. 3A), suggesting that this protective effect is indeed mediated via a7 nAChR activation.

In other models of oxidative stress injury, the neuroprotective effect of PNU282987 has been suggested to be mediated via a mechanism involving HO-1 (44). We tested the involvement of this heme-catabolizing enzyme under our experimental conditions. The protective effect of PNU282987 (10 μM) was associated with a 2.2-fold increase in HO-1 expression, as detected by Western blotting and as compared with untreated controls (Fig. 3B). This effect was reversed by BGT, suggesting that a7 nAChR activation induces the expression of HO-1. Inhibition of cell death by PNU282987 was also abrogated by tin (Sn)–protoporphyrin-IX (SnPP; 3 μM), an inhibitor of HO activity (Fig. 3A), corroborating the

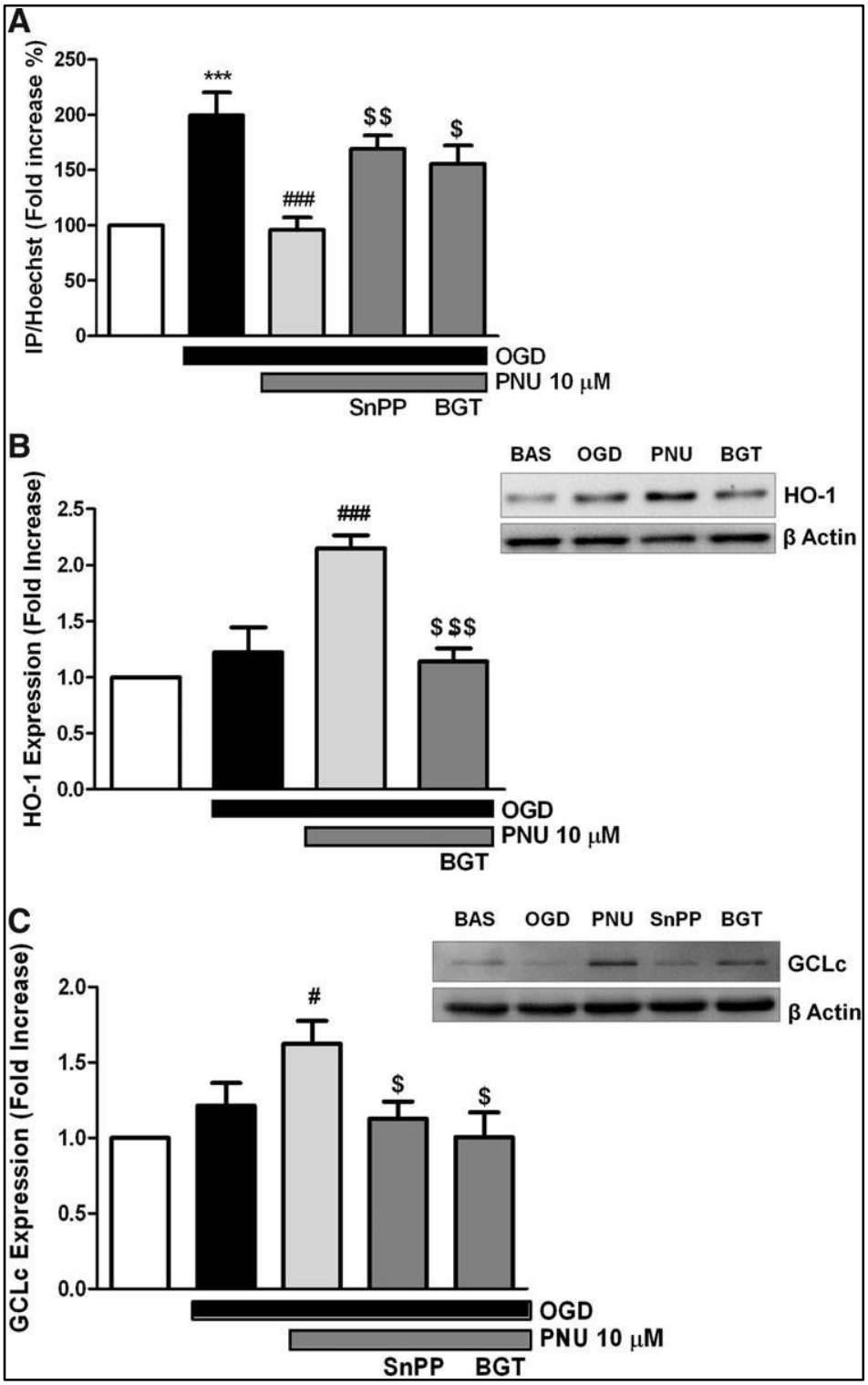

FIG. 3. Protection elicited by post-OGD treatment with PNU282987 is mediated by a7 nAChR and heme oxygenase-1 (HO-1). (A) OHCs were exposed to 15 min of OGD and then incubated with 10 μM PNU282987 for 24 h in the presence or absence of 100 nM a-bungarotoxin (BGT) and 3 μM tin (Sn)–protoporphyrin-IX (SnPP). Representative immunoblot of HO-1 (B) and glutamate cysteine ligase catalytic subunit (GCLc) (C) induction by PNU282987 in the absence or presence of 100 nM BGT and 3 μM SnPP. The histogram represents the densitometric quantification of HO-1 and GCLc induction using b-actin for normalization. Values are mean – SEM of six experiments, $^{***}p < 0.001$ compared with the untreated-slices, $^{###}p < 0.001$, $^{\#}p < 0.05$ with respect to the OGD-treated slices, $^{\$\$\$}p < 0.001$, $^{\$\$}p < 0.01$, and $^{\$}p < 0.05$ compared with the PNU282987 slices.

participation of HO-1 in the protective effect of PNU282987. We evaluated the induction of GCL-c, another phase II enzyme. As shown in Figure 3C, PNU282987 (10 μM) increased GCL-c expression by 1.6-fold, as compared with controls. This effect was inhibited by BGT and by SnPP, suggesting that a7 nAChR activation induces the expression of phase II enzymes, presumably conferring neuroprotection against OGD.

Given that HO-1 expression is tightly regulated by Nrf2 (2), we setup to determine the participation of this transcription factor in the protective effect of PNU282987. The neuroprotective effect of PNU282987 against OGD was lost in OHCs from $Nrf2^{-/-}$ versus $Nrf2^{+/+}$ mice (Fig. 4A). This was associated with the concomitant loss of HO-1 induction in OHC from $Nrf2^{-/-}$ versus $Nrf2^{+/+}$ mice, treated in both cases with

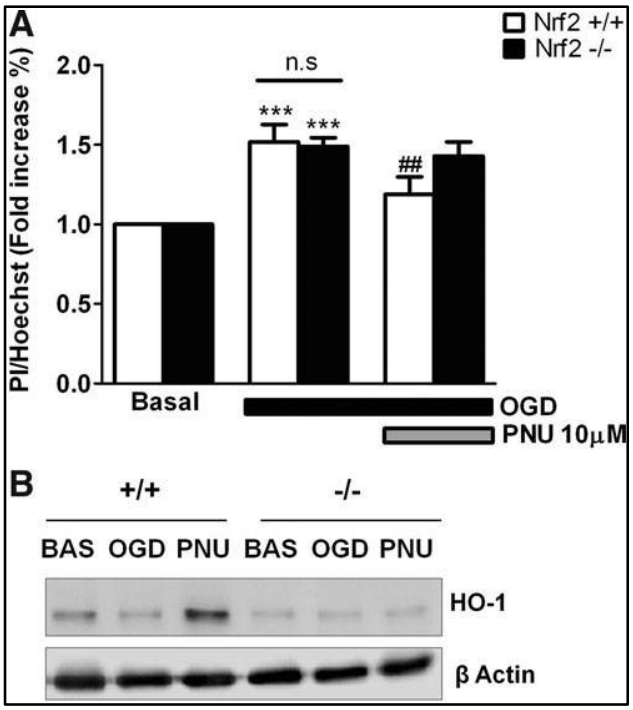

FIG. 4. Protection elicited by poststress treatment with PNU282987 is associated to the nuclear factor-erythroid-2-related factor 2 (Nrf2)/HO-1 axis. (A) Following the protocol shown in Figure 2A, the protective effect of post-OGD treatment with 10 μM PNU282987 was tested in organotypic slices of Nrf2 wild-type ($Nrf2^{+/+}$) and null mice ($Nrf2^{-/-}$). Data are mean – SEM of six different experiments; ***$p < 0.001$ compared with the untreated-slices, ##$p < 0.01$ with respect to OGD. (B) shows representative immunoblots of HO-1 induction under the different experimental conditions shown in A.

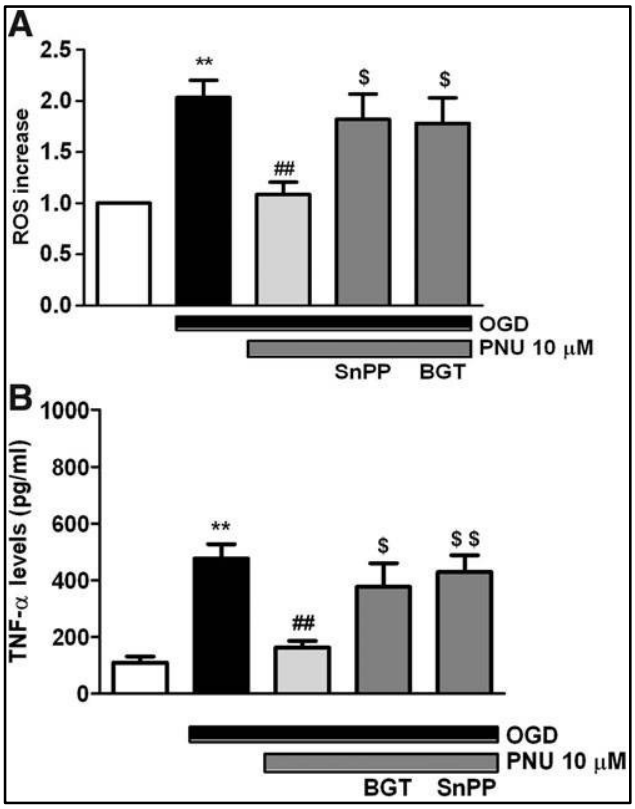

FIG. 5. PNU282987 reduces cellular reactive oxygen species (ROS) production and tumor necrosis factor (TNF)-a release caused by OGD/Reox. (A) Effect of PNU282987 on ROS production elicited by OGD/Reox. OHCs were subjected to 15 min of OGD followed by 24 h of reoxygenation in the presence or absence of 10 μM PNU282987, 100 nM BGT, and 3 μM SnPP. (B) TNF release in the OHC supernatant measured under the same experimental conditions. Data are means – SEM of five independent experiments; **$p < 0.01$ compared with the untreated-slices, $^{\#\#}p < 0.01$ with respect to the OGD-treated slices, $^{\$\$}p < 0.01$, $^{\$}p < 0.05$ compared with the PNU282987-treated slices.

PNU282987 (Fig. 4B). This suggests that the protective effect of PNU282987 acts via a mechanism that involves the induction of HO-1 by Nrf2.

Antioxidant and anti-inflammatory effect of PNU282987

There is accumulating evidence implicating ROS and inflammation as pivotal mediators of acute responses of the brain to ischemia and its chronic pathogenic progression (25, 31). OGD (15 min) followed by Reox (24 h) doubled the amount of ROS (measured by H_2DCFDA) produced in OHCs, as compared to the control (Fig. 5A). PNU282987 (10 μM) reduced ROS production significantly, as compared to the untreated controls. This effect was blocked by SnPP and by BGT as well, suggesting that the antioxidant effect triggered upon a7 nAChR activation is mediated by a mechanism involving HO-1.

To test the effects of PNU282987 on the production of cytokines induced by OGD/Reox, TNF and IL-10 were quantified by an enzyme-linked immunosorbent assay (ELISA) in the culture medium of OHCs. OGD (15 min) followed by Reox (24 h) increased TNF secretion, as compared to the control OHCs (477 – 50 pg/ml vs. 109 – 22 pg/ml). Treatment of OHCs with PNU 282987 10 μM reduced TNF release almost to the control levels (163 – 22 pg/ml). This inhibitory effect was prevented by SnPP (3 μM) as well as by BGT (100 nM) (429 – 59 pg/ml; 377 – 82 pg/ml, respectively). We did not observe changes in IL10 secretion in any of the conditions tested (data not shown). These results suggest that a7 nAChR activation inhibits the production of proinflammatory cytokines, TNF, via a mechanism involving the expression of HO-1.

Participation of microglia in HO-1 induction and neuroprotection induced by PNU282987 against OGD

PNU282987 induced by 1.5-fold the expression of HO-1 in isolated microglial cells, as assessed by Western blot (Supplementary Fig. S1; Supplementary Data are available online at www.liebertpub.com/ars). Microglial depletion from OHC using Mac1–sap (39) was confirmed by ionized calcium-binding adaptor molecule 1(IBA-1) staining (Fig. 6A, B) and was associated with increased cell death after OGD, in comparison to control OHCs. The protective effect of PNU282987 against OGD was impaired in microglia-depleted OHCs, as

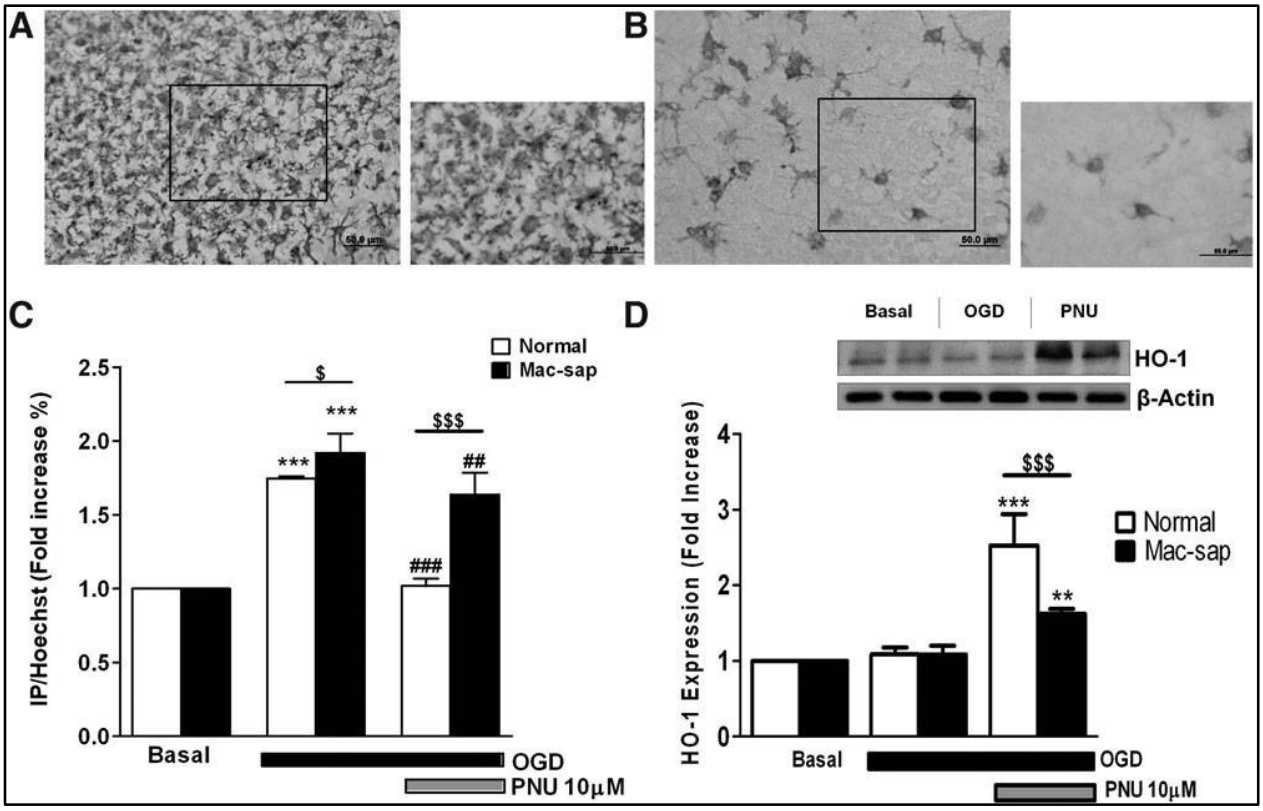

FIG. 6. Key role of microglia in the protective effect of PNU282987. The top part of the figure illustrates immunohistochemical expression of the microglial marker ionized calcium-binding adaptor molecule 1 in the CA1 pyramidal cell layer of OHCs. (A) shows an untreated slice and (B) slices treated with 5 nM of Mac1-sap, used to deplete microglia. To elicit toxicity, the protocol shown in Figure 2 was followed. (C) Densitometric measurements of PI uptake in depleted and nondepleted microglia OHCs. (D) The top part of the figure shows a representative immunoblot of HO-1 induction under the same experimental conditions as shown in (C); the bottom graph represents the densitometric quantification of HO-1, using b-actin for normalization. Data are means – SEM of six independent experiments, $^{***}p < 0.001$, $^{**}p < 0.01$ compared with the untreated slices, $^{###}p < 0.001$, $^{##}p < 0.01$ with respect to the OGD-treated slices, $^{\$\$\$}p < 0.001$, $^{\$}p < 0.05$, depleted versus nondepleted slices.

compared to the nondepleted OHCs (Fig. 6C). Induction of HO-1 expression by PNU282987 was also reduced in microglia-depleted OHCs, as compared to the control OHCs (Fig. 6D). This shows that a7 nAChR activation in microglia induces the expression of HO-1 in microglia.

PNU282987 reduces the cortical infarct volume through the induction of HO-1 expression

We used the photothrombotic model of stroke in mice to evaluate whether the protective effects of PNU282987 act under brain ischemic conditions in vivo (10). Following the protocol shown in Figure 7A, ischemia induced by photothrombosis caused a mean cortical infarct volume of 15.7% – 0.9%. Administration of PNU282987 (10 mg/kg), 1 h postphotothrombosis, reduced the infarct volume by 40% (9.4% – 0.4%). Administration of Zinc (III)–deuteroporphyrin IX-2,4 bisethylene glycol (ZnDPBG; 10 mg/kg), a potent HO inhibitor that crosses the BBB (24), did not alter the infarct volume, but prevented the neuroprotective effect of the a7 nAChR agonist PNU282987 to 14.6% – 0.8% (Fig. 7B).

To establish conclusively the involvement of HO-1, we compared the protective effect of PNU282987 against ischemia induced by photothrombosis in $Hmox1^{lox/lox}$ mice expressing normal levels of HO-1 versus $LysM^{Cre}Hmox1^{D/D}$ in which HO-1 expression is inhibited specifically in myeloid cells (see the Methods section and Supplementary Fig. S2), including in the microglia. PNU282987 reduced the infarct volume by 38% in $Hmox1^{lox/lox}$ mice, as compared to untreated $Hmox1^{lox/lox}$ mice. Reduction in the infarct volume correlated with improved motor coordination measured by hindpaw slips in the beam-walking test (BWT) (Fig. 7E). In contrast, PNU282987 failed to reduce the infarct volume or to improve motor coordination in $LysM^{Cre}Hmox1^{D/D}$ mice (Fig. 7C–E). This reveals that the expression of HO-1 in the myeloid compartment, and presumably in the microglia, is essential to support the neuroprotective effect of a7 nAChR against brain ischemia induced by photothrombosis.

Discussion

In the present study, we provide experimental evidence in vitro as well as in vivo, pointing to the crucial role of microglia in the neuroprotective effect afforded by the selective a7 nAChR agonist PNU282987 against brain ischemia. Although there is convincing evidence that a7 nAChR activation in macrophages exerts anti-inflammatory effects mediating the so-called cholinergic anti-inflammatory pathway (61), few

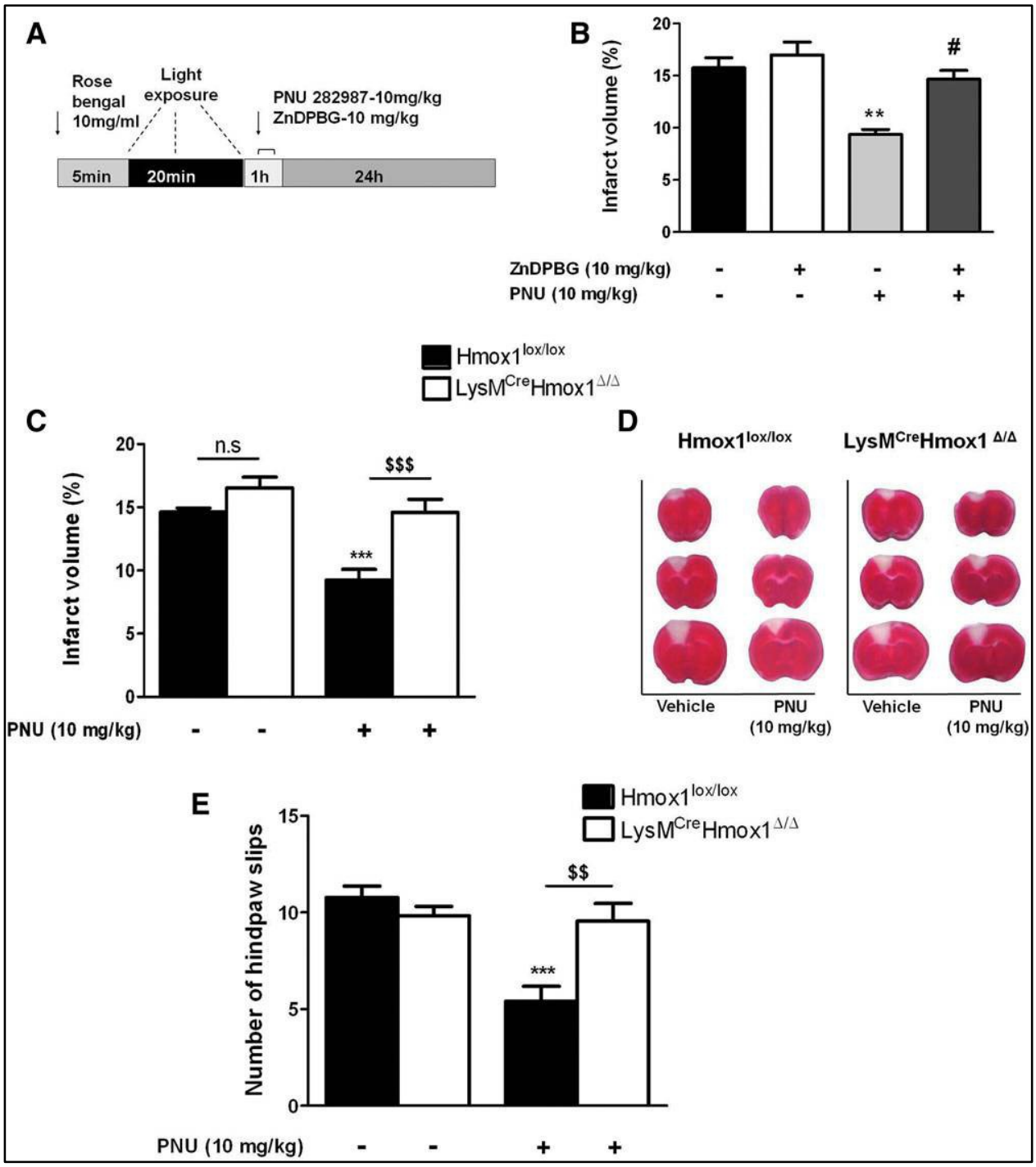

FIG. 7. PNU282987 reduces the infarct volume and promotes functional recovery in mice subjected to photothrombotic stroke depending on HO-1 expression. (A) illustrates the protocol used, in which PNU282987 (intraperitoneal [i.p] at 10 mg/kg) and/or zinc (III)–deuteroporphyrin IX-2,4 bisethylene glycol (ZnDPBG) (i.p. at 10 mg/kg) were administered 60 or 15 min after the thrombotic stroke, respectively. (B) Data are expressed as a percentage (%) of the cortical infarct volume in mice. Note that reduction of infarct in mice receiving PNU282987 was prevented by ZnDPBG. (C) Data are expressed as the percentage (%) of the cortical infarct volume in $LysM^{Cre}Hmox1^{D/D}$ versus $Hmox1^{lox/lox}$ mice subjected to photothrombotic stroke and receiving or not PNU282987 (10 mg/kg). (D) Representative photographs of the cortical infarcts of mice represented in (C). (E) Motor skills analyzed with the Beam-walk test 24 h after ischemia by quantification of hindpaw slips (see the Materials and Methods section) in the same animals as in (C). Data are expressed as mean – SEM of eight animals per group, in two independent experiments with the same trend. $^{**}p < 0.01$, compared with the ischemia plus saline group, $^{\#}p < 0.05$ in comparison with PNU treated animals, $^{***}p < 0.001$ in comparison with $Hmox1^{lox/lox}$ saline mice, $^{\$\$\$}p < 0.001$, $^{\$\$}p < 0.01$ $LysM^{Cre}Hmox1^{D/D}$ versus $Hmox1^{lox/lox}$. To see this illustration in color, the reader is referred to the web version of this article at www.liebertpub.com/ars

studies have addressed specifically whether this effect is also exerted in microglia, the resident macrophages of the brain. We provide evidence that a7 nAChR activation induces the expression of HO-1 in microglia, which is required to support the neuroprotective effect of PNU282987 against brain ischemia. This notion is supported by the following independent observations: (i) PNU282987 induces HO-1 expression at the concentration that afforded maximum protection against brain ischemia; (ii) the protective effect of PNU282987 is lost by inhibition of the HO activity (Figs. 2 and 3); (iii) induction of HO-1 by PNU282987 is ablated by deletion of the transcription factor Nrf2 (Fig. 4); (iv) the protective effect of PNU282987 is reversed by microglia deletion, an effect associated with the loss of HO-1 expression (Fig. 6); and (v) the protective effect of PNU282987 is ablated by specific deletion of HO-1 in myeloid cells, including the microglia (Fig. 7).

Signaling through nAChRs plays an important role in various processes such as neurite outgrowth, control and synthesis of neurotrophic factors, neuroprotection (20), as well as in the regulation of inflammation (48, 61). Moreover, signaling via a7 nAChR protects against neuronal death in different models of hemorrhagic brain injury (13, 29). We have also previously shown that a7 nAChR activation is protective in different *in vitro* models of ischemia/Reox (15, 44). Most of these studies have focused their attention on neuronal nicotinic receptors, while the participation of nAChRs in other brain cells such as astrocytes and microglia has been less studied. The results obtained in the present work indicate that a7 nAChRs expressed in microglia are key elements in promoting the protective effect of PNU282987. This notion is supported by the observation that the selective a7 nAChR antagonist a-BGT prevented the neuroprotective effect and the induction of phase II enzymes (HO-1 and GCL-c) by PNU282987, and hence the reduction of ROS production and TNF release (Fig. 5). Moreover, the protective effect of PNU282987 against brain ischemia is reduced by 70% upon microglial deletion (Fig. 6). These observations strongly suggest that the cholinergic anti-inflammatory pathway described for peripheral macrophages, as controlling systemic inflammation, may have a brain counterpart, where microglias, the resident macrophages of the brain, regulate inflammation via activation of the a7 nAChRs.

Recent findings have elucidated the cellular signaling pathways and molecular mechanisms that mediate adaptive stress response that typically involves the synthesis of various stress resistance proteins as the products of vitagenes, a group of genes strictly involved in preserving cellular homeostasis during stressful conditions (6). The vitagene family is composed of the heat shock proteins (Hsp) HO-1/Hsp32, Hsp70, and Hsp60, by the thioredoxin system and by sirtuin proteins. Nrf-2 is a master regulator of cellular redox homeostasis, controlling the expression of different genes that modulate the cellular redox status and inflammation (phase II enzymes), including HO-1 (22). Induction of HO-1 expression has generally been considered to provide an adaptive cytoprotective response against the toxicity of oxidative stress (17, 45, 59). *Hmox1*-deficient mice develop chronic inflammatory lesions that are similar to the ones observed in individuals lacking the HO-1 expression (64). Hence, compounds targeting the vitagene network could be a novel approach to delay various alterations in cells, tissues, and organs and potentially prevent and treat many different diseases, such as ischemia. The mechanisms regulating the salutary effects of HO-1 remain however to be fully established (52).

The protective effect of PNU282987 acts via activation of Nrf2, as demonstrated by the loss of this protective effect in OHCs from $Nrf2^{-/-}$ mice (Fig. 4A). This effect is associated with inhibition of HO-1 expression in microglial cells from OHCs $Nrf2^{-/-}$ *versus* $Nrf2^{+/+}$ (Fig. 4B and Supplementary Fig. S2). Recently, it has been hypothesized that pharmacological modulation of Nrf2 restores the cellular redox state through the expression of antioxidant phase II enzymes, downmodulating the pathological neuroinflammatory response of reactive microglia (21). Heme degradation by HO-1 in microglia generates CO (33), a gasotransmitter that can inhibit NADPH oxidase (55), the main enzyme responsible for microglial ROS production (4) promoting microglial activation during neuroinflammation (7). PNU282987 reduces ROS production as well as TNF release induced by brain ischemia, an effect mediated by the induction of HO-1 expression via a7 nAChR signaling (Fig. 5A, B). This corroborates the importance of the Nrf-2/HO-1 system in the control of the cellular redox state and modulation of the neuroinflammatory responses to ischemia. We infer that nAChR signaling modulates microglial activation via a mechanism mediated by Nrf2/HO-1, which inhibits ROS production.

Microglias have historically been viewed as immunocompetent cells that respond to inflammation by acting as antigen-presenting cells or secreting cytokines. The specific role of microglia in postischemic inflammation remains controversial. Resident microglia are activated rapidly in response to brain injury, within minutes of ischemia onset, and produce proinflammatory mediators, such TNF and IL-1b, which exacerbate brain damage (18, 37). Our data show that cell death induced by OGD was significantly higher in microglia-depleted OHCs compared to nondepleted slices (Fig. 6). Hence, in our model, microglial cells have a protective role in the brain against ischemic injury.

We found that expression of HO-1, presumably in the microglia, mediates the protective effect of PNU282987 against photothrombotic brain ischemia, as assessed in $Hmox1^{lox/lox}$ mice, expressing the normal levels of HO-1 *versus* $LysM^{Cre}$ $Hmox1^{D/D}$, in which HO-1 expression is inhibited specifically in myeloid cells, including in the microglia. Together with the data obtained in the OHC model, this suggests that expression of HO-1 by microglia is important to resolve the oxidative stress and neuroinflammation and, most importantly, to stop the progression of cell death induced by an ischemic episode. This is in line with the notion that microglia plays a central role in the regulation of brain ischemia and excitotoxic injury (32, 40, 41). We propose that pharmacologic modulation of HO-1 in microglia may be considered as a potential strategy against a brain ischemia-induced injury (62).

Materials and Methods

Animals and preparation of OHC

OHCs were conducted on 8–10-day-old Sprague-Dawley rats or wild-type C57BL/6 mice and Nrf2-knockout mice of the same littermates. Nrf2-knockout mice were kindly provided by Dr. Antonio Cuadrado (Department of Biochemistry, School of Medicine, Universidad Autó noma de Madrid). All animal assays were carried out following the European

Community Council Directive issued for these purposes and were approved by the Ethics Committee of the Facultad de Medicina, Universidad Autónoma de Madrid. Every effort was made to minimize the number of animals used and their suffering.

Cultures were prepared according to the methods described by Stoppini et al. (54) with some modifications. Briefly, 300-1m-thick hippocampal slices were prepared from rat or mice pups using a McIlwain tissue chopper, and separated in ice-cold Hank's balanced salt solution (HBSS) composed of (mM): glucose 15, $CaCl_2$ 1.3, KCl 5.36, NaCl 137.93, KH_2PO_4 0.44, Na_2HPO_4 0.34, $MgCl_2$ 0.49, $MgSO_4$ 0.44, NaHCO3 4.1, and HEPES 25; 100 U/ml penicillin and 0.100 mg/ml gentamicin. Approximately 4–6 slices were placed on Millicell 0.4-1m culture insert (Millipore) within each well of a six-well culture tray with the medium, where they remained for 7 days. The culture medium, which consisted of 50% minimal essential medium, 25% HBSS, and 25% heat-inactivated horse serum, were purchased from Life Technologies. The medium was supplemented with 3.7 mg/ml d-glucose, 2 mmol/l l-glutamine, and 2% of B-27 Supplement Minus antioxidants (Life Technologies), and 100 U/ml penicillin. OHCs were cultivated in a humidified atmosphere at 37°C and 5% CO_2, and the medium was changed twice a week.

Mice

C57BL/6 $Nrf2^{-/-}$ (22) and $Hmox1^{LoxP}$ (38) mice were generated by the laboratory of Dr. Masayuki Yamamoto (Tohoku University Graduate School of Medicine) and obtained through the RIKEN BioResource Center ($Nrf2^{-/-}$ mouse/C57BL6J and B6J.129P2-Hmox1 <tm1Mym >). C57BL/6 $LysM^{Cre}$ mice were generated by the laboratory of Dr. Forster (8) and obtained through the Jackson Laboratory (B6.129P2-Lyz2tm1(cre)Ifo/J Stock Number:004781). $LysM^{Cre}Hmox1^{D/D}$ mice used in this study were generated at the Instituto Gulbenkian de Ciência from $LysM^{Cre}Hmox1^{D/D}$ - $LysM^{Cre}Hmox1^{D/D}$. The $LysM^{Cre}Hmox1^{D/D}$ offspring is homozygous for the $LysM^{Cre}$ allele. Mice were genotyped by the polymerase chain reaction (PCR) from genomic DNA using the following primers for the Hmox1 allele (Hmox1 wild-type forward 5¢-CTCACTATGCAACTCTGTTGGAGG-3¢, Hmox1 wild-type reverse 5¢-GTCTGTAATCCTAGCACTCGAA-3¢ and $Hmox1^{LoxP}$ reverse 5¢-GGAAGGACAGCTTCTTGTA GTCG-3¢) and for the $LysM^{Cre}$ allele (mutant 5¢-CCCAGA AATGCCAGATTACG-3¢; common: 5¢-CTTGGGCTGCCAG AATTTCTC-3¢ and wild type 5¢-TTACAGTCGGCCAG GCTGAC-3¢). Mice were bred at the Instituto Gulbenkian de Ciência with food and water provided ad libitum. Mice were used at 6 to 12 weeks of age, and the littermates were used as controls.

Thioglycollate-induced peritoneal macrophages

Briefly, mice received (intraperitoneal [i.p], 2 ml) a 3% thioglycollate solution (w/v), and macrophages were obtained by peritoneal lavage 5 days, thereafter in phosphate-buffered saline (PBS; 5 ml).

Peritoneal macrophages were stained with an Alexa467-conjugated-anti-CD11b (M1/70; 1:50 dilution) mAb, and nonspecific Fc binding was inhibited using an anti-FcgIII/II receptor antibody (2.4G2; 1:50 dilution) in PBS 2% fetal calf serum (FCS) (20 min, 4°C). After washing and centrifugation (PBS 2% FCS; 666g, 2 min, 4°C), cells were sorted as $CD11b^+$ for the $Hmox1^{lox/lox}$ and as $CD11b^+DsRed^+$ or $CD11b^+DsRed^-$ for the $LysM^{Cre}Hmox1^{D/D}$. Cells were collected and analyzed by flow cytometry (FACSAria; BD Biosciences), using BD FACS-Diva Software (BD Biosciences) for acquisition. Postacquisition analysis was performed with FloJo software (Treestar).

RNA isolation and qRT-PCR

Briefly, mRNA was isolated from $CD11b^+$-sorted cells and extracted with the RNeasy Mini Kit (Qiagen). cDNA was synthesized from 0.3–0.5 µg of RNA using random hexamer primers (0.3 mg/reaction; Invitrogen) and dNTPs (0.5 mM/ reaction; Invitrogen) (5 min, 65°C). 5 · First Strand buffer (Invitrogen) was added in the presence of dithiothreitol (10 mM/reaction; Invitrogen) and RNAse Out recombinant ribonuclease inhibitor (40 U/reaction; Invitrogen) (2 min, 42°C). SuperScriptII reverse transcriptase (200 U/reaction; Invitrogen) was added completing a final volume of 20 µl (50 min, 42°C; 15 min, 70°C). One µ l of cDNA was used for PCRs (10 µl) using the Power SYBRGreen PCR master mix (Applied Biosystems) and optimal primer concentrations (previously determined for each transcript). PCR products were detected by quantitative real time-PCR (ABI-7900HT; Applied Biosystems) (2 min, 50°C, 10 min, 95°C, and 40 cycles of 15 s at 95°C, 1 min, 60°C). Primers used to amplify mouse mRNA transcripts were designed using the Primer3 software (Whitehead Institute for Biomedical Research, Steve Rozen and Helen Skaletsky) according to the specifications of the ABI-7900HT equipment (Applied Biosystems) and are listed below: Hmox1 5¢-AAGGAGGTACACATCCAAGCCGAG-3¢ and 5¢-GATATGGTACAAGGAAGCCATCACCAG-3¢; Glyceraldehyde 3-phosphate dehydrogenase (GAPDH) 5¢-AAC TTTGGCATTGTGGAAGG-3¢ and 5¢-ACACATTGGGGG TAGGAACA-3¢. The transcript number was calculated from the Ct of each gene using a 2^{-DDCT} method (relative number) and normalizing results to GAPDH.

Oxygen–glucose deprivation in OHCs

Oxygen–glucose deprivation was used as an in vitro model of cerebral ischemia. The inserts with slice cultures were placed in 1 ml of OGD solution composed of the following (in mM): NaCl 137.93, KCl 5.36, $CaCl_2$ 2, $MgSO_4$ 1.19, $NaHCO_3$ 26, KH_2PO_4 1.18, and 2-deoxyglucose 11 (Sigma-Aldrich). The cultures were then placed in an airtight chamber (Billups and Rothenberg), and were exposed to 5 min of 95% N_2/5% CO_2 gas flow to ensure oxygen deprivation. After that, the chamber was sealed for 15 min at 37°C. The control cultures were maintained for the same time under a normoxic atmosphere in a solution with the same composition as that described above (OGD solution), but containing glucose (15 mM) instead of 2-deoxyglucose. After the OGD period, the slice cultures were returned to their original culture conditions for 24 h (reoxygenation period).

Quantification of cell death in OHCs

Quantification of viability by MTT. The cell viability, virtually the mitochondrial activity of living cells, was measured using the quantitative colorimetric assay of MTT, as described previously (11) with some modifications. Briefly, 1 ml of the MTT-labeling reagent, at a final concentration of 0.5 mg/ml,

was added to the medium of each well at the end of the OGD-Reox period or normoxic period, and the plate was placed in a humidified incubator at 37°C with 5% CO_2 and 95% air (v/v) for an additional 30 min. Then, the insoluble formazan was dissolved with dimethyl sulfoxide; the colorimetric determination of MTT reduction was measured at 540 nm. Control cells treated under normoxic conditions with vehicle were taken as 100% viability.

Propidium iodide uptake. Cell death was determined in the CA1 region by staining the OHCs with PI. Thirty minutes before analyzing fluorescence, slices were incubated with PI (1 μg/ml) and Hoechst (5 μg/ml); Hoechst staining was used to normalize PI fluorescence with respect to the number of nuclei. Fluorescence was measured in a fluorescence-inverted NIKON Eclipse T2000-U microscope. The wavelengths of excitation and emission for PI and Hoechst were 530 or 350, and 580 or 460 nm, respectively. Images were taken at CA1 at magnifications of 10 · . The Metamorph programme version 7.0. was used for fluorescence analysis. To calculate cell death, we divided the mean PI fluorescence by the mean Hoechst fluorescence, as previously described (14). Data were normalized with respect to the control values that were considered as 1.

ROS measurement in OHCs

To measure the cellular ROS, we used the molecular probe H_2DCFDA as previously described (44). Briefly, organotypic hippocampal slices were loaded with 10 μM H_2DCFDA, which diffuses through the cell membrane and is hydrolyzed by intracellular esterases to the nonfluorescent form dichlorofluorescein (DCFH). DCFH reacts with intracellular H_2O_2 to form dichlorofluorescin, a green fluorescent dye. Fluorescence was measured in a fluorescence-inverted NIKON Eclipse T2000-U microscope. Wavelengths of excitation and emission were 485 and 520 nm, respectively.

Determination of cytokine levels in the culture medium of OHCs

TNF and IL-10 levels were measured by using specific ELISA kits. Supernatant samples were obtained at the indicated times and subjected to the ELISA analysis according to the recommendations of the supplier (R&D Systems-BioNova).

Immunotoxic depletion of microglial cells in OHCs

Hippocampal slices were cultured for 5 days and then exposed to 3 or 5 nM of the immunocomplex Mac1–sap (Advanced Targeting Systems) for 7 days. At the end of this period, the slices were fixed with paraformaldehyde 4% for immunohistochemistry. The OGD experiments in microglia-depleted OHCs were performed at the end of the immunotoxic treatments.

Histochemistry for microglia

The OHCs were fixed with 4% paraformaldehyde in 0.1 M phosphate buffer (PB, pH 7.4) and were subsequently cryoprotected for 2 days in 30% sucrose in 0.1 M PB. The endogenous peroxidase was inactivated with 1% H_2O_2, and the OHCs were then incubated in a blocking solution (PBS, 10% bovine serum albumin, and 10% normal goat serum) for 1 h, and rabbit anti-IBA1 was used as the primary antibody 1:1000 (Wako Chemicals, Rafer S.L) overnight. The secondary antibody was biotinylated goat anti-rabbit (Vector Labs; 1:200; 2 h) and was dissolved in a blocking solution. The OHCs were incubated in an avidin–biotin peroxidase complex (Kit ABC Elite®, 1:250 in PBS; Vector Laboratories) for 2 h and reacted with diaminobenzidine (0.05%; Sigma) with H_2O_2 (0.003% of the stock 30% solution). The intensity of the staining was checked every few minutes under a microscope, and when labeling was satisfactory, the reaction was stopped by rinsing the OHCs with a cold PB. After several washes with PB, the OHCs were dehydrated in ethanol, defatted with xylene, and coverslipped with DePeX. Negative controls for the specificity of the secondary antibody were prepared by omitting the primary antibody.

Immunoblotting and image analysis

After treatments, the slices were carefully separated from the inserts and lysed in 100 μl ice-cold lysis buffer (1% Nonidet P-40, 10% glycerol, 137 mM NaCl, 20 mM Tris–HCl, pH 7.5, 1 μg/ml leupeptin, 1 mM phenylmethylsulfonyl fluoride, 20 mM NaF, 1 mM sodium pyrophosphate, and 1 mM Na_3VO_4). Protein (30 μg) from this cell lysate was resolved by sodium dodecyl sulfate–polyacrylamide gel electrophoresis and transferred to the Immobilon-P membranes (Millipore Corp.). The membranes were incubated with anti-HO-1 (1:1000; Chemicon), anti-GCLc subunit (1:10000; a generous gift from Dr Cuadrado A), or anti-b-actin (1:100,000; Sigma). Appropriate peroxidase-conjugated secondary antibodies (1:10,000) were used to detect the proteins by enhanced chemiluminescence. Different band intensities corresponding to immunoblot detection of protein samples were quantified using the Scion Image program. Immunoblots correspond to a representative experiment that was repeated 4–5 times with similar results.

Microglial cell culture

Microglias were isolated using a mild trypsinization method as previously described (49) with brief modifications. Mixed glial cultures were prepared from the cerebral cortices of 3-day-old Sprague-Dawley rats. After mechanical dissociation, cells were seeded in Dulbecco's modified Eagle's medium (DMEM)/F12 with 20% of fetal bovine serum (FBS) at a density of 300,000 cells/ml and cultured at 37°C in humidified 5% CO_2/95% air. The medium was replaced after 5 days in vitro (DIV) for DMEM/F12 with 10% FBS. The confluency was achieved after 10–12 DIV. High enriched microglial cultures were obtained with a trypsin solution (0.25% trypsin and 1 mM EDTA) diluted 1:4 in DMEM-F12. This process resulted in the detachment of an upper layer of cells in one piece, and microglial cells were attached to the bottom of the well. A great majority of cells (99%) were positive for CD11b, as judged by the immunocytochemical criteria.

Photothombotic stroke model

All animal assays were carried out following the European Community Council Directive issued for these purposes and were approved by the Ethics Committee of the Facultad de Medicina, Universidad Autó noma de Madrid. Every effort was made to minimize the number of animals used and their

suffering. Mice were housed individually under controlled temperature and lighting conditions with food and water provided ad libitum. To induce ischemia, animals were anesthetized with 1.5% isoflurane in oxygen under spontaneous respiration. Mice were then placed in a stereotaxic frame (David Kopf Instruments), and the body temperature was maintained at 37°C – 0.5°C using a servo-controlled rectal probe-heating pad (Cibertec). A midline scalp incision was made, and the skull was exposed with removal of the periosteum, and both the bregma and lambda points were identified. A cold light (Zeiss KL 1500 LCD) was centered using a micromanipulator at 0.2 mm posterior and 1.5 mm lateral to bregma on the right side using a fiber optic bundle of 2 mm in diameter. According to the Paxinos mouse brain atlas, the primary motor cortex, secondary motor cortex, and primary somatosensory cortex (hindlimb and forelimb) are lying beneath this stereotaxic position. One milligram (0.1 ml) of the photosensitive dye Rose Bengal (Sigma-Aldrich) dissolved in sterile saline was injected i.p., and 5 min later, the brains were illuminated through the intact skull for 20 min. After completion of the surgical procedures, the incision was sutured, and the mice were allowed to recover.

Drug administration protocol

Mice were randomly divided into four groups: subjected to ischemia and treated with 0.9% NaCl sterile saline (ischemia control group), treated with 10 mg/kg PNU282987 dissolved in saline containing 5% DMSO, treated with ZnDPBG dissolved in DMSO, and diluted in physiological saline at a dose of 10 mg/kg (12), or with the combination of PNU282987 and ZnDPBG at the concentrations mentioned above. PNU282987 and ZnDPBG treatments were given i.p after ischemia (1 h and 15 min, respectively).

Measurement of infarct volume

Animals were sacrificed by decapitation 24 h after the ischemic insult. The brains were quickly removed and coronally sectioned into 1-mm-thick slices. For delineation of the infarct area, the brain slices were incubated in a 2% solution of triphenyltetrazolium chloride and then fixed in a buffered formalin solution, and the unstained area was defined as infarcted tissue. Morphometric determination of the cortical infarct volume was obtained using an unbiased stereological estimator of volume based on Cavalieri's principle (3).

Beam-walk test

Motor coordination of mice was assessed 24 h after the photothrombotic stroke by measuring the number of contralateral hindpaw slips in the Beam-walk apparatus (36, 46). This test takes place over three consecutive days: 2 days of training and 1 day of testing. In the BWT, mice have to go through a 520-mm beam with a flat surface of 10-mm width resting 50 cm above the tabletop on two poles. A black goal box (150 mm · 150 mm · 150 mm) is placed at the end of the beam as the finish point. The amounts of hindpaw slips that occur in the process were counted.

Statistics

Data are given as mean – SEM. Differences between the groups were determined by applying a one-way ANOVA followed by a Newman–Keuls post-hoc or two-way ANOVA, followed by a Bonferroni post hoc test when appropriate.

Acknowledgments

This work was supported in part by grants from Spanish Ministry of Science and Innovation Ref. SAF2009-12150 and SAF2012-32223 and the Spanish Ministry of Health (Instituto de Salud Carlos III) RETICS-RD06/0026 to MGL. E.P. and I.B. have a predoctoral fellowship from the Spanish Ministry of Economy. We would also like to thank the Fundación Teófilo Hernando for its continued support. Funding: Fundaç ão para a Ciência e Tecnologia (Portugal) grants to MPS: PTDC/BIA-BCM/101311/2008, PTDC/SAU-FCF/100762/2008, and PTDC/SAU-TOX/116627/2010) and European Community 6th Framework Grant LSH-2005-1.2.5-1 and 7th Framework Grant ERC-2011-AdG. 294709–DAMAGECONTROL. Ana Cunha was supported by a fellowship within the project PTDC/SAU-FCF/100762/2008 awarded to MPS. We also thank Sofia Rebelo (Instituto Gulbenkian de Ciência), who was responsible for the management of animals, and David Fdez Villa, responsible for the construction of the Beam-walk apparatus

Author Disclosure Statement

No competing financial interests exist.

References

1. Akamatsu Y, Haga M, Tyagi S, Yamashita K, Graca-Souza AV, Ollinger R, Czismadia E, May GA, Ifedigbo E, Otterbein LE, Bach FH, and Soares MP. Heme oxygenase-1-derived carbon monoxide protects hearts from transplant associated ischemia reperfusion injury. Faseb J 18: 771–772, 2004.
2. Alam J, Stewart D, Touchard C, Boinapally S, Choi AM, and Cook JL. Nrf2, a Cap'n'Collar transcription factor, regulates induction of the heme oxygenase-1 gene. J Biol Chem 274: 26071–26078, 1999.
3. Avendano C, Roda JM, Carceller F, and Diez-Tejedor E. Morphometric study of focal cerebral ischemia in rats: a stereological evaluation. Brain Res 673: 83–92, 1995.
4. Block ML, Zecca L, and Hong JS. Microglia-mediated neurotoxicity: uncovering the molecular mechanisms. Nat Rev Neurosci 8: 57–69, 2007.
5. Brouard S, Otterbein LE, Anrather J, Tobiasch E, Bach FH, Choi AM, and Soares MP. Carbon monoxide generated by heme oxygenase 1 suppresses endothelial cell apoptosis. J Exp Med 192: 1015–1026, 2000.
6. Calabrese V, Cornelius C, Dinkova-Kostova AT, Iavicoli I, Di Paola R, Koverech A, Cuzzocrea S, Rizzarelli E, and Calabrese EJ. Cellular stress responses, hormetic phytochemicals and vitagenes in aging and longevity. Biochim Biophys Acta 1822: 753–783, 2012.
7. Choi SH, Aid S, Kim HW, Jackson SH, and Bosetti F. Inhibition of NADPH oxidase promotes alternative and anti-inflammatory microglial activation during neuroinflammation. J Neurochem 120: 292–301, 2012.
8. Clausen BE, Burkhardt C, Reith W, Renkawitz R, and Forster I. Conditional gene targeting in macrophages and granulocytes using LysMcre mice. Transgenic Res 8: 265–277, 1999.
9. de Bilbao F, Arsenijevic D, Moll T, Garcia-Gabay I, Vallet P, Langhans W, and Giannakopoulos P. In vivo over-expression

of interleukin-10 increases resistance to focal brain ischemia in mice. J Neurochem 110: 12–22, 2009.
10. De Ryck M, Van Reempts J, Borgers M, Wauquier A, and Janssen PA. Photochemical stroke model: flunarizine prevents sensorimotor deficits after neocortical infarcts in rats. Stroke 20: 1383–1390, 1989.
11. Denizot F and Lang R. Rapid colorimetric assay for cell growth and survival. Modifications to the tetrazolium dye procedure giving improved sensitivity and reliability. J Immunol Methods 89: 271–277, 1986.
12. Duranski MR, Elrod JW, Calvert JW, Bryan NS, Feelisch M, and Lefer DJ. Genetic overexpression of eNOS attenuates hepatic ischemia-reperfusion injury. Am J Physiol Heart Circ Physiol 291: H2980–H2986, 2006.
13. Duris K, Manaenko A, Suzuki H, Rolland WB, Krafft PR, and Zhang JH. alpha7 nicotinic acetylcholine receptor agonist PNU-282987 attenuates early brain injury in a perforation model of subarachnoid hemorrhage in rats. Stroke 42: 3530–3536, 2011.
14. Egea J, Martin-de-Saavedra MD, Parada E, Romero A, Del Barrio L, Rosa AO, Garcia AG, and Lopez MG. Galantamine elicits neuroprotection by inhibiting iNOS, NADPH oxidase and ROS in hippocampal slices stressed with anoxia/reoxygenation. Neuropharmacology 62: 1082–1090, 2012.
15. Egea J, Rosa AO, Sobrado M, Gandia L, Lopez MG, and Garcia AG. Neuroprotection afforded by nicotine against oxygen and glucose deprivation in hippocampal slices is lost in alpha7 nicotinic receptor knockout mice. Neuroscience 145: 866–872, 2007.
16. Galvis G, Lips KS, and Kummer W. Expression of nicotinic acetylcholine receptors on murine alveolar macrophages. J Mol Neurosci 30: 107–108, 2006.
17. Gozzelino R, Jeney V, and Soares MP. Mechanisms of cell protection by heme oxygenase-1. Annu Rev Pharmacol Toxicol 50: 323–354, 2010.
18. Gregersen R, Lambertsen K, and Finsen B. Microglia and macrophages are the major source of tumor necrosis factor in permanent middle cerebral artery occlusion in mice. J Cereb Blood Flow Metab 20: 53–65, 2000.
19. Hajos M, Hurst RS, Hoffmann WE, Krause M, Wall TM, Higdon NR, and Groppi VE. The selective alpha7 nicotinic acetylcholine receptor agonist PNU-282987 [N-[(3R)-1-Azabicyclo[2.2.2]oct-3-yl]-4-chlorobenzamide hydrochloride] enhances GABAergic synaptic activity in brain slices and restores auditory gating deficits in anesthetized rats. J Pharmacol Exp Ther 312: 1213–1222, 2005.
20. Hejmadi MV, Dajas-Bailador F, Barns SM, Jones B, and Wonnacott S. Neuroprotection by nicotine against hypoxia-induced apoptosis in cortical cultures involves activation of multiple nicotinic acetylcholine receptor subtypes. Mol Cell Neurosci 24: 779–786, 2003.
21. Innamorato NG, Rojo AI, Garcia-Yague AJ, Yamamoto M, de Ceballos ML, and Cuadrado A. The transcription factor Nrf2 is a therapeutic target against brain inflammation. J Immunol 181: 680–689, 2008.
22. Itoh K, Chiba T, Takahashi S, Ishii T, Igarashi K, Katoh Y, Oyake T, Hayashi N, Satoh K, Hatayama I, Yamamoto M, and Nabeshima Y. An Nrf2/small Maf heterodimer mediates the induction of phase II detoxifying enzyme genes through antioxidant response elements. Biochem Biophys Res Commun 236: 313–322, 1997.
23. Jin R, Yang G, and Li G. Inflammatory mechanisms in ischemic stroke: role of inflammatory cells. J Leukoc Biol 87: 779–789, 2010.
24. Johnson RA, Lavesa M, Askari B, Abraham NG, and Nasjletti A. A heme oxygenase product, presumably carbon monoxide, mediates a vasodepressor function in rats. Hypertension 25: 166–169, 1995.
25. Jung JE, Kim GS, Chen H, Maier CM, Narasimhan P, Song YS, Niizuma K, Katsu M, Okami N, Yoshioka H, Sakata H, Goeders CE, and Chan PH. Reperfusion and neurovascular dysfunction in stroke: from basic mechanisms to potential strategies for neuroprotection. Mol Neurobiol 41: 172–179, 2010.
26. Kawahara R, Yasuda M, Hashimura H, Amagase K, Kato S, and Takeuchi K. Activation of alpha7 nicotinic acetylcholine receptors ameliorates indomethacin-induced small intestinal ulceration in mice. Eur J Pharmacol 650: 411–417, 2011.
27. Kim YS, Zhuang H, Koehler RC, and Dore S. Distinct protective mechanisms of HO-1 and HO-2 against hydroperoxide-induced cytotoxicity. Free Radic Biol Med 38: 85–92, 2005.
28. Kox M, Pompe JC, Peters E, Vaneker M, van der Laak JW, van der Hoeven JG, Scheffer GJ, Hoedemaekers CW, and Pickkers P. alpha7 Nicotinic acetylcholine receptor agonist GTS-21 attenuates ventilator-induced tumour necrosis factor-alpha production and lung injury. Br J Anaesth 107: 559–566, 2011.
29. Krafft PR, Altay O, Rolland WB, Duris K, Lekic T, Tang J, and Zhang JH. alpha7 Nicotinic acetylcholine receptor agonism confers neuroprotection through GSK-3beta inhibition in a mouse model of intracerebral hemorrhage. Stroke 43: 844–850, 2012.
30. Kreutzberg GW. Microglia: a sensor for pathological events in the CNS. Trends Neurosci 19: 312–318, 1996.
31. Lakhan SE, Kirchgessner A, and Hofer M. Inflammatory mechanisms in ischemic stroke: therapeutic approaches. J Transl Med 7: 97, 2009.
32. Lalancette-Hebert M, Gowing G, Simard A, Weng YC, and Kriz J. Selective ablation of proliferating microglial cells exacerbates ischemic injury in the brain. J Neurosci 27: 2596–2605, 2007.
33. Lee S and Suk K. Heme oxygenase-1 mediates cytoprotective effects of immunostimulation in microglia. Biochem Pharmacol 74: 723–729, 2007.
34. Lehrmann E, Kiefer R, Christensen T, Toyka KV, Zimmer J, Diemer NH, Hartung HP, and Finsen B. Microglia and macrophages are major sources of locally produced transforming growth factor-beta1 after transient middle cerebral artery occlusion in rats. Glia 24: 437–448, 1998.
35. Lester HA, Dibas MI, Dahan DS, Leite JF, and Dougherty DA. Cys-loop receptors: new twists and turns. Trends Neurosci 27: 329–336, 2004.
36. Luong TN, Carlisle HJ, Southwell A, and Patterson PH. Assessment of motor balance and coordination in mice using the balance beam. J Vis Exp, 2011. DOI: 10.3791/2376.
37. Mabuchi T, Kitagawa K, Ohtsuki T, Kuwabara K, Yagita Y, Yanagihara T, Hori M, and Matsumoto M. Contribution of microglia/macrophages to expansion of infarction and response of oligodendrocytes after focal cerebral ischemia in rats. Stroke 31: 1735–1743, 2000.
38. Mamiya T, Katsuoka F, Hirayama A, Nakajima O, Kobayashi A, Maher JM, Matsui H, Hyodo I, Yamamoto M, and Hosoya T. Hepatocyte-specific deletion of heme oxygenase-1 disrupts redox homeostasis in basal and oxidative environments. Tohoku J Exp Med 216: 331–339, 2008.

39. Montero M, Gonzalez B, and Zimmer J. Immunotoxic depletion of microglia in mouse hippocampal slice cultures enhances ischemia-like neurodegeneration. Brain Res 1291: 140–152, 2009.
40. Narantuya D, Nagai A, Sheikh AM, Masuda J, Kobayashi S, Yamaguchi S, and Kim SU. Human microglia transplanted in rat focal ischemia brain induce neuroprotection and behavioral improvement. PLoS One 5: e11746, 2010.
41. Neumann J, Gunzer M, Gutzeit HO, Ullrich O, Reymann KG, and Dinkel K. Microglia provide neuroprotection after ischemia. Faseb J 20: 714–716, 2006.
42. Otterbein LE, Bach FH, Alam J, Soares M, Tao Lu H, Wysk M, Davis RJ, Flavell RA, and Choi AM. Carbon monoxide has anti-inflammatory effects involving the mitogen-activated protein kinase pathway. Nat Med 6: 422–428, 2000.
43. Otterbein LE, Soares MP, Yamashita K, and Bach FH. Heme oxygenase-1: unleashing the protective properties of heme. Trends Immunol 24: 449–455, 2003.
44. Parada E, Egea J, Romero A, del Barrio L, Garcia AG, and Lopez MG. Poststress treatment with PNU282987 can rescue SH-SY5Y cells undergoing apoptosis via alpha7 nicotinic receptors linked to a Jak2/Akt/HO-1 signaling pathway. Free Radic Biol Med 49: 1815–1821, 2010.
45. Poss KD and Tonegawa S. Reduced stress defense in heme oxygenase 1-deficient cells. Proc Natl Acad Sci U S A 94: 10925–10930, 1997.
46. Quinn LP, Perren MJ, Brackenborough KT, Woodhams PL, Vidgeon-Hart M, Chapman H, Pangalos MN, Upton N, and Virley DJ. A beam-walking apparatus to assess behavioural impairments in MPTP-treated mice: pharmacological validation with R-(-)-deprenyl. J Neurosci Methods 164: 43–49, 2007.
47. Rock RB, Gekker G, Aravalli RN, Hu S, Sheng WS, and Peterson PK. Potentiation of HIV-1 expression in microglial cells by nicotine: involvement of transforming growth factor-beta 1. J Neuroimmune Pharmacol 3: 143–149, 2008.
48. Rosas-Ballina M, Ochani M, Parrish WR, Ochani K, Harris YT, Huston JM, Chavan S, and Tracey KJ. Splenic nerve is required for cholinergic antiinflammatory pathway control of TNF in endotoxemia. Proc Natl Acad Sci U S A 105: 11008–11013, 2008.
49. Saura J, Tusell JM, and Serratosa J. High-yield isolation of murine microglia by mild trypsinization. Glia 44: 183–189, 2003.
50. Shin EJ, Chae JS, Jung ME, Bing G, Ko KH, Kim WK, Wie MB, Cheon MA, Nah SY, and Kim HC. Repeated intracerebroventricular infusion of nicotine prevents kainate-induced neurotoxicity by activating the alpha7 nicotinic acetylcholine receptor. Epilepsy Res 73: 292–298, 2007.
51. Soares MP and Bach FH. Heme oxygenase-1: from biology to therapeutic potential. Trends Mol Med 15: 50–58, 2009.
52. Soares MP, Marguti I, Cunha A, and Larsen R. Immunoregulatory effects of HO-1: how does it work? Curr Opin Pharmacol 9: 482–489, 2009.
53. Stevens TR, Krueger SR, Fitzsimonds RM, and Picciotto MR. Neuroprotection by nicotine in mouse primary cortical cultures involves activation of calcineurin and L-type calcium channel inactivation. J Neurosci 23: 10093–10099, 2003.
54. Stoppini L, Buchs PA, and Muller D. A simple method for organotypic cultures of nervous tissue. J Neurosci Methods 37: 173–182, 1991.
55. Taille C, El-Benna J, Lanone S, Boczkowski J, and Motterlini R. Mitochondrial respiratory chain and NAD(P)H oxidase are targets for the antiproliferative effect of carbon monoxide in human airway smooth muscle. J Biol Chem 280: 25350–25360, 2005.
56. Tenhunen R, Marver HS, and Schmid R. The enzymatic conversion of heme to bilirubin by microsomal heme oxygenase. Proc Natl Acad Sci U S A 61: 748–755, 1968.
57. Tsoyi K, Jang HJ, Kim JW, Chang HK, Lee YS, Pae HO, Kim HJ, Seo HG, Lee JH, Chung HT, and Chang KC. Stimulation of alpha7 nicotinic acetylcholine receptor by nicotine attenuates inflammatory response in macrophages and improves survival in experimental model of sepsis through heme oxygenase-1 induction. Antioxid Redox Signal 14: 2057–2070, 2011.
58. Urata Y, Honma S, Goto S, Todoroki S, Iida T, Cho S, Honma K, and Kondo T. Melatonin induces gamma-glutamylcysteine synthetase mediated by activator protein-1 in human vascular endothelial cells. Free Radic Biol Med 27: 838–847, 1999.
59. Vile GF, Basu-Modak S, Waltner C, and Tyrrell RM. Heme oxygenase 1 mediates an adaptive response to oxidative stress in human skin fibroblasts. Proc Natl Acad Sci U S A 91: 2607–2610, 1994.
60. Vitali SH, Mitsialis SA, Liang OD, Liu X, Fernandez-Gonzalez A, Christou H, Wu X, McGowan FX, and Kourembanas S. Divergent cardiopulmonary actions of heme oxygenase enzymatic products in chronic hypoxia. PLoS One 4: e5978, 2009.
61. Wang H, Yu M, Ochani M, Amella CA, Tanovic M, Susarla S, Li JH, Wang H, Yang H, Ulloa L, Al-Abed Y, Czura CJ, and Tracey KJ. Nicotinic acetylcholine receptor alpha7 subunit is an essential regulator of inflammation. Nature 421: 384–388, 2003.
62. Weinstein JR, Koerner IP, and Moller T. Microglia in ischemic brain injury. Future Neurol 5: 227–246, 2010.
63. Wilde GJ, Pringle AK, Wright P, and Iannotti F. Differential vulnerability of the CA1 and CA3 subfields of the hippocampus to superoxide and hydroxyl radicals in vitro. J Neurochem 69: 883–886, 1997.
64. Yachie A, Niida Y, Wada T, Igarashi N, Kaneda H, Toma T, Ohta K, Kasahara Y, and Koizumi S. Oxidative stress causes enhanced endothelial cell injury in human heme oxygenase-1 deficiency. J Clin Invest 103: 129–135, 1999.
65. Yang C, Zhang X, Fan H, and Liu Y. Curcumin upregulates transcription factor Nrf2, HO-1 expression and protects rat brains against focal ischemia. Brain Res 1282: 133–141, 2009.

Address correspondence to:
Prof. Manuela G. Lopez
Instituto Teófilo Hernando
Departamento de Farmacología
Facultad de Medicina
Universidad Autónoma de Madrid
C/Arzobispo Morcillo 4
E-28029 Madrid
Spain

E-mail: manuela.garcia@uam.es

Date of first submission to ARS Central, April 24, 2012; date of final revised submission, December 18, 2012; date of acceptance, January 11, 2013.

Abbreviations Used

BBB ¼ blood–brain barrier
BGT ¼ bungarotoxin
BV ¼ biliverdin
CO ¼ carbon monoxide
DCFH ¼ dichlorofluorescein
ELISA ¼ enzyme-linked immunosorbent assay
GCL-c ¼ glutamate cysteine ligase catalytic subunit
GSH ¼ glutathione
HBSS ¼ Hank's balanced salt solution
HO-1 ¼ hemoxygenase-1
IBA1 ¼ ionized calcium-binding adaptor molecule 1
IL ¼ interleukin
MTT ¼ 3-(4,5-dimethylthiazol-2-yl)-2,5-diphenyltetrazolium bromide
nAChR ¼ nicotinic acetylcholine receptor
NADPH ¼ nicotinamide adenine dinucleotide phosphate
NOX ¼ NADPH oxidase
Nrf2 ¼ nuclear factor-erythroid-2-related factor 2
OGD ¼ oxygen and glucose deprivation
OHCs ¼ organotypic hippocampal cultures
PBS ¼ phosphate-buffered saline
PI ¼ propidium iodide
Reox ¼ reoxygenation
ROS ¼ reactive oxygen species
SnPP ¼ tin (Sn)–protoporphyrin-IX
TNF ¼ tumor necrosis factor
ZnDPBG ¼ zinc (III)–deuteroporphyrin IX-2,4 bisethylene glycol

Contents lists available at ScienceDirect

Free Radical Biology & Medicine

journal homepage: www.elsevier.com/locate/freeradbiomed

Original Contribution

Microglial HO-1 induction by curcumin provides antioxidant, anti-neuroinflammatory and cytoprotective effects

Esther Parada [a,b], Javier Egea [a,b], Blanca Prieto [a,b,d], Carlos Avendaño[d], Manuela G. López [a,b,*]

[a] Instituto Teófilo Hernando, Facultad de Medicina, Universidad Autónoma de Madrid, 4-28029 Madrid, Spain
[b] Departamento de Farmacología y Terapéutica, Facultad de Medicina, Universidad Autónoma de Madrid, 4-28029 Madrid, Spain
[c] Servicio de Farmacología Clínica, Hospital Universitario de la Princesa, Madrid, Spain
[d] 3Departamento de Anatom'ıa, Histolog'ıa y Neurociencia, Facultad de Medicina, Universidad Auto'noma de Madrid, Madrid, Spain.

RESUMEN

En este estudio nos planteamos estudiar el efecto protector de la curcumina en cultivos gliales, así como el mecanismo implicado en dicho proceso. Para ello, hemos tratado cultivos gliales mixtos de rata con rotenona (30 µM) más oligomicina-A (10µM) (rot/oligo) y/o lipopolisacárido (LPS). La co-incubacion de rot/oligo más LPS-1ug/ml, durante 16 h, produjo un 50 % de muerte celular.

Usando el protocolo mencionado anteriormente, la curcumina (10 µM) produjo glioprotección significativa. Los cultivos de glia expuestos 24 h a 10 µM de curcumina vieron aumentada la expresión de la enzima antioxidante hemo oxigenasa- 1 (HO - 1). La glioprotección observada se relaciona con la inducción de esta enzima ya que la Sn (IV) protoporfirina-IX , un inhibidor de hemo oxigenasa- 1 (HO-1), previno la protección ofrecida por la curcumina . Por otra parte, el aumento de ROS inducido por el tratamiento con rot/oligo + LPS-1ug/ml también fue revertido por la curcumina vía HO-1. Adicionalmente, la curcumina también redujo la liberación de NO observada en los cultivos gliales tratados con LPS, así como el fenotipo de activación microglial.

Cuando los cultivos gliales mixtos fueron separados específicamente después de los tratamientos, para estudiar la expresión de iNOS en astrocitos y en microglia de forma independiente, observamos que la sobreexpresión de iNOS inducida por LPS se produjo solo en la microglía, pero no en los astrocitos. La curcumina redujo esta inducción de iNOS por un mecanismo que implica HO-1. Estos resultados sugieren que la curcumina induce HO-1 en la microglia para proporcionar citoprotección.

Contents lists available at ScienceDirect

Free Radical Biology & Medicine

journal homepage: www.elsevier.com/locate/freeradbiomed

Original Contribution

Microglial HO-1 induction by curcumin provides antioxidant, anti-neuroinflammatory and cytoprotective effects

Esther Parada [a,b,c], Javier Egea [a,b,c], Blanca Prieto [a,b,], Carlos Avendaño[d], Manuela G. López [a,b,c*]

[a] Instituto Teófilo Hernando, Facultad de Medicina, Universidad Autónoma de Madrid, 4-28029 Madrid, Spain
[b] Departamento de Farmacología y Terapéutica, Facultad de Medicina, Universidad Autónoma de Madrid, 4-28029 Madrid, Spain
[c] Servicio de Farmacología Clínica, Hospital Universitario de la Princesa, Madrid, Spain
[d] 3Departamento de Anatom'ıa, Histolog'ıa y Neurociencia, Facultad de Medicina, Universidad Auto'noma de Madrid, Madrid, Spain.

a b s t r a c t

Glia plays a critical role in maintaining neuronal cell homeostasis under oxidative and inflammatory conditions, such as those that occur in neurodegeneration. Induction of hemoxigenase 1 (HO-1), an enzyme that affords antioxidant and anti-inflammatory actions, facilitates neuroprotection. This study was planned to evaluate if the antioxidant curcumin could induce HO-1 in glial cells to afford antioxiative and anti-neuroinflammatory effects. We have used rat glial cell cultures exposed to the combination of an oxidative (rotenone plus oligomycin A) and pro-inflammatory (lipopolysaccharide-LPS) stimuli (RO/LPS) for 16 h; this stimuli induced around 50 % reduction of glial viability. When glial cells were exposed to curcumin (10 μM) in the presence of the toxics, it afforded significant glialprotection and, reduction of reactive oxygen species, nitrates, and inducible nitric oxide synthase; all these effects were blocked when the HO-1 inhibitor SnPP was added to the medium. Glial cultures incubated with curcumin (10 and 20 μM) for 16 h, showed significantly increase of HO-1 protein. Induction of iNOS by the toxic stimuli (RO/LPS) was predominantly expressed in microglial cells, a very slight and non-significant effect was observed in astrocytes; this effect was inhibited by curcumin in a HO-1 dependent manner. Analysis of the microglial phenotype showed that the toxics favored a round phagocytic pattern while the presence of curcumin favored the microglial alternative phenotype. Inhibition of HO-1 promoted the phagocytic phenotype. In conclusion, when glial cells are exposed to an inflammatory and oxidative environment, curcumin induces the antioxidant enzyme HO-1, preferentially in the microglia, to provide cytoprotection.

Curcumin is the main curcuminoid present in the rhizomes of *Curcuma longa*, it is the active ingredient of culinary herbs and spices traditionally used in South and Southeast Asia. Curcumin shows promising pharmacological activities due to its antioxidant and anti-inflammatory actions and has demonstrated beneficial effects for the treatment of various chronic inflammatory diseases (Maheshwari *et al.* 2006). Treatment with curcumin is being tested in several clinical trials which are ongoing, involving different diseases like pancreatic cancer, psoriasis, Alzheimer's disease, epilepsy (Gupta *et al.* 2013, Monroy *et al.* 2013, Hatcher *et al.* 2008). Curcumin has also immuno-regulatory properties by modulating the activation of T-cells, B-cells, neutrophils, natural killer cells and macrophages (Jagetia & Aggarwal 2007).

* Corresponding author. Instituto Teófilo Hernando, Facultad de Medicina, Universidad Autónoma de Madrid, 4-28029 Madrid, Spain. Fax: +34 914975380.
E-mail address: manuela.garcia@uam.es (M.G. López).

The anti-inflammatory effects of curcumin involve different mechanism of actions; for example, it can regulate the activation of transcription factors like activating protein-1 (AP-1) and nuclear factor kappa B (NF-κB) in monocytes or macrophages, or it can block the induction of cyclooxygenase-2 (COX-2) (Rahman *et al.* 2006, Aggarwal & Shishodia 2006). Furthermore, curcumin by down-regulating intercellular signaling proteins such as protein kinase C, has shown to inhibit the release of proinflamatory cytokines like IL1β, IL-6 and TNF (Shishodia 2013).

Focusing in the central nervous sistem (CNS), microglia constitute the resident macrophages in this location and plays an important role in neuronal homeostasis and innate immune regulation. Ramified microglia continuously scans the surrounding environment searching for pathogens or cellular debris to ensure the correct functioning of brain homeostasis (Hanisch & Kettenmann 2007, Streit 2002). Furthermore, neurons send inhibitory signals which prevent microglial toxicity. Dangerous signals polarize microglia towards a pro-inflammatory phenotype increasing the production of nitric oxide (NO) and reactive oxygen species (ROS) (Qin *et al.* 2002), which promotes the release of pro-inflammatory cytokines such as TNF, IL-1, IL-6 and IL-12 (Allan & Rothwell 2001). Under normal conditions,

polarization of microglia is resolved by a long-lasting repair stage known as alternative phase. On the other hand, chronic microglial activation leads to chronic inflammation which has been identified in most neurodegenerative diseases (Schwartz *et al.* 2006, Block *et al.* 2007). Curcumin inhibits LPS-induced microglial activation through inhibition of NO production (Jung *et al.* 2006) and reduction of the release of pro-inflammatory cytokines like IL6, IL1β and TNF (Lee *et al.* 2007, Zhang *et al.* 2010). Finally, it has been demonstrated that curcumin attenuates microglial migration and triggers the alternative microglial phenotype, which has anti-inflammatory and neuroprotective actions (Karlstetter *et al.* 2011).

The transcription factor Nuclear factor erythroid-2-related factor 2 (Nrf2) tightly controls redox homeostasis of cells. Nrf2 is a crucial player in the antioxidant protection of microglial cells avoiding dangerous effects of oxidative stress and over-activation of the pro-inflammatory phenotype. Nrf2 controls the expression of more than 100 genes related to redox homeostasis. Among these genes, several data strongly point to HO-1 as an important enzyme in immunomodulation. HO-1 end-products reduce classic monocyte activation by inhibiting ROS production and TLR-4 signaling. Moreover, treatment with anti-inflammatory cytokine IL-10 up-regulates HO-1 and promotes acquisition of the alternative phase. In microglia, HO-1 positive cells preferentially activate the alternative program after traumatic brain injury. Furthermore, HO-1 over-expression in microglia is critical in the neuroprotective effect observed after brain ischemia (Parada *et al.* 2013).

Although the antioxidant/antiiflammatory actions of curcumin are well documented in the periphery, in this study we have focused on how curcumin can regulate these actions in the CNS by exposing glial cultures to LPS (inflammatory stimuli) and rotenone- oligomycin A (oxidative stimuli). Our results show that curcumin promotes the acquisition of alternative microglial phenotype in an HO-1-dependent manner, reduces iNOS induction and ROS production, to protect glial cells against oxidative/inflammatory stimuli.

Materials and methods

Mixed glial culture

Mixed glial cultures were prepared from cerebral cortices of 3-day-old Sprague Dawley rats as previously described (Saura *et al.* 2003). Briefly, after removing the meninges and blood vessels, the forebrains were gently dissociated by repeated pipetting in Dulbecco's modified Eagle' (DMEM) /F12 medium. After mechanical dissociation, cells were seeded in DMEM/F12 with 20 % of Fetal Bovine Serum (FBS) at a density of 300,000 cells/ml and cultured at 37 °C in humidified 5 % CO_2/95 % air. Medium was replaced after 5 days *in vitro* (DIV) for DMEM/F12 with 10 % FBS. Confluence was achieved after 10–12 DIV.

Isolation of microglia and astrocytes

Microglia and astrocytes were isolated using a mild trypsinization method as previously described (Saura et al. 2003) with brief modifications. After 10-12 DIV, the following steps were conducted to obtain different purified fractions of microglia and astrocytes: **(1st)** microglia located in the upper part of the culture was isolated by shaking the mixed glia-containing flasks for 15 min at 200 rpm, the supernatant was collected (**highly enriched microglia 1**), **(2nd)** cells were then treated with trypsin solution (0.25 % trypsin, 1 mM EDTA) diluted 1:4 in DMEM-F12, this process resulted in the detachment of an upper layer of cells in one piece (**highly enriched astrocytes**), and, (3rd) microglial cells that were attached to the bottom of the well were detached (**highly enriched microglia 2**). For a schematic picture see supplemental data 1. A great majority of microglia and astrocytes were positive for Iba1 and GFAP respectively, measured by western blot

measured at 540 nm. Control cells treated with vehicle (MEM/F-12) were taken as 100% viable.

Quantification of viability by MTT in glia cells

Cell viability, virtually the mitochondrial activity of living cells, was measured by a quantitative colorimetric assay with MTT, as described previously (Denizot & Lang 1986) Briefly, 50 µl of the MTT labeling reagent, at a final concentration of 0.5 mg/ml, was added to the DMEM/F-12 of each well at the end of the RO/LPS (rotenone + Lipopolysaccharide) period; then, the plate was placed in a humidified incubator at 37 °C with 5% CO_2 and 95 % air (v/v) for an additional 2 h. Thereafter, the insoluble formazan was dissolved with dimethyl sulfoxide; colorimetric determination of MTT reduction was measured at the wavelength of 540 nm. Control cells treated with vehicle (DMEM/F-12) were taken as 100 % viable.

ROS measurement

To measure cellular ROS, we used the molecular probe H_2DCFDA (Ha *et al.* 1997). Glial cells were loaded with 5 µM H_2DCFDA, which diffuses through the cell membrane and is hydrolyzed by intracellular esterases to the non-fluorescent form dichlorofluorescein (DCFH). DCFH reacts with intracellular H_2O_2 to form dichlorofluorescin, a green-fluorescent dye. Fluorescence was measured in a fluorescence microplate reader (FLUOstar Galaxy; BMG Labtech, Offenburg, Germany). Wavelengths of excitation and emission were 485 and 520 nm, respectively.

Immunoblotting and image analysis

After the various treatments, glia cells (5×10^6) were washed once with cold phosphate-buffered saline and lysed in 100 µl ice-cold lysis buffer (1 % Nonidet P-40, 10 % glycerol, 137 mM NaCl, 20 mM Tris–HCl, pH 7.5, 1 µg/ml leupeptin, 1 mM phenylmethylsulfonyl fluoride, 20 mM NaF, 1 mM sodium pyrophosphate, and 1 mM Na3VO4). Protein (30 µg) from this cell lysate was resolved by SDS–PAGE and transferred to Immobilon-P membranes (Millipore Corp., Billerica, MA, USA). Membranes were incubated with anti-iNOS/NOS Type II (1:1000; Santa Cruz Biotechnology, Santa Cruz, CA, USA), anti-HO-1 (1:1000; Chemicon, Temecula, CA, USA), anti-β-actin (1:100,000; Sigma), anti-Iba1 (1:1000; ionized calcium-binding adapter molecule 1; Wako Chemicals, Rafer S.L, Madrid, Spain), or anti-GFAP (1:1000 Millipore Corp., Billerica, MA, USA). Appropriate peroxidase-conjugated secondary antibodies (1:10,000) were used to detect proteins by enhanced chemiluminescence. Different band intensities corresponding to immunoblot detection of protein samples were quantified using the Scion Image program. Immunoblots correspond to a representative experiment that was repeated three or four times with similar results.

Determination of NO^{2-} based on the Griess Reaction

To determine NO^{2-} produced from LPS-treated cells. After 16 h activation, the cell culture supernatant from each sample was collected and an equal volume of Griess reagents (Marzinzig *et al.* 1997) were added. After 5 min incubation at room temperature, light absorption was measured at 550 nm in a microplate reader ((FLUOstar Galaxy; BMG Labtech, Offenburg, Germany). Nitrite release of control cells treated with vehicle (DMEM/F-12) was taken as 100 %.

Shape factor determination

Given the basically two-dimensional arrangement of cells in our material, cell size and surface could be estimated by applying (Howard *et al.* 2005) The apparent area of the Iba 1-immunostained cell profiles was estimated by point counting, superimposing a regular lattice of points on confocal photomicrographs of the cells.

On the same cells, the length of their cytoplasmic boundary was estimated by randomly superimposing a Merz grid. The grid consists of repetitions of a rectangle that contains a sinuous line formed by two succesive semicircumferences in opposed directions. This is the test line, with built-in isotropy in 2D, and the intersections (*I*) between this line and the cell boundary are recorded to estimate the length (*L*) of each profile by the simple equation:

$$\hat{L} = \frac{\pi}{2} \cdot \frac{a}{l} \cdot \frac{1}{asf} \cdot \sum I$$

where *a/l* is the grid constant (area of the rectangle divided by the length of the test line, that is, 2d/Π), and *asf* is the fraction of the area sampled by the grid (1, in our design).

The surface and length values obtained for each cell were then used to compute a simple shape descriptor, to gain a –undoubtedly biased, but still informative- quantitative measure of the degree of circularity of the profile by

$$Circ = \frac{4\pi a_i}{b_i^2}$$

where *a* is the estimated area of the cell *I*, and *b* is its cytoplasmic boundary length.

Stadisctics

Data are given as means ± SEM. Differences between groups were determined by applying a one-way ANOVA followed by a Newman–Keuls test or Student t test when appropriate. Differences were considered statistically significant when $p < 0.05$.

Results

Cell death induced by rot/oligo plus LPS

We first established the experimental conditions that were most appropriate to induce cell death with the combination of an oxidative oxidative stress stimuli, using the mitochondrial complex I inhibitor rotenone at 30 µM and complex V inhibitor oligomycin A at 10 µM (RO), together with a pro-inflammatory stimuli with lipopolysaccharide-LPS (0.1, 1 and 10 µg/ml). For this purpose, cells were incubated for different time periods (8, 16 or 24 h) with the toxics and, at the end of each period, cell viability was assed by the MTT method.

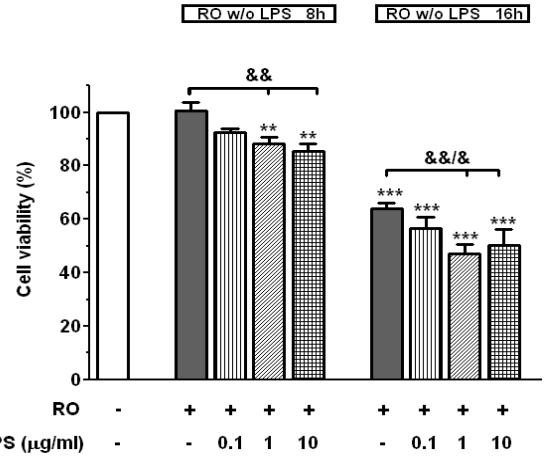

Fig1. Time-dependent cell death induced by rotenone plus oligomycin A in the absence or presence of LPS. To elicited cell death, mixed glia cultures were treated with 30 µM rotenone plus 10 µM oligomycin (RO) for various times (8 and 16 h). RO stimulus was also combined with increasing concentrations of LPS (0.1, 1 and 10 µg/ml). Cell viability was measured using the MTT assay. Data are means ± SEM of six different cell batches; ***p<0.001 and **p<0.01 significantly different from basal cells; &&p<0.01 and &p< 0.05 compared to toxic potentiation of RO *versus* RO plus LPS

As represented in **Fig 1**, RO incubated alone for 8 h had no significant effect on cell viability but when incubated for 16 h, it reduced viability to 40 %. LPS (0.1, 1 and 10 µg/ml) incubated alone for 8, 16 or 24 h had no effect on cell viability when compared to basal (Data not shown). Interestingly, when the inflammatory stimulus with LPS was added to RO, a significant reduction in cell viability was achieved, both when the 8 or 16 h incubation protocol was used. However, the maximum toxic effect was achieved when RO was combined with LPS-1µg/ml during 16 h; this combination reduced cell viability to 46 % with respect to RO alone (63 %). Therefore, for future experiments, we selected 16 h incubation with RO plus LPS 1µg/ml (from now on termed **RO/LPS**) since it afforded a good window for recovery opportunity.

Curcumin affords protection against RO/LPS

Curcumin is widely used to afford neuroprotection against various cytotoxic stimuli, such as okadaic acid (Rajasekar et al. 2013), amyloid beta (Hoppe et al. 2013) or ischemia/reperfusion (Kim et al. 2012b). However, little is known about the effect of curcumin in glial cells. Following the protocol shown on the top part of **Fig. 2**, 16 h incubation with RO plus LPS 1µg/ml reduced cell viability to 46%, measured as reduction of MTT. To test the protective properties of curcumin, we co-incubated mixed-glial cultures with increasing concentrations of curcumin (1, 3, 10 and 20 µM) and the toxic stimuli for 16h; with these fixed conditions, curcumin afforded cytoprotection at 10 and 20 µM; the maximum protective effect was achieved at 10 µM (60 % cytoprotection).

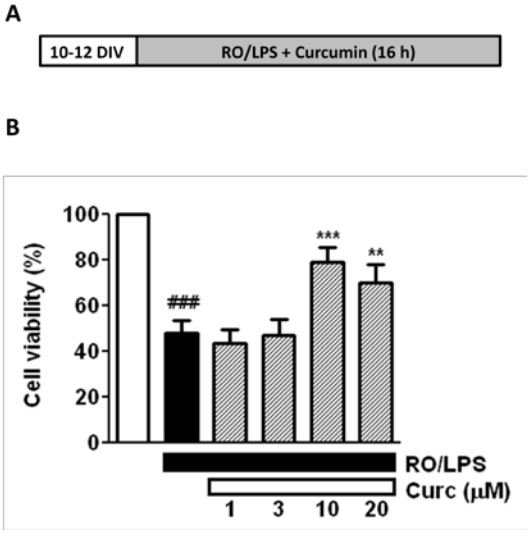

Fig2. Curcumin afforded cytoprotection against RO and LPS 1µg/ml. Following the protocol shown in on the top part of the figure, mixed glial cultures were co-incubated with RO plus LPS-1µg/ml (RO/LPS) and increasing concentrations of curcumin (1, 3, 10 and 20 µM) for 16 h, at the end of this period, cell viability was measured using the MTT assay. Data are means ± SEM of six different cell batches; ###p<0.001 significantly different from basal cells; ***p<0.001 and **p< 0.01 in comparison with RO/LPS treated cells

Curcumin protects glia cells by inducing HO-1 against RO/LPS

Once the beneficial effect of curcumin was observed, we wanted to test the importance of HO-1 induction in the protective mechanism of curcumin. According to the protocol shown in Fig XXX, cells were co-incubated with RO/LPS plus curcumin 10 µM, in the absence or presence of tin (IV) protoporphyrin (SnPP 3 µM, an inhibitor of HO-1 activity). SnPP significantly prevented the protective effect afforded by curcumin 10 µM (**Fig. 3A**). The possibility that curcumin was affording protection by inducing HO-1 was tested in the following experiment. Mixed-glial cultures were incubated for 16 h with vehicle or increased concentrations of curcumin (1, 3, 10 and 20 µM) and cell lysates were resolved by SDS–PAGE and analyzed by immunoblot with anti-HO-1 antibody (**Fig. 3B**). Curcumin 10 µM and 20 µM significantly increased (by 2.7 and 7.2-fold, respectively) the amount of HO-1 expression compared with control cells. These experiments show that curcumin increases the expression of HO-1 at the concentrations where protection was observed, and this over-expression is related with its protective effect.

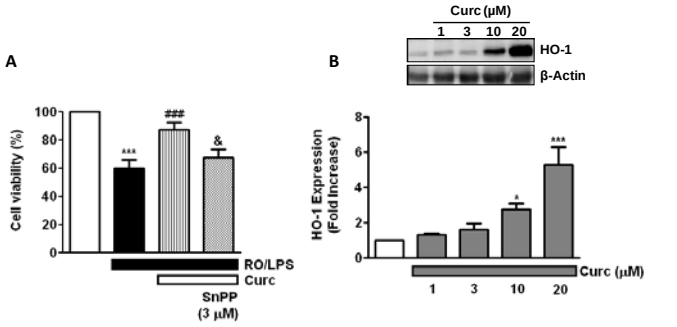

Fig3. **Curcumin-10 μM afforded cytoprotection against RO/LPS through HO-1 induction.** Following the protocol shown in Fig. 2A, mixed glial cultures were treated with RO/LPS and curcumin-10 μM in the presence or absence of tin (Sn)protoporphyrin-IX 3μM (SnPP) for 16 h **(A)** Mixed glial cultures were treated with increasing concentrations of curcumin (1, 3,10 and 20 μM) for 16 h , after this period cells were collected for inmunoblot of HO-1 (B). The histogram presents the densitometric quantification of HO-1 induction using β-actin for normalization. Values are means ± SEM of six experiments. ***p<0.001 and *p<0.05 in comparison with basal; $^{\#\#\#}$p<0.001 with respect to RO/LPS; $^{\&}$p<0.05 significantly different from curcumin.

Curcumin reduces reactive oxygen species (ROS) generated by RO/LPS via HO-1 induction

Oxidative stress is a common characteristic of many neurodegenerative diseases that can drive to cell death through excessive production of ROS. Therefore, we analyzed ROS production with the fluorescence probe H_2DFCDA using the protocol previously shown in **Fig. 2**. Glial cells were incubated with LPS 1μg/ml, RO or with the combination of both toxic stimuli (RO/LPS) for 16 h. This stimulus produced a significant increase of ROS in comparison with the control cells (**Fig. 4**). However, the maximum amount of ROS was achieved with the toxic combination RO/LPS. The antioxidant properties of curcumin were tested by incubating the cells with RO/LPS plus curcumin 10 μM for 16 h; under these conditions, ROS production was reduced near to basal levels. To corroborate the involvement of HO-1 induction in this effect, we incubated the cells with curumin-10 μM plus SnPP-3 μM. As expected, SnPP prevented the antioxidant effect afforded by curcumin (**Fig. 4**), indicating that HO-1 participates in the control of redox homeostasis by curcumin.

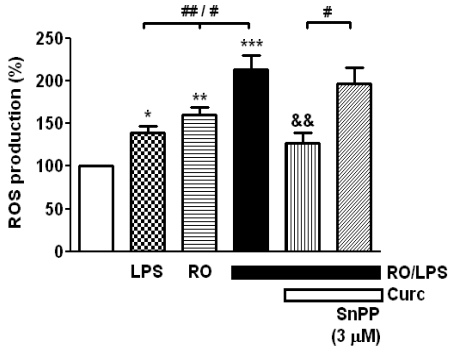

Fig 4. Curcumin reduces ROS production induced by RO and/or LPS by a mechanism that implicates HO-1. Mixed glial cultures were co-incubated with RO and LPS alone or combined (RO/LPS) for 16 h. Another set of glial cultures were treated with RO/LPS plus curcumin-10 μM in the presence or absence of the HO-1 inhibitor SnPP-3μM. ROS production under the different experimental conditions was measured with the fluorescent probe H_2DCFDA and normalized with respect to basal production (100 %). Data correspond to the means ± SEM of five different cell batches; ***p<0.001, **p<0.01 and *p<0.05 compared to basal; $^{\&\&}$p<0.05 with respect to RO/LPS; $^{\#\#}$p<0.01 and $^{\#}$p<0.05 as is indicated.

through HO-1 induction

It has been reported that curcumin can attenuate LPS-induced pro-inflammatory responses in glial cell cultures (Wang *et al.* 2010, Lee et al. 2007); however, the mechanism involved in theese effects is still poorly understood. To assess the ability of curcumin to regulate nitric oxide release by LPS stimulation, we exposed mixed glial cultures to LPS 1 μg/ml, with or without curcumin 10 μM for 16 h; thereafter, supernatants were removed and assayed for nitrite content. Controls (considered as 100 %) were supernatants of cells treated with fresh medium for 16 h. As shown in **Fig. 5A**, nitrite release was increased by **3.8**-fold in LPS 1 μg/ml treated cells; the presence of curcumin significantly reduced nitrite release induced by LPS. To explore the participation of HO-1 in the reduction of nitrite release upon an inflammatory stimulus, glial cells were incubated with 3 μM SnPP, a HO-1 inhibitor, in the presence of curcumin and LPS. Under these experimental conditions, curcumin reduction of LPS-nitrite release was prevented by SnPP, suggesting that HO-1 was participating in the protective pathway of curcumin.

Astrocyte/microglia intercellular communication is crucial for the maintenance of many intracellular signals (Pascual *et al.*, Liu *et al.*). Often, this interaction is lost when subcultures of both cell types are performed separately. To avoid this, we wanted to create a method that would allow us to analyze the behavior of astrocytes and microglia independently, after having treated them in a mixed culture. To address this issue we have established a protocol that allows separation of microglia and astrocytes after being co-cultured (see Material and Methods section and Suplemental data). Using this approach, we wanted to study iNOS expression under LPS treatment and evaluate if curcumin was regulating the expression of this inducible enzyme in a specific glial cell type. For this purpose, mixed glial cell cultures were incubated with LPS 1 μg/ml with or without curcumin 10 μM, for 16 h. At the end of this period, astrocytes and microglia were specifically isolated from the initial mixed glial culture (see Materials and Methods) and iNOS expression was assessed by western blotting. Interestingly, LPS caused a significant increase of iNOS in microglial cells but not in astrocytes, and this induction was remarkably reduced in curcumin treated microglia (**Fig. 5B**). To further evaluate the involvement of HO-1 induction in this effect, curcumin was incubated in the presence or absence of SnPP-3 μM; under these experimental conditions, SnPP reverted the reduction of iNOS caused by curcumin in LPS treated microglia (**Fig. 5B**).

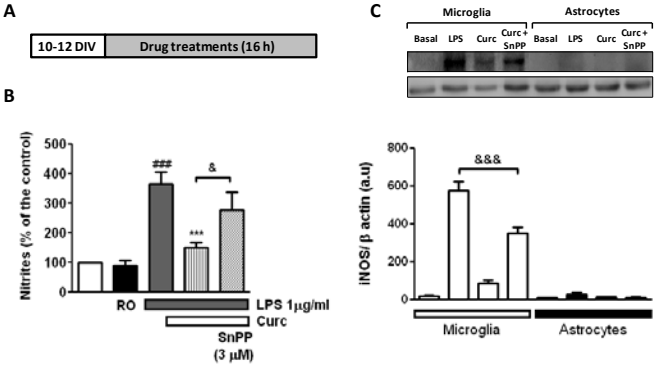

Fig 5. Curcumin reduces NO production and microglial iNOS overexpression against LPS via HO-1. (A) Illustrates the experimental protocol used**.** Mixed glial cultures were treated with RO plus LPS-1μg/ml and curcumin-10μM in the presence or absence of SnPP-3μM for 16 h. After this period supernatant was collected to determine NO production measured by griess reaction. **(B)** Represents the average data, expressed as percentage of control, obtained for each experimental condition indicated in the graph. **(C)** The top part of the figure shows a representative immunoblot of iNOS measured in isolated microglia and astrocytes, after exposing the mixed cultures to the experimental conditions used in figure A (see Material and Methods). Values are means ± SEM of six experiments. $^{\#\#\#}$p<0.001 in comparison with basal cells; ***p<0.001 significantly different from LPS treated cells; $^{\&\&\&}$p<0.001 and $^{\&}$p<0.05 compares the indicated bars.

Curcumin prevents LPS-nitrite release and iNOS over-expression Curcumin reduced iNOS expression in microglia involves HO-1

induction

To corroborate results shown in Fig. 5 we studied iNOS expression induced by LPS and the effect of curcumin 10 µM measured by innunofluorescence. Following the protocol shown in Fig. 5A, mixed glial cultures were treated with LPS 1 µg/ml in the presence or absence of curcumin 10 µM. Curcumin was incubated with or without SnPP 3µM to test the involvement of HO-1. induction. When the experiment was ended, cells were fixed and labeled by using different antibodies such as anti-Iba1 (microglial marker), DAPI (nuclear marker) and anti-iNOS. As previously observed, iNOS expression was evident only in cells treated with LPS or LPS plus curcumin-SnPP (Fig. 6). Taken together, these results indicate that curcumin can reduce iNOS overexpression-induced by LPS by a mechanism that involves HO-1 induction

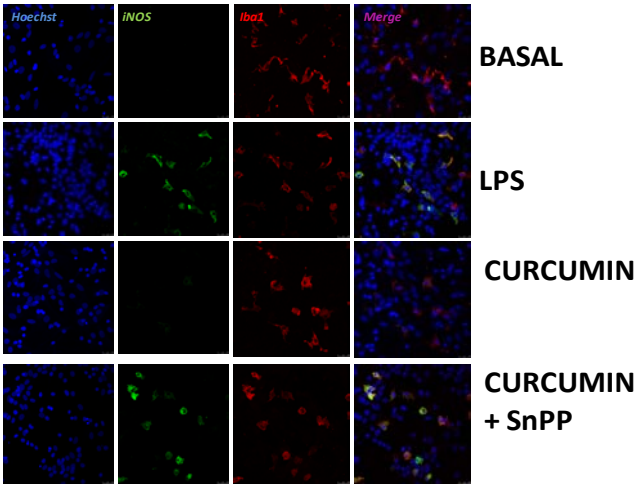

Fig 6. Curcumin reduces microglial iNOS overexpresion induced by LPS via HO-1. Immunofluorescence with anti-Iba1 (red), anti-iNOS (green) and Hoechst (blue) following the experimental conditions shown in Fig. 5A, cells were treated with LPS-1µg/ml with or without curcumin-10µM (in the presence or absence of SnPP-3µM).

Curcumin prevents LPS induced microglial pro-inflammatory phenotype via HO-1 induction

Ameboid microglia is considered a type of activated microglia phenotype linked to a phagocyte state (Giulian & Baker 1986). This state is characterized by an enlargement of the cell bodies and retraction of the microglial branches. Following the experimental conditions mentioned above, we decided to quantify the microglial phenotype changes. For this purpose, shape factor equation was used to determine microglial circularity (see Materials and Methods). Shape factor values of LPS-treated microglia cells (labeled with anti-Iba1) were four times higher than the values observed in control cells; curcumin 10 µM reduced this effect. To determine the participation of HO-1 in curcumin´s effect, the inhibitor of HO- 1,SnPP-3 µM, was used. Surprisingly, SnPP not only prevented the effects of curcumin, but the shape factor values were higher than those observed with the incubation of LPS alone (**Fig. 7B**). For control purposes, a parallel group of cells were incubated with LPS plus SnPP-3 µM; under these conditions, shape factor values were also higher than those observed with LPS alone. Therefore, HO-1 inhibition seems to shift microglial phenotype to ameboid morphology.

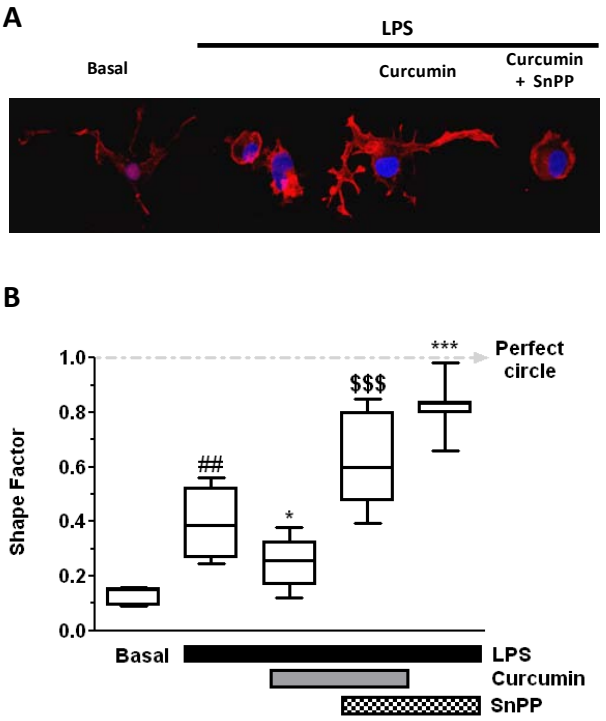

Fig 7. Curcumin reduces the microglial shape factor index increase induced by LPS by a mechanism that implicates HO-1. Following the protocol shown in Fig. 5A, cells were treated with LPS-1 µg/ml with or without curcumin-10 µM (in the presence or absence of SnPP-3µM). **(A)** shows representative images of microglial phenotype in the different conditions mentioned above. **(B)** Represents stereological quantification of microglial circularity, expressed as shape factor (see Materials and Methods). Data are mean ± SEM of at least 300 cells $^{\#\#}p<0.01$ in comparison with basal; $^{***}p<0.001$, $^{*}p<0.05$ with respect to LPS; $^{\$\$\$}p<0.001$ significantly different from curcumin treated cells.

Discussion

In the present study, we provide experimental evidence *in vitro* of the antioxidant and anti-inflammatory effect of curcumin in RO/LPS-treated mixed glial cultures. Curcumin induces HO-1 expression, which reduces oxidative stress, iNOS overexpression, microglial activated phenotype and NO production, thus promoting the resolution of microglial inflammation.

Curcumin has a well-known inhibitory role on pro-inflammatory gene expression in microglia. Recent studies show a noticeable inhibitory effect of curcumin against HIV-1 gp120-induced neuronal damage (Guo *et al.* 2013). Furthermore, curcumin inhibits the activation of microglial cells by inhibiting the production of NO and diminishing the release of cytokines such as IL6 and TNF (Zhang et al. 2010, Kim *et al.* 2012a). The protective effect of curcumin seems to be related to its anti-inflammatory actions, since curcumin protects dopaminergic neurons against microglia-mediated neurotoxicity but fails to exert neuroprotection in microglia-depleted cultures (Guo et al. 2013). Here, we have shown that curcumin´s anti-inflammatory effects depend on HO-1 induction. The immunomodulatory role of HO-1 was firstly described in peripheral macrophages, where HO-1 byproducts biliverdin and carbon monoxide inhibit NAD(P)H oxidase and TLR4 signaling, reducing macrophage activation. Furthermore, treatment with the anti-inflammatory cytokine IL-10 results in induction of HO-1 (Gomez-Hurtado *et al.* 2011). HO-1 also has an immunomodulatory role in the CNS. After traumatic brain injury, CD163/HO-1 positive microglia and infiltrated macrophages exhibit an anti-inflammatory and neuroprotective phenotype (Zhang *et al.* 2012). These results indicate that induction of HO-1 could be important in the fine regulation between classical and alternative phenotypes of microglia.

There are two main transcription factors that strongly regulate

redox homeostasis, i.e. NFkB and Nrf2. NFkB is considered the master regulator of microglial inflammatory responses to brain infections. LPS induces its translocation to the nucleus promoting the expression of iNOS, NO production, and finally the release of pro-inflammatory cytokines (Greenberg *et al.* 1998, Rossol *et al.* 2011). It is well documented that curcumin inhibits NFkB activation, and consequently iNOS induction and NO production (Greenberg et al. 1998, Deshpande *et al.* 1997) Here, we have shown that iNOS induction was controlled by HO-1 over-expression induced by curcumin. HO-1 is a phase II antioxidant enzyme induced by translocation of the transcription factor Nrf2. The effect of Nrf2 has been described in different *in vivo* models where Nrf2 null mice have enhanced vulnerability to asthma (Rangasamy *et al.* 2005) or emphysema (Rangasamy *et al.* 2004). Moreover, LPS produced an enhanced inflammatory response in Nrf2 KO mice compared to control mice (Thimmulappa *et al.* 2006). There is increasing evidence about the crosstalk between HO-1 expression and IL10 release (Chen *et al.* 2013, Mandal *et al.* 2010)

The role of HO-1 induced by LPS is still controversial, some authors assert that HO-1 induced by LPS regulates the expression of proinflammatory markers, thus contributing to increased cell damage and immune response (Dodd & Filipov 2011, Chen *et al.* 2013). However, the opposite effect of HO-1 is also described. When HO-1 is induced by LPS, it can also have an important anti-inflammatory role, inhibiting the release of pro-inflammatory cytokines such as TNF and IL-6 (Wang *et al.* 2009). Our data concerning the shape factor values of the microglia support the anti-inflammatory role of HO-1, even when is induced by LPS.

Age is the major risk factor for neurodegenerative diseases. As brain ages there is an increase in pro-inflammatory and a decrease in anti-inflammatory gene signaling. Evidence points to a dysregulated immune response in aged microglia. Chronically primed microglia exhibits an excessive pro-inflammatory cytokine release in response to LPS injection (Godbout *et al.* 2005, Sparkman & Johnson 2008). Furthermore, aged microglia seems to be inefficient to solve inflammation, showing a decreased phagocytic activity and neuroprotective effects (Ye & Johnson 2001, Nolan *et al.* 2005) To date there is no effective treatment for repairing a damaged brain. The idea of a microglia-targeted therapy is under debate. Therapies aimed at restoring the neuroprotective and repairing profile of microglia would lead to the control of excessive microglial activation. Our data point that control of microglial activation through HO-1 overexpression, which has a potent antioxidant and anti-inflammatory activity (Jayasooriya *et al.* 2013), could be a novel strategy to restore the repairing profile of microglia. Recently, we have shown that HO-1 overexpression in microglia is critical for the neuroprotective effect shown in brain ischemia (Parada *et al.*). Therefore, curcumin could be a strong candidate because of its promising pharmacological activities as antioxidant, neuroprotectant and anti-inflammatory drug.

In conclusion, we suggest that curcumin induces a microglial anti-inflammatory phenotype by reducing iNOS expression and NO production. We have also reported cytoprotective and antioxidant properties of curcumin in mixed glia cultures. All these effects of curcumin are dependent on the expression of the antioxidant enzyme HO-1.

Acknowledgments

This work was supported BY grants from the Spanish Ministerio de Economía y Competitividad Ref. SAF2012-32223 and the Spanish Ministry of Health (Instituto de Salud Carlos III) RENEVAS-RETICS-RD06/0026. We would also like to thank the continued support of Fundación Teófilo Hernando.

References

Aggarwal, B. B. and Shishodia, S. (2006) Molecular targets of dietary agents for prevention and therapy of cancer. *Biochem Pharmacol,* **71,** 1397-1421.

Allan, S. M. and Rothwell, N. J. (2001) Cytokines and acute neurodegeneration. *Nat Rev Neurosci,* **2,** 734-744.

Block, M. L., Zecca, L. and Hong, J. S. (2007) Microglia-mediated neurotoxicity: uncovering the molecular mechanisms. *Nat Rev Neurosci,* **8,** 57-69.

Chen, C., Zhang, F., Zhang, Z., Peng, M., Wang, Y. and Chen, Y. (2013) TLR4 signaling-induced heme oxygenase upregulation in the acute lung injury: role in hemorrhagic shock and two-hit induced lung inflammation. *Mol Biol Rep,* **40,** 1167-1172.

Denizot, F. and Lang, R. (1986) Rapid colorimetric assay for cell growth and survival. Modifications to the tetrazolium dye procedure giving improved sensitivity and reliability. *J Immunol Methods,* **89,** 271-277.

Deshpande, R., Khalili, H., Pergolizzi, R. G., Michael, S. D. and Chang, M. D. (1997) Estradiol down-regulates LPS-induced cytokine production and NFkB activation in murine macrophages. *Am J Reprod Immunol,* **38,** 46-54.

Dodd, C. A. and Filipov, N. M. (2011) Manganese potentiates LPS-induced heme-oxygenase 1 in microglia but not dopaminergic cells: role in controlling microglial hydrogen peroxide and inflammatory cytokine output. *Neurotoxicology,* **32,** 683-692.

Giulian, D. and Baker, T. J. (1986) Characterization of ameboid microglia isolated from developing mammalian brain. *J Neurosci,* **6,** 2163-2178.

Godbout, J. P., Chen, J., Abraham, J., Richwine, A. F., Berg, B. M., Kelley, K. W. and Johnson, R. W. (2005) Exaggerated neuroinflammation and sickness behavior in aged mice following activation of the peripheral innate immune system. *Faseb J,* **19,** 1329-1331.

Gomez-Hurtado, I., Zapater, P., Bellot, P., Pascual, S., Perez-Mateo, M., Such, J. and Frances, R. (2011) Interleukin-10-mediated heme oxygenase 1-induced underlying mechanism in inflammatory down-regulation by norfloxacin in cirrhosis. *Hepatology,* **53,** 935-944.

Greenberg, S. S., Jie, O., Zhao, X. and Wang, J. F. (1998) Role of PKC and tyrosine kinase in ethanol-mediated inhibition of LPS-inducible nitric oxide synthase. *Alcohol,* **16,** 167-175.

Guo, L., Xing, Y., Pan, R., Jiang, M., Gong, Z., Lin, L., Wang, J., Xiong, G. and Dong, J. (2013) Curcumin protects microglia and primary rat cortical neurons against HIV-1 gp120-mediated inflammation and apoptosis. *PLoS One,* **8,** e70565.

Gupta, S. C., Patchva, S. and Aggarwal, B. B. (2013) Therapeutic roles of curcumin: lessons learned from clinical trials. *Aaps J,* **15,** 195-218.

Ha, H. C., Woster, P. M., Yager, J. D. and Casero, R. A., Jr. (1997) The role of polyamine catabolism in polyamine analogue-induced programmed cell death. *Proc Natl Acad Sci U S A,* **94,** 11557-11562.

Hanisch, U. K. and Kettenmann, H. (2007) Microglia: active sensor and versatile effector cells in the normal and pathologic brain. *Nat Neurosci,* **10,** 1387-1394.

Hatcher, H., Planalp, R., Cho, J., Torti, F. M. and Torti, S. V. (2008) Curcumin: from ancient medicine to current clinical trials. *Cell Mol Life Sci,* **65,** 1631-1652.

Hoppe, J. B., Haag, M., Whalley, B. J., Salbego, C. G. and Cimarosti, H. (2013) Curcumin protects organotypic hippocampal slice cultures from Abeta1-42-induced synaptic toxicity. *Toxicol In Vitro,* **27,** 2325-2330.

Howard, C.V., Reed, M. G (2005) Unbiased stereology. Three-dimensional measurement in microscopy. Oxford, Bios Scientific

Jagetia, G. C. and Aggarwal, B. B. (2007) "Spicing up" of the immune system by curcumin. *J Clin Immunol,* **27,** 19-35.

Jayasooriya, R. G., Lee, K. T., Lee, H. J., Choi, Y. H., Jeong, J. W. and Kim, G. Y. (2013) Anti-inflammatory effects of beta-hydroxyisovalerylshikonin in BV2 microglia are mediated through suppression of the PI3K/Akt/NF-kB pathway and activation of the Nrf2/HO-1 pathway. *Food Chem Toxicol*.

Jung, K. K., Lee, H. S., Cho, J. Y. et al. (2006) Inhibitory effect of curcumin on nitric oxide production from lipopolysaccharide-activated primary microglia. *Life Sci,* **79,** 2022-2031.

Karlstetter, M., Lippe, E., Walczak, Y., Moehle, C., Aslanidis, A., Mirza, M. and Langmann, T. (2011) Curcumin is a potent modulator of microglial gene expression and migration. *J Neuroinflammation,* **8,** 125.

Kim, K. H., Lee, E. N., Park, J. K. et al. (2012a) Curcumin attenuates TNF-alpha-induced expression of intercellular adhesion

molecule-1, vascular cell adhesion molecule-1 and proinflammatory cytokines in human endometriotic stromal cells. *Phytother Res*, **26,** 1037-1047.
Kim, Y. S., Kwon, J. S., Cho, Y. K., Jeong, M. H., Cho, J. G., Park, J. C., Kang, J. C. and Ahn, Y. (2012b) Curcumin reduces the cardiac ischemia-reperfusion injury: involvement of the toll-like receptor 2 in cardiomyocytes. *J Nutr Biochem*, **23,** 1514-1523.
Lee, H. S., Jung, K. K., Cho, J. Y., Rhee, M. H., Hong, S., Kwon, M., Kim, S. H. and Kang, S. Y. (2007) Neuroprotective effect of curcumin is mainly mediated by blockade of microglial cell activation. *Pharmazie*, **62,** 937-942.
Liu, W., Tang, Y. and Feng, J. Cross talk between activation of microglia and astrocytes in pathological conditions in the central nervous system. *Life Sci*, **89,** 141-146.
Maheshwari, R. K., Singh, A. K., Gaddipati, J. and Srimal, R. C. (2006) Multiple biological activities of curcumin: a short review. *Life Sci*, **78,** 2081-2087.
Mandal, P., Pritchard, M. T. and Nagy, L. E. (2010) Anti-inflammatory pathways and alcoholic liver disease: role of an adiponectin/interleukin-10/heme oxygenase-1 pathway. *World J Gastroenterol*, **16,** 1330-1336.
Marzinzig, M., Nussler, A. K., Stadler, J., Marzinzig, E., Barthlen, W., Nussler, N. C., Beger, H. G., Morris, S. M., Jr. and Bruckner, U. B. (1997) Improved methods to measure end products of nitric oxide in biological fluids: nitrite, nitrate, and S-nitrosothiols. *Nitric Oxide*, **1,** 177-189.
Monroy, A., Lithgow, G. J. and Alavez, S. (2013) Curcumin and neurodegenerative diseases. *Biofactors*, **39,** 122-132.
Nolan, Y., Maher, F. O., Martin, D. S., Clarke, R. M., Brady, M. T., Bolton, A. E., Mills, K. H. and Lynch, M. A. (2005) Role of interleukin-4 in regulation of age-related inflammatory changes in the hippocampus. *J Biol Chem*, **280,** 9354-9362.
Parada, E., Egea, J., Buendia, I., Negredo, P., Cunha, A. C., Cardoso, S., Soares, M. P. and Lopez, M. G. The Microglial alpha7-Acetylcholine Nicotinic Receptor Is a Key Element in Promoting Neuroprotection by Inducing Heme Oxygenase-1 via Nuclear Factor Erythroid-2-Related Factor 2. *Antioxid Redox Signal*, **19,** 1135-1148.
Parada, E., Egea, J., Buendia, I., Negredo, P., Cunha, A. C., Cardoso, S., Soares, M. P. and Lopez, M. G. (2013) The microglial alpha7-acetylcholine nicotinic receptor is a key element in promoting neuroprotection by inducing heme oxygenase-1 via nuclear factor erythroid-2-related factor 2. *Antioxid Redox Signal*, **19,** 1135-1148.
Pascual, O., Ben Achour, S., Rostaing, P., Triller, A. and Bessis, A. Microglia activation triggers astrocyte-mediated modulation of excitatory neurotransmission. *Proc Natl Acad Sci U S A*, **109,** E197-205.
Qin, L., Liu, Y., Cooper, C., Liu, B., Wilson, B. and Hong, J. S. (2002) Microglia enhance beta-amyloid peptide-induced toxicity in cortical and mesencephalic neurons by producing reactive oxygen species. *J Neurochem*, **83,** 973-983.
Rahman, I., Biswas, S. K. and Kirkham, P. A. (2006) Regulation of inflammation and redox signaling by dietary polyphenols. *Biochem Pharmacol*, **72,** 1439-1452.
Rajasekar, N., Dwivedi, S., Tota, S. K., Kamat, P. K., Hanif, K., Nath, C. and Shukla, R. (2013) Neuroprotective effect of curcumin on okadaic acid induced memory impairment in mice. *Eur J Pharmacol*, **715,** 381-394.
Rangasamy, T., Cho, C. Y., Thimmulappa, R. K. et al. (2004) Genetic ablation of Nrf2 enhances susceptibility to cigarette smoke-induced emphysema in mice. *J Clin Invest*, **114,** 1248-1259.
Rangasamy, T., Guo, J., Mitzner, W. A. et al. (2005) Disruption of Nrf2 enhances susceptibility to severe airway inflammation and asthma in mice. *J Exp Med*, **202,** 47-59.
Rossol, M., Heine, H., Meusch, U., Quandt, D., Klein, C., Sweet, M. J. and Hauschildt, S. (2011) LPS-induced cytokine production in human monocytes and macrophages. *Crit Rev Immunol*, **31,** 379-446.
Saura, J., Tusell, J. M. and Serratosa, J. (2003) High-yield isolation of murine microglia by mild trypsinization. *Glia*, **44,** 183-189.
Schwartz, M., Butovsky, O., Bruck, W. and Hanisch, U. K. (2006) Microglial phenotype: is the commitment reversible? *Trends Neurosci*, **29,** 68-74.
Shishodia, S. (2013) Molecular mechanisms of curcumin action: gene expression. *Biofactors*, **39,** 37-55.
Sparkman, N. L. and Johnson, R. W. (2008) Neuroinflammation associated with aging sensitizes the brain to the effects of infection or stress. *Neuroimmunomodulation*, **15,** 323-330.
Streit, W. J. (2002) Microglia as neuroprotective, immunocompetent cells of the CNS. *Glia*, **40,** 133-139.
Thimmulappa, R. K., Scollick, C., Traore, K. et al. (2006) Nrf2-dependent protection from LPS induced inflammatory response and mortality by CDDO-Imidazolide. *Biochem Biophys Res Commun*, **351,** 883-889.
Wang, H. M., Zhao, Y. X., Zhang, S., Liu, G. D., Kang, W. Y., Tang, H. D., Ding, J. Q. and Chen, S. D. (2010
) PPARgamma agonist curcumin reduces the amyloid-beta-stimulated inflammatory responses in primary astrocytes. *J Alzheimers Dis*, **20,** 1189-1199.
Wang, X. M., Kim, H. P., Nakahira, K., Ryter, S. W. and Choi, A. M. (2009) The heme oxygenase-1/carbon monoxide pathway suppresses TLR4 signaling by regulating the interaction of TLR4 with caveolin-1. *J Immunol*, **182,** 3809-3818.
Ye, S. M. and Johnson, R. W. (2001) An age-related decline in interleukin-10 may contribute to the increased expression of interleukin-6 in brain of aged mice. *Neuroimmunomodulation*, **9,** 183-192.
Zhang, L., Wu, C., Zhao, S., Yuan, D., Lian, G., Wang, X., Wang, L. and Yang, J. (2010) Demethoxycurcumin, a natural derivative of curcumin attenuates LPS-induced pro-inflammatory responses through down-regulation of intracellular ROS-related MAPK/NF-kappaB signaling pathways in N9 microglia induced by lipopolysaccharide. *Int Immunopharmacol*, **10,** 331-338.
Zhang, Z., Zhang, Z. Y., Wu, Y. and Schluesener, H. J. (2012) Lesional accumulation of CD163+ macrophages/microglia in rat traumatic brain injury. *Brain Res*, **1461,** 102-110.

Supplemental data 1

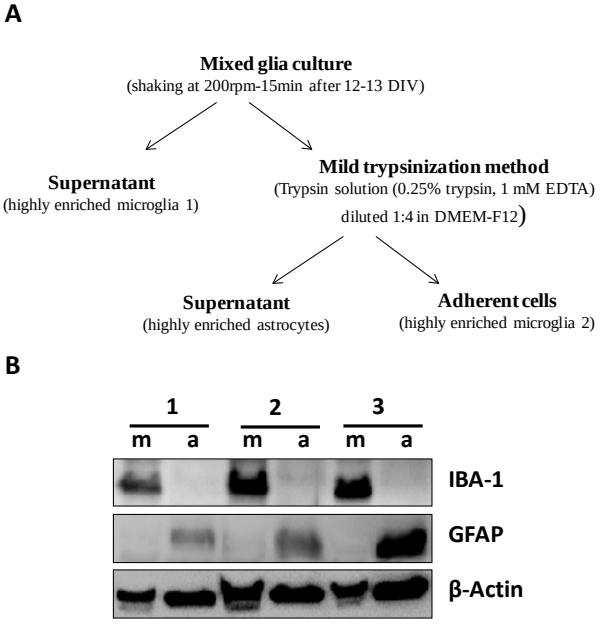

Supplemental data 1. Specific isolation of microglia and astrocyte cells from mixed glial cultures. Panel **(A)** shows the protocol used to separate specifically microglia (m) and astrocyte (a) from a mixed glia culture. Representative inmunoblots of GFAP (astrocyte marker), Iba1 (microglia marker) and β-actin after the end of this protocol. Samples of three different experiments are shown **(B).**

Este trabajo de investigación se ha centrado en determinar los efectos neuroprotectores y anti-inflamatorios mediados por la activación de receptores nicotínicos neuronales en modelos relacionados con la isquemia cerebral. Los resultados derivados de esta tesis ponen de manifiesto una vía de señalización que implica los receptores nicotínicos del subtipo α7 y la inducción de la enzima hemoxigenasa- 1(HO-1) vía Nrf2, así como la especial relevancia de la microglía en dicho proceso.

En el primer estudio, nos centramos en determinar el efecto neuroprotector del agonista de los nAChRs α7, PNU282997, ante un estímulo de isquemia in vitro. Para ello, se incubaron células SH-SY5Y con una combinación de los bloqueantes de los complejos mitocondriales I y V, rotenona y oligomicina A (rot/oligo), durante 8 h; estos bloqueantes de la cadena respiratorio mitocondrial ocasionaron una muerte celular entorno al 30 %. El tipo de muerte celular provocada por la combinación de rotenona y oligomicina A, fue fundamentalmente de tipo apoptótica; este hallazgo reviste gran interés pues, tal como se citó en la Introducción, en la zona de penumbra isquémica, que es la zona susceptible de rescate farmacológico, las células mueren principalmente por mecanismos de apoptosis y autofagia En estas condiciones de isquemia in vitro, el agonista de los receptores α7, PNU282987, incubado durante 16 h, después de las 8h de exposición a los tóxicos, fue capaz de ofrecer protección celular. Además de incrementar la viabilidad celular, disminuyó marcadores de apoptosis tales como la anexina-5 y la caspasa-3 activa. El hecho de que el PNU282987 fuera capaz de ofrecer neuroprotección después de haber expuesto las células a los tóxicos, reviste gran interés desde el punto de vista de aplicación clínica ya que los pacientes que han padecido un ictus son tratados horas después de haber sufrido dicho evento (Lacy *et al.* 2001; Hossmann 2012).

El agonista nicotínico α7, PNU282987, también redujo los niveles de ROS y aumentó la expresión de la enzima antioxidante HO-1. La importancia de la sobreexpresión de esta enzima y su relación con la activación de receptores nicotínicos estaba precedida por estudios anteriores del grupo, en los cuales se describió que el efecto citoprotector y antinociceptivo de la epibatidina estaba mediado, en parte, por la inducción de esta enzima antioxidante de fase II (Egea *et al*. 2007; Egea *et al.* 2009). En nuestro trabajo, hemos observado que los efectos neuroprotectores del PNU282987 se revierten en presencia de un inhibidor de la actividad de esta enzima, la SnPP (protoporfirina de estaño IV). Por tanto, estos resultados indican que los efectos

neuroprotectores observados con el PNU282987, incubado después de los tóxicos, estarían mediados en gran parte por la inducción de la enzima HO-1.

La relación entre la activación de los receptores nicotínicos y la regulación del estrés oxidativo celular es aún controvertida. Algunos autores afirman que la activación de los receptores α7 nAChR (usando generalmente nicotínica, como agonista de este receptor) produce un aumento de ROS dependiente de la entrada de Ca2+ al interior celular (Escubedo *et al*. 2009; Tsoyi *et al.* 2011). Sin embargo, otros trabajos, incluidos los de nuestro grupo, han observado lo contrario (Taveira *et al.* 2013; Zhang *et al.* 2013b). Una posible explicación a esta discordancia podría ser debida a la entrada de Ca2+ al interior celular por este receptor. Estudios previos de nuestro grupo demostraron que sólo es posible ver entrada de Ca2+ por el nAChR α7 cuando el agonista está en presencia de un modulador alostérico positivo de éste receptor (del Barrio et al. 2011). El aumento de Ca2+ producido por la activación de nAChR α7 va asociado a una activación de proteínas dependientes de Ca2+, como PKC y CaMKII, tras la cual se produce la activación de NAPH oxidasa, generando así ROS (Tsoyi *et al.* 2011). Es por esto por lo que en nuestros trabajos observamos una reducción en los niveles ROS y no un aumento de estos, ya que no hemos detectado ni entrada de Ca2+, ni activación de proteínas dependientes de este ion por activación de receptores α7 nAChR.

Para ahondar en cuáles serían las rutas de señalización intracelulares que podría estar activando el PNU282987, nos centramos en dos proteínas clásicas de supervivencia celular, la PIK3/AKT y la JAK2. Varios estudios han descrito la importancia de la fosforilación de AKT y JAK2 en enfermedades neurodegenerativas como el Parkinson, el Alzheimer o la isquemia (Shioda *et al.* 2009; Bencherif and Lippiello 2010; Wang *et al.* 2012). Recientemente, se ha descubierto que la proteína JAK2 se encuentra físicamente unida al receptor nicotínico α7, al realizarse ensayos de co-inmunoprecipitación de ambas proteínas (Shaw *et al.* 2002; Marrero and Bencherif 2009). Los efectos neuroprotectores del PNU282987 se previnieron mediante inhibidores selectivos de estas rutas intracelulares, además la incubación de las células con PNU282987 aumentó significativamente la fosforilación de ambas proteínas. Sabemos que la activación de AKT y JAK2 pueden dar lugar a la futura sobreexpresión de HO-1 (Shih *et al*. 2010; Zhang *et al*. 2013a). Por tanto, el conjunto de resultados de

este estudio indican que la vía de señalización implicada en el mecanismo neuroprotector del PNU282987 es α7nAChR/Jak2/AKT/HO-1.

Una vez establecido el efecto neuroprotector del agonista nAChR α7, en un modelo de toxicidad isquémica in vitro, en células de neuroblastoma humano, en un segundo estudio nos planteamos estudiar el efecto neuroprotector de la galantamina en un modelo más complejo. Seleccionamos la galantamina porque es un inhibidor de la acetilcolinesterasa empleado actualmente en clínica para tratar a los enfermos de Alzheimer, y también porque teníamos datos previos del grupo en el que habíamos demostrado que poseía efectos neuroprotectores por un mecanismo dependiente de receptores nicotínicos (Arias *et al*. 2004; Lorrio *et al*. 2007). En el segundo trabajo de esta tesis, hemos empleamos rodajas de hipocampo de rata sometidas a un periodo de privación de oxígeno y glucosa, seguido de otro de re-oxigenación con la idea de reproducir una situación de hipoxia/reperfusión *in vitro*. En estas condiciones experimentales, la galantamina, al igual que habíamos observado en el trabajo previo con el PNU282987, ofreció neuroprotección mediante un mecanismo que implica los receptores nicotínicos y las quinasas JAK2, PI3K y Akt. Aunque la activación de JAK2 por agonistas nicotínicos ha sido descrita con anterioridad (Marrero and Bencherif 2009), desconocíamos la relación entre la galantamina y esta proteína en concreto. En nuestro estudio, la incubación de las rodajas con galantamina durante 30 minutos, aumento la fosforilación de JAK2, y la adición de un inhibidor de la fosforilación de ésta revirtió su efecto protector, quedando así patente la importancia de esta proteína en el mecanismo de acción de la galantamina.

La galantamina se ha descrito como un fármaco cuya actividad dual (inhibidor de acetilcolinesterasa y modulador alostérico de receptores) produce neuroprotección frente a distintas enfermedades neurodegenerativas, aumenta la liberación de neurotransmisores y mejora la plasticidad sináptica (Ago *et al*. 2011). Se ha observado, tanto in vivo como in vitro, una relación directa entre la protección por galantamina y la activación de receptores nicotínicos (Arias *et al*. 2004). De hecho, en nuestros experimentos, mecamilamina (un antagonista no selectivo de receptores nicotínicos) revirtió los efectos neuroprotectores de galantamina. Aunque la participación de los receptores nicotínicos en el mecanismo protector de galantamina parece inequívoca, no hay que olvidar que la galantamina también puede potenciar las corrientes pre-sinápticas gabaérgica y glutamatérgica. En este sentido, los agonistas gabaergicos han

mostrado ser eficaces en modelos experimentales de isquemia, por lo que la galantamina podría ejercer su efecto, en parte también, a través de éste mecanismo de acción.

Otro de los aspectos que hemos explorado, en cuanto al mecanismo de acción de la galantamina, es su posible acción antiinflamatoria. Varios estudios aseguran que los efectos positivos de los inhibidores de acetilcolinesterasa frente a la enfermedad de Alzheimer, son debidos a su capacidad para aumentar los niveles de ACh en la hendidura sináptica, y por su capacidad anti-neuroinflamatoria (Tabet 2006). Los datos de nuestro estudio muestran que la galantamina puede ejercer un efecto antiinflamatorio, al impedir la translocación al núcleo de p65 durante la POG/reoxigenación.

La galantamina también mostró un marcado efecto antioxidante, al reducir los niveles de ROS y la activación de NAD(P)H oxidasa (NOX) e iNOS. La activación de NOX es considerada como la mayor fuente de ROS tras un evento isquémico (Abramov *et al.* 2007). De hecho, los compuestos inhibidores de esta actividad NOX son considerados como una buena estrategia terapéutica frente a la isquemia (Walder *et al*. 1997; Chen *et al*. 2009). La inhibición adicional de la iNOS puede suponer un efecto antioxidante complementario al de la inhibición de la NOX, ya que al reducirse la producción de NO y también de radicales $O2^-$, al estar inhibida la NOX, no se generan radicales peroxinitritos que son altamente reactivos (Kalyanaraman 2013). Teniendo en cuenta la capacidad antioxidante, anti-neuroinflamatoria y neuroprotectora de la galantamina, nuestros resultados señalan a la galantamina como un agente potencialmente eficaz frente la isquemia/reoxigenación. Estos datos se encuentran en la línea de trabajos anteriores del grupo, donde se ha visto el potencial efecto neuroprotector de la galantamina en un modelo de isquemia global en jerbo (Lorrio *et al.* 2009); en este estudio, el tratamiento de los animales con galantamina hasta 3h después de haber inducido la isquemia global, disminuyó de forma significativa el número de neuronas apoptóticas en la región hipocampal CA1.

Hasta ahora, habíamos comprobado que mitigar el estrés oxidativo, creado durante una situación de isquemia, suponía una buena estrategia para reducir el daño neuronal. También sabíamos que la actuación sobre los receptores nicotínicos, ya sea con el PNU282987 o con la galantamina, ocasionaba la activación de una ruta de

señalización de supervivencia que implica las quinasas JAK2, PI3K, Akt para, finalmente, inducir la enzima antioxidante HO-1, y así proteger las células SH-SY5Y y las rodajas de hipocampo ante un estímulo isquémico.

En base a los hallazgos anteriormente mencionados, a que la melatonina es una neurohormona con potentes propiedades antioxidante y, que resultados previos del grupo mostraban que la asociación de concentraciones subefectivas de galantamina y melatonina ofrecían un efecto neuroprotector sinérgico (Romero *et al.* 2010), nos planteamos profundizar en el mecanismo neuroprotector de la melatonina y su relación con los receptores nicotínicos en un modelo de isquemia/reperfusión. Aunque el modelo agudo de privación de oxígeno y glucosa empleado en el trabajo anterior (Egea *et al.* 2012), es un buen método para estudiar los mecanismos que suceden inmediatamente después a un evento isquémico, si queremos analizar los procesos a más largo plazo, resulta ineficaz. Por ello, en este nuevo estudio establecimos un modelo de privación de oxigeno y glucosa en cultivos organotípicos de rodajas de hipocampo de rata. En el cultivo organotípico, las rodajas se preservan en un coctel de nutrientes que permite la viabilidad de éstas por más tiempo (hasta 15 días), además de mantener conservadas las estructuras fisiológicas características de las rodajas de hipocampo (Stoppini *et al*. 1991). En este modelo experimental, optimizamos las condiciones de privación de oxígeno y glucosa, seguido de una fase de re-oxigenación que nos permitiera obtener una ventana de muerte neuronal adecuada, para evaluar los efectos neuroprotectores de la melatonina; las condiciones que, finalmente, establecimos fueron las de 15 minutos de POG seguido de 24 h de re-oxigenación. Estas condiciones fueron similares a las que usamos posteriormente en el modelo in vivo.

Al igual que habíamos observado en el primer trabajo con el PNU282987 (la melatonina fue capaz de prevenir la muerte celular cuando se administró después del estímulo tóxico; la ventana máxima fue de 2 h. Estos resultados están de acuerdo con otros que describen que la melatonina puede ofrecer protección cuando se administra después de tóxico (Manev *et al*. 1996). También, en el estudio de Nair y colaboradores, la administración de melatonina, 2 h después de ocluir la arteria cerebral media en la rata, redujo el volumen de infarto, la expresión de iNOS, y además, promovió la neurogenesis (Nair *et al*. 2011; Chern *et al*. 2012). Nuestros resultados se encuentran en la línea de estas investigaciones, ya que hemos visto el efecto neuroprotector y antioxidante de melatonina, cuando es administrada post-POG .

El efecto neuroprotector de la melatonina, observado en los cultivos organotípicos privados de oxígeno y glucosa, fue posteriormente corroborado en un modelo *in vivo*. Concretamente, utilizamos el modelo de isquemia focal inducido mediante fototrombosis en el ratón. Aunque este modelo está descrito en la literatura (Zou *et al.* 2006), hemos introducido algunas modificaciones que permiten correlacionar el volumen de infarto con un déficit funcional. Para ello, hemos realizado una modificación de las coordenadas estereotáxicas, que nos permiten inducir un infarto cerebral de la corteza motora, que corresponde con la movilidad de la pata delantera y trasera contralateral al hemisferio dañado; ello nos permite, mediante la prueba de la barra horizontal, analizar la capacidad motora de los animales (Quinn *et al.* 2007; Luong *et al.* 2011). En este modelo de ictus fototrombótico, observamos que la administración de 15 mg/kg de melatonina, inmediatamente después de la isquemia, produjo una mejora del déficit motor, así como una reducción significativa del volumen de infarto.

Existen antecedentes bibliográficos que muestran que la melatonina modula la respuesta central y periférica de los receptores nAChRs (Markus *et al.* 1996; Markus *et al.* 2003). Así, la contracción del conducto deferente de ratas sacrificadas por la mañana en respuesta a la acetilcolina, es 6 veces mayor que en ratas sacrificadas por la tarde. Éstos resultados concuerdan con la mayor cantidad plasmática de melatonina en ese espacio del día. También se ha observado, recientemente, que la melatonina disminuye la permeabilidad de la mucosa duodenal por un mecanismo dependiente de los nAChR (Sommansson *et al.* 2013). Esta interrelación, entre las acciones de la melatonina y los nAChR, nos hizo presuponer que esta neurohormona podría estar ejerciendo sus efectos neuroprotectores mediante la inducción de la HO-1, por un mecanismo dependiente de nAChRs, tal como habíamos observados en el primer y segundo trabajo de esta tesis (Parada *et al.* 2010; Egea *et al* 2013). Efectivamente, los efectos neuroprotectores de la melatonina fueron bloqueados por el antagonista de la HO-1, la SnPP, y por los bloqueantes selectivos de los nAChRs α7, la bungarotoxina y la metilacconitina. Estos resultados, en cierto modo, venían a confirmar resultados previos del grupo en los que demostrábamos que, concentraciones subefectivas de galantamina y melatonina ofrecían una neuroprotección sinérgica por un mecanismo dependiente de la expresión de HO-1 (Romero *et al.* 2010).

Con la idea de profundizar en el mecanismo por el cual la melatonina estaba induciendo HO-1 y, basándonos en datos previos, que mostraban que la melatonina puede favorecer la translocación al núcleo de Nrf2 y, consecuentemente la inducción de HO-1 en macrófagos (Aparicio-Soto *et al*. 2013), neuronas (Permpoonputtana and Govitrapong 2013) o células endoteliales (Tao *et al.* 2013)., decidimos realizar los experimentos de privación de oxigeno y glucosa en cultivos organotípicos de ratones nulos para Nrf2, (que como hemos visto en la introducción, es un factor de transcripción implicado en la expresión de HO-1). En estos ratones deficientes de Nrf2, la protección mediada por melatonina se perdía en un 40 %; quedando así patente la importancia que tenía la inducción de esta enzima en el mecanismo protector de melatonina. El conjunto de estos resultados nos muestran que la melatonina puede ofrecer un efecto neuroprotector, incluso cuando se administra después del insulto isquémico, mediante un mecanismo que implica, en gran parte, la inducción de la HO-1 vía nAChRs α7.

Hasta ahora nos habíamos centrado, fundamentalmente, en la neurona como la célula diana y, en los efectos antioxidantes mediados por la inducción de Nrf2 y HO-1 para explicar los efectos neuroprotectores asociados a la activación de los nAChRs α7, tanto en modelos *in vitro* como *in vivo* de isquemia cerebral. Llegados a este punto, nos llamó la atención los resultados descritos por el grupo de Kevin Tracey que ponían de manifiesto que el receptor nicotínico α7 nAChR de los macrófagos, es el regulador del efecto antiinflamatorio periférico, conseguido tras la estimulación del nervio vago; así se establece la teoría "The Cholinergic Antiinflammatory Pathway" (Borovikova *et al*. 2000; Wang *et al*. 2003). Dado que en los procesos de isquemia cerebral se produce una reconocida respuesta inflamatoria que contribuye a la neurodegeneración neuronal post-ictus (Perry et al. 2010), nos planteamos investigar si los efectos descritos a nivel periférico por el grupo de Tracey, tendrían un reflejo a nivel del SNC. Para ello, centramos nuestra atención en las células inmunomoduladoras del SNC, las células de la microglía.

Usando el protocolo de privación de oxigeno y glucosa en cultivo organotípico de rodaja de hipocampo, el agonista de nAChRs α7, PNU282987, ofreció protección significativa, a la misma concentración a la que inducía la máxima expresión de HO-1. Este efecto neuroprotector fue revertido por la co-incubación del PNU282987 con un

inhibidor de la actividad de HO-1. Para corroborar estos resultados, usamos ratones nulos para el factor de transcripción Nrf2. Tal y como era de esperar, la protección que ofrecía el PNU282987 sólo fue significativa en los cultivos de rodajas de hipocampo de ratón salvaje y no en la de los ratones nulos Nrf2.

La mayoría de los trabajos que existían sobre protección mediada por receptores nicotínicos, se centraban en los subtipos neuronales, sin embargo, poco se sabía de la participación de los receptores nAChR gliales. Observamos que el PNU282987 redujo los niveles de TNF, una de las principales citoquinas pro-inflamatorias, y éste efecto se revertía por α-bungarotoxina, un antagonista selectivo del subtipo nAChRs α7. La microglia, es la célula glial mayoritaria, a nivel del SNC, que puede liberar TNF; de hecho, algunos autores dudan de la presencia de TNF o TNFR1 (receptor de TNF) en los astrocitos (Badiola *et al.* 2009). Para evaluar la importancia de la activación del subtipo α7 nAChR microglial en nuestras condiciones, usamos una toxina que se acumula en la microglia y la destruye, de forma selectiva, sin afectar al resto de poblaciones celulares (astrocitos y neuronas). En cultivos organotípicos tratados con esta toxina, y por tanto depletadas de microglia, la protección obtenida con el PNU282987 incubado post privación de oxigeno y glucosa, se redujo en un 70 %. Estos resultados apoyan la teoría que nos hablan del papel neuroprotector de la microglia en isquemia y de su respuesta anti-inflamatoria, en compensación a la agresión que sucede durante un evento isquémico (Weinstein *et al.* 2010; Gomes-Leal 2012).

El papel antioxidante y anti-inflamatorio de Nrf2 y HO-1, ha sido descrito con anterioridad en varias ocasiones (véase introducción). Podemos decir que nuestro grupo es pionero en estudiar la sobreexpresión de esta enzima a través de la activación de receptores nAChR (Egea *et al.* 2007). Después de esto, otros grupos han reproducido este hecho al describir la importancia de HO-1 en el efecto anti-inflamatorio y citoprotector de nicotina, en modelos de sepsis e isquemia/reperfusión hepática (Tsoyi *et al.* 2011; Park *et al.* 2013). Para estudiar la importancia que tenía la sobre-expresión de HO-1 en la microglia, en el efecto neuroprotector del PNU282987, realizamos experimentos de isquemia focal in vivo, comparando la respuesta de ratones $Hmox^{lox/lox}$ (expresan niveles normales de HO-1) con ratones LysMCre $Hmox^{\Delta/\Delta}$ (no se expresa HO-1 en células de estirpe mieloide, incluida la microglía). Usando el protocolo de isquemia por fototrombosis descrito en el trabajo anterior (Parada *et al.* 2013), administramos a los ratones 10 mg/kg de PNU282987 -1h después de la isquemia, esto

produjo una reducción del volumen de infarto, así como una mejora del déficit motor. Este hecho, se observó en los ratones que expresaban niveles normales de HO-1 (Hmoxlox/lox); sin embargo, no se observó protección significativa en los ratones deficientes en HO-1 en microglia (LysMCre HmoxΔ/Δ). En conjunto de los resultados de este estudio refuerzan la importancia que tiene la expresión de HO-1 en la microglía para el control de la inflamación, el estrés oxidativo y la protección celular. Y pone de manifiesto, por vez primera, que la teoría colinérgica antiinflamatoria mediada por nAChRs α7 a nivel periférico, tiene su reflejo a nivel central en la microglía.

Los resultados conseguidos en las células de neuroblastoma humano SH-SY5Y, en el primer trabajo de esta tesis, señalaban la importancia de la activación de los receptores α7 nAChR neuronales, sin embargo, los resultados de este cuarto trabajo demuestran la enorme participación que posee la activación de este subtipo de receptor en la microglia, es por esto por lo que tampoco debemos descartar la posible contribución de los receptores α7 nAChR en astrocitos, oligodendrocitos u otros tipos celulares, que encontramos en el SNC.

Los resultados del cuarto estudio de esta tesis (Parada *et al.* 2013), nos llevaron a plantearnos un estudio más exhaustivo acerca de la expresión de HO-1 en glía y su participación en la inflamación. Para ello, usamos un inductor natural de Nrf2/HO-1, la curcumina. La curcumina es un compuesto natural presente en los rizomas de la planta Curcuma longa, posee numerosas actividades farmacológicas, incluyendo antimicrobianas, antioxidantes y antitumorales quimioterapéuticas (Maheshwari *et al*. 2006; Hatcher *et al*. 2008). Aunque ha mostrado tener efectos anti-inflamatorios en macrófagos (Zhong *et al*. 2013), sus efectos a nivel central, han sido hasta ahora poco estudiados. El estrés oxidativo y la inflamación son características típicas de la patología isquémica. Por tanto, quisimos aunar estos dos factores para producir una lesión en las células de glía. Como agente oxidativo, recurrimos a la mezcla de rot/oligo (ya vista anteriormente), que produce estrés mitocondrial y como agente inflamatorio usamos la endotoxina conocida como LPS (lipopolisacárido bacteriano). La incubación de curcumina 10 μM, durante 16 h, en cultivos mixtos gliales sometidos a este coctel tóxico, produjo un aumento significativo de la viabilidad celular. Observamos que la curcumina tenía un efecto citoprotector, anti-inflamatorio y antioxidante, dependiente de la expresión de HO-1, ya que dichos efectos beneficiosos se evitaron en presencia de un inhibidor selectivo de la actividad HO-1. Estos datos, son concordantes con los que

encontramos en la literatura en microglia, donde se ha visto que la curcumina reduce los niveles de ROS, TNF y MCP-1 frente a la toxicidad inducida por VIH-gp120 (Guo *et al*. 2013); en astrocitos, también se ha descrito el efecto antioxidante y anti-inflamatorio de curcumina, tanto *in vivo* como *in vitro* (Erlank *et al.* 2011; Gui *et al*. 2013).

Existen dos factores de transcripción principales implicados en el mantenimiento de la homeostasia celular, estos son el NFkB y el Nrf2. El factor de transcripción NFkB está considerado como el más importante en la regulación de la respuesta inflamatoria microglial en infecciones del SNC. Cuando tratamos la microglía con LPS, se produce la translocación al núcleo de esta proteína, promoviendo la expresión de iNOS, la producción de NO y, finalmente, la liberación de citoquinas pro-inflamatorias (Jobin *et al.* 1999). Entre los mecanismos de acción de la curcumina, destacan el de inhibir las activación de NFkB y la consecuente inducción de iNOS (Maheshwari *et al.* 2006). Aunque este hecho se ha constatado en macrófagos y microglia (Ben *et al*. 2011; Karlstetter *et al.* 2011), aún se desconocen los mecanismos por los cuales se produce. Nosotros evaluamos en este estudio, la producción de NO en cultivos sometidos al estímulo pro-inflamatorio del LPS y tratados con curcumina. En estas condiciones, la curcumina redujo la producción de nitritos hasta niveles cercanos a la basal, este hecho, fue revertido por un inhibidor selectivo de la actividad de HO-1. Para averiguar si este efecto estaba ocurriendo en microglía o astrocitos, decidimos diseñar un protocolo que nos permitiese separar ambos tipos celulares, después de realizar los tratamientos farmacológicos. De esta manera, podríamos evaluar los cambios bioquímicos independientemente, sin interrumpir la señalización intercelular que existe entre astrocitos y microglía (Liu *et al*. 2011; Pascual *et al*. 2011). Lo primero que nos llamó la atención de estos experimentos, es que sólo la microglía y no los astrocitos, sobreexpresaron iNOS cuando eran tratados con LPS. Aunque existen muchos estudios realizados en cultivos de astrocitos donde se ha visto ésta sobre-expresión de iNOS con LPS, existen otros autores que, usando el mismo estímulo tóxico, han observado diferencias en la expresión de iNOS entre astrocitos y microglia (Guo and Bhat 2006; Bi *et al.* 2013). Otro hecho que nos llamó la atención fue la reducción de iNOS que observamos en las células tratadas con curcumina, fenómeno que se revirtió con la incubación de un inhibidor de la actividad de HO-1.

Tras constatar estos resultados con experimentos de inmunofluorescencia, nos dimos cuenta de la morfología cambiante que adquiría la microglía con los distintos

tratamientos. Las células de microglía en condiciones basales tenían una forma característica, es decir, alargada y ramificada; sin embargo, las tratadas con LPS mostraban un aspecto ovalado o redondo, y las células que habíamos incubado con curcumina, de nuevo presentaban una morfología más ramificada. Decidimos cuantificar estos cambios, usando un factor clásico de forma que sería: 4*Π*Area/Perimetro2. Usando ésta fórmula, obtenemos valores entre 0 y 1, donde un círculo perfecto tendría el valor de 1. Cuando la microglia fue descrita por Rio Hortega, éste definió tres estados principales: ameboide, ramificada e intermedia. Aunque ahora sabemos que esta clasificación puede entrañar más complejidad, el fenotipo ameboide sigue estando asociado a un estado fagocítico de la célula, propio de la activación microglial. En nuestros experimentos, y analizando más de 300 células, observamos que el LPS produce un "redondeado" celular significativo, que se revierte por el tratamiento con curcumina. El uso de un inhibidor de la actividad de HO-1 devolvió a las células un fenotipo ameboide, indicando así la importancia de esta enzima en la regulación del fenotipo antiinflamatorio de la microglia.

El binomio LPS/HO-1 suscita mucha controversia tanto en la función como en la expresión de HO-1. Para empezar, aunque la mayor parte de la literatura existente asegura que el tratamiento de macrófagos/microglia con LPS induce HO-1 (Chen *et al*. 2013b; Zhou *et al*. 2013), algunos autores no han visto cambios en la expresión de esta proteína usando incluso las mismas dosis / tiempo de incubación de LPS (Lee and Chau 2002; Lee *et al.* 2012). Si esta inducción se produjese, esclarecer su función, sería sin duda, la siguiente cuestión a debatir. Algunos autores aseveran que la HO-1 inducida por LPS regula la expresión de marcadores pro-inflamatorios, contribuyendo así al incremento del daño celular y la respuesta inmune (Dodd and Filipov 2011; Chen *et al*. 2013a). Sin embargo, otros autores aseguran todo lo contrario, cuando se induce HO-1 por tratamiento con LPS, ésta puede tener también un papel anti-inflamatorio muy importante, inhibiendo la liberación de citoquinas pro-inflamatorias como TNF e IL6, inducidas por activación de los receptores TLR4 (Wang *et al.* 2009). Nuestros datos se encuentran en la línea de estas últimas hipótesis, ya que el redondeado celular que obtuvimos con LPS fue significativamente menor que el que se observó al tratar las células de microglia con LPS más un inhibidor de la actividad de HO-1. Infiriendo así la importancia que tiene la expresión de HO-1 en el control de la actividad glial y la respuesta anti-inflamatoria.

La conclusión general de esta tesis doctoral, podría resumirse así: La activación de los receptores nicotínicos del subtipo alfa-7 confiere propiedades antiinflamatorias, antioxidantes y neuroprotectoras ante diferentes estímulos citotóxicos mediante un mecanismo que implica, fundamentalmente, la inducción de HO-1 vía Nrf2

Conclusiones parciales:

Articulo1: *Poststress treatment with PNU282987 can rescue SH-SY5Y cells undergoing apoptosis via α7 nicotinic receptors linked to a Jak2/Akt/HO-1 signaling pathway*

- La administración, post-estimulo oxidante, del agonista selectivo α7 PNU282987, previene la muerte de las células de neuroblastoma humano SH-SY5Y, mediante la activación de la ruta neuroprotectora α7 nAChR/Jak2/AKT/HO-1.

Articulo 2: *Galantamine elicits neuroprotection by inhibiting iNOS, NADPH oxidase and ROS in hippocampal slices stressed with anoxia/reoxygenation*

- La galantamina, un inhibidor de la acetilcolinesterasa empleado en el tratamiento del Alzheimer, activa una ruta de supervivencia celular que implica los receptores α7 y la fosforilación de JAK2 en un modelo agudo de isquemia reperfusion, en rodajas de hipocampo de rata. Además, la galantamina mostró propiedades antiinflamatorias ya que inhibió la traslocación al núcleo de NFkB, la inducción de iNOS y la producción de NO.

Articulo 3: *Neuroprotective effect of melatonin against ischemia is partially mediated by alpha-7 nicotinic receptor modulation and HO-1 overexpression*

- La melatonina administrada post-isquemia, tanto en modelos *in vitro* como *in vivo*, proporciona efecto neuroprotector y antioxidante por un mecanismo que implica la modulación de los receptores nicotínicos α7 y la inducción de HO-1 vía Nrf2

Articulo 4: *The Microglial α7-Acetylcholine Nicotinic Receptor Is a Key Element in Promoting Neuroprotection by Inducing Heme Oxygenase-1 via Nuclear Factor Erythroid-2-Related Factor 2*

- Los receptores nicotínicos α7 nAChR microgliales desempeñan un papel predominante en el mantenimiento del efecto neuroprotector y antiinflamatorio en modelos de isquemia *in vivo* e *in vitro;* dicho efecto se relaciona con la traslocación al núcleo de Nrf2 y la expresión de HO-1. Este estudio demuestra que a nivel central también existe un control colinérgico antiinflamatorio mediado por los receptores α7 microgliales, tal como se ha demostrado a nivel periférico en los macrófagos.

Articulo 5: *Microglial HO-1 induction by curcumin provides antioxidant, anti-neuroinflammatory and cytoprotective effects*

- La curcumina, un aditivo alimentario que induce Nrf2, ofrece glioprotección ante un estímulo tóxico que combina inflamación y estrés oxidativo (LPS+rot/oligo). El mecanismo glioprotector se relaciona son su capacidad para reducir los niveles de nitritos, iNOS, ROS y activación microglial; todos estos efectos fueron dependientes de la inducción de HO-1, primordialmente en la población microglial.

Abramov A. Y., Scorziello A. and Duchen M. R. (2007) Three distinct mechanisms generate oxygen free radicals in neurons and contribute to cell death during anoxia and reoxygenation. J Neurosci 27, 1129-1138.

Ago Y., Koda K., Takuma K. and Matsuda T. (2011) Pharmacological aspects of the acetylcholinesterase inhibitor galantamine. J Pharmacol Sci 116, 6-17.

Allan S. M. and Rothwell N. J. (2003) Inflammation in central nervous system injury. Philos Trans R Soc Lond B Biol Sci 358, 1669-1677.

Aparicio-Soto M., Alarcon-de-la-Lastra C., Cardeno A., Sanchez-Fidalgo S. and Sanchez-Hidalgo M. (2013) Melatonin modulates microsomal prostaglandin E synthase 1 and nuclear factor-E2-related factor-2-regulated antioxidant enzyme expressions in LPS-induced murine peritoneal macrophages. Br J Pharmacol.

Arias E., Ales E., Gabilan N. H., Cano-Abad M. F., Villarroya M., Garcia A. G. and Lopez M. G. (2004) Galantamine prevents apoptosis induced by beta-amyloid and thapsigargin: involvement of nicotinic acetylcholine receptors. Neuropharmacology 46, 103-114.

Ashrafian H., Czibik G., Bellahcene M., Aksentijevic D., Smith A. C., Mitchell S. J., Dodd M. S., Kirwan J., Byrne J. J., Ludwig C., Isackson H., Yavari A., Stottrup N. B., Contractor H., Cahill T. J., Sahgal N., Ball D. R., Birkler R. I., Hargreaves I., Tennant D. A., Land J., Lygate C. A., Johannsen M., Kharbanda R. K., Neubauer S., Redwood C., de Cabo R., Ahmet I., Talan M., Gunther U. L., Robinson A. J., Viant M. R., Pollard P. J., Tyler D. J. and Watkins H. (2012) Fumarate is cardioprotective via activation of the Nrf2 antioxidant pathway. Cell Metab 15, 361-371.

Ay I., Lu J., Ay H. and Gregory Sorensen A. (2009) Vagus nerve stimulation reduces infarct size in rat focal cerebral ischemia. Neurosci Lett 459, 147-151.

Babbs C. F. (1985) Role of iron ions in the genesis of reperfusion injury following successful cardiopulmonary resuscitation: preliminary data and a biochemical hypothesis. Ann Emerg Med 14, 777-783.

Badiola N., Malagelada C., Llecha N., Hidalgo J., Comella J. X., Sabria J. and Rodriguez-Alvarez J. (2009) Activation of caspase-8 by tumour necrosis factor receptor 1 is necessary for caspase-3 activation and apoptosis in oxygen-glucose deprived cultured cortical cells. Neurobiol Dis 35, 438-447.

Barone F. C. and Feuerstein G. Z. (1999) Inflammatory mediators and stroke: new opportunities for novel therapeutics. J Cereb Blood Flow Metab 19, 819-834.

Bartus R. T., Dean R. L., 3rd, Beer B. and Lippa A. S. (1982) The cholinergic hypothesis of geriatric memory dysfunction. Science 217, 408-414.

Battista D., Ferrari C. C., Gage F. H. and Pitossi F. J. (2006) Neurogenic niche modulation by activated microglia: transforming growth factor beta increases neurogenesis in the adult dentate gyrus. Eur J Neurosci 23, 83-93.

Ben P., Liu J., Lu C., Xu Y., Xin Y., Fu J., Huang H., Zhang Z., Gao Y., Luo L. and Yin Z. (2011) Curcumin promotes degradation of inducible nitric oxide synthase and suppresses its enzyme activity in RAW 264.7 cells. Int Immunopharmacol 11, 179-186.

Bencherif M. and Lippiello P. M. (2010) Alpha7 neuronal nicotinic receptors: the missing link to understanding Alzheimer's etiopathology? Med Hypotheses 74, 281-285.

Bergey G. K. (2013) Neurostimulation in the treatment of epilepsy. Exp Neurol 244, 87-95.

Bi J., Jiang B., Zorn A., Zhao R. G., Liu P. and An L. J. (2013) Catalpol inhibits LPS plus IFN-gamma-induced inflammatory response in astrocytes primary cultures. Toxicol In Vitro 27, 543-550.

Bianchi M. E. (2007) DAMPs, PAMPs and alarmins: all we need to know about danger. J Leukoc Biol 81, 1-5.

Bitner R. S., Bunnelle W. H., Decker M. W., Drescher K. U., Kohlhaas K. L., Markosyan S., Marsh K. C., Nikkel A. L., Browman K., Radek R., Anderson D. J., Buccafusco J. and Gopalakrishnan M. (2010) In vivo pharmacological characterization of a novel selective alpha7 neuronal nicotinic acetylcholine receptor agonist ABT-107: preclinical considerations in Alzheimer's disease. J Pharmacol Exp Ther 334, 875-886.

Block M. L., Zecca L. and Hong J. S. (2007) Microglia-mediated neurotoxicity: uncovering the molecular mechanisms. Nat Rev Neurosci 8, 57-69.

Borovikova L. V., Ivanova S., Zhang M., Yang H., Botchkina G. I., Watkins L. R., Wang H., Abumrad N., Eaton J. W. and Tracey K. J. (2000) Vagus nerve stimulation attenuates the systemic inflammatory response to endotoxin. Nature 405, 458-462.

Broughton B. R., Reutens D. C. and Sobey C. G. (2009) Apoptotic mechanisms after cerebral ischemia. Stroke 40, e331-339.

Burton N. C., Kensler T. W. and Guilarte T. R. (2006) In vivo modulation of the Parkinsonian phenotype by Nrf2. Neurotoxicology 27, 1094-1100.

Calabrese V., Boyd-Kimball D., Scapagnini G. and Butterfield D. A. (2004) Nitric oxide and cellular stress response in brain aging and neurodegenerative disorders: the role of vitagenes. In Vivo 18, 245-267.

Corbin J., Methot N., Wang H. H., Baenziger J. E. and Blanton M. P. (1998) Secondary structure analysis of individual transmembrane segments of the nicotinic acetylcholine receptor by circular dichroism and Fourier transform infrared spectroscopy. J Biol Chem 273, 771-777.

Chen C., Zhang F., Zhang Z., Peng M., Wang Y. and Chen Y. (2013a) TLR4 signaling-induced heme oxygenase upregulation in the acute lung injury: role in hemorrhagic shock and two-hit induced lung inflammation. Mol Biol Rep 40, 1167-1172.

Chen H., Song Y. S. and Chan P. H. (2009) Inhibition of NADPH oxidase is neuroprotective after ischemia-reperfusion. J Cereb Blood Flow Metab 29, 1262-1272.

Chen H. G., Xie K. L., Han H. Z., Wang W. N., Liu D. Q., Wang G. L. and Yu Y. H. (2013b) Heme oxygenase-1 mediates the anti-inflammatory effect of molecular hydrogen in LPS-stimulated RAW 264.7 macrophages. Int J Surg.

Chern C. M., Liao J. F., Wang Y. H. and Shen Y. C. (2012) Melatonin ameliorates neural function by promoting endogenous neurogenesis through the MT2 melatonin receptor in ischemic-stroke mice. Free Radic Biol Med 52, 1634-1647.

Cheyuo C., Jacob A., Wu R., Zhou M., Coppa G. F. and Wang P. (2011) The parasympathetic nervous system in the quest for stroke therapeutics. J Cereb Blood Flow Metab 31, 1187-1195.

Dajas-Bailador F. A., Lima P. A. and Wonnacott S. (2000) The alpha7 nicotinic acetylcholine receptor subtype mediates nicotine protection against NMDA excitotoxicity in primary hippocampal cultures through a Ca(2+) dependent mechanism. Neuropharmacology 39, 2799-2807.

Danton G. H. and Dietrich W. D. (2003) Inflammatory mechanisms after ischemia and stroke. J Neuropathol Exp Neurol 62, 127-136.

Davalos D., Grutzendler J., Yang G., Kim J. V., Zuo Y., Jung S., Littman D. R., Dustin M. L. and Gan W. B. (2005) ATP mediates rapid microglial response to local brain injury in vivo. Nat Neurosci 8, 752-758.

Davinelli S., Willcox D. C. and Scapagnini G. (2012) Extending healthy ageing: nutrient sensitive pathway and centenarian population. Immun Ageing 9, 9.

Degterev A., Huang Z., Boyce M., Li Y., Jagtap P., Mizushima N., Cuny G. D., Mitchison T. J., Moskowitz M. A. and Yuan J. (2005) Chemical inhibitor of nonapoptotic cell death with therapeutic potential for ischemic brain injury. Nat Chem Biol 1, 112-119.

del Barrio L., Egea J., Leon R., Romero A., Ruiz A., Montero M., Alvarez J. and Lopez M. G. (2011a) Calcium signalling mediated through alpha7 and non-alpha7 nAChR stimulation is differentially regulated in bovine chromaffin cells to induce catecholamine release. Br J Pharmacol 162, 94-110.

Del Barrio L., Martin-de-Saavedra M. D., Romero A., Parada E., Egea J., Avila J., McIntosh J. M., Wonnacott S. and Lopez M. G. (2011b) Neurotoxicity induced by okadaic acid in the human neuroblastoma SH-SY5Y line can be differentially prevented by alpha7 and beta2* nicotinic stimulation. Toxicol Sci 123, 193-205.

Del Rio-Hortega P. (1921) Studies on neuroglia: Glia with very few processes (oligodendroglia) by PA-o del RA-o-Hortega. 1921. Clin Neuropathol 31, 440-459.

del Rio-Hortega P. (1993) Art and artifice in the science of histology. 1933. Histopathology 22, 515-525.

Dodd C. A. and Filipov N. M. (2011) Manganese potentiates LPS-induced heme-oxygenase 1 in microglia but not dopaminergic cells: role in controlling microglial hydrogen peroxide and inflammatory cytokine output. Neurotoxicology 32, 683-692.

Dong D. L., Zhang Y., Lin D. H., Chen J., Patschan S., Goligorsky M. S., Nasjletti A., Yang B. F. and Wang W. H. (2007) Carbon monoxide stimulates the Ca2(+)-activated big conductance k channels in cultured human endothelial cells. Hypertension 50, 643-651.

Donnelly-Roberts D. L., Xue I. C., Arneric S. P. and Sullivan J. P. (1996) In vitro neuroprotective properties of the novel cholinergic channel activator (ChCA), ABT-418. Brain Res 719, 36-44.

Duris K., Manaenko A., Suzuki H., Rolland W. B., Krafft P. R. and Zhang J. H. (2011) alpha7 nicotinic acetylcholine receptor agonist PNU-282987 attenuates early brain injury in a perforation model of subarachnoid hemorrhage in rats. Stroke 42, 3530-3536.

Durukan A. and Tatlisumak T. (2007) Acute ischemic stroke: overview of major experimental rodent models, pathophysiology, and therapy of focal cerebral ischemia. Pharmacol Biochem Behav 87, 179-197.

Egea J., Rosa A. O., Cuadrado A., Garcia A. G. and Lopez M. G. (2007) Nicotinic receptor activation by epibatidine induces heme oxygenase-1 and protects chromaffin cells against oxidative stress. J Neurochem 102, 1842-1852.

Egea J., Rosa A. O., Lorrio S., del Barrio L., Cuadrado A. and Lopez M. G. (2009) Haeme oxygenase-1 overexpression via nAChRs and the transcription factor Nrf2 has antinociceptive effects in the formalin test. Pain 146, 75-83.

Egea J., Martin-de-Saavedra M. D., Parada E., Romero A., Del Barrio L., Rosa A. O., Garcia A. G. and Lopez M. G. (2012) Galantamine elicits neuroprotection by inhibiting iNOS, NADPH oxidase and ROS in hippocampal slices stressed with anoxia/reoxygenation. Neuropharmacology 62, 1082-1090.

Emsley H. C. and Hopkins S. J. (2008) Acute ischaemic stroke and infection: recent and emerging concepts. Lancet Neurol 7, 341-353.

Erlank H., Elmann A., Kohen R. and Kanner J. (2011) Polyphenols activate Nrf2 in astrocytes via H2O2, semiquinones, and quinones. Free Radic Biol Med 51, 2319-2327.

Escubedo E., Camarasa J., Chipana C., Garcia-Rates S. and Pubill D. (2009) Involvement of nicotinic receptors in methamphetamine- and MDMA-induced neurotoxicity: pharmacological implications. Int Rev Neurobiol 88, 121-166.

Ferchmin P. A., Perez D., Eterovic V. A. and de Vellis J. (2003) Nicotinic receptors differentially regulate N-methyl-D-aspartate damage in acute hippocampal slices. J Pharmacol Exp Ther 305, 1071-1078.

Ferenbach D. A., Kluth D. C. and Hughes J. (2010) Hemeoxygenase-1 and renal ischaemia-reperfusion injury. Nephron Exp Nephrol 115, e33-37.

Fisher M., Feuerstein G., Howells D. W., Hurn P. D., Kent T. A., Savitz S. I. and Lo E. H. (2009) Update of the stroke therapy academic industry roundtable preclinical recommendations. Stroke 40, 2244-2250.

Folbergrova J., Zhao Q., Katsura K. and Siesjo B. K. (1995) N-tert-butyl-alpha-phenylnitrone improves recovery of brain energy state in rats following transient focal ischemia. Proc Natl Acad Sci U S A 92, 5057-5061.

Foresti R., Bains S. K., Pitchumony T. S., de Castro Bras L. E., Drago F., Dubois-Rande J. L., Bucolo C. and Motterlini R. (2013) Small molecule activators of the Nrf2-HO-1

antioxidant axis modulate heme metabolism and inflammation in BV2 microglia cells. Pharmacol Res 76, 132-148.

Francis P. T., Palmer A. M., Snape M. and Wilcock G. K. (1999) The cholinergic hypothesis of Alzheimer's disease: a review of progress. J Neurol Neurosurg Psychiatry 66, 137-147.

Frolich L., Ashwood T., Nilsson J. and Eckerwall G. (2011) Effects of AZD3480 on cognition in patients with mild-to-moderate Alzheimer's disease: a phase IIb dose-finding study. J Alzheimers Dis 24, 363-374.

Galluzzi L. and Kroemer G. (2008) Necroptosis: a specialized pathway of programmed necrosis. Cell 135, 1161-1163.

Gill A. J. and Kolson D. L. (2013) Dimethyl fumarate modulation of immune and antioxidant responses: application to HIV therapy. Crit Rev Immunol 33, 307-359.

Gomes-Leal W. (2012) Microglial physiopathology: how to explain the dual role of microglia after acute neural disorders? Brain Behav 2, 345-356.

Gotti C. and Clementi F. (2004) Neuronal nicotinic receptors: from structure to pathology. Prog Neurobiol 74, 363-396.

Green A. R. (2002) Why do neuroprotective drugs that are so promising in animals fail in the clinic? An industry perspective. Clin Exp Pharmacol Physiol 29, 1030-1034.

Gregersen R., Lambertsen K. and Finsen B. (2000) Microglia and macrophages are the major source of tumor necrosis factor in permanent middle cerebral artery occlusion in mice. J Cereb Blood Flow Metab 20, 53-65.

Gui H. Y., Chen R. N., Peng Y., Hu J. H., Mao Z., Ning R., Shang W., Liu W., Xiong J., Hu G. and Yang J. (2013) Curcumin Protects against 1-Methyl-4-phenylpyridinium Ion- and Lipopolysaccharide-Induced Cytotoxicities in the Mouse Mesencephalic Astrocyte via Inhibiting the Cytochrome P450 2E1. Evid Based Complement Alternat Med 2013, 523484.

Guo G. and Bhat N. R. (2006) Hypoxia/reoxygenation differentially modulates NF-kappaB activation and iNOS expression in astrocytes and microglia. Antioxid Redox Signal 8, 911-918.

Guo L., Xing Y., Pan R., Jiang M., Gong Z., Lin L., Wang J., Xiong G. and Dong J. (2013) Curcumin protects microglia and primary rat cortical neurons against HIV-1 gp120-mediated inflammation and apoptosis. PLoS One 8, e70565.

Hanisch U. K. and Kettenmann H. (2007) Microglia: active sensor and versatile effector cells in the normal and pathologic brain. Nat Neurosci 10, 1387-1394.

Hatcher H., Planalp R., Cho J., Torti F. M. and Torti S. V. (2008) Curcumin: from ancient medicine to current clinical trials. Cell Mol Life Sci 65, 1631-1652.

Hong Y., Yan W., Chen S., Sun C. R. and Zhang J. M. (2010) The role of Nrf2 signaling in the regulation of antioxidants and detoxifying enzymes after traumatic brain injury in rats and mice. Acta Pharmacol Sin 31, 1421-1430.

Hossmann K. A. (2012) The two pathophysiologies of focal brain ischemia: implications for translational stroke research. J Cereb Blood Flow Metab 32, 1310-1316.

Hosur V. and Loring R. H. (2011) alpha4beta2 nicotinic receptors partially mediate anti-inflammatory effects through Janus kinase 2-signal transducer and activator of transcription 3 but not calcium or cAMP signaling. Mol Pharmacol 79, 167-174.

Hsu J. T., Kuo C. J., Chen T. H., Wang F., Lin C. J., Yeh T. S., Hwang T. L. and Jan Y. Y. (2012) Melatonin prevents hemorrhagic shock-induced liver injury in rats through an Akt-dependent HO-1 pathway. J Pineal Res 53, 410-416.

Hu X., Li P., Guo Y., Wang H., Leak R. K., Chen S., Gao Y. and Chen J. (2012) Microglia/macrophage polarization dynamics reveal novel mechanism of injury expansion after focal cerebral ischemia. Stroke 43, 3063-3070.

Immenschuh S., Baumgart-Vogt E. and Mueller S. (2010) Heme oxygenase-1 and iron in liver inflammation: a complex alliance. Curr Drug Targets 11, 1541-1550.

Innamorato N. G., Rojo A. I., Garcia-Yague A. J., Yamamoto M., de Ceballos M. L. and Cuadrado A. (2008) The transcription factor Nrf2 is a therapeutic target against brain inflammation. J Immunol 181, 680-689.

Itoh K., Chiba T., Takahashi S., Ishii T., Igarashi K., Katoh Y., Oyake T., Hayashi N., Satoh K., Hatayama I., Yamamoto M. and Nabeshima Y. (1997) An Nrf2/small Maf heterodimer mediates the induction of phase II detoxifying enzyme genes through antioxidant response elements. Biochem Biophys Res Commun 236, 313-322.

Jin R., Yang G. and Li G. (2010) Inflammatory mechanisms in ischemic stroke: role of inflammatory cells. J Leukoc Biol 87, 779-789.

Jin Z., Gao F., Flagg T. and Deng X. (2004) Nicotine induces multi-site phosphorylation of Bad in association with suppression of apoptosis. J Biol Chem 279, 23837-23844.

Jobin C., Bradham C. A., Russo M. P., Juma B., Narula A. S., Brenner D. A. and Sartor R. B. (1999) Curcumin blocks cytokine-mediated NF-kappa B activation and proinflammatory gene expression by inhibiting inhibitory factor I-kappa B kinase activity. J Immunol 163, 3474-3483.

Jones S., Sudweeks S. and Yakel J. L. (1999) Nicotinic receptors in the brain: correlating physiology with function. Trends Neurosci 22, 555-561.

Jordan J., Segura T., Brea D., Galindo M. F. and Castillo J. (2008) Inflammation as therapeutic objective in stroke. Curr Pharm Des 14, 3549-3564.

Kahle M. P. and Bix G. J. (2012) Successfully Climbing the "STAIRs": Surmounting Failed Translation of Experimental Ischemic Stroke Treatments. Stroke Res Treat 2012, 374098.

Kalappa B. I., Sun F., Johnson S. R., Jin K. and Uteshev V. V. (2013) A positive allosteric modulator of alpha7 nAChRs augments neuroprotective effects of endogenous nicotinic agonists in cerebral ischaemia. Br J Pharmacol 169, 1862-1878.

Kalyanaraman B. (2013) Teaching the basics of redox biology to medical and graduate students: Oxidants, antioxidants and disease mechanisms. Redox Biol 1, 244-257.

Karlstetter M., Lippe E., Walczak Y., Moehle C., Aslanidis A., Mirza M. and Langmann T. (2011) Curcumin is a potent modulator of microglial gene expression and migration. J Neuroinflammation 8, 125.

Kawamata J. and Shimohama S. (2011) Stimulating nicotinic receptors trigger multiple pathways attenuating cytotoxicity in models of Alzheimer's and Parkinson's diseases. J Alzheimers Dis 24 Suppl 2, 95-109.

Kiefer R., Streit W. J., Toyka K. V., Kreutzberg G. W. and Hartung H. P. (1995) Transforming growth factor-beta 1: a lesion-associated cytokine of the nervous system. Int J Dev Neurosci 13, 331-339.

Kim S. W., Lee H. K., Shin J. H. and Lee J. K. (2013) Up-down Regulation of HO-1 and iNOS Gene Expressions by Ethyl Pyruvate via Recruiting p300 to Nrf2 and Depriving It from p65. Free Radic Biol Med 65C, 468-476.

Komara J. S., Nayini N. R., Bialick H. A., Indrieri R. J., Evans A. T., Garritano A. M., Hoehner T. J., Jacobs W. A., Huang R. R., Krause G. S. and et al. (1986) Brain iron delocalization and lipid peroxidation following cardiac arrest. Ann Emerg Med 15, 384-389.

Kono H. and Rock K. L. (2008) How dying cells alert the immune system to danger. Nat Rev Immunol 8, 279-289.

Krafft P. R., Caner B., Klebe D., Rolland W. B., Tang J. and Zhang J. H. (2013) PHA-543613 preserves blood-brain barrier integrity after intracerebral hemorrhage in mice. Stroke 44, 1743-1747.

Krafft P. R., Altay O., Rolland W. B., Duris K., Lekic T., Tang J. and Zhang J. H. (2011) alpha7 nicotinic acetylcholine receptor agonism confers neuroprotection through GSK-3beta inhibition in a mouse model of intracerebral hemorrhage. Stroke 43, 844-850.

Lacy C. R., Suh D. C., Bueno M. and Kostis J. B. (2001) Delay in presentation and evaluation for acute stroke: Stroke Time Registry for Outcomes Knowledge and Epidemiology (S.T.R.O.K.E.). Stroke 32, 63-69.

Lalancette-Hebert M., Gowing G., Simard A., Weng Y. C. and Kriz J. (2007) Selective ablation of proliferating microglial cells exacerbates ischemic injury in the brain. J Neurosci 27, 2596-2605.

Lee I. S., Lim J., Gal J., Kang J. C., Kim H. J., Kang B. Y. and Choi H. J. (2011) Anti-inflammatory activity of xanthohumol involves heme oxygenase-1 induction via NRF2-ARE signaling in microglial BV2 cells. Neurochem Int 58, 153-160.

Lee M. Y., Seo C. S., Lee J. A., Shin I. S., Kim S. J., Ha H. and Shin H. K. (2012) Alpinia katsumadai H(AYATA) seed extract inhibit LPS-induced inflammation by induction of heme oxygenase-1 in RAW264.7 cells. Inflammation 35, 746-757.

Lee T. S. and Chau L. Y. (2002) Heme oxygenase-1 mediates the anti-inflammatory effect of interleukin-10 in mice. Nat Med 8, 240-246.

Lin H. Y., Huang B. R., Yeh W. L., Lee C. H., Huang S. S., Lai C. H., Lin H. and Lu D. Y. (2014) Antineuroinflammatory effects of lycopene via activation of adenosine monophosphate-activated protein kinase-alpha1/heme oxygenase-1 pathways. Neurobiol Aging 35, 191-202.

Lindstrom J. M. (2003) Nicotinic acetylcholine receptors of muscles and nerves: comparison of their structures, functional roles, and vulnerability to pathology. Ann N Y Acad Sci 998, 41-52.

Liu A. J., Zang P., Guo J. M., Wang W., Dong W. Z., Guo W., Xiong Z. G., Wang W. Z. and Su D. F. (2012) Involvement of acetylcholine-alpha7nAChR in the protective effects of arterial baroreflex against ischemic stroke. CNS Neurosci Ther 18, 918-926.

Liu S., Zhen G., Meloni B. P., Campbell K. and Winn H. R. (2009) Rodent Stroke Model Guidelines for Preclinical Stroke Trials (1st Edition). J Exp Stroke Transl Med 2, 2-27.

Liu W., Tang Y. and Feng J. (2011) Cross talk between activation of microglia and astrocytes in pathological conditions in the central nervous system. Life Sci 89, 141-146.

Loboda A., Jazwa A., Grochot-Przeczek A., Rutkowski A. J., Cisowski J., Agarwal A., Jozkowicz A. and Dulak J. (2008) Heme oxygenase-1 and the vascular bed: from molecular mechanisms to therapeutic opportunities. Antioxid Redox Signal 10, 1767-1812.

Lorrio S., Negredo P., Roda J. M., Garcia A. G. and Lopez M. G. (2009) Effects of memantine and galantamine given separately or in association, on memory and hippocampal neuronal loss after transient global cerebral ischemia in gerbils. Brain Res 1254, 128-137.

Lorrio S., Sobrado M., Arias E., Roda J. M., Garcia A. G. and Lopez M. G. (2007) Galantamine postischemia provides neuroprotection and memory recovery against transient global cerebral ischemia in gerbils. J Pharmacol Exp Ther 322, 591-599.

Lu D. Y., Tsao Y. Y., Leung Y. M. and Su K. P. (2010) Docosahexaenoic acid suppresses neuroinflammatory responses and induces heme oxygenase-1 expression in BV-2 microglia: implications of antidepressant effects for omega-3 fatty acids. Neuropsychopharmacology 35, 2238-2248.

Luong T. N., Carlisle H. J., Southwell A. and Patterson P. H. (2011) Assessment of motor balance and coordination in mice using the balance beam. J Vis Exp.

Lloyd-Jones D. M. (2010) Cardiovascular risk prediction: basic concepts, current status, and future directions. Circulation 121, 1768-1777.

Mabuchi T., Kitagawa K., Ohtsuki T., Kuwabara K., Yagita Y., Yanagihara T., Hori M. and Matsumoto M. (2000) Contribution of microglia/macrophages to expansion of infarction and response of oligodendrocytes after focal cerebral ischemia in rats. Stroke 31, 1735-1743.

Madinier A., Bertrand N., Mossiat C., Prigent-Tessier A., Beley A., Marie C. and Garnier P. (2009) Microglial involvement in neuroplastic changes following focal brain ischemia in rats. PLoS One 4, e8101.

Maheshwari R. K., Singh A. K., Gaddipati J. and Srimal R. C. (2006) Multiple biological activities of curcumin: a short review. Life Sci 78, 2081-2087.

Manev H., Uz T., Kharlamov A. and Joo J. Y. (1996) Increased brain damage after stroke or excitotoxic seizures in melatonin-deficient rats. Faseb J 10, 1546-1551.

Markus R. P., Zago W. M. and Carneiro R. C. (1996) Melatonin modulation of presynaptic nicotinic acetylcholine receptors in the rat vas deferens. J Pharmacol Exp Ther 279, 18-22.

Markus R. P., Santos J. M., Zago W. and Reno L. A. (2003) Melatonin nocturnal surge modulates nicotinic receptors and nicotine-induced [3H]glutamate release in rat cerebellum slices. J Pharmacol Exp Ther 305, 525-530.

Marrero M. B. and Bencherif M. (2009) Convergence of alpha 7 nicotinic acetylcholine receptor-activated pathways for anti-apoptosis and anti-inflammation: central role for JAK2 activation of STAT3 and NF-kappaB. Brain Res 1256, 1-7.

McColl B. W., Allan S. M. and Rothwell N. J. (2009) Systemic infection, inflammation and acute ischemic stroke. Neuroscience 158, 1049-1061.

Mehta S. L., Manhas N. and Raghubir R. (2007) Molecular targets in cerebral ischemia for developing novel therapeutics. Brain Res Rev 54, 34-66.

Mergenthaler P., Dirnagl U. and Meisel A. (2004) Pathophysiology of stroke: lessons from animal models. Metab Brain Dis 19, 151-167.

Merson T. D., Binder M. D. and Kilpatrick T. J. (2010) Role of cytokines as mediators and regulators of microglial activity in inflammatory demyelination of the CNS. Neuromolecular Med 12, 99-132.

Miyamoto O., Pang J., Sumitani K., Negi T., Hayashida Y. and Itano T. (2003) Mechanisms of the anti-ischemic effect of vagus nerve stimulation in the gerbil hippocampus. Neuroreport 14, 1971-1974.

Morgan S. C., Taylor D. L. and Pocock J. M. (2004) Microglia release activators of neuronal proliferation mediated by activation of mitogen-activated protein kinase, phosphatidylinositol-3-kinase/Akt and delta-Notch signalling cascades. J Neurochem 90, 89-101.

Muller F. J., Snyder E. Y. and Loring J. F. (2006) Gene therapy: can neural stem cells deliver? Nat Rev Neurosci 7, 75-84.

Nair S. M., Rahman R. M., Clarkson A. N., Sutherland B. A., Taurin S., Sammut I. A. and Appleton I. (2011) Melatonin treatment following stroke induction modulates L-arginine metabolism. J Pineal Res 51, 313-323.

Narantuya D., Nagai A., Sheikh A. M., Masuda J., Kobayashi S., Yamaguchi S. and Kim S. U. (2010) Human microglia transplanted in rat focal ischemia brain induce neuroprotection and behavioral improvement. PLoS One 5, e11746.

Neumann J., Sauerzweig S., Ronicke R., Gunzer F., Dinkel K., Ullrich O., Gunzer M. and Reymann K. G. (2008) Microglia cells protect neurons by direct engulfment of invading

neutrophil granulocytes: a new mechanism of CNS immune privilege. J Neurosci 28, 5965-5975.

Nimura T., Weinstein P. R., Massa S. M., Panter S. and Sharp F. R. (1996) Heme oxygenase-1 (HO-1) protein induction in rat brain following focal ischemia. Brain Res Mol Brain Res 37, 201-208.

Nixon R. A. (2013) The role of autophagy in neurodegenerative disease. Nat Med 19, 983-997.

Nouhi F., Tusi S. K., Abdi A. and Khodagholi F. (2011) Dietary supplementation with tBHQ, an Nrf2 stabilizer molecule, confers neuroprotection against apoptosis in amyloid beta-injected rat. Neurochem Res 36, 870-878.

Paine A., Eiz-Vesper B., Blasczyk R. and Immenschuh S. (2010) Signaling to heme oxygenase-1 and its anti-inflammatory therapeutic potential. Biochem Pharmacol 80, 1895-1903.

Parada E., Buendia I., León R., Negredo P., Romero A., Cuadrado A., López MG., Egea J. (2013) Neuroprotective effect of melatonin against ischemia is partially mediated by alpha-7 nicotinic receptor modulation and HO-1 overexpression. J Pineal Res 18

Parada E., Egea J., Buendia I., Negredo P., Cunha AC., Cardoso S., Soares MP., López MG. (2013) The microglial α7-acetylcholine nicotinic receptor is a key element in promoting neuroprotection by inducing heme oxygenase-1 via nuclear factor erythroid-2-related factor 2. Antioxid Redox Signal, 19(11), 1135-1148

Parada E., Egea J., Romero A., del Barrio L., García AG., López MG. (2010) Poststress treatment with PNU282987 can rescue SH-SY5Y cells undergoing apoptosis via α7 nicotinic receptors linked to a Jak2/Akt/HO-1 signaling pathway. Free Radic Biol Med. 49(11), 1815-1821

Parfenova H., Basuroy S., Bhattacharya S., Tcheranova D., Qu Y., Regan R. F. and Leffler C. W. (2006) Glutamate induces oxidative stress and apoptosis in cerebral vascular endothelial cells: contributions of HO-1 and HO-2 to cytoprotection. Am J Physiol Cell Physiol 290, C1399-1410.

Park J., Kang J. W. and Lee S. M. (2013) Activation of the cholinergic anti-inflammatory pathway by nicotine attenuates hepatic ischemia/reperfusion injury via heme oxygenase-1 induction. Eur J Pharmacol 707, 61-70.

Pascual O., Ben Achour S., Rostaing P., Triller A. and Bessis A. (2011) Microglia activation triggers astrocyte-mediated modulation of excitatory neurotransmission. Proc Natl Acad Sci U S A 109, E197-205.

Permpoonputtana K. and Govitrapong P. (2013) The anti-inflammatory effect of melatonin on methamphetamine-induced proinflammatory mediators in human neuroblastoma dopamine SH-SY5Y cell lines. Neurotox Res 23, 189-199.

Perry V. H., Nicoll J. A. and Holmes C. (2010) Microglia in neurodegenerative disease. Nat Rev Neurol 6, 193-201.

Phillips J. T. and Fox R. J. (2013) BG-12 in multiple sclerosis. Semin Neurol 33, 56-65.

Posadas I., Lopez-Hernandez B. and Cena V. (2013) Nicotinic receptors in neurodegeneration. Curr Neuropharmacol 11, 298-314.

Poss K. D. and Tonegawa S. (1997) Reduced stress defense in heme oxygenase 1-deficient cells. Proc Natl Acad Sci U S A 94, 10925-10930.

Quinn L. P., Perren M. J., Brackenborough K. T., Woodhams P. L., Vidgeon-Hart M., Chapman H., Pangalos M. N., Upton N. and Virley D. J. (2007) A beam-walking apparatus to assess behavioural impairments in MPTP-treated mice: pharmacological validation with R-(-)-deprenyl. J Neurosci Methods 164, 43-49.

Rezaie P. and Male D. (2002) Mesoglia & microglia--a historical review of the concept of mononuclear phagocytes within the central nervous system. J Hist Neurosci 11, 325-374.

Rock R. B., Gekker G., Hu S., Sheng W. S., Cheeran M., Lokensgard J. R. and Peterson P. K. (2004) Role of microglia in central nervous system infections. Clin Microbiol Rev 17, 942-964, table of contents.

Romero A., Egea J., Garcia A. G. and Lopez M. G. (2010) Synergistic neuroprotective effect of combined low concentrations of galantamine and melatonin against oxidative stress in SH-SY5Y neuroblastoma cells. J Pineal Res 49, 141-148.

Ryter S. W. and Tyrrell R. M. (2000) The heme synthesis and degradation pathways: role in oxidant sensitivity. Heme oxygenase has both pro- and antioxidant properties. Free Radic Biol Med 28, 289-309.

Ryter S. W., Alam J. and Choi A. M. (2006) Heme oxygenase-1/carbon monoxide: from basic science to therapeutic applications. Physiol Rev 86, 583-650.

Safar P. (1986) Cerebral resuscitation after cardiac arrest: a review. Circulation 74, IV138-153.

Shaw S., Bencherif M. and Marrero M. B. (2002) Janus kinase 2, an early target of alpha 7 nicotinic acetylcholine receptor-mediated neuroprotection against Abeta-(1-42) amyloid. J Biol Chem 277, 44920-44924.

Shih R. H., Lee I. T., Hsieh H. L., Kou Y. R. and Yang C. M. (2010) Cigarette smoke extract induces HO-1 expression in mouse cerebral vascular endothelial cells: involvement of c-Src/NADPH oxidase/PDGFR/JAK2/STAT3 pathway. J Cell Physiol 225, 741-750.

Shioda N., Han F. and Fukunaga K. (2009) Role of Akt and ERK signaling in the neurogenesis following brain ischemia. Int Rev Neurobiol 85, 375-387.

Smedlund K., Tano J. Y., Margiotta J. and Vazquez G. (2011) Evidence for operation of nicotinic and muscarinic acetylcholine receptor-dependent survival pathways in human coronary artery endothelial cells. J Cell Biochem 112, 1978-1984.

Sommansson A., Nylander O. and Sjoblom M. (2013) Melatonin decreases duodenal epithelial paracellular permeability via a nicotinic receptor-dependent pathway in rats in vivo. J Pineal Res 54, 282-291.

STAIR G. R. f. S. R. P. N. a. and Development. R. D. (1999) Recommendations for standards regarding preclinical neuroprotective and restorative drug development. Stroke 30, 2752-2758.

Stangel M. and Linker R. A. (2013) Dimethyl fumarate (BG-12) for the treatment of multiple sclerosis. Expert Rev Clin Pharmacol 6, 355-362.

Stocker R., Yamamoto Y., McDonagh A. F., Glazer A. N. and Ames B. N. (1987) Bilirubin is an antioxidant of possible physiological importance. Science 235, 1043-1046.

Stoppini L., Buchs P. A. and Muller D. (1991) A simple method for organotypic cultures of nervous tissue. J Neurosci Methods 37, 173-182.

Sun F., Jin K. and Uteshev V. V. (2013) A type-II positive allosteric modulator of alpha7 nAChRs reduces brain injury and improves neurological function after focal cerebral ischemia in rats. PLoS One 8, e73581.

Tabet N. (2006) Acetylcholinesterase inhibitors for Alzheimer's disease: anti-inflammatories in acetylcholine clothing! Age Ageing 35, 336-338.

Tao R. R., Huang J. Y., Shao X. J., Ye W. F., Tian Y., Liao M. H., Fukunaga K., Lou Y. J., Han F. and Lu Y. M. (2013) Ischemic injury promotes Keap1 nitration and disturbance of antioxidative responses in endothelial cells: a potential vasoprotective effect of melatonin. J Pineal Res 54, 271-281.

Taveira M., Sousa C., Valentao P., Ferreres F., Teixeira J. P. and Andrade P. B. (2013) Neuroprotective effect of steroidal alkaloids on glutamate-induced toxicity by preserving mitochondrial membrane potential and reducing oxidative stress. J Steroid Biochem Mol Biol 140C, 106-115.

Taylor R. A. and Sansing L. H. (2013) Microglial Responses after Ischemic Stroke and Intracerebral Hemorrhage. Clin Dev Immunol 2013, 746068.

Thimmulappa R. K., Lee H., Rangasamy T., Reddy S. P., Yamamoto M., Kensler T. W. and Biswal S. (2006a) Nrf2 is a critical regulator of the innate immune response and survival during experimental sepsis. J Clin Invest 116, 984-995.

Thimmulappa R. K., Scollick C., Traore K., Yates M., Trush M. A., Liby K. T., Sporn M. B., Yamamoto M., Kensler T. W. and Biswal S. (2006b) Nrf2-dependent protection from LPS induced inflammatory response and mortality by CDDO-Imidazolide. Biochem Biophys Res Commun 351, 883-889.

Thrift A. G., Dewey H. M., Macdonell R. A., McNeil J. J. and Donnan G. A. (2001) Incidence of the major stroke subtypes: initial findings from the North East Melbourne stroke incidence study (NEMESIS). Stroke 32, 1732-1738.

Tracey K. J. (2002) The inflammatory reflex. Nature 420, 853-859.

Tsoyi K., Jang H. J., Kim J. W., Chang H. K., Lee Y. S., Pae H. O., Kim H. J., Seo H. G., Lee J. H., Chung H. T. and Chang K. C. (2011) Stimulation of alpha7 nicotinic acetylcholine receptor by nicotine attenuates inflammatory response in macrophages and improves

survival in experimental model of sepsis through heme oxygenase-1 induction. Antioxid Redox Signal 14, 2057-2070.

Vijgen G. H., Bouvy N. D., Leenen L., Rijkers K., Cornips E., Majoie M., Brans B. and van Marken Lichtenbelt W. D. (2013) Vagus nerve stimulation increases energy expenditure: relation to brown adipose tissue activity. PLoS One 8, e77221.

Walder C. E., Green S. P., Darbonne W. C., Mathias J., Rae J., Dinauer M. C., Curnutte J. T. and Thomas G. R. (1997) Ischemic stroke injury is reduced in mice lacking a functional NADPH oxidase. Stroke 28, 2252-2258.

Wang G., Pan J. and Chen S. D. (2012a) Kinases and kinase signaling pathways: potential therapeutic targets in Parkinson's disease. Prog Neurobiol 98, 207-221.

Wang H., Yu M., Ochani M., Amella C. A., Tanovic M., Susarla S., Li J. H., Wang H., Yang H., Ulloa L., Al-Abed Y., Czura C. J. and Tracey K. J. (2003) Nicotinic acetylcholine receptor alpha7 subunit is an essential regulator of inflammation. Nature 421, 384-388.

Wang Q., Wang F., Li X., Yang Q., Li X., Xu N., Huang Y., Zhang Q., Gou X., Chen S. and Xiong L. (2012b) Electroacupuncture pretreatment attenuates cerebral ischemic injury through alpha7 nicotinic acetylcholine receptor-mediated inhibition of high-mobility group box 1 release in rats. J Neuroinflammation 9, 24.

Wang X. (2005) Investigational anti-inflammatory agents for the treatment of ischaemic brain injury. Expert Opin Investig Drugs 14, 393-409.

Wang X. M., Kim H. P., Nakahira K., Ryter S. W. and Choi A. M. (2009) The heme oxygenase-1/carbon monoxide pathway suppresses TLR4 signaling by regulating the interaction of TLR4 with caveolin-1. J Immunol 182, 3809-3818.

Weinstein J. R., Koerner I. P. and Moller T. (2010) Microglia in ischemic brain injury. Future Neurol 5, 227-246.

White B. C., Krause G. S., Aust S. D. and Eyster G. E. (1985) Postischemic tissue injury by iron-mediated free radical lipid peroxidation. Ann Emerg Med 14, 804-809.

Wijayanti N., Katz N. and Immenschuh S. (2004) Biology of heme in health and disease. Curr Med Chem 11, 981-986.

Wilkinson W. J. and Kemp P. J. (2011) Carbon monoxide: an emerging regulator of ion channels. J Physiol 589, 3055-3062.

Willis D., Moore A. R., Frederick R. and Willoughby D. A. (1996) Heme oxygenase: a novel target for the modulation of the inflammatory response. Nat Med 2, 87-90.

Wonnacott S. (1997) Presynaptic nicotinic ACh receptors. Trends Neurosci 20, 92-98.

Xu M. and Zhang H. L. (2011) Death and survival of neuronal and astrocytic cells in ischemic brain injury: a role of autophagy. Acta Pharmacol Sin 32, 1089-1099.

Xu S. Y. and Pan S. Y. (2013) The failure of animal models of neuroprotection in acute ischemic stroke to translate to clinical efficacy. Med Sci Monit Basic Res 19, 37-45.

Yang C., Zhang X., Fan H. and Liu Y. (2009) Curcumin upregulates transcription factor Nrf2, HO-1 expression and protects rat brains against focal ischemia. Brain Res 1282, 133-141.

Yet S. F., Layne M. D., Liu X., Chen Y. H., Ith B., Sibinga N. E. and Perrella M. A. (2003) Absence of heme oxygenase-1 exacerbates atherosclerotic lesion formation and vascular remodeling. Faseb J 17, 1759-1761.

Yilmaz G. and Granger D. N. (2008) Cell adhesion molecules and ischemic stroke. Neurol Res 30, 783-793.

Zhang M., An C., Gao Y., Leak R. K., Chen J. and Zhang F. (2013a) Emerging roles of Nrf2 and phase II antioxidant enzymes in neuroprotection. Prog Neurobiol 100, 30-47.

Zhang T., Liang X., Shi L., Wang L., Chen J., Kang C., Zhu J. and Mi M. (2013b) Estrogen Receptor and PI3K/Akt Signaling Pathway Involvement in S-(-)Equol-Induced Activation of Nrf2/ARE in Endothelial Cells. PLoS One 8, e79075.

Zhao J., Kobori N., Aronowski J. and Dash P. K. (2006) Sulforaphane reduces infarct volume following focal cerebral ischemia in rodents. Neurosci Lett 393, 108-112.

Zhong Y., Liu T., Lai W., Tan Y., Tian D. and Guo Z. (2013) Heme oxygenase-1-mediated reactive oxygen species reduction is involved in the inhibitory effect of curcumin on lipopolysaccharide-induced monocyte chemoattractant protein-1 production in RAW264.7 macrophages. Mol Med Rep 7, 242-246.

Zhou Z. H., Kumari N., Nekhai S., Clouse K. A., Wahl L. M., Yamada K. M. and Dhawan S. (2013) Heme oxygenase-1 induction alters chemokine regulation and ameliorates human immunodeficiency virus-type-1 infection in lipopolysaccharide-stimulated macrophages. Biochem Biophys Res Commun 435, 373-377.

Zou L. Y., Cheung R. T., Liu S., Li G. and Huang L. (2006) Melatonin reduces infarction volume in a photothrombotic stroke model in the wild-type but not cyclooxygenase-1-gene knockout mice. J Pineal Res 41, 150-156.